

**MATERIAL EVALUATION STUDY  
BALLAST AND FOUNDATION MATERIALS  
RESEARCH PROGRAM**



**JANUARY 1977**

DOCUMENT IS AVAILABLE TO THE PUBLIC THROUGH  
THE NATIONAL TECHNICAL INFORMATION SERVICE,  
SPRINGFIELD, VIRGINIA 22161

Prepared for  
**U. S. DEPARTMENT OF TRANSPORTATION  
FEDERAL RAILROAD ADMINISTRATION  
Office of Research and Development  
Washington, D.C. 20590**

01-Track & Structures

## NOTICE

This document is disseminated under the sponsorship of the Department of Transportation in the interest of information exchange. The United States Government assumes no liability for its contents or use thereof.

1. Report No. FRA-OR&D-77-02	2. Government Accession No.	3. Recipient's Catalog No.	
4. Title and Subtitle Materials Evaluation Study - Ballast and Foundation Materials Research Program		5. Report Date January 1977	6. Performing Organization Code
7. Author(s) Knutson, R. M., Thompson, M. R., Mullin, T., and Tayabji, S. D.		8. Performing Organization Report No.	
9. Performing Organization Name and Address Department of Civil Engineering University of Illinois, Urbana-Champaign Campus Urbana, Illinois 61801		10. Work Unit No.	11. Contract or Grant No. DOT-FR-30038
12. Sponsoring Agency Name and Address Office of Research & Development Federal Railroad Administration, U. S. Dept. of Trans. 2100 2nd Street, S. W. Washington, D.C. 20590		13. Type of Report and Period Covered Technical Report	
14. Sponsoring Agency Code		15. Supplementary Notes	
16. Abstract <p>This report presents the results of Phase IV - Materials Evaluation Study, of the Ballast and Foundation Materials Research Program. Emphasis is on characterizing the response of the structural support elements (subgrade, subballast, and ballast) with respect to in service loading conditions. Properties of the subgrade, the subballast, and the ballast that significantly influence track structure behavior and performance have been identified.</p> <p>Part A of the report includes the evaluation of the resilient (elastic) response and permanent strain response of 7 ballast and subballast materials. Part B contains plastic strain and degradation results of ballast materials subject to long term (1 million repetitions) loading. Part C includes the evaluation of resilient response and permanent strain response of ten subgrade soils. Thermal regime characterization, including freeze-thaw analysis is presented in Part D. A comprehensive summary and conclusions are given in Part E.</p>			
17. Key Words Ballast, Subballast, Subgrade, Ballast Testing, Subgrade Testing, Repeated Load Triaxial Testing, Thermal Regime Characterization, Conventional Railway Track Support System		18. Distribution Statement Document is available to the public from: National Technical Information Service 5285 Port Royal Road Springfield, Virginia 22161	
19. Security Classif. (of this report) Unclassified	20. Security Classif. (of this page) Unclassified	21. No. of Pages 332	22. Price

## PREFACE

This report has been generated as part of a sub-contract between the Association of American Railroads Research and Test Department, and the University of Illinois.

This sub-contract is part of a larger contract which is a cooperative effort between the Federal Railroad Administration and the Association of American Railroads on improved track structures. The entire program is in response to recognition of the desire for a more durable track structure. To this end, the program is a multi-task effort involving 1) the development of empirical and analytical tools for the description of the track structure so that the economic trade-offs among track construction parameters such as tie size, rail size, ballast depth and cross section, type, subgrade type, stiffness may be determined, 2) methodologies to upgrade the existing track structures to withstand new demands in loading, 3) development of performance specifications for track components, and 4) investigating the effects of various levels of maintenance.

This particular report presents the results of Ballast and Foundation Materials Evaluation Study. Emphasis is on characterizing the response of the structural support elements (subgrade, subballast, and ballast) with respect to in-service loading conditions.

A special note of thanks is given to Mr. William S. Autrey, Chief Engineer of Santa Fe, Mr. R. M. Brown, Chief Engineer of Union Pacific, Mr. F. L. Peckover, Engineer of Geotechnical Services, Canadian National Railway, Mr. C. E. Webb, Asst. Vice President, Southern Railway System, as they have served in the capacity of members of the Technical Review Committee for this Ballast and Foundation Materials program, and Dr. R. M. McCafferty as the Contracting Officer's Technical Representative of the FRA on the entire research program.

G. C. Martin  
Director-Dynamics Research  
Principal Investigator  
Track Structures Research Program  
Association of American Railroads

## FOREWORD

The Department of Civil Engineering of the University of Illinois at Urbana Champaign is currently conducting a broad based research program entitled "Ballast and Foundation Materials Research Program". The University of Illinois is serving as a sub-contractor to the Association of American Railroads. The research program is sponsored by the U. S. Department of Transportation, Federal Railroad Administration.

The research program consists of six work phases which are detailed below:

- Phase I - Technical Data Bases (completed)
- Phase II - Development of Structural Model and Materials Evaluation Procedures (completed)
- Phase III - Parameter Studies and Sensitivity Analyses (completed)
- Phase IV - Materials Evaluation Study (this report)
- Phase V - Economic Evaluation
- Phase VI - Preparation of Conclusions, Summary and Recommendations

This report presents the results of Work Phase IV. Emphasis is on characterizing the response of the structural support elements (subgrade, subballast, and ballast) with respect to in service loading conditions. Properties of the subgrade, the subballast, and the ballast that significantly influence track structure behavior and performance have been identified. Because of the varied nature of the subject matter and because it is felt that some of the subjects may be of particular interest to the individual user, the report is organized into five separate parts.

Part A includes the evaluation of 7 ballast and subballast materials. Particular attention is paid to the resilient (elastic) response and to the permanent strain response, especially under mixed loading conditions.

Part B is a presentation of the plastic strain and degradation results of ballast materials subjected to long term (1 million repetitions) loading.

The results of investigations of the plastic strain response and the resilient behavior of subgrade materials are presented in Part C. Ten soils were studied, and emphasis was given to determining the effects of changes in density and moisture conditions.

Environmental conditions, including freeze-thaw analysis, and the results of changes in those conditions forms Part D of the report.

Although summary and conclusions sections are included in the individual parts, a comprehensive summary and conclusions section is presented in Part E because it was felt that the casual reader would better appreciate the overall thrust of the study through such a section.

## TABLE OF CONTENTS

CHAPTER	Page
PART A . . . . .	1
1 INTRODUCTION . . . . .	1
1.1 Statement of the Problem . . . . .	1
1.2 Objective and Scope . . . . .	2
2 LITERATURE SURVEY . . . . .	5
2.1 Concept of Resilient Modulus . . . . .	5
2.2 Laboratory Investigations . . . . .	6
2.2.1 Stress History . . . . .	6
2.2.2 Frequency and Duration of Load Application . . . . .	9
2.2.3 Geometric Characteristics of Aggregate . . . . .	9
2.2.4 Gradation . . . . .	12
2.2.5 Degree of Compaction . . . . .	13
2.2.6 Degree of Saturation . . . . .	14
2.2.7 Stress Level . . . . .	14
2.2.8 Specimen Size . . . . .	15
2.3 Factors Affecting the Permanent Deformation Characteristics of Granular Materials . . . . .	17
2.4 Summary . . . . .	28
3 LABORATORY TESTING PROGRAM . . . . .	31
3.1 Ballast . . . . .	31
3.1.1 Description of Materials . . . . .	31
3.1.2 Characterization Tests . . . . .	34
3.1.3 Static Triaxial Tests . . . . .	34
3.2 Testing Program . . . . .	34
3.2.1 Testing Equipment . . . . .	39
3.2.2 Instrumentation . . . . .	42
3.2.3 Specimen Preparation . . . . .	43
3.2.4 Testing Sequence . . . . .	50
4 RESILIENT MODULUS RESULTS . . . . .	61
4.1 Introduction . . . . .	61
4.2 Computation of Resilient Modulus . . . . .	61
4.3 Results of Resilient Testing Program . . . . .	61
4.4 Correlation with Characterization Test Results . . . . .	97
4.5 Analysis of Variance Results . . . . .	100
4.6 Summary . . . . .	104
5 PRESENTATION AND ANALYSIS OF RESULTS FOR PLASTIC BEHAVIOR . . . . .	105
5.1 Introduction . . . . .	105
5.2 Plastic Strain Results . . . . .	106
5.3 Linear Regression Analysis . . . . .	106

CHAPTER	Page
5.4	Correlations with Characterization Test Results . . . 156
5.5	Analysis of Variance . . . . . 164
5.5.1	Effects of Gradation . . . . . 164
5.5.2	Effects of Material Type . . . . . 167
5.5.3	Effects of Degree of Compaction . . . . . 170
5.6	Comparisons with Hyperbolic Stress-Strain Law . . . . 173
5.7	Summary . . . . . 175
6	SUMMARY AND CONCLUSIONS . . . . . 179
6.1	Summary . . . . . 179
6.2	Conclusions . . . . . 179
PART B	. . . . . 181
7	INTRODUCTION . . . . . 181
7.1	Statement of the Problem . . . . . 181
7.2	Objective and Scope . . . . . 181
8	LITERATURE SURVEY . . . . . 183
8.1	General . . . . . 183
8.2	Permanent Deformation . . . . . 183
8.2.1	Laboratory Investigations of Permanent Deformation Behavior . . . . . 183
8.2.2	Field Correlations . . . . . 185
8.3	Degradation . . . . . 185
8.3.1	Laboratory Degradation Studies . . . . . 186
8.3.2	Field Degradation Studies . . . . . 188
8.4	Summary . . . . . 189
9	LABORATORY TESTING PROGRAM . . . . . 191
9.1	Ballast . . . . . 191
9.1.1	Description of Materials . . . . . 191
9.1.2	Characterization Tests . . . . . 191
9.2	Testing Program . . . . . 191
9.2.1	Triaxial Equipment . . . . . 194
9.2.2	Instrumentation . . . . . 194
9.2.3	Specimen Preparation . . . . . 194
9.2.4	Testing Sequence . . . . . 194
9.2.5	Degradation Measurement . . . . . 195
10	PRESENTATION AND ANALYSIS OF PERMANENT DEFORMATION BEHAVIOR . . . . . 197
10.1	Introduction . . . . . 197
10.2	Plastic Strain Results for Primary Testing Series . . . 197
10.2.1	Regression Analysis . . . . . 197

CHAPTER	Page
10.2.2 Relationship of Plastic Strain to Material Properties . . . . .	197
10.3 Results for Low Confining Pressure Specimens . . . . .	207
11 PRESENTATION AND ANALYSIS OF DEGRADATION RESULTS . . . . .	211
11.1 Introduction . . . . .	211
11.2 Criteria . . . . .	211
11.3 Correlations with Material Properties . . . . .	211
11.4 Correlations with Plastic Strain . . . . .	211
11.5 Nature of Fines . . . . .	213
12 SUMMARY AND CONCLUSIONS . . . . .	215
12.1 Summary . . . . .	215
12.2 Conclusions . . . . .	215
PART C . . . . .	217
13 FOUNDATION MATERIAL TESTING PROGRAM AND PROCEDURES . . . . .	217
13.1 General . . . . .	217
13.2 Soils . . . . .	217
13.3 Testing Program and Procedures . . . . .	217
13.3.1 Specimen Preparation . . . . .	220
13.3.2 Specimen Testing . . . . .	220
14 FOUNDATION MATERIAL TEST RESULTS . . . . .	223
14.1 Resilience Test Results . . . . .	223
14.2 Permanent Deformation Test Results . . . . .	232
14.3 Summary and Conclusions . . . . .	262
PART D . . . . .	265
15 TEMPERATURE REGIME CHARACTERIZATION . . . . .	265
15.1 Introduction . . . . .	265
15.2 Description of the Heat Transfer Model . . . . .	265
15.3 Input Parameters Required for the Model . . . . .	266
15.4 Limitations of the Heat Transfer Model . . . . .	270
15.5 Evaluation of the Thermal Properties of Subgrade and Ballast . . . . .	271
16 TEMPERATURE REGIME EVALUATION . . . . .	281
16.1 Initial Analyses . . . . .	281
16.2 Laboratory Evaluation of Ballast Thermal Properties . . . . .	284
16.3 Selection of Ballast Thermal Properties . . . . .	290
16.4 Discussion of Results . . . . .	293
16.5 Conclusions . . . . .	297

CHAPTER	Page
PART E	
17 SUMMARY AND CONCLUSIONS . . . . .	299
17.1 Summary . . . . .	299
17.2 Conclusions . . . . .	300
LIST OF REFERENCES . . . . .	305

## LIST OF TABLES

Table		Page
2.1	Summary of Repeated Load Tests of Granular Materials.	16
3.1	AREA Recommended Ballast Gradations . . . . .	32
3.2	Amounts of Ballast Used by Material Type . . . . .	33
3.3	Standard Characterization Test References . . . . .	36
3.4	Characterization Test Results . . . . .	37
3.5	Static Triaxial Test Results . . . . .	38
3.6	Summary of Primary Test Specimen Properties . . . . .	53
3.7	Reference Section Parameters . . . . .	54
3.8	Standard Test Sequence . . . . .	59
4.1	Results of Resilient Modulus Testing Program . . . . .	62
4.2	Correlation Coefficients for Regression Analyses of Resilient and Characterization Test Results . . . . .	98
4.3	Randomized Complete Block Analyses of Resilient Test Results . . . . .	101
4.4	Randomized Complete Block Analysis of Resilient Test Results by Material Type . . . . .	102
5.1	Regression Analyses of Plastic Strain Results during Conditioning Phase . . . . .	148
5.2	Regression Analysis of Plastic Strain at Stress Levels Other Than Conditioning . . . . .	149
5.3	Stress Factor Results . . . . .	155
5.4	Correlation of Plastic Strain Results for 32 Specimens . . . . .	157
5.5	Correlation of Plastic Strain Results for 14 No. 4 Gradation Specimens . . . . .	158
5.6	Correlation of Plastic Strain Results for 6 No. 4 Gradation Specimens . . . . .	160
5.7	Correlation of Plastic Strain Results for 9 No. 4 Gradation Specimens . . . . .	161

Table	Page
5.8 Correlation of Regression Results . . . . .	162
5.9 Correlation of Stress Factor Results . . . . .	163
5.10 RCB Analysis of Plastic Strain Results by Gradation . . . . .	166
5.11 CRD Analysis of Stress Factor Results by Gradation . . . . .	168
5.12 RCB Analysis of Plastic Strain Results by Material Type . . . . .	169
5.13 CRD Analysis of Stress Factor Results . . . . .	171
5.14 RCB Analysis of Regression Results by Compaction Level . . . . .	172
5.15 CBR Analysis of Stress Factor Results by Void Ratio . . . . .	174
5.16 Comparisons with Hyperbolic Stress-Strain Law Results . . . . .	176
8.1 Comparison of Field and Laboratory Ballast Degradation (References 28 and 53) . . . . .	190
9.1 Characterization Test Results . . . . .	193
9.2 Test Specimen Properties . . . . .	196
10.1 Permanent Strain and Regression Results for Long Term Testing . . . . .	198
10.2 Correlation Matrix for the Physical and Mechanical Properties of Ballasts Tested . . . . .	205
11.1 Degradation Results for Long Term Testing . . . . .	212
13.1 Soils Used . . . . .	218
14.1 Permanent Strain Relations for the Soils Used . . . . .	259
15.1 Description of Climatological Data Card for a First Order ESSA Weather Bureau Station (Reference 57) . . . . .	268
15.2 Thermal Conductivity of Some Rock Forming Minerals (Reference 73) . . . . .	274
15.3 Grain Sizes of the Sorted Aggregate (Reference 74) . . . . .	276
15.4 Thermal Conductivity Results of Six Crushed Stone Aggregate (Reference 74) . . . . .	277
15.5 Results of Ballast Thermal Conductivity Calculations . . . . .	278
16.1 Initial Results of Temperature Regime Evaluation . . . . .	283

Table		Page
16.2	Results of Temperature Regime Evaluation ( $K_B = 0.5$ and $0.75 \text{ Btu/ft-hr-}^\circ\text{F}$ ) . . . . .	294
16.3	Results of Temperature Regime Evaluation ( $K_B = 1.0$ $\text{Btu/ft-hr-}^\circ\text{F}$ ) . . . . .	295

## LIST OF FIGURES

Figure	Page
2.1 Resilient Modulus as a Function of the Sum of Principal Stresses . . . . .	7
2.2 Resilient Modulus as a Function of Confining Pressure . . . . .	8
2.3 Cumulative Plastic Strain as a Function of Stress Level . . . . .	18
2.4 Effect of Stress Sequence on Permanent Strain Response . . . . .	23
2.5 Effect of Stress Level on Permanent Strain Response, No. 1 . . . . .	24
2.6 Effect of Stress Level on Permanent Strain Response, No. 2 . . . . .	25
2.7 Schematic of Repeated Loading Response for Triaxial Compression . . . . .	26
2.8 Schematic of Possible Stress Paths in Triaxial Compression . . . . .	27
3.1 Ballast Gradations Tested . . . . .	35
3.2 Schematic of Triaxial Cell . . . . .	40
3.3 Overall View of Testing Equipment . . . . .	41
3.4 Compaction Mold . . . . .	45
3.5 Compaction Equipment . . . . .	46
3.6 Typical Completed Specimen . . . . .	48
3.7 Gradation of CA-10 . . . . .	49
3.8 Typical Gradations and Permeabilities . . . . .	51
3.9 Gradations of Two "Well Graded" Specimens . . . . .	52
3.10 Cumulative Plastic Strain Results for a No. 5 Gradation, Medium Density Limestone Specimen . . . . .	56
3.11 Plastic Strain Results for a No. 5 Gradation, Medium Density Limestone Specimen . . . . .	57
4.1 Relationship between $E_r$ and $\theta$ for No. 4 Gradation Limestone, Medium Density . . . . .	64
4.2 Relationship between $E_r$ and $\theta$ for No. 4 Gradation Granitic Gneiss, Medium Density . . . . .	65

Figure		Page
4.3	Relationship between $E_r$ and $\theta$ for No. 4 Gradation Chicago Blast Furnace Slag, Medium Density . . . . .	66
4.4	Relationship between $E_r$ and $\theta$ for No. 4 Gradation Basalt, Medium Density . . . . .	67
4.5	Relationship between $E_r$ and $\theta$ for No. 4 Gradation Crushed Gravel, Medium Density . . . . .	68
4.6	Relationship between $E_r$ and $\theta$ for No. 4 Gradation Gravel, Medium Density . . . . .	69
4.7	Relationship between $E_r$ and $\theta$ for No. 4 Gradation Limestone, Low Density . . . . .	70
4.8	Relationship between $E_r$ and $\theta$ for No. 4 Gradation Granitic Gneiss, Low Density . . . . .	71
4.9	Relationship between $E_r$ and $\theta$ for No. 4 Gradation Chicago Blast Furnace Slag, Low Density . . . . .	72
4.10	Relationship between $E_r$ and $\theta$ for No. 4 Gradation Gravel, Low Density . . . . .	73
4.11	Relationship between $E_r$ and $\theta$ for No. 4 Gradation Limestone, High Density . . . . .	74
4.12	Relationship between $E_r$ and $\theta$ for No. 4 Gradation Granitic Gneiss, High Density . . . . .	75
4.13	Relationship between $E_r$ and $\theta$ for No. 4 Gradation Chicago Blast Furnace Slag, High Density . . . . .	76
4.14	Relationship between $E_r$ and $\theta$ for No. 4 Gradation Gravel, High Density . . . . .	77
4.15	Relationship between $E_r$ and $\theta$ for No. 5 Gradation Limestone, Medium Density . . . . .	78
4.16	Relationship between $E_r$ and $\theta$ for No. 5 Gradation Basalt, Medium Density . . . . .	79
4.17	Relationship between $E_r$ and $\theta$ for No. 5 Gradation Gravel, Medium Density . . . . .	80
4.18	Relationship between $E_r$ and $\theta$ for No. 5 Gradation Kansas Test Track Slag, Medium Density . . . . .	81

Figure	Page
4.19 Relationship between $E_r$ and $\theta$ for No. 5 Gradation Limestone, Low Density . . . . .	82
4.20 Relationship between $E_r$ and $\theta$ for No. 5 Gradation Granitic Gneiss, Low Density . . . . .	83
4.21 Relationship between $E_r$ and $\theta$ for No. 5 Gradation Kansas Test Track Slag, Low Density . . . . .	84
4.22 Relationship between $E_r$ and $\theta$ for No. 5 Gradation Limestone, High Density . . . . .	85
4.23 Relationship between $E_r$ and $\theta$ for No. 5 Gradation Kansas Test Track Slag, High Density . . . . .	86
4.24 Relationship between $E_r$ and $\theta$ for Well Graded ( $n = 2/3$ ) Limestone, Medium Density . . . . .	87
4.25 Relationship between $E_r$ and $\theta$ for Well Graded ( $n = 2/3$ ) Granitic Gneiss, Medium Density . . . . .	88
4.26 Relationship between $E_r$ and $\theta$ for Well Graded ( $n = 2/3$ ) Chicago Blast Furnace Slag, Medium Density . . . . .	89
4.27 Relationship between $E_r$ and $\theta$ for Well Graded ( $n = 2/3$ ) Basalt, Medium Density . . . . .	90
4.28 Relationship between $E_r$ and $\theta$ for Well Graded ( $n = 2/3$ ) Gravel, Medium Density . . . . .	91
4.29 Relationship between $E_r$ and $\theta$ for Well Graded ( $n = 1/2$ ) Limestone, Medium Density, No. 1 . . . . .	92
4.30 Relationship between $E_r$ and $\theta$ for Well Graded ( $n = 1/2$ ) Limestone, Medium Density, No. 2 . . . . .	93
4.31 Relationship between $E_r$ and $\theta$ for CA-10 Gradation Limestone, Medium Density . . . . .	94
4.32 Relationship between $E_r$ and $\theta$ for CA-10 Gradation Limestone, High Density . . . . .	95
5.1 Effect of Density on Plastic Strain Response for No. 5 Gradation Limestone . . . . .	107
5.2 Effect of Density on Plastic Strain Response for No. 5 Gradation Kansas Test Track Slag . . . . .	108

Figure		Page
5.3	Effects of Gradation and Density on Plastic Strain Response for Limestone	. 109
5.4	Effects of Gradation and Density on Plastic Strain Response for Granitic Gneiss	. 110
5.5	Effects of Gradation and Density on Plastic Strain Response for Chicago Blast Furnace Slag	. 111
5.6	Effects of Crushing, Density, and Gradation on Plastic Strain Response for Gravel	. 112
5.7	Effects of Density and Gradation on Plastic Strain Response for Limestone	. 113
5.8	Effects of Gradation on Plastic Strain Response for Basalt	. 114
5.9	Effects of Material Type and Density on Plastic Strain Response	. 115
5.10	Effect of Stress Level on Plastic Strain Response of No. 5 Gradation Limestone, Medium Density	. 116
5.11	Effect of Stress Level on Plastic Strain Response of No. 5 Gradation Limestone, High Density	. 117
5.12	Effect of Stress Level on Plastic Strain Response of No. 4 Gradation Limestone, Low Density	. 118
5.13	Effect of Stress Level on Plastic Strain Response of No. 4 Gradation Limestone, Medium Density	. 119
5.14	Effect of Stress Level on Plastic Strain Response of No. 4 Gradation Limestone, High Density	. 120
5.15	Effect of Stress Level on Plastic Strain Response of Well Graded ( $n = 2/3$ ) Limestone, Medium Density	. 121
5.16	Effect of Stress Level on Plastic Strain Response of Well Graded ( $n = 1/2$ ) Limestone, Medium Density, No. 1	. 122
5.17	Effect of Stress Level on Plastic Strain Response of Well Graded ( $n = 1/2$ ) Limestone, Medium Density, No. 2	. 123
5.18	Effect of Stress Level on Plastic Strain Response of CA-10 Gradation Limestone, Medium Density	. 124
5.19	Effect of Stress Level on Plastic Strain Response of CA-10 Gradation Limestone, High Density	. 125

Figure	Page
5.20	Effect of Stress Level on Plastic Strain Response of No. 5 Gradation Granitic Gneiss, Low Density . . . . . 126
5.21	Effect of Stress Level on Plastic Strain Response of No. 4 Gradation Granitic Gneiss, Low Density . . . . . 127
5.22	Effect of Stress Level on Plastic Strain Response of No. 4 Gradation Granitic Gneiss, Medium Density . . . . . 128
5.23	Effect of Stress Level on Plastic Strain Response of No. 4 Gradation Granitic Gneiss, High Density . . . . . 129
5.24	Effect of Stress Level on Plastic Strain Response of Well Graded ( $n = 2/3$ ) Granitic Gneiss, Medium Density . . . . . 130
5.25	Effect of Stress Level on Plastic Strain Response of No. 4 Gradation Chicago Blast Furnace Slag, Low Density . . . . . 131
5.26	Effect of Stress Level on Plastic Strain Response of No. 4 Gradation Chicago Blast Furnace Slag, Medium Density . . . . . 132
5.27	Effect of Stress Level on Plastic Strain Response of No. 4 Gradation Chicago Blast Furnace Slag, High Density . . . . . 133
5.28	Effect of Stress Level on Plastic Strain Response of Well Graded ( $n = 2/3$ ) Chicago Blast Furnace Slag, Medium Density . . . . . 134
5.29	Effect of Stress Level on Plastic Strain Response of No. 5 Gradation Basalt, Medium Density . . . . . 135
5.30	Effect of Stress Level on Plastic Strain Response of No. 4 Gradation Basalt, Medium Density . . . . . 136
5.31	Effect of Stress Level on Plastic Strain Response of Well Graded ( $n = 2/3$ ) Basalt, Medium Density . . . . . 137
5.32	Effect of Stress Level on Plastic Strain Response of No. 4 Gradation Crushed Gravel, Medium Density . . . . . 138
5.33	Effect of Stress Level on Plastic Strain Response of No. 5 Gradation Gravel, Medium Density . . . . . 139
5.34	Effect of Stress Level on Plastic Strain Response of No. 4 Gradation Gravel, Low Density . . . . . 140
5.35	Effect of Stress Level on Plastic Strain Response of No. 4 Gradation Gravel, Medium Density . . . . . 141

Figure	Page
5.36 Effect of Stress Level on Plastic Strain Response of No. 4 Gradation Gravel, High Density . . . . .	142
5.37 Effect of Stress Level on Plastic Strain Response of Well Graded (n = 2/3) Gravel, Medium Density . . . . .	143
5.38 Effect of Stress Level on Plastic Strain Response of No. 5 Gradation Kansas Test Track Slag, Low Density . . . . .	144
5.39 Effect of Stress Level on Plastic Strain Response of No. 5 Gradation Kansas Test Track Slag, Medium Density . . . . .	145
5.40 Effect of Stress Level on Plastic Strain Response of No. 5 Gradation Kansas Test Track Slag, High Density . . . . .	146
9.1 Ballast Gradation Tested and Limits for No. 4 Ballast . . . . .	192
10.1 Effect of Number of Loading Cycles on Plastic Strain for Limestone . . . . .	199
10.2 Effect of Number of Loading Cycles on Plastic Strain for Granitic Gneiss . . . . .	200
10.3 Effect of Number of Loading Cycles on Plastic Strain for Chicago Blast Furnace Slag . . . . .	201
10.4 Effect of Number of Loading Cycles on Plastic Strain for Basalt . . . . .	202
10.5 Effect of Number of Loading Cycles on Plastic Strain for Gravel . . . . .	203
10.6 Effect of Number of Loading Cycles on Plastic Strain for Crushed Gravel . . . . .	204
10.7 Low Confining Pressure Results for Limestone . . . . .	209
10.8 Low Confining Pressure Results for Gravel . . . . .	210
13.1 Schematic Diagram of Kneading Compaction Apparatus . . . . .	219
13.2 Schematic Diagram of Resilience Testing Equipment Used with Fine-Grained Soils . . . . .	201
14.1 Resilient Modulus-Repeated Deviator Stress Relation for Applying . . . . .	224
14.2 Resilient Modulus-Repeated Deviator Stress Relation for Cecil . . . . .	225
14.3 Resilient Modulus-Repeated Deviator Stress Relation for Davidson . . . . .	226

Figure	Page
14.4 Resilient Modulus-Repeated Deviator Stress Relation for Drummer B . . . . .	227
14.5 Resilient Modulus-Repeated Deviator Stress Relation for Fayette B . . . . .	228
14.6 Resilient Modulus-Repeated Deviator Stress Relation for Fayette C . . . . .	229
14.7 Resilient Modulus-Repeated Deviator Stress Relation for Greenville . . . . .	230
14.8 Resilient Modulus-Repeated Deviator Stress Relation for Norfolk . . . . .	231
14.9 Permanent Strain-Number of Load Repetition Relation for Davidson B <sub>2</sub> . . . . .	233
14.10 Permanent Strain-Number of Load Repetition Relation for Dickenson C . . . . .	236
14.11 Permanent Strain-Number of Load Repetition Relation for Drummer B . . . . .	239
14.12 Permanent Strain-Number of Load Reepetition Relation for Fayette B . . . . .	242
14.13 Permanent Strain-Number of Load Repetition Relation for Fayette C . . . . .	245
14.14 Permanent Strain-Number of Load Repetition Relation for the Kansas Test Track Soil . . . . .	248
14.15 Permanent Strain-Number of Load Repetition Relation for Norfolk B <sub>2</sub> . . . . .	250
14.16 Deviator Stress-Permanent Strain Relation at 5000 load applications for Davidson B <sub>2</sub> . . . . .	253
14.17 Deviator Stress-Permanent Strain Relation at 5000 load applications for Dickenson C . . . . .	254
14.18 Deviator Stress-Permanent Strain Relation at 5000 load applications for Drummer B . . . . .	255
14.19 Deviator Stress-Permanent Strain Relation at 5000 load applications for Fayette B . . . . .	255
14.20 Deviator Stress-Permanent Strain Relation at 5000 load applications for Fayette C . . . . .	256

Figure		Page
14.21	Deviator Stress-Permanent Strain Relation at 5000 load applications for the Kansas Test Track Soil. . . . .	257
14.22	Deviator Stress-Permanent Strain Relation at 5000 load applications for Norfolk B <sub>2</sub> . . . . .	258
14.23	Effect of One Freeze-Thaw Cycle on Permanent Deformation for Drummer B . . . . .	261
15.1	Intrinsic Factors Which Influence Frost Action (Reference 52) . . . . .	269
16.1	Material Properties for Idealized Ballast-Subgrade System . . . . .	282
16.2	Laboratory Gradation Used to Evaluate Ballast Thermal Properties . . . . .	285
16.3	Effects of Depth on Heat Transfer in Limestone Ballast . . . . .	287
16.4	Material Properties Used to Simulate Laboratory Conditions . . . . .	288
16.5	Effects of Thermal Conductivity on Heat Transfer in Ballast Materials . . . . .	289
16.6	Effects of Heat Capacity on Heat Transfer in Ballast Materials . . . . .	291
16.7	Effects of Density on Heat Transfer in Ballast Materials . . . . .	292

PART A  
CHAPTER 1

INTRODUCTION

1.1 Statement of the Problem

Railroads have long used ballast to provide support for the rail-tie system and to provide a free draining medium. Two of the problems related to the performance of ballast materials are the excessive elastic deformations caused by the rapid application and removal of the wheel loads, and the accumulation of large plastic deformations resulting from many repetitions of individual wheel loads.

Excessive elastic deformations in the ballast can cause shortening of the rail-tie life because of fatigue resulting from increased bending stresses. In addition the ride quality of both freight and passenger cars is reduced if the elastic deformations in the conventional railway track support system (CRTSS) are excessive.

The plastic deformations necessitate continual realignment of the rail-tie system by addition of ballast. Present maintenance practice is to tamp only the portion of the ballast near the rail and to leave the center undisturbed. The practice results in the addition of ballast primarily in the proximity of the rails; ballast pockets result (1)\*. The ballast pockets serve as traps for water; the result is almost continual saturation of the subgrade, thus worsening an often bad situation. Continued maintenance therefore is not always a satisfactory solution.

---

\* Numbers in parentheses refer to entries in the List of References.

Modern analytical models can be used to improve the present experience oriented design of rail-tie support systems. However before modern techniques can be applied adequate input in the form of material response parameters must be obtained. To date, such information has been lacking. The response of granular materials has been shown to be stress dependent, i.e., the response of the material depends upon the applied state of stress. Therefore to accurately predict the structural response of the CRTSS, the test method used to evaluate the granular materials should simulate the in service dynamic stress conditions.

Several investigations (2, 3, 4, 5) of the repeated load behavior of granular materials have been made. Both rigid confinement and triaxial equipment have been used to study dense graded aggregates and sand, but little work has been done involving open graded aggregate such as ballast. In addition, most of the research has been directed toward studies of the elastic (resilient) properties of the material; little attention has been paid to the plastic behavior of aggregate subjected to repeated load conditions.

Repeated load triaxial testing of a variety of aggregate types would appear to be the most appropriate method for investigating the elastic as well as the plastic behavior of ballast materials. Previous investigations in which actual loading conditions were closely simulated have given excellent results for convenient application to finite element techniques.

## 1.2 Objective and Scope

The objective of this research was to investigate the effects of material type and gradational changes on both the elastic and plastic

repeated load behavior of ballast. The importance of stress history, stress level, and degree of compaction on the response of the materials was also included.

It was intended that the results be used for material characterization input to advanced structural models, such as the Illi-Track procedure (6). Such methods are necessary to adequately predict CRTSS structural response and to aid in the design of the rail-tie support system.

The work was divided into four phases. Phase I involved the literature survey discussed in Chapter 2. The literature survey was concerned primarily with repeated load testing of granular materials and the factors influencing the results of such tests.

During Phase II, samples of several types of ballast were obtained, and the materials were subjected to several standard characterization tests to enable later correlations with the repeated load behavior of the aggregates. The results are included in Chapter 3.

Phase III, the laboratory testing program, also is included in Chapter 3. Based on the results of preliminary tests, a standard procedure was developed for testing cylindrical specimens subjected to constant confining pressure and a repeated deviator stress. Both elastic and plastic deformations were carefully monitored during the test program. So that comparisons could be made, several types of materials (basalt, limestone, slag, etc.) and various gradations were included in the laboratory study.

Data reduction and analysis, Phase IV, are included in Chapters 4 and 5. The resilient modulus portion of the program is presented in Chapter 4. Equations were developed to relate resilient modulus to the sum of the

principal stresses, and the significance of the variables considered is presented. The analysis of the permanent deformation data recorded during testing and the attempts to relate permanent deformation to material properties, to gradation, to compaction level, and to stress level are presented in Chapter 5.

Chapter 6 includes the summary and conclusions reached during the study.

CHAPTER 2  
LITERATURE SURVEY

### 2.1 Concept of Resilient Modulus

Modern analytical techniques for predicting the structural response in layered systems require better characterization of the dynamic response of materials than can be obtained from static testing methods. It is desirable to evaluate the response of granular materials under laboratory conditions which simulate the in service conditions.

To evaluate the repeated load behavior of granular materials, several investigators (2, 3, 4, 5) have used the conventional triaxial cell with a repeated deviator stress and either constant or pulsed confining pressure. In addition, some tests of rigidly confined materials have been attempted with varying degrees of success.

Several investigators have used the concept of resilient modulus\* to describe the behavior of granular materials subjected to repeated loading conditions. Values of resilient modulus,  $E_r$ , at several stress states are obtained from laboratory testing. To account for the stress dependent nature of the materials several predictive equations have been developed; two of the more widely used equations are the following:

$$E_r = K\theta^n \quad (2.1)$$

and

$$E_r = K' \sigma_3^m \quad (2.2)$$

---

\* Resilient modulus is defined as the repeated deviator stress divided by the recoverable portion of the axial strain.

where

$K$ ,  $K'$ ,  $n$ , and  $m$  are constants determined from regression analysis of the laboratory data;  $\sigma_3$  is the confining pressure; and  $\theta$  represents the first stress invariant,  $\sigma_1 + \sigma_2 + \sigma_3$ .

Typical results are shown in Figures 2.1 and 2.2.

Some of the more important findings of previous investigations and some of the factors affecting resilient response of granular materials are discussed in Section 2.2.

## 2.2 Laboratory Investigations

As previously noted, most of the repeated load tests of granular materials have emphasized the characterization of the resilient behavior of sands or dense graded aggregates. Much of the important work on repeated load testing of aggregates has been effectively summarized in Reference 7. One of the important conclusions was that repeated load triaxial testing was the most suitable method for evaluating the resilient response of granular materials. A more recent summary of repeated load triaxial testing is included in Allen (5).

The remainder of this section will describe some of the factors influencing the results of repeated load triaxial testing.

### 2.2.1 Stress History

It has been shown (3, 5) that if a specimen has not been overstressed the resilient response measured after approximately 100 load cycles will be representative of the material behavior throughout a complex stress history. The consensus is that one specimen can be used to measure the

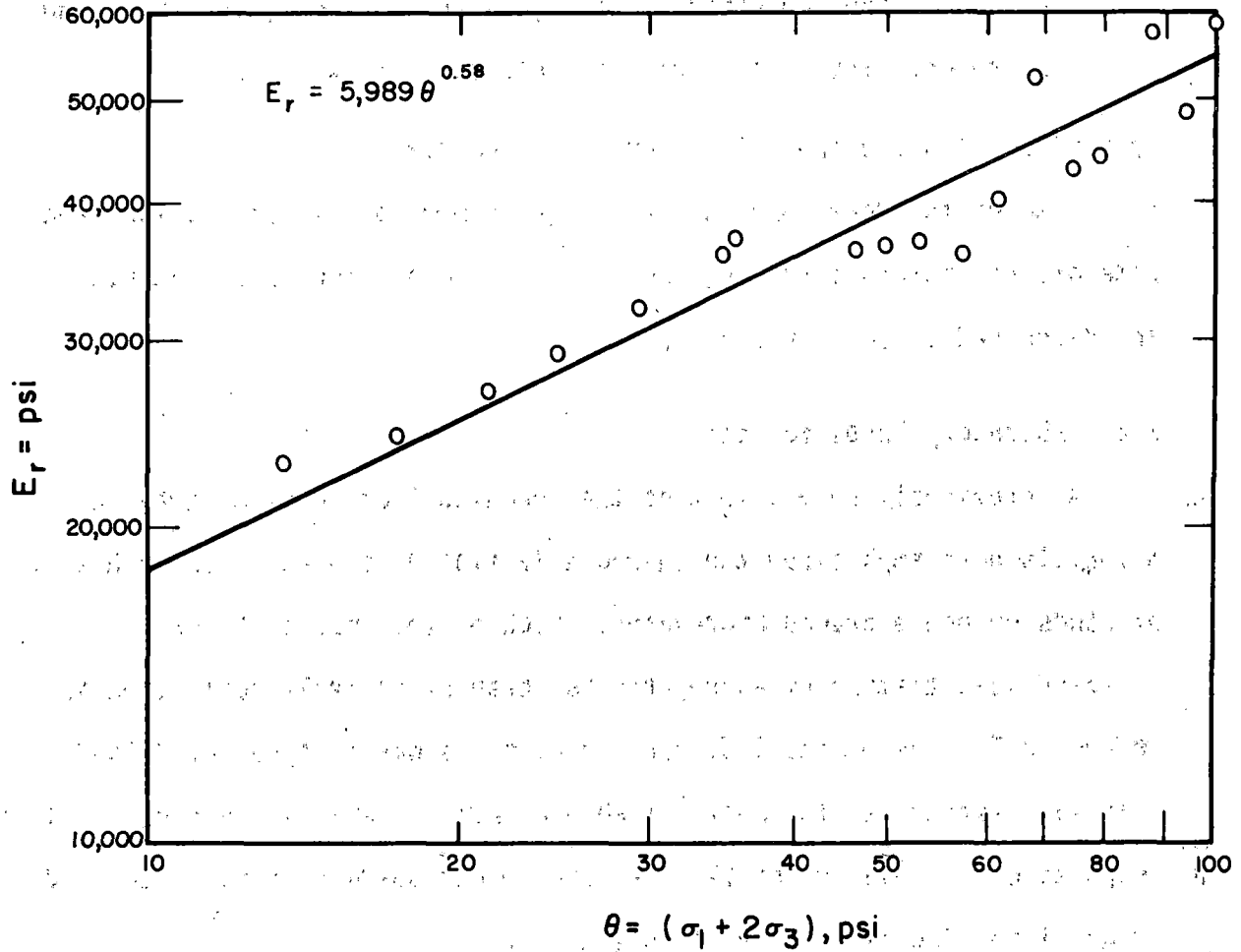


Figure 2.1. Resilient Modulus as a Function of the Sum of Principal Stresses (Reference 5).

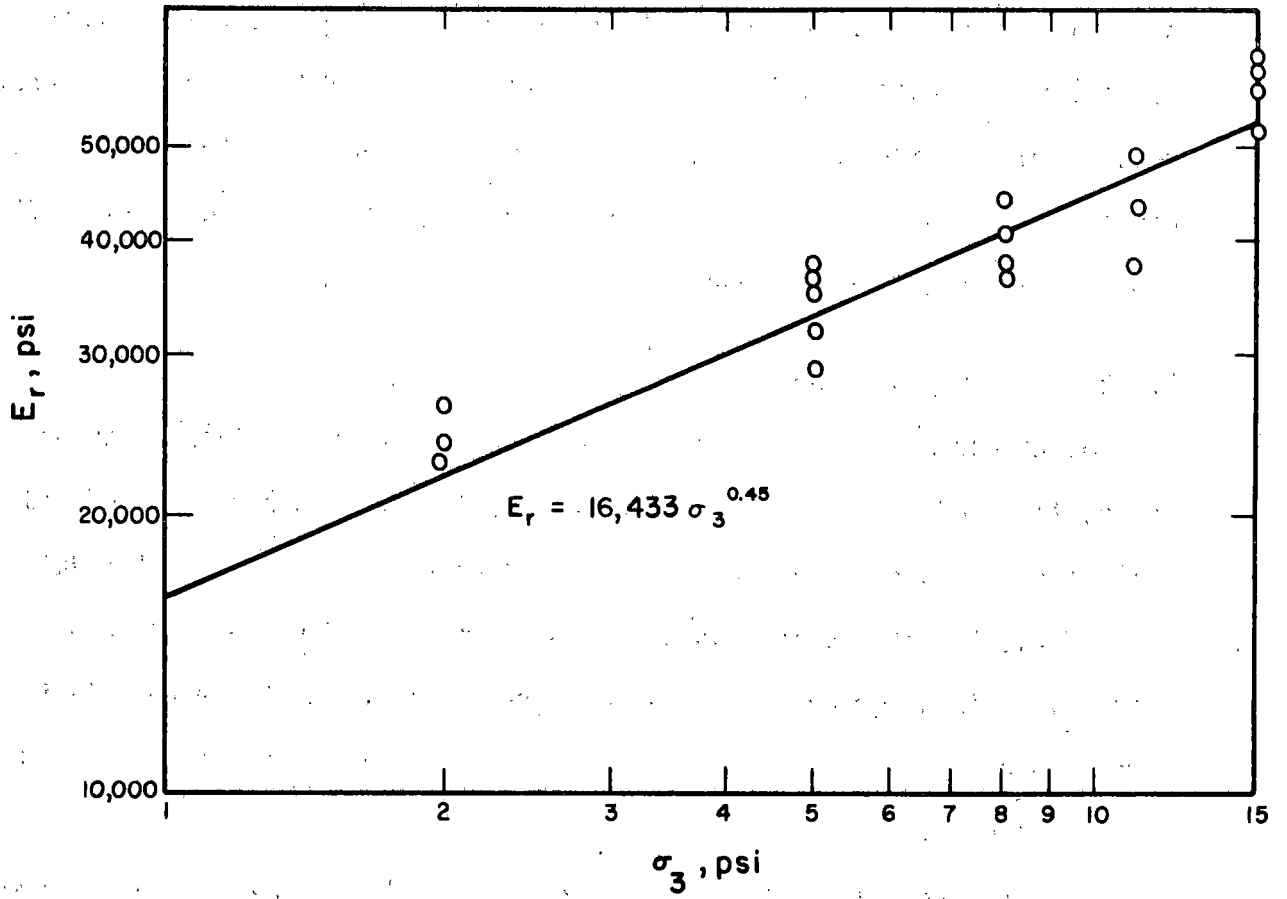


Figure 2.2. Resilient Modulus as a Function of Confining Pressure (Reference 5).

resilient response at several stress levels and that the sequence of stress application has no significant effect on the results.

Morgan (8) determined that the resilient modulus of sand tested in triaxial apparatus increased as the number of load applications increased but reached a constant value after approximately 10,000 load cycles. From tests of well graded aggregates, Allen (5) concluded the effects of stress history were small if the specimen had been conditioned for at least 1000 repetitions to eliminate adverse seating effects.

### 2.2.2 Frequency and Duration of Load Application

Hicks and Monismith (3) observed no influence on resilient modulus values for load durations in the range of 0.1 to 0.25 seconds. Seed and colleagues (7) concluded the change in the magnitude of resilient modulus of sand due to changes in load duration was small. For repeated load triaxial tests on granular materials Allen (5) found that the resilient modulus did not change for values of pulse duration in the range of 0.10 to 1.00 seconds.

Kalcheff and Hicks (9) varied the frequency of load application from 10 to 80 repetitions per minute and concluded resilient modulus was virtually insensitive to changes in frequency.

### 2.2.3 Geometric Characteristics of Aggregate

Huang (10) has defined geometric characteristics as the shape, angularity, and surface texture of aggregate materials. Because geometric characteristics of aggregate differ according to material type (limestone, basalt, slag, etc.) it is desirable to measure those characteristics.

Two of the methods for measuring shape, angularity, and surface texture are the Particle Index Test (10) and the Pouring Test of Ishai and Tons (11).

The Particle Index Test compares the void ratio of single sized aggregate to that of uniform spheres. Recently the Particle Index Test has been made a tentative ASTM standard. Typical values of particle index range from zero for highly polished aluminum spheres to near 20 for rough aggregate such as slag.

The Pouring Test expresses the geometric irregularity (volume, specific gravity, and aggregate porosity) of aggregate. The test is conducted by allowing aggregate to flow through an orifice into a container. The aggregate is leveled and weighed. The packing specific gravity,  $G_p$ , is determined by comparing the weight of the aggregate to the weight of glass beads needed to fill the container. The geometric irregularity is expressed by the specific rugosity,  $S_{rv}$ . The specific rugosity of smooth spheres is zero. Typical values of specific rugosity range from near 2 for beach pebbles to more than 20 for slag (11).

Although neither of the above measurements has been related to the repeated load behavior of aggregate, studies have tied particle index to compaction, static strength, and field performance. Huang, et al. (12) from tests of several different compacted materials found an almost linear relationship between void ratio and particle index; the aggregates showing higher particle index values had the highest void ratios.

Huang, et al. (12) also studied the effects of geometric characteristics on the strength of well graded aggregate systems. Several materials (gravel, mine chat, crushed stone) were tested in triaxial apparatus, using confining

pressures of 5, 15, and 30 psi (34, 103, and 207 kN/m<sup>2</sup>). The results consistently showed that both maximum stress difference and angle of shearing resistance increased as particle index increased.

A study by Thompson (13) on factors influencing field performance of soil-aggregate mixtures compared Burgraaff shear strength with the particle index values of gravel and crushed stone mixtures. No significant correlation could be established between particle index and the Burgraaff shear values possibly because particle index is based on the coarse aggregate fraction (plus No. 4) of the mixture, and for the mixtures tested an average of only 26% was retained on the No. 4 sieve. Thus the particle index of the preponderance of the material was not controlled which may have adversely affected the results of the tests. Because in general ballast consists of particles larger than the No. 4 sieve the particle index of ballast could be more easily controlled for comparative testing.

Although neither Particle Index nor the Pouring Test results has been related to repeated load performance some qualitative analyses have been made.

From tests conducted on well graded crushed gravel and crushed rock, Hicks and Monismith (3) concluded that resilient modulus at a given stress level increased with increasing particle angularity. Haynes and Yoder (2) observed higher resilient modulus values for gravel specimens than for crushed stone when both were compacted to the same relative density.

Allen (5) conducted repeated load triaxial tests on crushed stone, gravel, and a blend of the two. In general the resilient modulus values of the crushed stone were slightly higher than those of the gravel; the

resilient modulus of the blend generally was between the crushed stone and the gravel. Allen (5) concluded material type (gravel versus crushed stone) was not a major factor affecting the resilient response of granular materials.

#### 2.2.4 Gradation

Although differences in gradation are readily observed from the results of sieve analyses, it is difficult to represent a particular gradation by a single meaningful number. An attempt was made by Hudson (14) to estimate gradations through the use of the gradation parameter,  $\bar{A}$ . The gradation parameter is defined as the logarithm to the base 2 of the ratio of 54.8 to the effective mean diameter in millimeters of a particular size fraction.

The value of  $\bar{A}$  for a size fraction can be computed from

$$2^{\bar{A}} = \frac{54.8}{\bar{d}} \quad (2.3)$$

where

$$\bar{d} = \frac{0.443 (d_1 - d_2)}{\log (d_1/d_2)} \quad (2.4)$$

$d_1$  = size of larger sieve in millimeters, and

$d_2$  = size of smaller sieve in millimeters.

The gradation parameter of the aggregate system is the weighted mean of the values of the individual size fractions.

Although gradation estimators such as that of Hudson are available, few studies have attempted to relate them to repeated load behavior of aggregate systems.

Most of the studies of gradation effects on resilient response have involved either variations in the amount of material passing the No. 200 sieve or blends of materials. Hicks and Monismith (3) observed decreases in the resilient modulus values of well graded materials as the fines content was increased.

Barksdale (4) tested various soil-aggregate blends and concluded 20% soil, 80% aggregate blends exhibited higher values of resilient modulus at low stress state than did 40% soil, 60% aggregate specimens. At higher stress levels the situation was reversed. Haynes and Yoder (2) observed little change in resilient modulus values of well graded aggregates for changes in the amount of material passing the No. 200 sieve ranging from 6.2 to 11.5 percent.

#### 2.2.5 Degree of Compaction

Ballast is placed in the field in a fairly loose state, and tamping is used to increase the density of the material beneath the ties. It is generally acknowledged that the ballast underneath the tie undergoes increases in density due to the repeated loading of traffic. Because of the changes in the in-service density of ballast and because ballast in the field is not well confined, it is important to examine the response at various densities.

The effect of the degree of compaction on resilient modulus is not well understood. Although several studies have included density as a variable, the conclusions have not been consistent. Hicks and Monismith (3) obtained higher resilient modulus values for samples compacted to higher densities, although the variations were slight.

Trollope, et al., (15) found that the resilient modulus of high density dry sand was as much as 50% greater than the resilient modulus of the same material in a loose state.

Allen (5) investigated the response of crushed stone and gravel materials and a blend of both. In general the resilient modulus increased as density increased (AASHTO Method T-99 versus AASHTO Method T-180); the effect was most pronounced, although not without exception, at the lower values of the sum of principal stresses,  $\theta$ .

#### 2.2.6 Degree of Saturation

For dense graded granular materials, increased levels of saturation generally resulted in decreased modulus values (2). The effect was more pronounced for gravels than for crushed materials.

The results of research by Thompson (42) confirmed previous findings that resilient deformations increase and thus resilient modulus decreases as the degree of saturation increases.

#### 2.2.7 Stress Level

All of the previous studies of elastic response of granular materials have shown that the most significant factor affecting the resilient modulus is the stress state.

Figures 2.1 and 2.2 show typical constitutive relationships based on Equations 2.1 and 2.2, respectively. Although the model based on confining pressure gives good results, the first stress invariant,  $\theta$ , model is preferable because it affords better correlation coefficients and reduced scatter. The two figures depict typical results for the two models for a

single specimen, and effectively show the advantages of the model based on the first stress invariant.

Most of the investigations to date have been accomplished using constant confining pressure, but recently some studies have used cyclic confining pressure as well as cyclic deviator stress (5, 16). Allen and Thompson (17) concluded that although the constant confining pressure tests overestimated the resilient modulus, the use of the constant confining pressure triaxial test was justified as a means of characterizing the resilient response of granular materials.

#### 2.2.8 Specimen Size

Two geometrical considerations affect static triaxial test results: specimen height to diameter ratio, and specimen diameter to maximum particle size ratio. Bishop and Green (18) concluded the sample height should be at least twice the diameter in order to minimize adverse end effects. Studies by Holtz and Gibbs (19) and by Leslie (20) indicated that to obtain good test results the specimen diameter should be 4 to 20 times the maximum particle size. Proportions of the large size particles greater than 50 percent require the ratio to be closer to 20.

As already pointed out the above recommendations apply to static testing. Apparently there have been no studies extending the results to repeated load testing although it is believed the same recommendations are applicable.

The results of some of the more important resilient testing investigations are included in Table 2.1.

Table 2.1. Summary of Repeated Load Tests of Granular Materials.\*

Reference	Material	Factors Investigated
Haynes and Yoder (2)	Gravel and Crushed Stone	Effects of moisture content and gradation on $E_r$
Hicks and Monismith (3)	Well Graded Crushed Gravel and Crushed Stone	Effects of material type, gradation, density and degree of saturation on $E_r$
Barksdale (4)	Soil-Aggregate Blends	Stress level effects on plastic strain; gradation and moisture effects on $E_r$
Allen (5)	Gravel and Crushed Stone	Effects of cyclic confining pressure, material type, and stress history on $E_r$
Kalcheff and Hicks (9)	Crushed Stone	Gradation; frequency of loading, stress history effects on $E_r$ ; stress history effects on plastic strain behavior
ORE (25)	Ballast	Permanent deformation and $E_r$
Brown and Hyde (30)	Crushed Stone	Effects of cyclic confining pressure on $E_r$ ; effect of stress history on plastic strain behavior

\*Selected References Only.

### 2.3 Factors Affecting the Permanent Deformation Characteristics of Granular Materials

Most of the factors affecting resilient behavior of granular materials discussed in the previous section probably influence the repeated load plastic strain behavior in similar manners although few studies actually have examined the various factors. Some of the results of studies on permanent deformation characteristics of granular materials are included in this section.

Barksdale (4) tested several types of dense graded materials in triaxial apparatus. One of the most important conclusions from Barksdale's study was that for low deviator stresses the rate of plastic strain accumulation decreases as the number of load applications increases, but beyond a critical value of deviator stress the rate of plastic strain accumulation increases with increasing numbers of load applications. Typical results are shown in Figure 2.3. As shown in the figure, the trend for the rate of plastic strain accumulation to increase was established prior to the application of 5000 load cycles. In addition Barksdale showed that blends of 20% soil, 80% aggregate experienced significantly lower plastic strains than 40% soil, 60% aggregate blends. Barksdale also concluded that for a 5 percent reduction in maximum density (T-180) the repeated load plastic strain at various numbers of load applications almost doubled, but for increases in density beyond maximum, little reduction in plastic strain was observed.

An interesting method for predicting permanent axial strain caused by repeated loading was proposed by Barksdale (4). Barksdale modified the hyperbolic stress-strain methods of Kondner (21) and Duncan and Chang (22) and developed the following expression for predicting the permanent

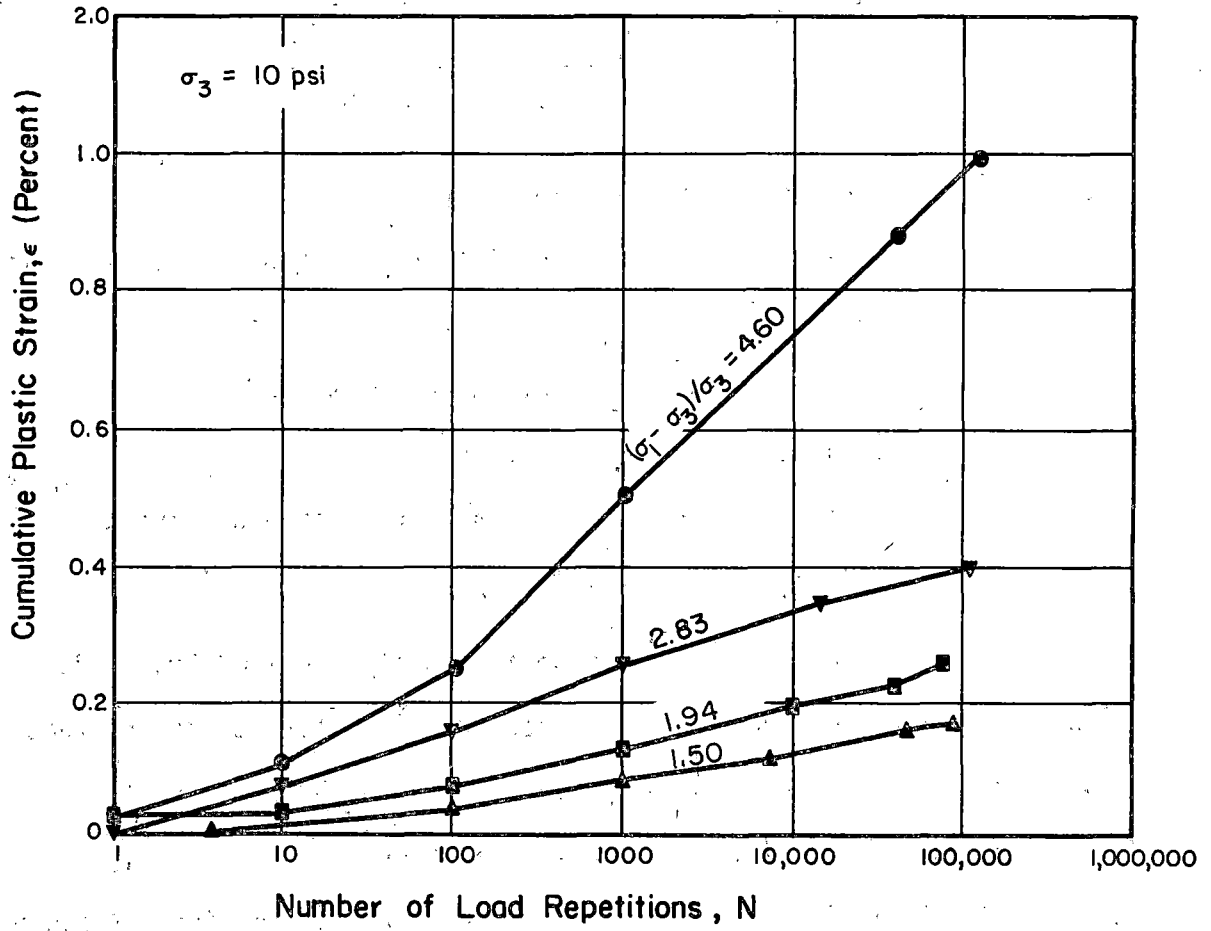


Figure 2.3. Cumulative Plastic Strain as a Function of Stress Level (Reference 4).

strain after 100,000 load cycles for well graded materials:

$$\epsilon_p = \frac{(\sigma_1 - \sigma_3)/E_i}{1 - \frac{(\sigma_1 - \sigma_3)(1 - \sin \phi) R_f}{2(C \cos \phi + \sigma_3 \sin \phi)}} \quad (2.5)$$

where  $\epsilon_p$  = permanent axial strain,

$E_i$  = a relationship defining the initial tangent modulus, psi,

$C$  = cohesion, psi,

$\phi$  = angle of internal friction, degrees, and

$R_f$  = a ratio relating the stress difference at failure to the stress difference which the stress-strain curve approaches at infinite strain.

Allen (5) found that an increase in density from T-99 to T-180 resulted in decreased accumulated repeated load deformations and that crushed material experienced less plastic strain than did gravel.

Haynes and Yoder (2) tested well graded crushed stone and gravel materials and found that repeated load permanent deformations depend on density and on degree of saturation. Low density and high degree of saturation resulted in the highest levels of permanent deformations.

Lau (23) conducted repeated load triaxial tests on sand and found that the permanent strain increased as both the number of load cycles and the ratio of repeated deviator stress to maximum static deviator stress increased. The latter result was more pronounced for high confining pressures than for low confining pressures.

Repeated load triaxial testing of ballast (conforming to the Canadian National Railways gradation) was accomplished by Olowekere (24). It was concluded that a substantial portion of the permanent deformation occurred during the first loading cycle and the deformation occurred at a decreasing rate for subsequent cycles. Olowekere also concluded that permanent strain increased as the applied deviator stress increased and as the confining pressure decreased.

The Office for Research and Experiments, ORE, (25), from repeated load triaxial testing of ballast, arrived at the following predictive equation:

$$\epsilon_p = 0.082 (100n - 38.2) (\sigma_1 - \sigma_3)^2 (1 + 0.2 \log N) \quad (2.6)$$

where  $\epsilon_p$  = permanent axial strain after N cycles,

$n$  = initial porosity,

$\sigma_1 - \sigma_3$  = deviator stress, kgf/cm<sup>2</sup>, and

$N$  = number of repeated loading cycles.

Although Equation 2.6 shows the permanent strain to be proportional to porosity, to number of cycles of loading, and to deviator stress squared, ORE has not included the confining pressure as a factor directly influencing permanent strain. It should be noted that according to Equation 2.6 the first 100 cycles of loading are extremely important. No information on the standard error of estimate for Equation 2.6 was included by ORE.

Snyder (26) used a series of arcs and springs to provide confinement in a unique form of triaxial test. Granular materials were subjected to repeated loading, and the plastic strain was monitored. Snyder concluded

that as the maximum size of the aggregate increased it better resisted permanent deformation and except at very high levels of deviator stress the plastic deformation was linear with respect to the logarithm of the number of load cycles.

Holubec (27) concluded from repeated load triaxial tests performed on dense graded aggregates that the permanent strain depended on both the magnitude of the cyclic deviator stress and the confining pressure and that cohesion was a significant factor in resisting plastic strain. Other conclusions of the study by Holubec were that crushed gravel resisted repeated load deformations better than did crushed stone and that high densities better resisted plastic strain. Holubec concluded that variation in the angle of internal friction was not an important factor in determining the plastic strain behavior of granular materials.

Another important study involving aggregate was done by Wong (28). One dimensional repeated load testing of several types of ballast was accomplished using an oedometer. The conclusion was that the vertical strain increased only slightly with increases in the repeated axial stress. In addition, the vertical deformations did not correlate with the mechanical properties (Los Angeles abrasion, crushing value, flakiness index, specific gravity) of the aggregates. A continuation of the study of Wong was done by Bishop (29). An important conclusion was that the plastic strain due to repeated loading was a function of the type of ballast, although no analysis by type was included.

Two important studies (9, 30) have shown that, unlike resilient strains, plastic strain accumulations are dependent on the stress

application sequence. The total plastic strain was less when the specimen was subjected to gradually increasing stress levels than when the highest stress level was applied first. Typical results are included in Figures 2.4, 2.5, and 2.6.

A recent study by Lade and Duncan (31) offers a reasonable explanation for the stress history effects on permanent deformation behavior. Their theory is that elastic strain is determined primarily by the elastic deformations of individual particles, but plastic strain results from sliding between particles. When a triaxial specimen (constant confining pressure) of a cohesionless material is subjected to an initial load, large plastic deformation is caused by the rearrangement of particles. The plastic deformation is accompanied by smaller elastic deformation. When the specimen is unloaded and reloaded to the previous stress level, theoretically only elastic deformation will be observed. However, in the actual case some additional plastic strain accumulates with each loading cycle. If after several repeated loading cycles the specimen is subjected to a deviator stress greater than that previously experienced, the stress-strain curve will continue in the direction of the original curve. An example of this type of sequence is shown in Figure 2.7.

The effect can also be explained in terms of stress path and stress level. The stress path for a triaxial sample subjected to an increasing axial stress while the confining pressure is held constant is shown as the vertical line in Figure 2.8. Stress level, as defined by Lade and Duncan, refers to "the fraction of the soil strength which is mobilized." The failure line in Figure 2.8 represents the maximum possible stress level

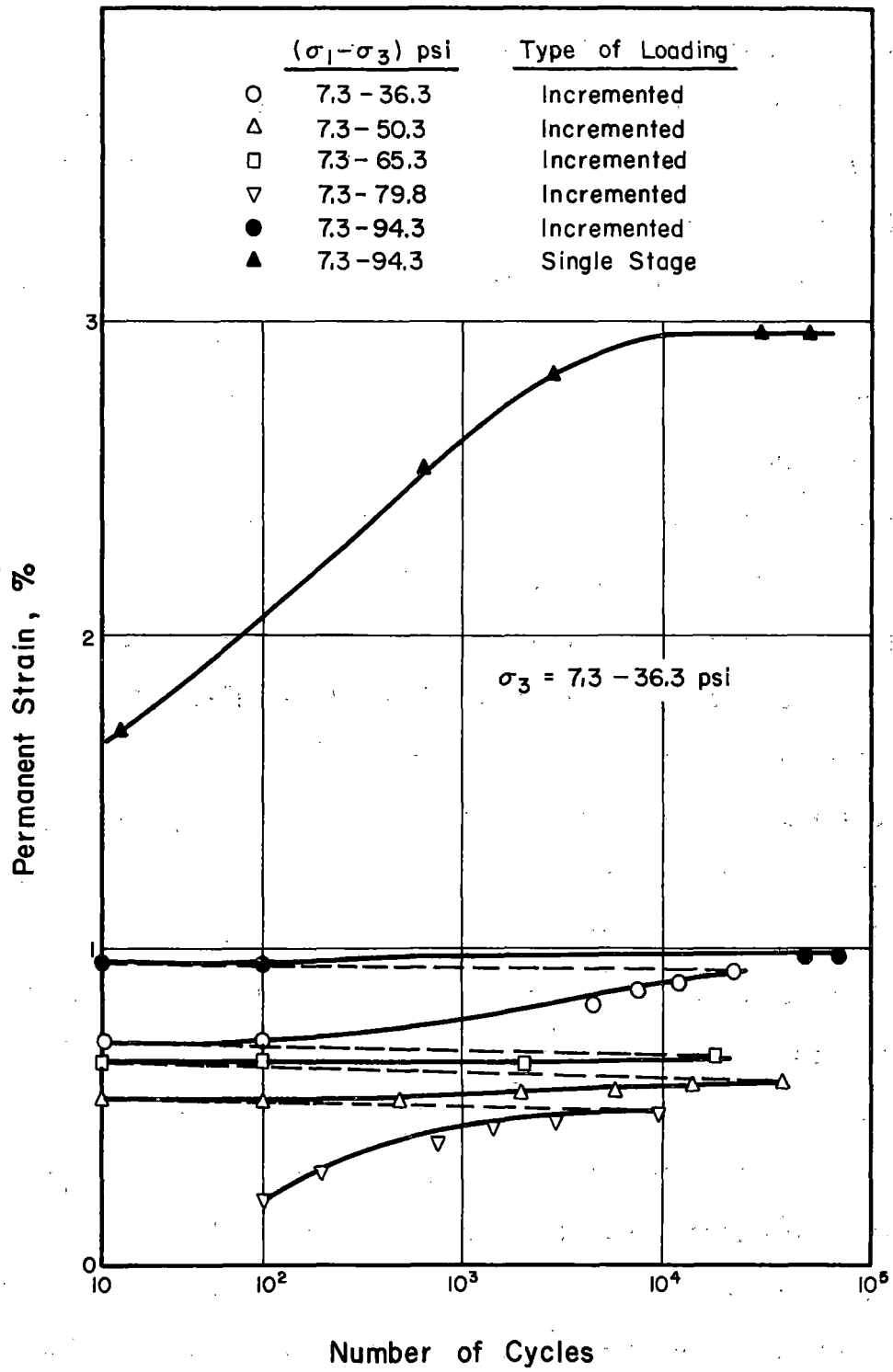


Figure 2.4. Effect of Stress Sequence on Permanent Strain Response. (Reference 30).

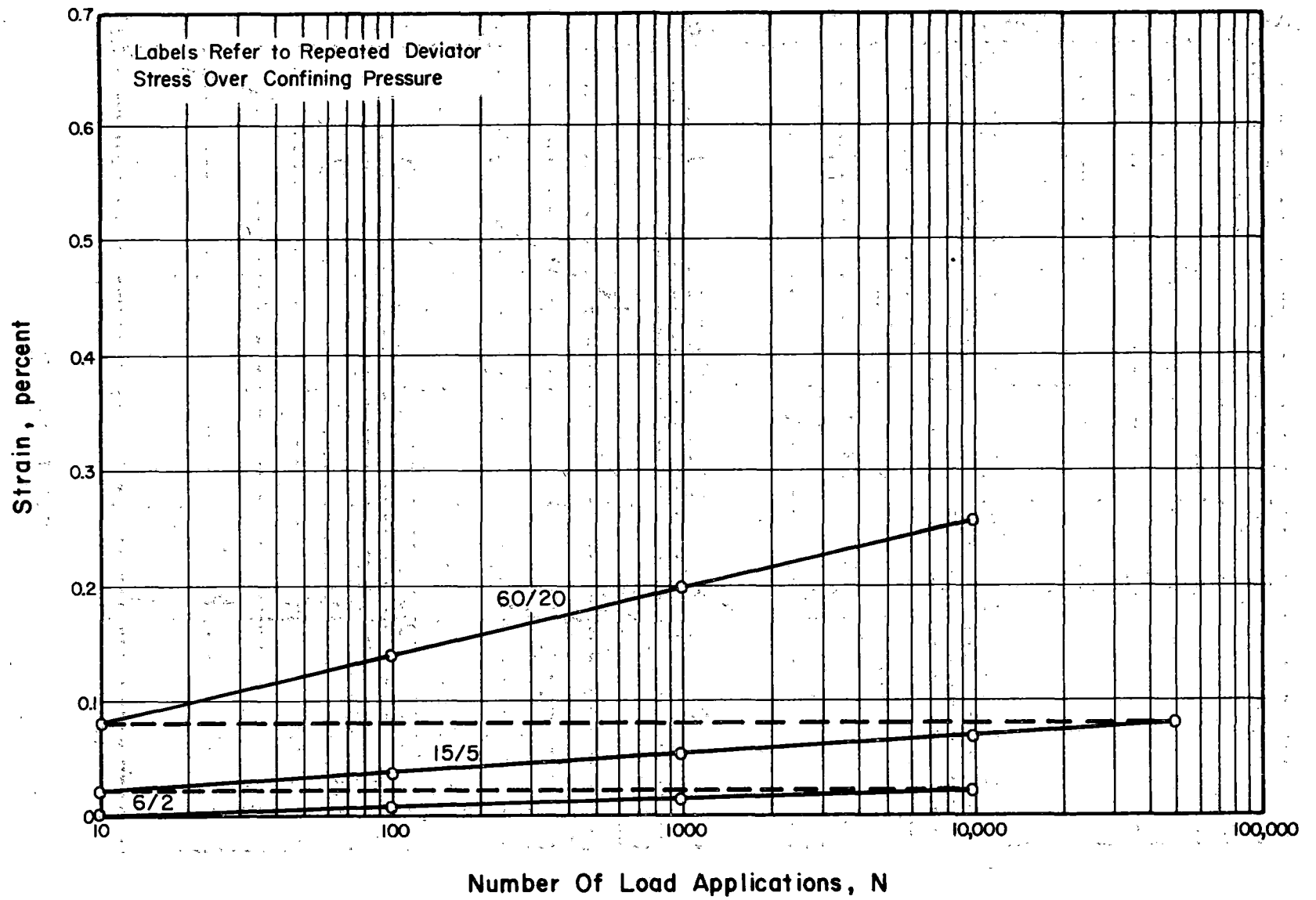


Figure 2.5. Effect of Stress Level on Permanent Strain Response, No. 1 (Reference 9).

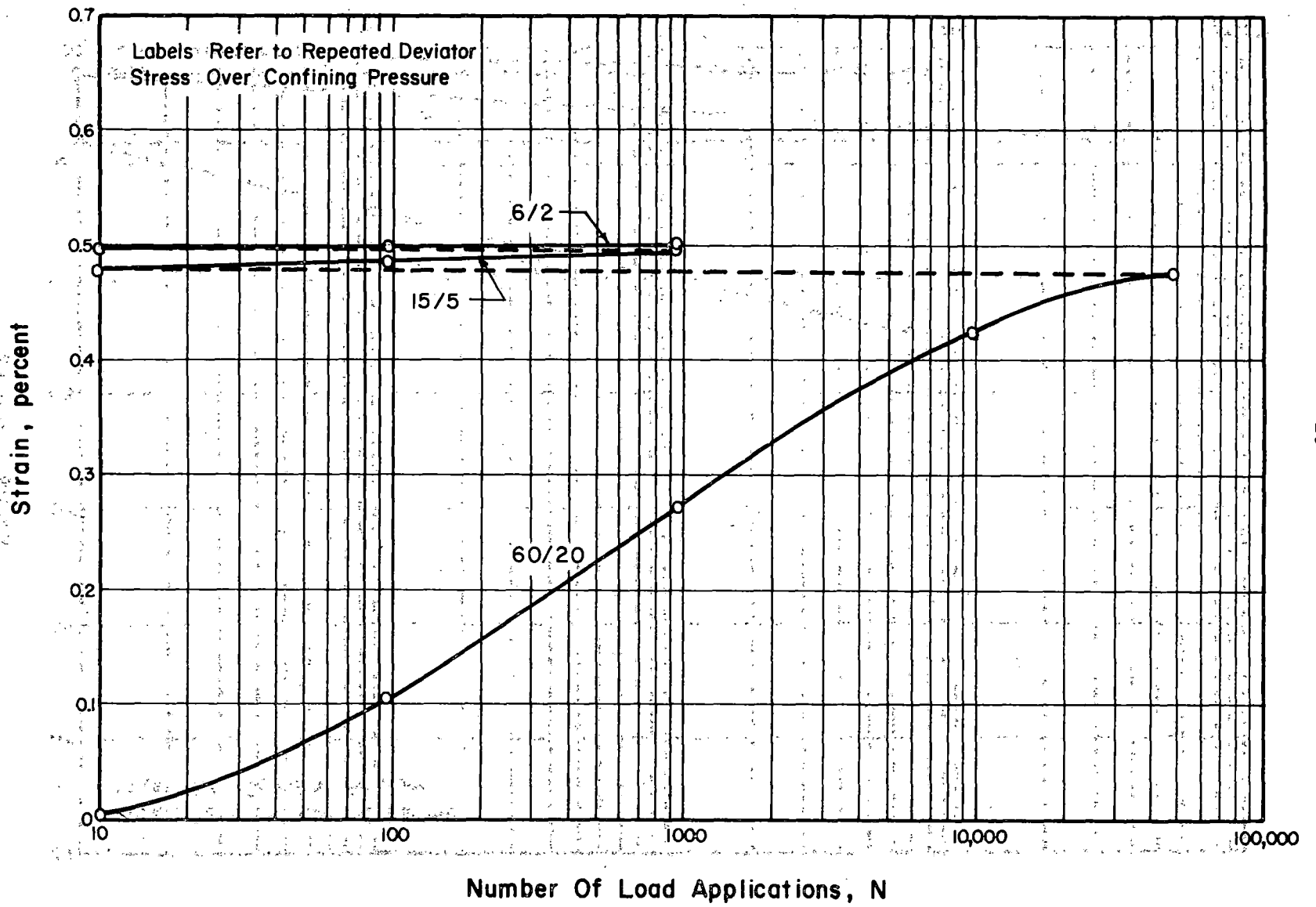


Figure 2.6. Effect of Stress Level on Permanent Strain Response, No. 2 (Reference 9).

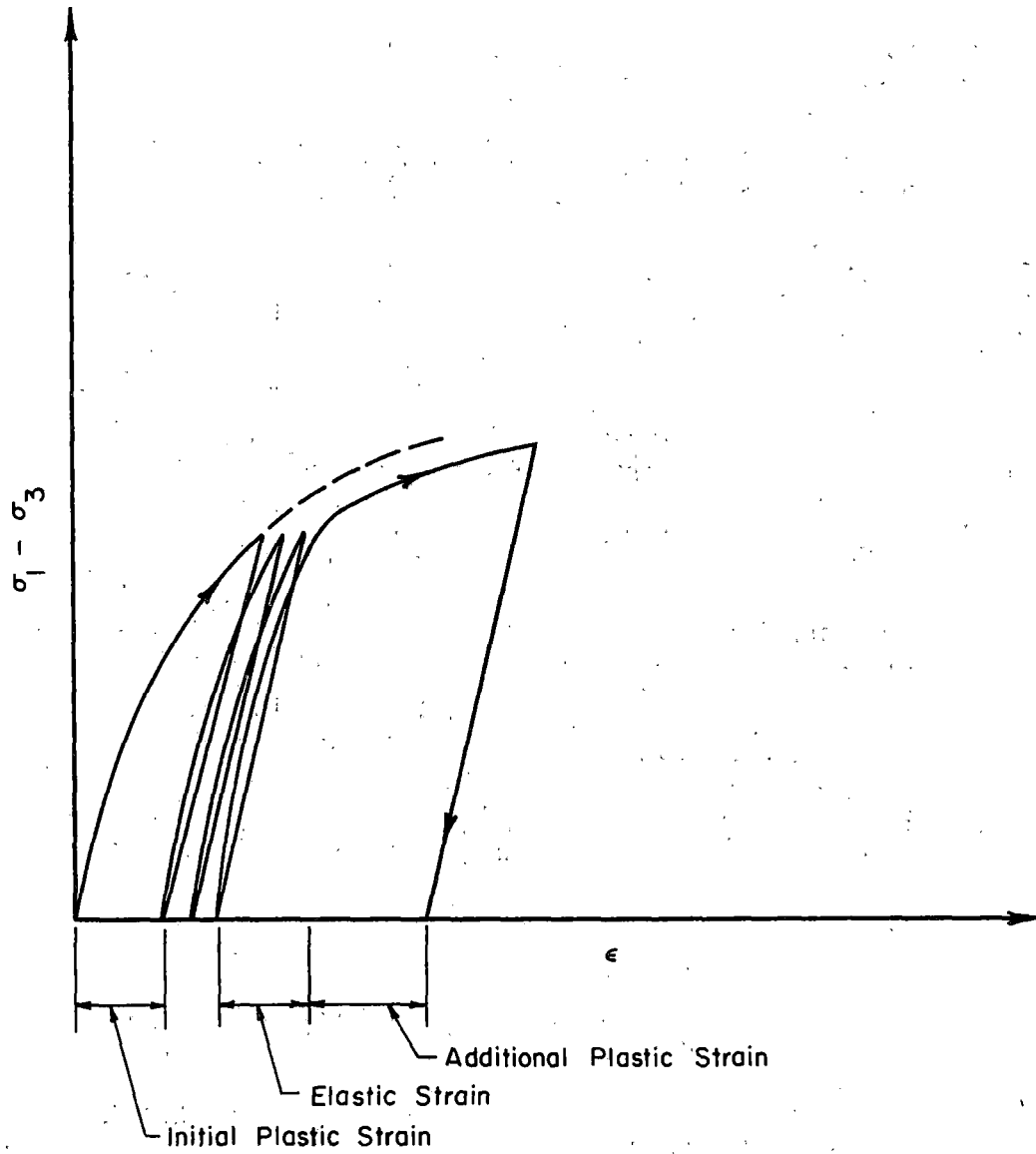


Figure 2.7. Schematic of Repeated Loading Response for Triaxial Compression.

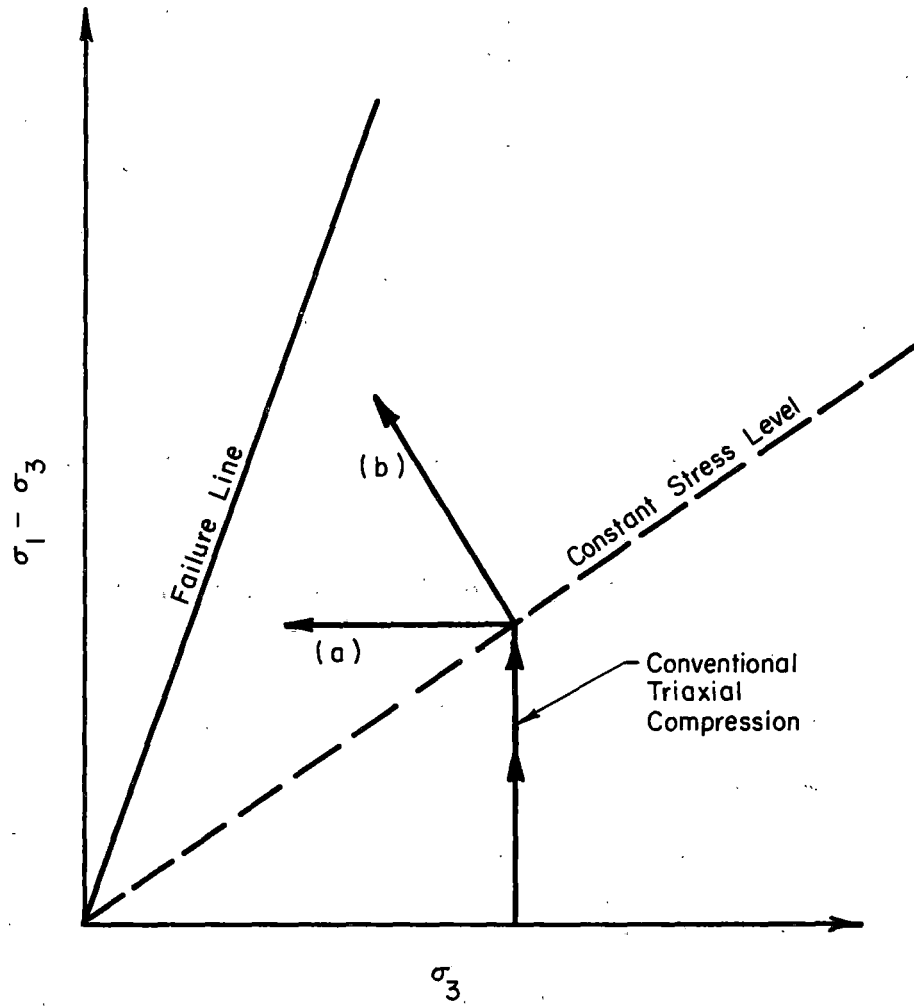


Figure 2.8. Schematic of Possible Stress Paths in Triaxial Compression.

for the material. Primary loading occurs when the stress level is increased beyond the previous maximum. Lines (a) and (b) in Figure 2.8 are stress paths for primary loading compared to that represented by the vertical line. Plastic strain occurs during the primary loading phase. If the specimen is subjected to repeated loading at the original stress level, theoretically only elastic strains will occur. Or stated another way, large additional plastic strain results if the specimen is subjected to a stress level greater than previous stress levels. They concluded that stress changes are of three types: primary loading, unloading, and reloading, and that only primary loading causes large plastic strains. Thus stress history affects repeated load response, specifically the permanent deformation characteristics.

Field evidence of the importance of the maximum loading conditions (or primary loading) on the permanent deformation of ballast has been presented by ORE (32). They concluded that smaller loads cause "negligible settlement" and that "small numbers of large dynamic loads ... determine the deterioration of the track level, rather than the general level of the axle loads."

#### 2.4 Summary

Table 2.1 summarizes some of the important studies of the resilient and plastic behavior of granular materials. The most important variables are generally believed to be the magnitudes of the repeated deviator stress and confining pressure, the number of load applications, and the density. Additional factors such as material type and gradation, stress history,

and the duration and frequency of load application affect the results of repeated load tests, but the effects are not well known. More research is needed to determine the repeated load behavior of ballast and to relate gradation and material type to performance under in service conditions. Chapter 3 describes a laboratory testing program designed to measure elastic and plastic deformations of several types of ballast under various conditions of repeated loading.

## CHAPTER 3

### LABORATORY TESTING PROGRAM

#### 3.1 Ballast

Several types (limestone, granite, slag, etc.) and gradations of materials are used for ballast. The standard gradations recommended by the American Railway Engineering Association (AREA) are shown in Table 3.1; the No. 4 and No. 5 gradations are used more frequently than are the others. Table 3.2 includes typical ballast material types and the amount of each used for the years 1971 and 1972. To gain knowledge of the behavioral effects due to material type, aggregates from several different sources were selected for characterization and for repeated load testing.

##### 3.1.1 Description of Materials

Seven materials commonly used for ballast were chosen so that comparisons of their repeated load behavior and natural properties could be made.

Because limestone is the most commonly used ballast type, preliminary testing was conducted using a dolomitic limestone obtained from a quarry near Kankakee, Illinois. The same limestone was used in the main testing program also.

The other materials obtained were a blast furnace slag from Chicago; granitic gneiss from a quarry near Columbus, Georgia; basalt from New Jersey; crushed and uncrushed gravels from a pit near McHenry, Illinois; and a second type of blast furnace slag from the Kansas Test Track. The original source of the Kansas Test Track slag was Pueblo, Colorado.

Table 3.1. AREA Recommended Ballast Gradations (Reference 33).

Size No.	Nominal Size Square Opening	Amounts Finer Than Each Sieve (Square Opening) Percent by Weight									
		3"	2-1/2"	2"	1-1/2"	1"	3/4"	1/2"	3/8"	No. 4	No. 8
24	2-1/2"-3/4"	100	90-100		25-60		0-10	0-5			
3	2"-1"		100	95-100	35-70	0-15		0-5			
4	1-1/2"-3/4"			100	90-100	20-55	0-15		0-5		
5	1"-3/8"				100	90-100	40-75	15-35	0-15	0-5	
57	1"-No. 4				100	95-100		25-60		0-10	0-5

(1 inch = 2.54 cm)

Table 3.2. Amounts of Ballast Used by Material Type (Reference 79).

Material	Amount, Short tons	
	1971	1972
Limestone and Dolomite	6,153,000	7,250,000
Granite	5,388,000	6,162,000
Slag (air cooled blast furnace)	3,174,000	3,686,000
Gravel	2,347,000	2,229,000
Other Stone	1,538,000	N.A.
Trap Rock	989,000	2,332,000
Steel Slag	855,000	1,327,000
Sandstone and Quartzite	610,000	1,014,000

N. A. = Data Not Available

With the exception of the Kansas Test Track slag, the materials were sieved and each size of material was stored in a separate container for recombining into the desired gradations. The various ballast gradations of the samples tested are shown in Figure 3.1.

### 3.1.2 Characterization Tests

In order to relate the results of the repeated load tests to the physical properties of the materials, standard tests were performed. The standard tests and references are included in Table 3.3. In addition, an amplified discussion of the various test procedures is included in Reference 39.

The results of the tests are summarized in Table 3.4.

### 3.1.3 Static Triaxial Tests

To enable comparisons with the hyperbolic stress strain law (4, 21, 22) static triaxial tests were performed on medium density, No. 4 ballast gradation specimens of limestone, granitic gneiss, Chicago slag, basalt, gravel, and crushed gravel. Only two levels of confining pressure, 5 and 15 psi (34 and 103 kN/m<sup>2</sup>), were used. The results are presented in Table 3.5. The values for  $\phi$  shown are taken from the tangents to the respective failure circles on the Mohr-Coulomb failure envelope.

## 3.2 Testing Program

Since the purpose of the research was to study the behavior of ballast materials under simulated loading conditions, the repeated load triaxial test was selected as the primary method.

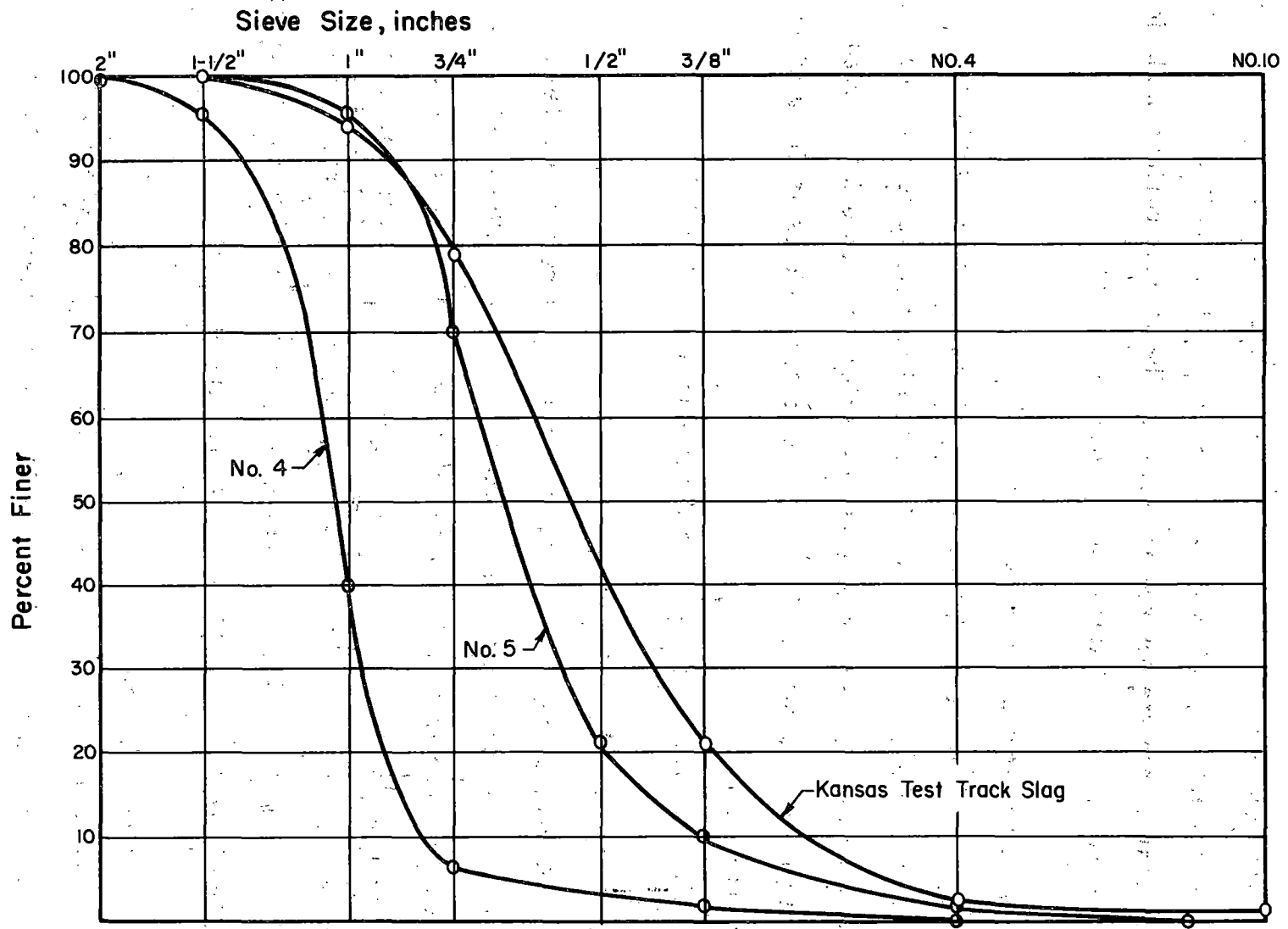


Figure 3.1. Ballast Gradations Tested.

Table 3.3. Standard Characterization Test References.

Test	Designation		
	ASTM <sup>(a)</sup>	AASHTO <sup>(b)</sup>	British Standard <sup>(c)</sup>
Particle Index	Tentative <sup>(d)</sup>		
Specific Gravity	C 127	T 85	
Los Angeles Abrasion	C 131	T 96	
Gradation Parameter <sup>(e)</sup>			
Flakiness Index			812-15
Soundness	C 88	T 104	
Crushing Value			812-34

(a) Reference 35

(b) Reference 36

(c) Reference 37

(d) Reference 38

(e) Reference 14

Table 3.4. Characterization Test Results.

Material	Gradation	Particle Index	Specific Gravity	Los Angeles Abrasion Loss, %	Gradation Parameter	Flakiness Index	Soundness Loss, %	Crushing Value
Limestone			2.626	34.2				22.7
	No. 5	13.80			1.846	17.52	12.3	
	No. 4	13.75			1.074	16.78	18.5	
	Well graded	14.09			2.039	17.33	15.3	
	n=1/2	14.07			2.295	17.04	14.5	
	n=1/2	14.07			2.178	17.04	14.5	
CA-10	13.90			4.959	13.00	14.5		
Granitic Gneiss			2.679	34.7				26.1
	No. 5	13.61			1.846	15.60	0.23	
	No. 4	13.45			1.074	14.39	0.25	
Well graded	13.68			2.039	15.71	0.26		
Chicago Blast Furnace Slag			2.133	37.8				37.3
	No. 4	15.68			1.074	3.59	0.75	
Well graded	16.63			2.039	3.76	0.87		
Basalt			2.775	12.3				12.4
	No. 5	15.10			1.846	19.69	6.14	
	No. 4	15.40			1.074	17.33	4.93	
Well graded	14.83			2.039	16.11	4.86		
Crushed Gravel			2.678	28.0				20.0
	No. 4	11.85			1.074	10.12	7.45	
Gravel			2.658	23.2				13.8
	No. 5	7.54			1.846	4.03	5.06	
	No. 4	10.17			1.074	5.79	5.78	
	Well graded	8.86			2.039	6.58	5.84	
Kansas Test Track Blast Furnace Slag			2.521	26.7				25.2
	No. 5	14.10			1.846	5.39	0.87	

Table 3.5. Static Triaxial Test Results.

<u>Material Type</u>	<u>Gradation</u>	<u>Density (pcf)</u>	<u>Confining Pressure (psi)</u>	<u>Maximum Deviator Stress (psi)</u>	<u>φ (degrees)</u>
Limestone	No. 4	97	5	32.9	45
		97	15	73.4	28
Granitic Gneiss	No. 4	97	5	42.3	46
		97	15	63.1	15
Chicago Blast Furnace Slag	No. 4	70	5	31.7	47
		70	15	59.5	18
Basalt	No. 4	95	5	36.6	46
		97	15	81.0	35
Crushed Gravel	No. 4	102	5	27.0	42
		102	15	68.9	32
Gravel	No. 4	105	5	26.9	44
		105	15	78.6	44

Note: 1 psi = 6.894 kN/m<sup>2</sup>

### 3.2.1 Testing Equipment

A U.S. Army Engineer Waterways Experiment Station triaxial cell design was modified, and the cell was fabricated at the University of Illinois. Because of the large maximum size of the aggregate to be tested, the cell was constructed with an inside diameter of 11 inches (279 mm) to provide the capability for testing 8 inch (203 mm) diameter cylindrical specimens 16 inches (406 mm) high. A schematic diagram of the triaxial cell is shown in Figure 3.2, and an overall view of the equipment is shown in Figure 3.3.

The confining pressure was supplied by means of air pressure and was not cycled during the tests. The repeated deviator stress was applied by a hydraulically actuated piston; control was by means of a closed loop electronic system. Input for the load control was provided by a function generator connected through electronic controls to the hydraulic actuator.

Several investigators (3, 5, 7) have experimented with changes in the duration of the repeated load and have found no significant dependence of the resilient behavior on the duration of load, especially if the duration is on the order of 0.10 to 0.15 seconds. Unfortunately the effects of duration of load on the permanent deformation behavior of granular materials is not known.

The effect on resilient behavior of the frequency of applied load was studied by Seed, et al. (7). So long as the frequency was in the range of those expected in service the effect on the resilient response was slight. From repeated load triaxial tests of ballast ORE (32) concluded that there was little influence on permanent deformation results for frequencies in the range of 0.1 to 30 hertz.

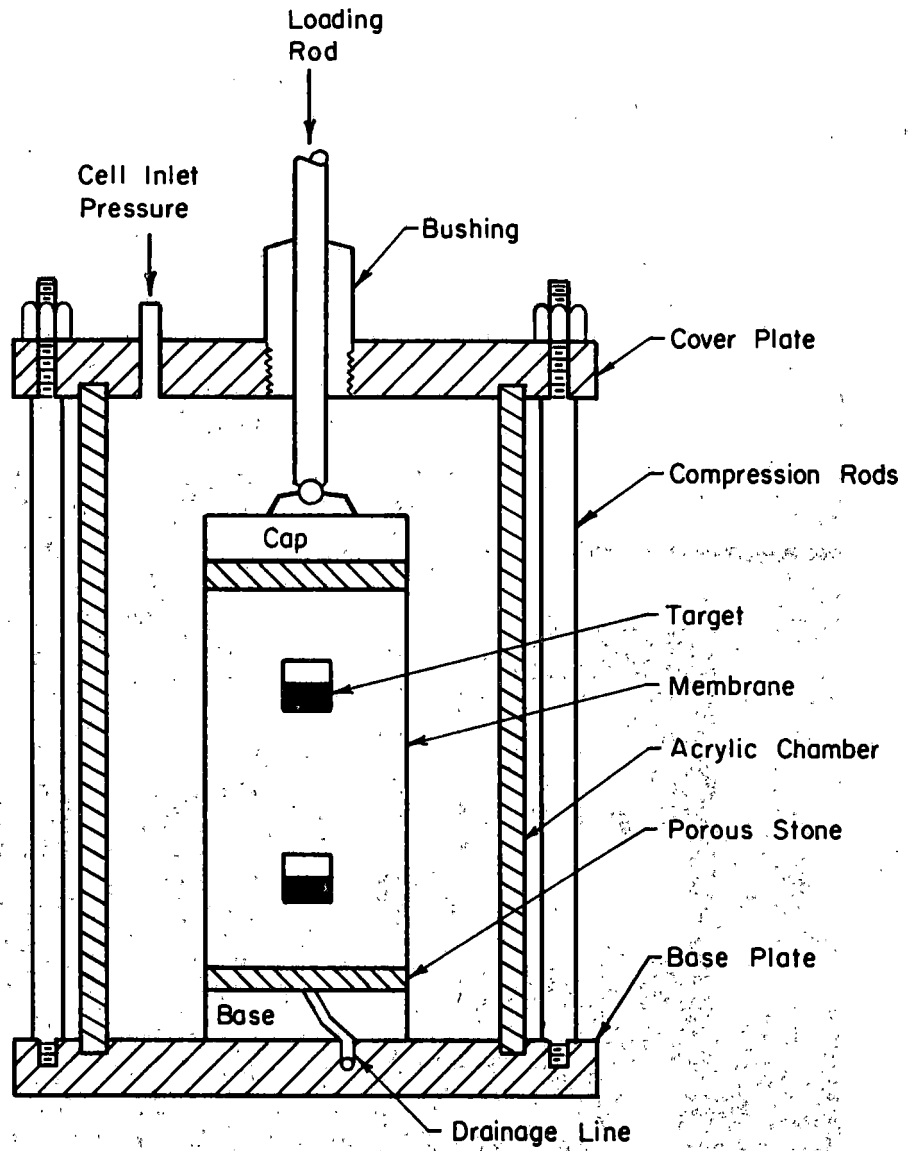
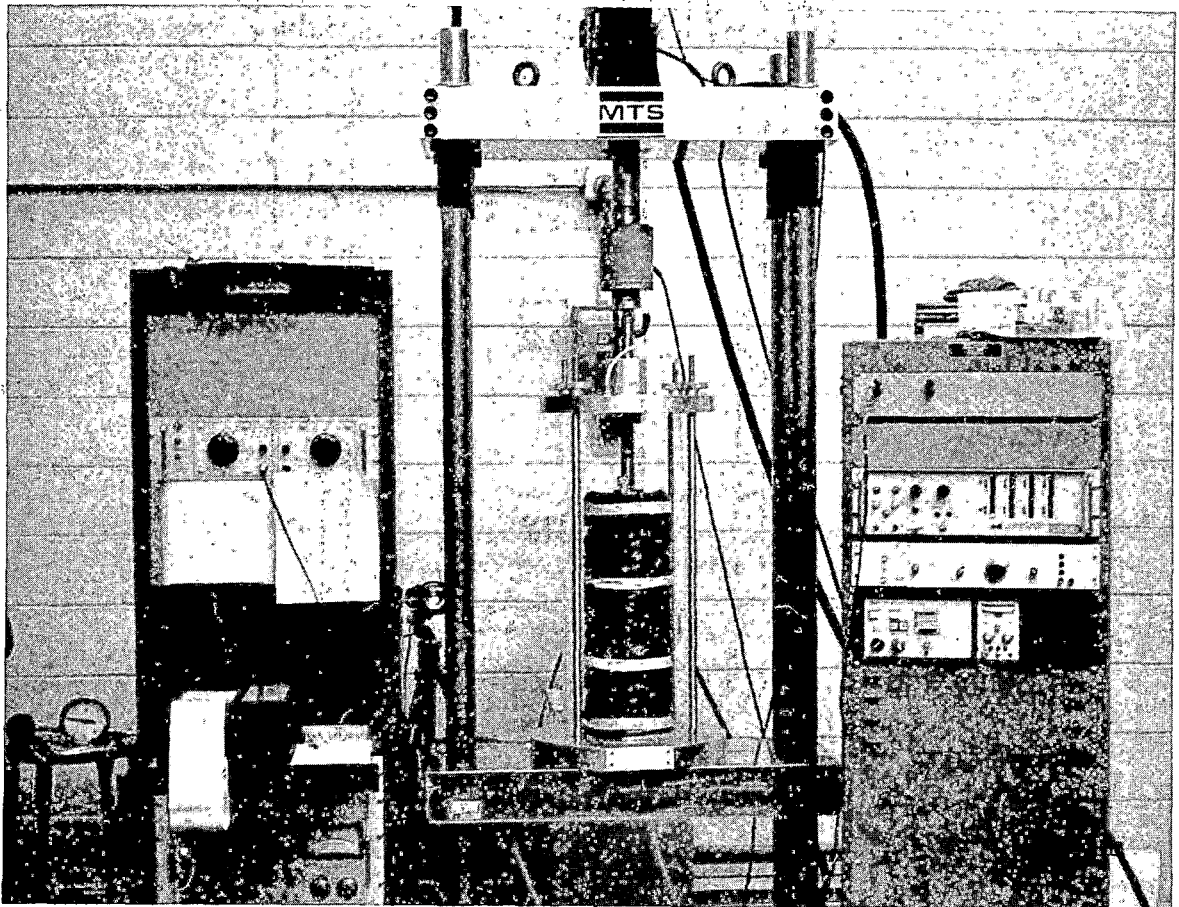


Figure 3.2. Schematic of Triaxial Cell.



- 1) Strip Chart Recorders
- 2) Test Specimen
- 3) Control Console
- 4) Load Cell

Figure 3.3. Overall View of Testing Equipment.

To satisfy the constraints of the equipment and to approximate the in service conditions a frequency of 50 applications per minute and a haversine load pulse of 0.15 seconds duration were selected.

The spacing of trucks on rolling stock varies, and the pulse caused by the second truck on one car overlaps that of the first truck on the following car. These two factors cause problems in analyzing the in service frequency and duration of loading of ballast. The frequency (50 cycles per minute) and duration of load (0.15 seconds) selected are equivalent to a train speed on the order of 80 mph.

### 3.2.2 Instrumentation

The triaxial chamber pressure was monitored by a gauge on the air supply line located immediately adjacent to the pressure regulator. The axial load was monitored by means of a load cell mounted between the hydraulic actuator and the loading rod. A two channel high speed strip chart recorder was used to observe the output of the load cell.

Two methods were used to observe the axial deformations. The primary method for measuring the resilient deformation was by two electronic-optical scanners. The collimators measured the vertical motion of black and white targets placed at the upper and lower quarter points of the specimen. Each target consisted of one black and one white rectangular strip, 1 1/4 by 2 1/2 inches (32 by 64 mm) each, which were held to the specimen membrane by doubled sided tape. The chamber pressure insured the membrane was molded firmly to the specimen thereby eliminating slippage between specimen and targets. The movements of the targets were sensed by the optical heads and converted into an electrical signal; the difference in

movements was recorded as output on the strip recorder.

The primary method for measuring the permanent deformations was by a linear variable differential transformer (LVDT) mounted at the top of the hydraulic actuator. The LVDT signal was recorded simultaneously with the collimator signal so that the permanent as well as the resilient deformations were observed.

The LVDT measured deformations over the entire specimen length, and was used as a backup to and for comparison with the optical method of obtaining resilient deformations.

The optical heads were mounted independently on a geared stand and a dial indicator was used to measure the relative distance the heads were rezeroed; a backup means of measuring the permanent deformations was thereby provided.

### 3.2.3 Specimen Preparation

Because one of the objectives of this study was to determine the effects of gradation and maximum size on ballast behavior two different sample sizes were used. Samples 6 inches (152 mm) in diameter were used for the No. 5 ballast gradation which has a maximum particle size of 1 1/2 inches (38 mm). The No. 4 ballast gradation has a maximum particle size of 2 inches (51 mm), and therefore larger samples 8 inches (203 mm) in diameter were used. Thus a diameter to maximum particle size ratio of 4 was maintained.

All of the prepared samples had a height to diameter ratio of 2:1 or more to minimize the end effects on deformation measurements as reported by Bishop and Green (18) and Duncan and Dunlop (40).

To minimize segregation and to insure gradation control each specimen was weighed out by thirds for each of the size fractions and each third was placed in a separate container. With the exception of the CA-10 specimens, the aggregate was washed to remove the fines, drained, and compacted immediately.

The specimens were prepared in a split mold clamped to the sample base as shown in Figure 3.4. A rubber membrane was used inside the mold, and a vacuum was applied through the attached tubing to hold the membrane against the mold.

Because of the open graded nature of ballast, vibratory compaction was selected. Compaction was accomplished by a method similar to that described by Rostron, et al. (41) which used a vibratory hammer and a compaction foot slightly smaller in diameter than that of the mold. The compaction equipment is shown in Figure 3.5.

To determine the compaction characteristics of the aggregate and for a check on degradation during compaction, limestone of No. 5 ballast gradation was compacted in the standard split mold for various times using the vibratory compactor. The results showed that little increase in density was attained for compaction times greater than 45 seconds and that gradation change for the limestone due to compaction was extremely small. For example, the amount of material passing the No. 4 sieve increased from 2.5 percent to 4.0 percent after compaction for 45 seconds per layer. The increase was less (less than 1 percent) for the shorter compaction times.

Because densities are generally not specified when ballast is placed, no attempt was made to attain specific densities. Instead three degrees

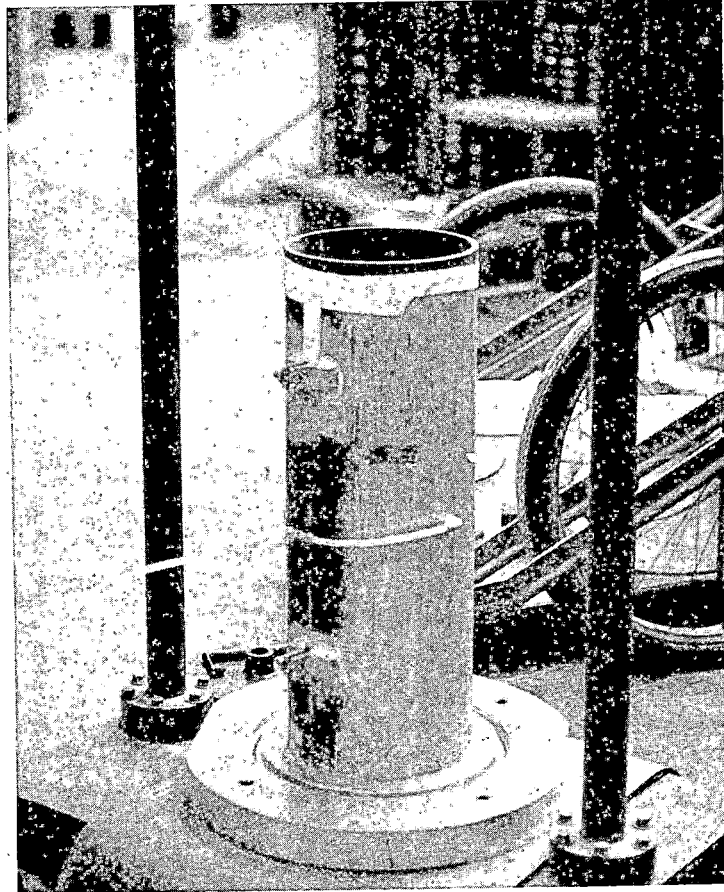


Figure 3.4. Compaction Mold.

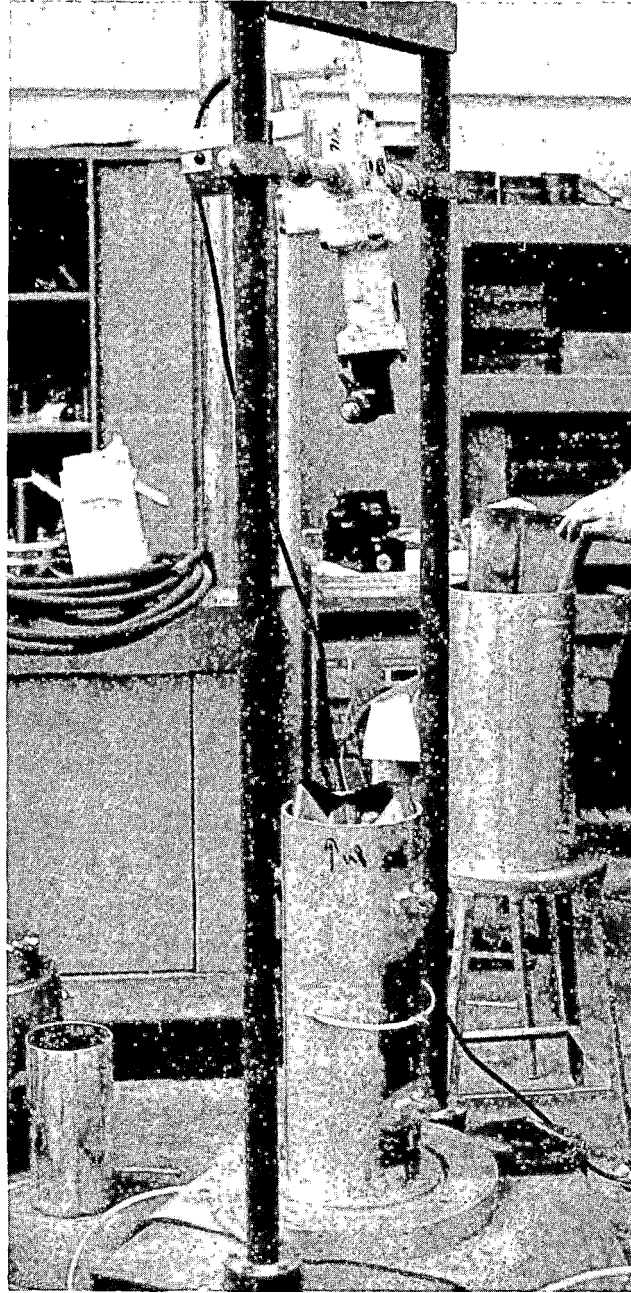


Figure 3.5. Compaction Equipment.

of compaction were selected. For low density specimens, each layer of aggregate was placed and rodded 10 times. For medium density specimens each layer was compacted for 5 seconds with the vibratory hammer, and for the high density specimens each of the three layers was vibrated for 45 seconds.

After compaction the height of the specimen was recorded, the mold was removed, and a second membrane was placed over the specimen because almost without exception the original membrane was punctured during compaction. A typical completed sample is shown in Figure 3.6.

In addition to the No. 4 and No. 5 ballast gradations tested, two other gradations were used. For comparison with the open graded materials, two CA-10 (a standard Illinois Department of Transportation gradation) limestone specimens were tested. The CA-10 gradation used is shown in Figure 3.7. The specimens were compacted at 6 percent moisture content, or slightly dry of the optimum as determined by AASHTO T-99. Two levels of compaction, 5 seconds per layer and 45 seconds per layer, were used for the CA-10 specimens of medium and high density, respectively.

The grain size distribution for a dense graded material can be determined through use of the Talbot equation:

$$p = 100 \left( \frac{d}{D} \right)^n \quad (3.1)$$

where  $d$  is the sieve size in question,  $p$  is the percent of material finer than the sieve,  $D$  is the maximum size of the aggregate, and  $n$  is an exponent, usually between  $1/3$  and  $1/2$ .

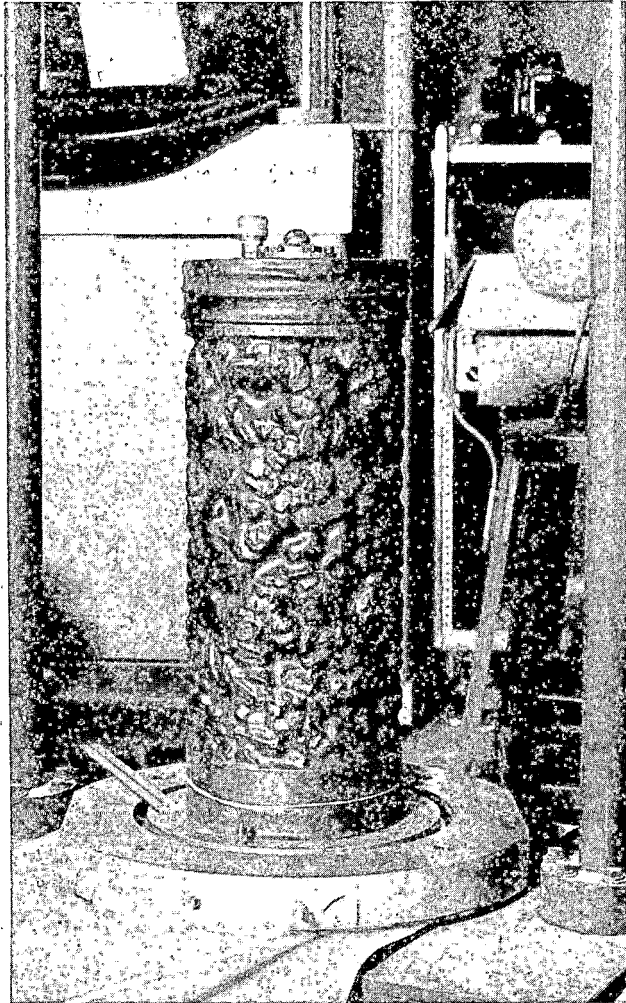


Figure 3.6. Typical Completed Specimen.

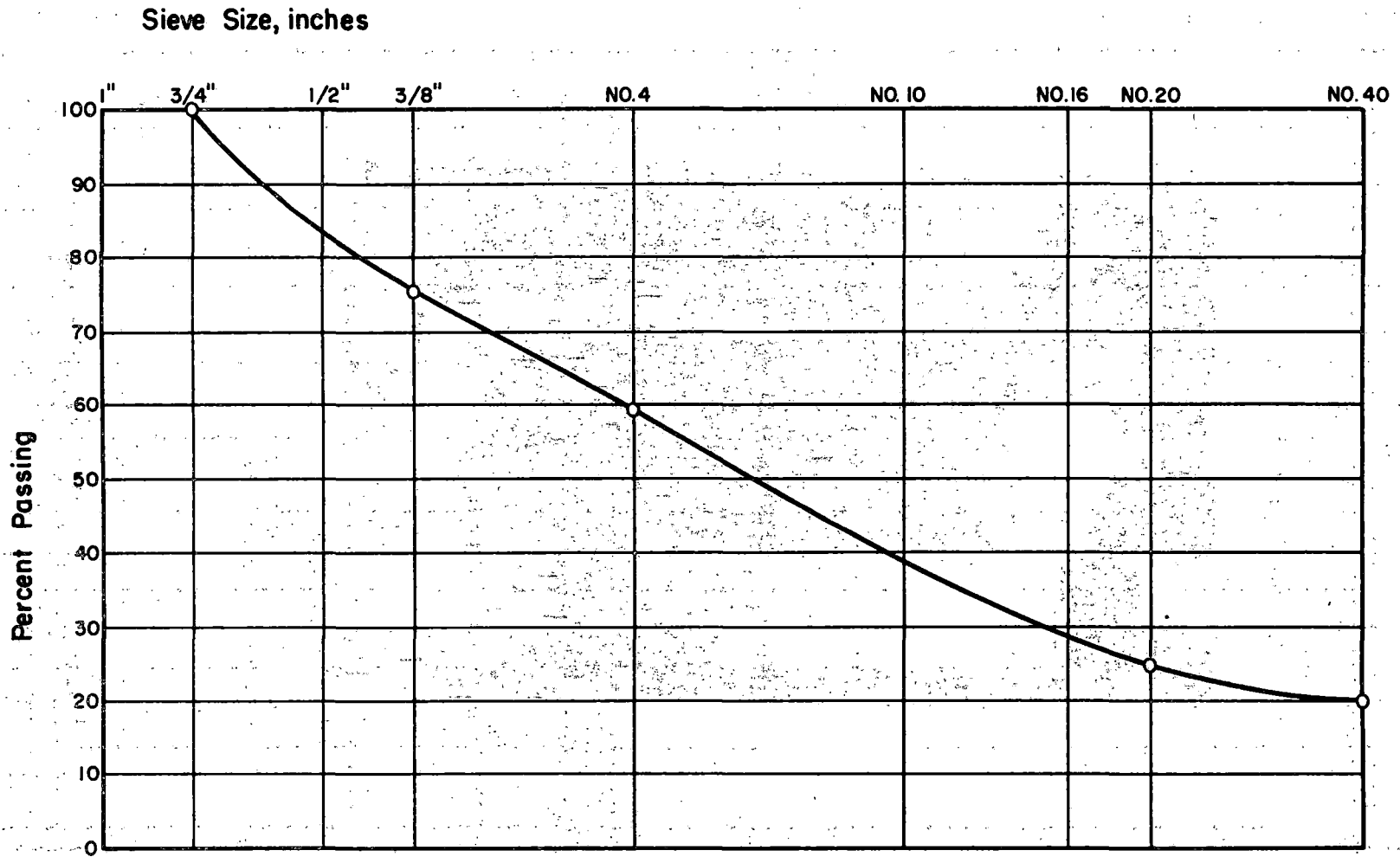


Figure 3.7. Gradation of CA-10.

Usually maximum density for an aggregate will occur if the exponent,  $n$ , is  $1/2$ . To evaluate the effects of a slight change in gradation from current ballast specifications, the Talbot equation with an exponent equal to  $2/3$  was used. The gradation results from the Talbot equation were maintained only through No. 4 sieve. To ensure a high permeability rate no material finer than the No. 16 sieve was used. The gradation selected and the permeabilities of some other coarse materials are shown in Figure 3.8. A conservative estimate of the permeability of the "well graded" material is 5000 feet (1500 m) per day. Two other specimens with gradations obtained using an exponent of  $1/2$  for the Talbot equation were also tested. The smallest material in these two specimens was coarser than the No. 10 sieve; the gradations are shown in Figure 3.9. All of the well graded specimens were compacted for 5 seconds for each of the three layers. A summary of the primary test specimens and their material types, gradations, densities, and void ratios is included in Table 3.6.

#### 3.2.4 Testing Sequence

From finite element analysis of CRTSS (6) values were obtained for the stresses at various points in the ballast. The reference section parameters are described in Table 3.7. Representative values of deviator stress of 45 psi ( $310 \text{ kN/m}^2$ ) and confining pressure of 15 psi ( $103 \text{ kN/m}^2$ ) (or a stress ratio hereafter shown simply as 45/15) were selected, and preliminary tests were conducted using two medium density No. 5 ballast gradation specimens. The densities of the samples were 104 and 103 pcf ( $1670$  and  $1650 \text{ kg/m}^3$ ), respectively. To check on stress history effects on permanent strain behavior of open graded materials the first sample

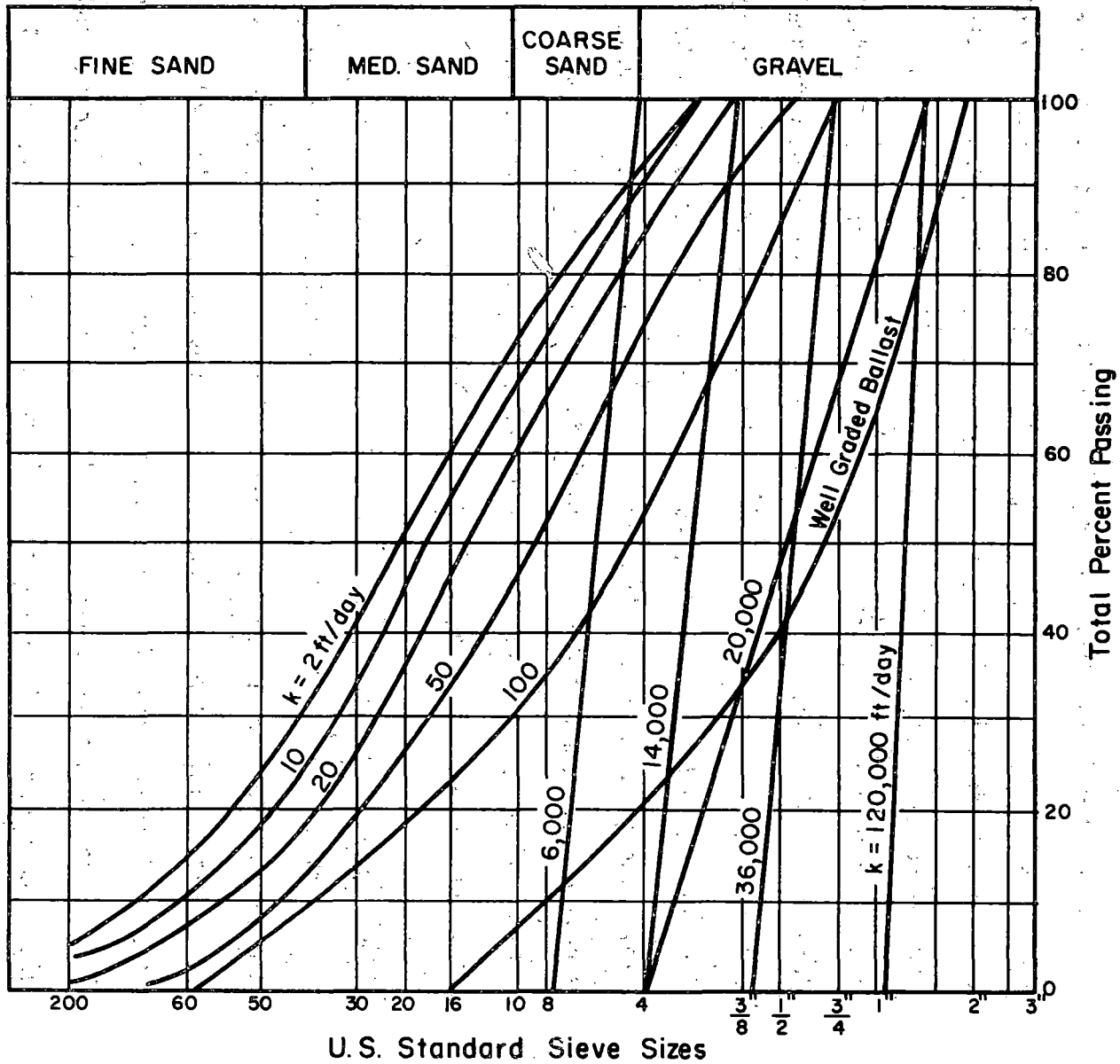


Figure 3.8. Typical Gradations and Permeabilities (Reference 43).

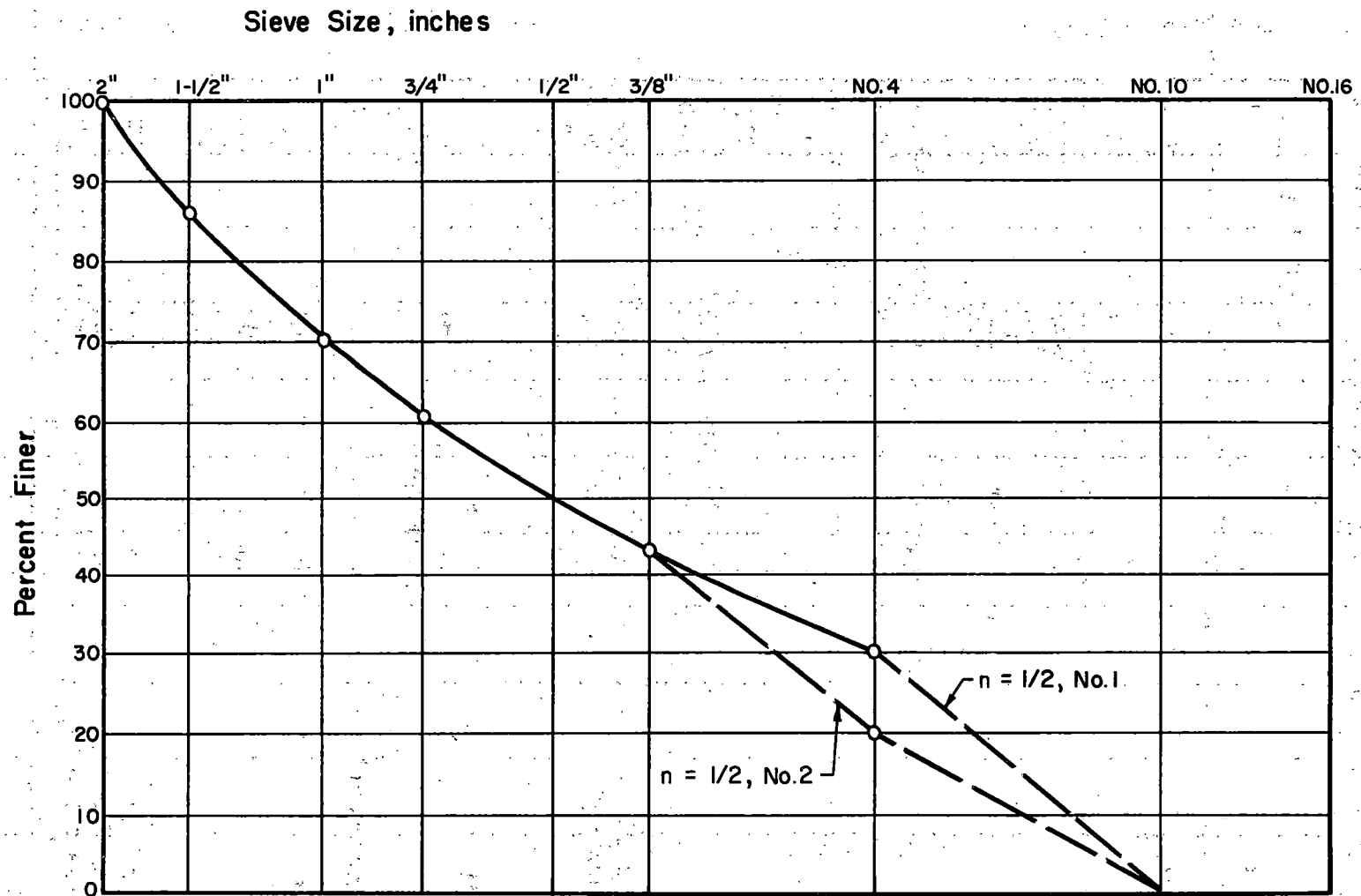


Figure 3.9. Gradations of Two "Well Graded" Specimens.

Table 3.6. Summary of Primary Test Specimen Properties.

Material Type	Gradation	Compaction		Void Ratio
		Level*	Density (pcf)	
Limestone	No. 5	Low	90.3	0.81
	No. 5	Med	103.2	0.59
	No. 5	High	106.8	0.55
	No. 4	Low	88.9	0.84
	No. 4	Med	95.9	0.71
	No. 4	High	99.0	0.66
	well graded	Med	111.9	0.46
	n = 1/2	Med	112.1	0.46
	n = 1/2	Med	112.1	0.46
	CA-10	Med	123.8	0.32
CA-10	High	130.6	0.25	
Granitic Gneiss	No. 5	Low	89.3	0.87
	No. 4	Low	93.0	0.76
	No. 4	Med	97.5	0.71
	No. 4	High	102.3	0.63
	well graded	Med	114.6	0.46
Chicago Blast Furnace Slag	No. 4	Low	66.7	1.00
	No. 4	Med	71.0	0.87
	No. 4	High	73.2	0.82
	well graded	Med	86.3	0.54
Basalt	No. 5	Med	107.5	0.63
	No. 4	Med	95.3	0.82
	well graded	Med	115.7	0.50
Crushed Gravel	No. 4	Med	100.8	0.66
Gravel	No. 5	Med	126.7	0.31
	No. 4	Low	102.4	0.62
	No. 4	Med	107.5	0.54
	No. 4	High	112.1	0.48
	well graded	Med	131.7	0.26
Kansas Test Track Blast Furnace Slag	No. 5	Low	90.8	0.73
	No. 5	Med	98.9	0.59
	No. 5	High	100.9	0.56

\* Low - rodded 10 blows per layer  
 Med - 5 seconds per layer vibration  
 High - 45 seconds per layer vibration

Table 3.7. Reference Section Parameters (Reference 6).

Rail - 136 lb/yd (68 kg/m) rail

$I = 94.00 \text{ in}^4 (3954 \text{ cm}^4)$

$E = 30,000 \text{ ksi} (207,000 \text{ MN/m}^2)$

Ties - Timber ties

Width = 8 in. (20.3 cm)

Thickness = 7 in. (17.8 cm)

Length = 8 ft (2.44 m)

Tie Spacing = 20 in. (50.8 cm)

Compressive Modulus = 1,250 ksi (8618 MN/m<sup>2</sup>)

Effective bearing length under each rail = 18 in. (45.7 cm)

Ballast - Crushed stone ballast, AREA No. 4 Gradation

$\mu = 0.35$

Ballast Depth = 12 in. (30.5 cm)

Subballast - none

Subgrade (Embankment Material) - Depth = 275.0 in. (6.99 m)

$\mu = 0.47$

was tested using gradually increasing stress levels. The permanent strain results are shown in Figure 3.10. A second sample was tested at 45 psi ( $310 \text{ kN/m}^2$ ) repeated deviator stress and 15 psi ( $103 \text{ kN/m}^2$ ) confining pressure. The results are shown in Figure 3.11. The total permanent strain realized during the gradually increasing stress level sequence was less than that obtained when the specimen was first subjected to a high stress level. The results are similar to those of Kalcheff and Hicks (9) and of Brown and Hyde (30), although their results were obtained using dense graded crushed stone.

Although it was recognized that stress history affects the permanent strain results it was decided that valuable information could be obtained by subjecting each specimen to a standard conditioning phase (5000 load applications at 45 psi ( $310 \text{ kN/m}^2$ ) repeated deviator stress and 15 psi ( $103 \text{ kN/m}^2$ ) confining pressure). During the conditioning phase readings of the accumulated permanent deformation were taken at 10, 100, 1000, and 5000 load applications. Following the conditioning phase, the second phase of the testing program was started. After the specimens were tested for resilient modulus at 7 different stress levels, the plastic strain portion of the testing sequence was begun. To observe any change in the resilient behavior a second resilient modulus test was conducted after the 5000 load applications of the 60/15 stress ratio, although two of the samples failed before the second resilient modulus test could be conducted.

Based on data presented by Barksdale (4) 5000 was selected as the number of cycles to be run at each stress level because most of the curves of permanent strain versus logarithm of the number of cycles had either

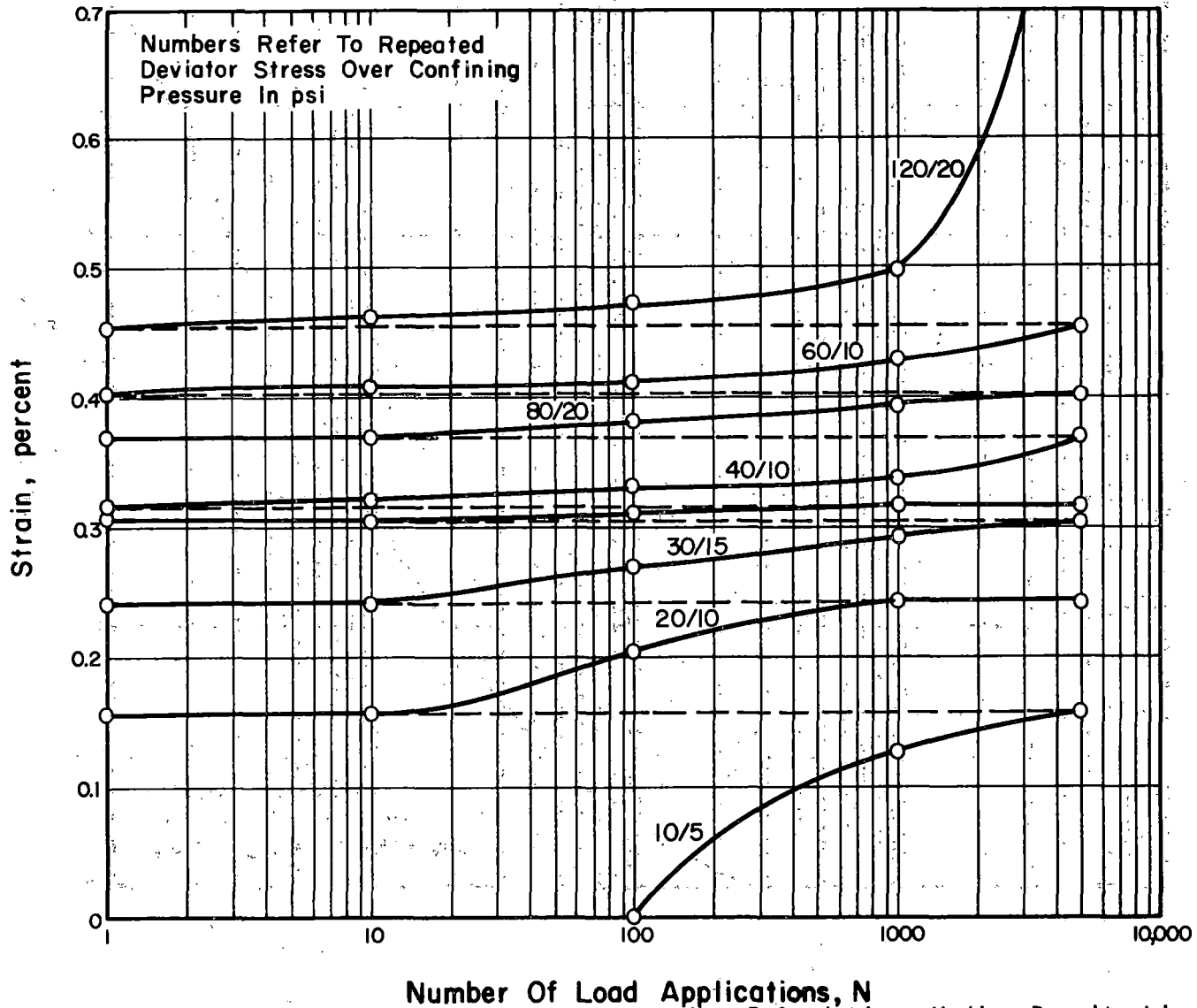


Figure 3.10. Cumulative Plastic Strain Results for a No. 5 Gradation, Medium Density Limestone Specimen.

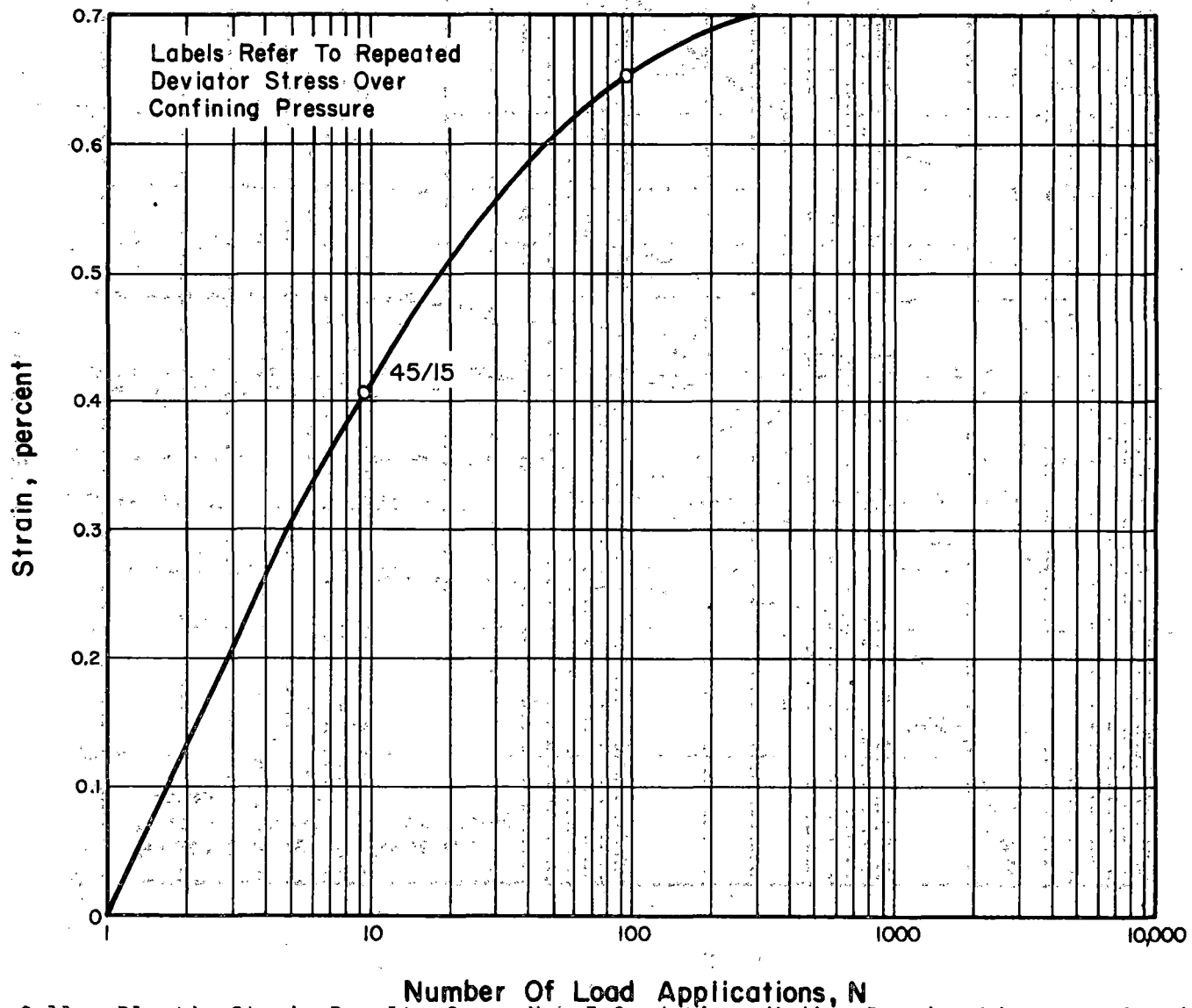


Figure 3.11. Plastic Strain Results for a No. 5 Gradation, Medium Density Limestone Specimen.

leveled off or had started to increase dramatically by the time 5000 loads had been applied.

The complete testing sequence is presented in Table 3.8.

Table 3.8. Standard Test Sequence.

Phase	$\sigma_3$ psi	$\sigma_D$ psi	$\sigma_D/\sigma_3$ psi	Number of Repetitions (1)	Readings (2)
I. Conditioning	15	45	3	5000	10 100 1000 5000
II. Primary					
a. Resilient	15	60	4		
	15	30	2		
	10	40	4		
	10	20	2		
	5	20	4		
	5	15	3		
	5	10	2		
b. Permanent	5	20	4	5000	(2)
	15	60	4	5000	(2)
c. Resilient (3)					
d. Permanent	5	30	6	5000	(2)
	5	40	8	5000	(2)
	15	90	6	5000	(2)
	15	120	8	5000	(2)

- (1) 5000 or until failure  
(2) same as for conditioning phase  
(3) same as the first resilient

## CHAPTER 4

### RESILIENT MODULUS RESULTS

#### 4.1 Introduction

The results of the resilient testing portion of the program are presented in this chapter. The resilient modulus values obtained after the conditioning phase are compared with those obtained following the repeated load testing at a stress level higher than that used during conditioning. Correlations of the material characterization values shown in Chapter 3 with the resilient modulus test results are presented. Also included in Chapter 4 are analyses of differences in the resilient behavior due to material type, density, and gradation.

#### 4.2 Computation of Resilient Modulus

The resilient modulus,  $E_r$ , has been defined (Chapter 2) as the repeated deviator stress divided by the recoverable axial strain. The methods of instrumentation used in the test procedure and the output from the strip recorder are included in Chapter 3. Because the resilient modulus for a granular material is not constant but varies with the state of stress, analysis of the  $E_r$  values at various stress levels can be used to develop a regression line depicting the stress dependent behavior. The results from the regression analysis are used in the form of Equation 2.1.

#### 4.3 Results of Resilient Testing Program

Table 4.1 summarizes the results of the resilient modulus versus first stress invariant regression analyses including the standard errors

Table 4.1. Results of Resilient Modulus Testing Program.

Material Type	Gradation	Compaction Level	After Conditioning			After the 5000 Cycles at $\sigma_D/\sigma_3 = 60/15$		
			Slope, n	Intercept, K, psi	Standard Error of Estimate	Slope, n	Intercept, K, psi	Standard Error of Estimate
Limestone	No. 5	Low	0.40	11,234	0.021	0.44 <sup>(a)</sup>	9320 <sup>(a)</sup>	0.014
		Med	0.52	5640	0.018	0.52	5545	0.029
		High	0.54	7296	0.035	0.48	7851	0.025
	No. 4	Low	0.51	6513	0.035	0.54	5293	0.018
		Med	0.47	5883	0.022	0.57	4948	0.033
		High	0.46	8636	0.022	0.52	6363	0.026
	Well graded	Med	0.59	5149	0.016	0.67	3287	0.027
		Med	0.65	4281	0.018	0.60	5069	0.017
		Med	0.61	4733	0.017	0.66	3268	0.018
	CA-10	Med	0.65	2598	0.011	0.73	1702	0.007
High		0.60	4186	0.006	0.59	3582	0.017	
Granitic Gneiss	No. 5	Low	0.19*	34,127	0.047	0.43	10,172	0.022
	No. 4	Low	0.60	5128	0.009	0.60	4124	0.029
		Med	0.53	6819	0.022	failed		
	Well graded	High	0.52	8076	0.024	0.54	7384	0.016
		Med	0.56	7092	0.013	0.65	4215	0.021
Chicago Slag	No. 4	Low	0.64	4122	0.020	0.68	2974	0.020
		Med	0.71	3466	0.018	0.81	1433	0.036
		High	0.63	5269	0.018	0.77	1957	0.008
	Well graded	Med	0.70	4899	0.015	0.70	4259	0.024
Basalt	No. 5	Med	0.47	8944	0.029	0.46	9249	0.023
	No. 4	Med	0.65	4725	0.022	0.52	7963	0.031
	Well graded	Med	0.60	7145	0.015	0.65	5962	0.012
Crushed Gravel	No. 4	Med	0.56	7864	0.025	0.50	10,147	0.029
Gravel	No. 5	Med	0.59	5388	0.025	0.59	6756	0.030
	No. 4	Low	0.53	8228	0.035	failed		
		Med	0.49	10,431	0.040	0.57	7531	0.028
		High	0.38	25,187	0.015	0.47	14,772	0.025
	Well graded	Med	0.60	7781	0.016	0.57	8070	0.032
Kansas Test Track Slag	No. 5	Low	0.58	5626	0.008	0.53	7864	0.012
		Med	0.49	13,092	0.011	0.46	16,784	0.014
	High	0.58	8244	0.027	0.68	3525	0.020	

\* Not significant at  $\alpha = 0.01$ .

(a) Results after 20,000 cycles at  $\sigma_D/\sigma_3 = 45/15$ .

of estimate. As noted with one exception all were significant at  $\alpha = 0.01$ .

Although the standard errors of estimate appear to be extremely low they are associated with the prediction of the logarithm of  $E_r$ . As an illustration of the actual error in the prediction of the resilient modulus, consider the following example:

$$E_r = 6513 \theta^{0.51}$$

$$\text{standard error, } S_{xy} = 0.035$$

therefore,  $\log E_r = [\log 6513 + 0.51 \log \theta] \pm 0.035$ , which yields, for  $\theta$  equal to 100 psi (689 kN/m<sup>2</sup>),  $4.834 \pm 0.035$ , a range for  $E_r$  of 62,951 to 73,961 psi (434 to 510 MN/m<sup>2</sup>). The error in the prediction of  $E_r$  is therefore considerably larger than the standard error of estimate. Also although the standard error of estimate is constant on the logarithmic scale, the error in the prediction of  $E_r$  is greater for large values of  $\theta$  than for small values.

Figures 4.1 through 4.32 depict the results of the resilient modulus portion of the testing program. Analysis of the results is in subsequent sections.

Figures 4.1 through 4.6 show the relationships between resilient modulus,  $E_r$ , and the sum of principal stresses,  $\theta$ , for 6 specimens of different material types but of the same gradation (No. 4 ballast) and compactive effort (medium). With the exception of the granitic gneiss, two sets of data representing values immediately after the conditioning phase and following the 5000 cycles of 60 psi (414 kN/m<sup>2</sup>) repeated deviator stress and 15 psi (103 kN/m<sup>2</sup>) confining pressure are shown.

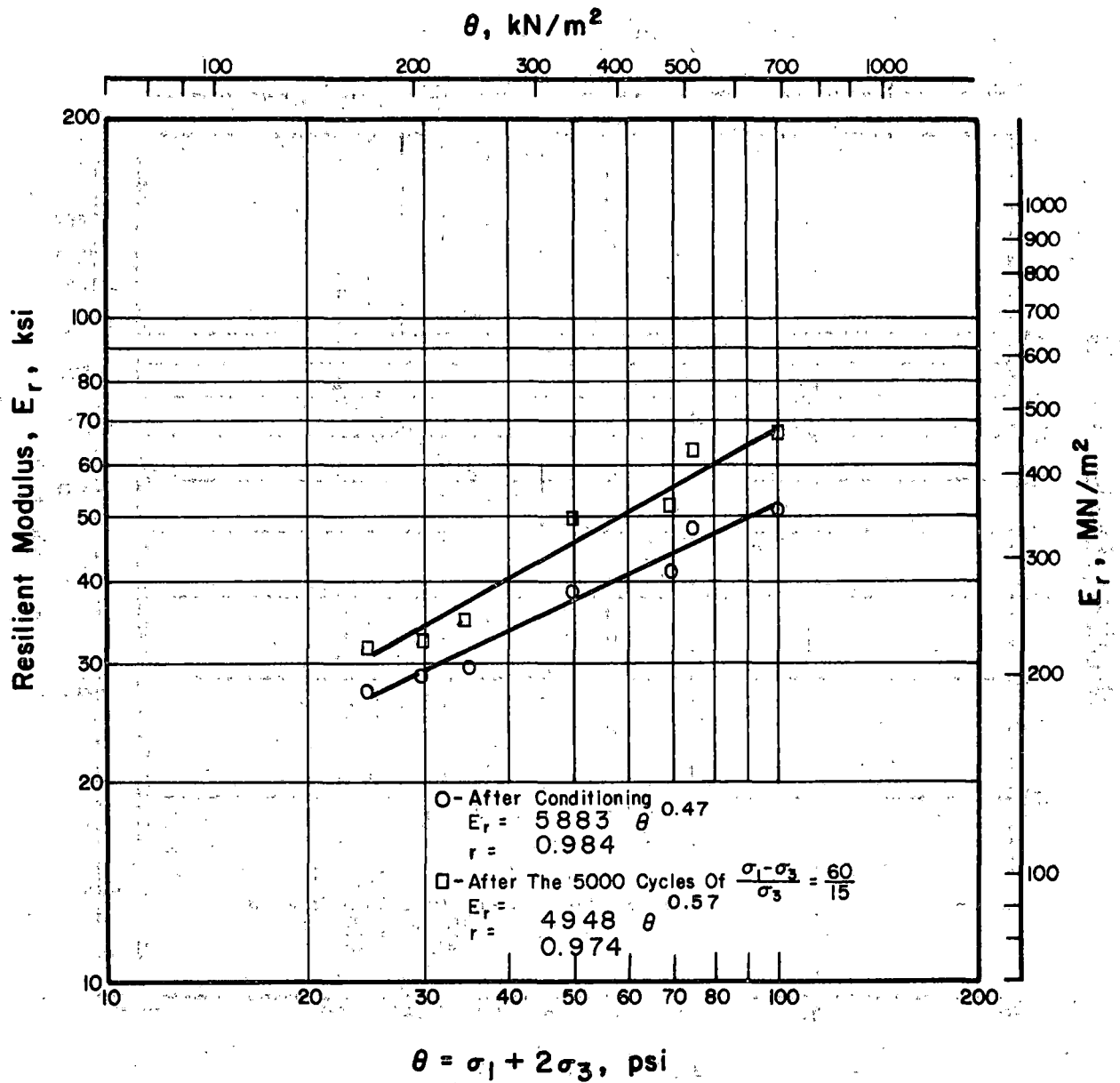


Figure 4.1. Relationship between  $E_r$  and  $\theta$  for No. 4 Gradation Limestone, Medium Density.

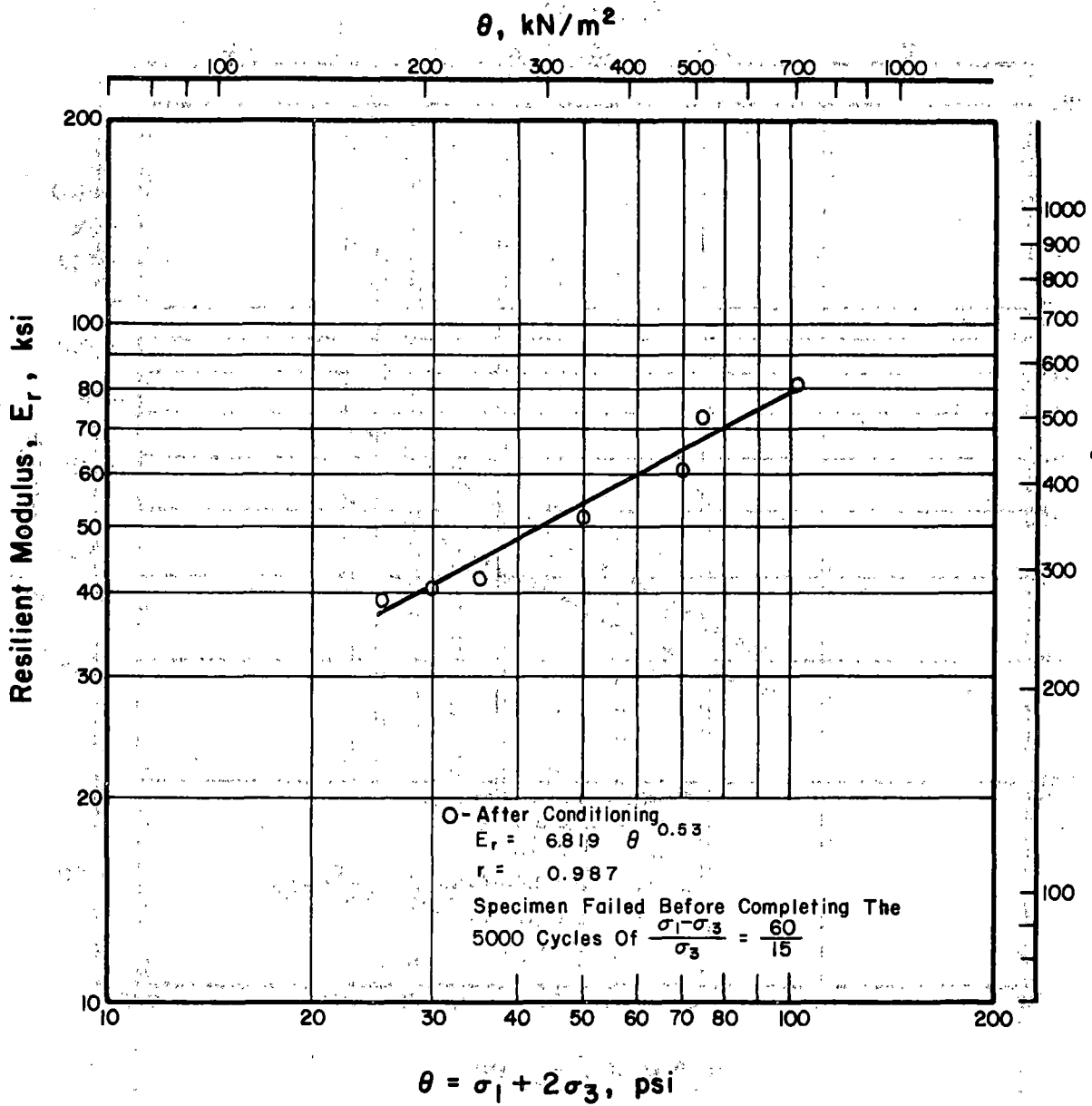


Figure 4.2. Relationship between  $E_r$  and  $\theta$  for No. 4 Gradation Granitic Gneiss, Medium Density.

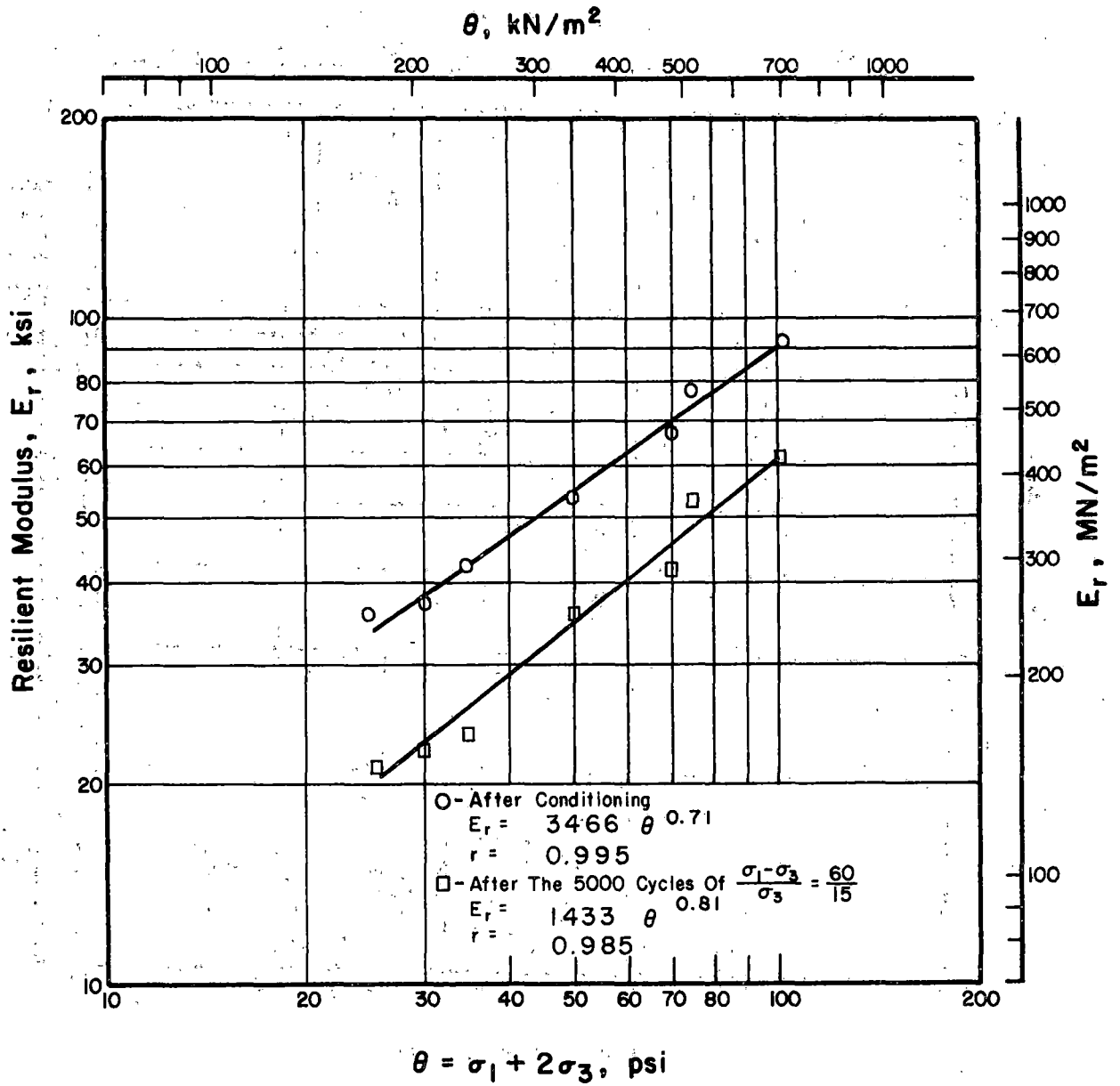


Figure 4.3. Relationship between  $E_r$  and  $\theta$  for No. 4 Gradation Chicago Blast Furnace Slag, Medium Density.

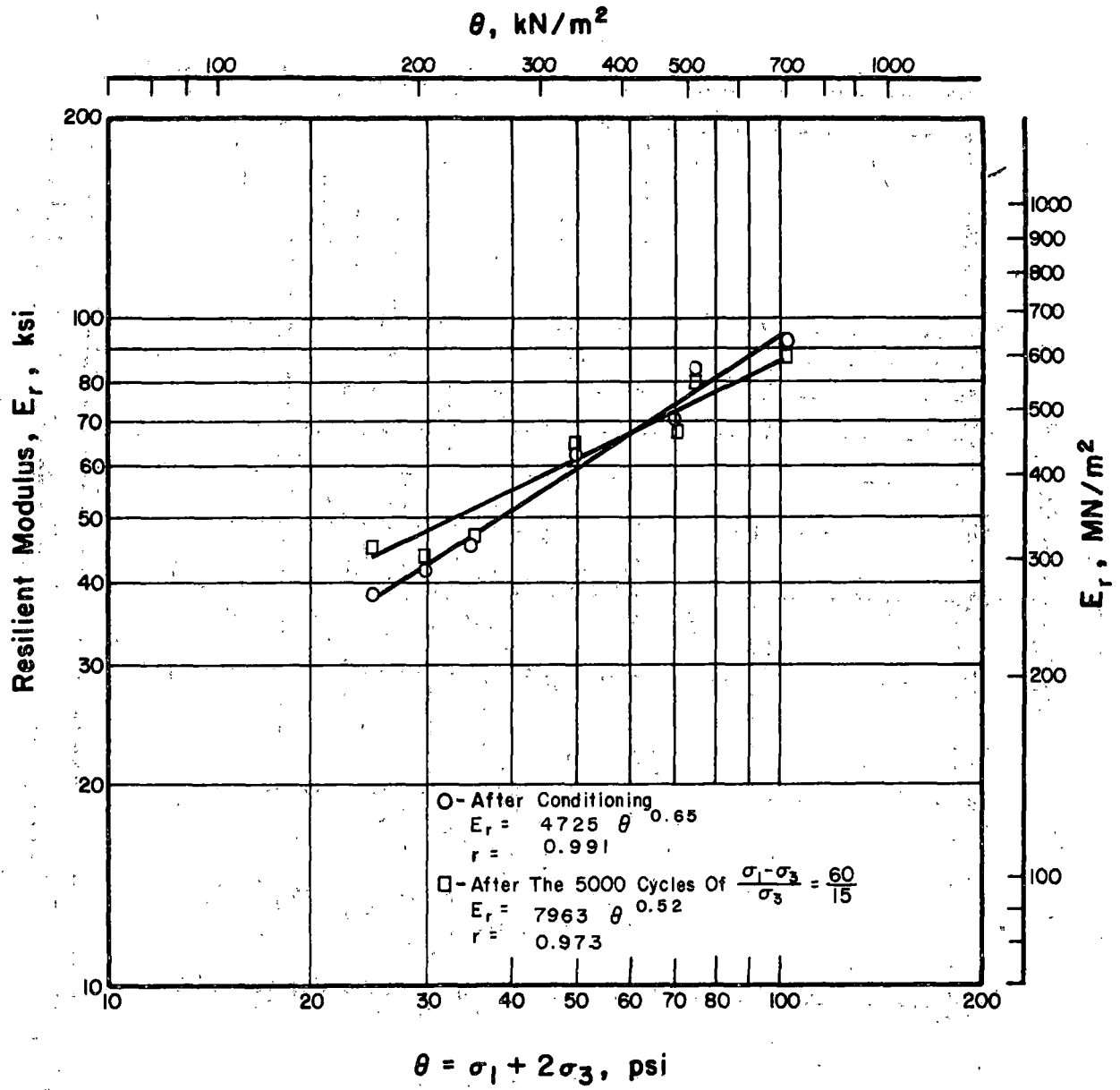


Figure 4.4. Relationship between  $E_r$  and  $\theta$  for No. 4 Gradation Basalt, Medium Density.

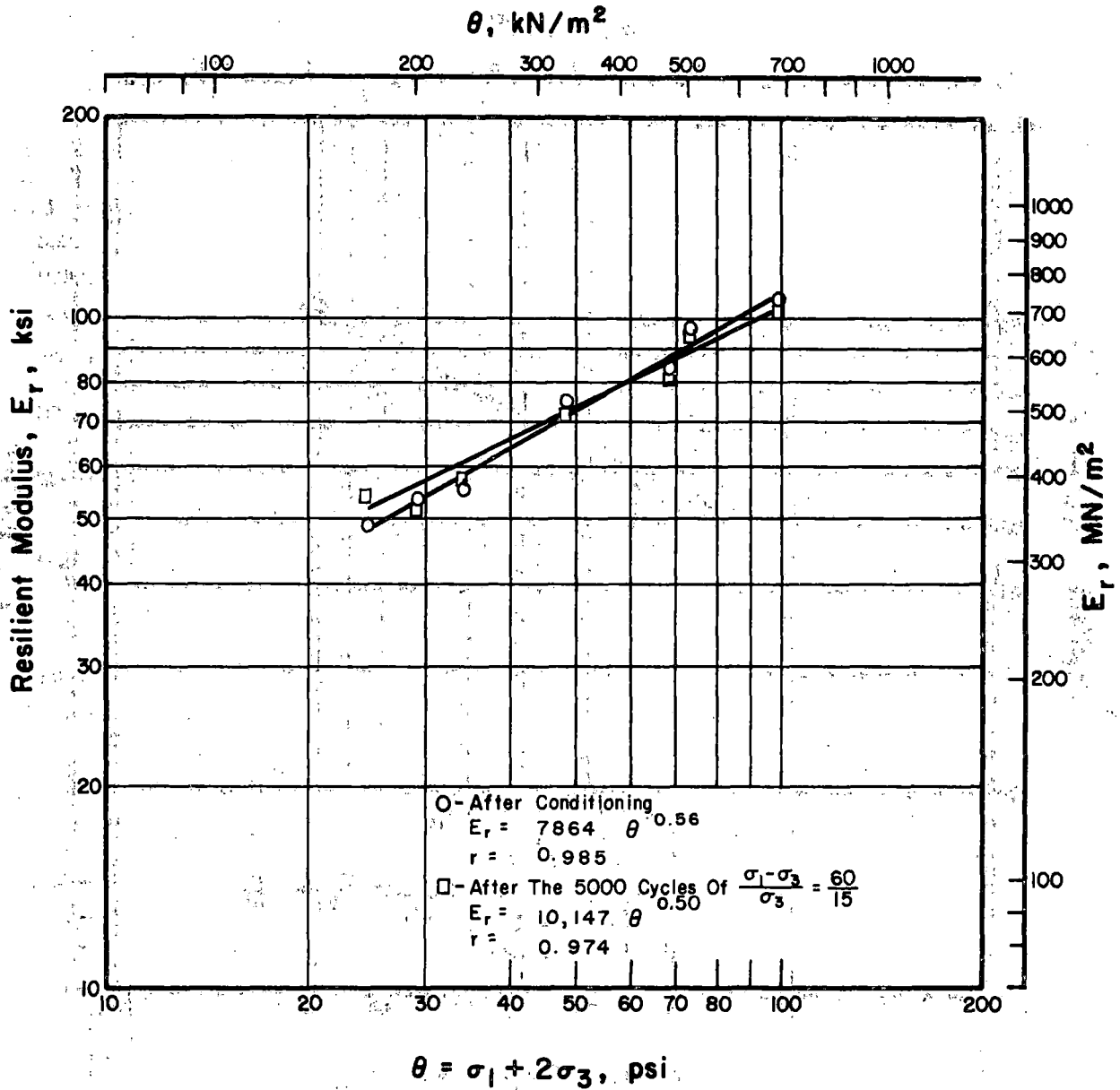


Figure 4.5. Relationship between  $E_r$  and  $\theta$  for No. 4 Gradation Crushed Gravel, Medium Density.

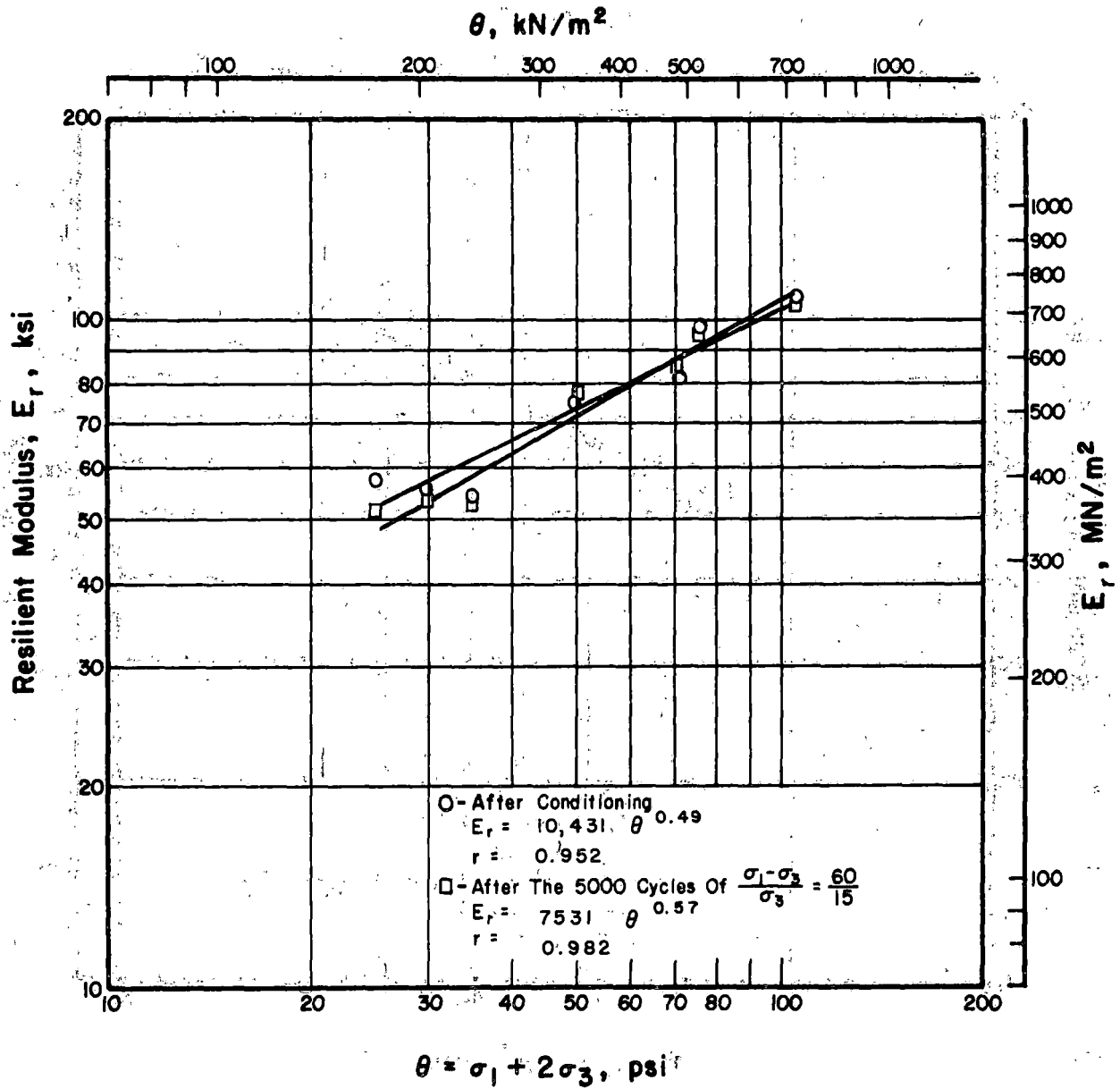


Figure 4.6. Relationship between  $E_r$  and  $\theta$  for No. 4 Gradation Gravel, Medium Density.

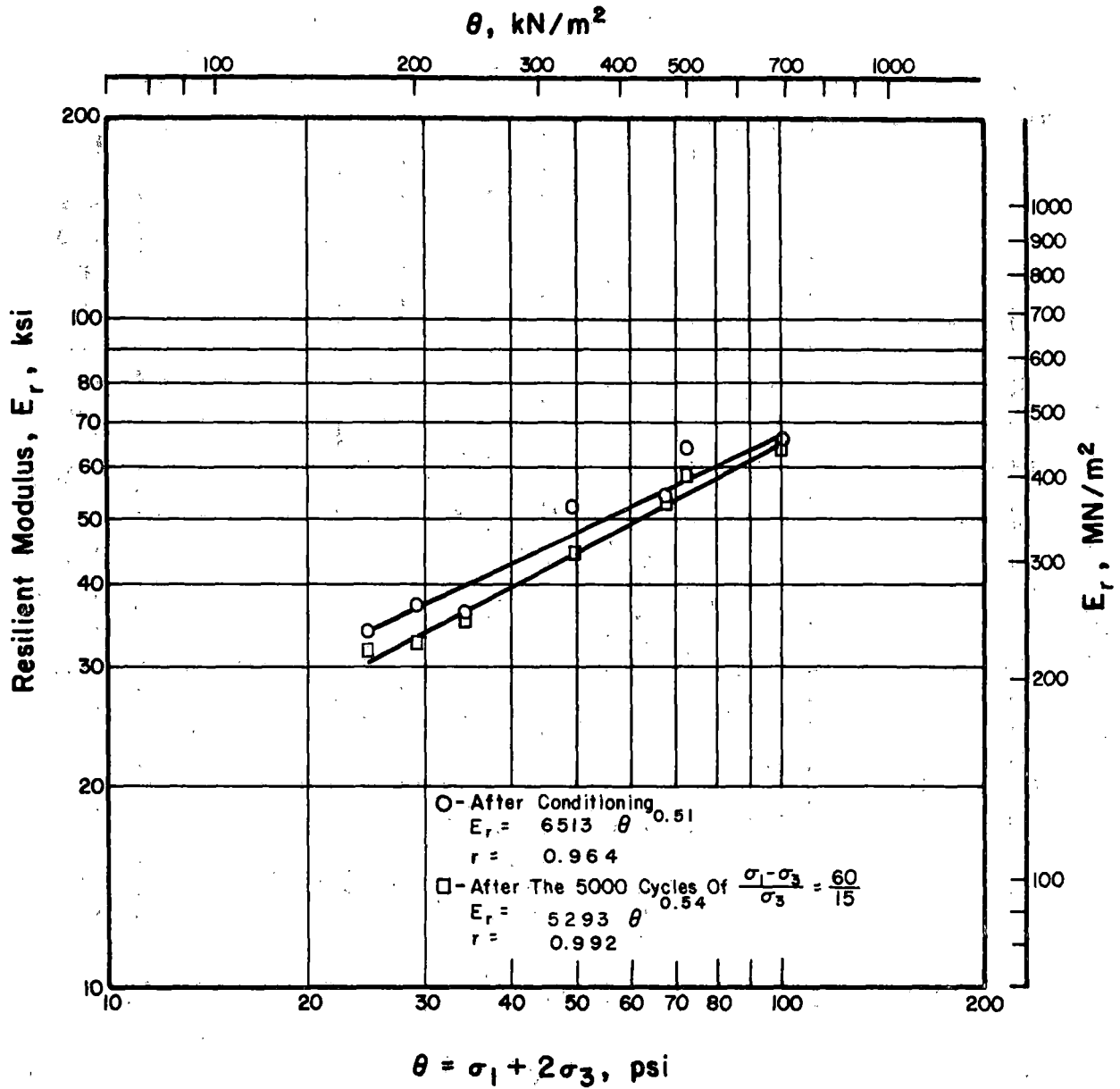


Figure 4.7. Relationship between  $E_r$  and  $\theta$  for No. 4 Gradation Limestone, Low Density.

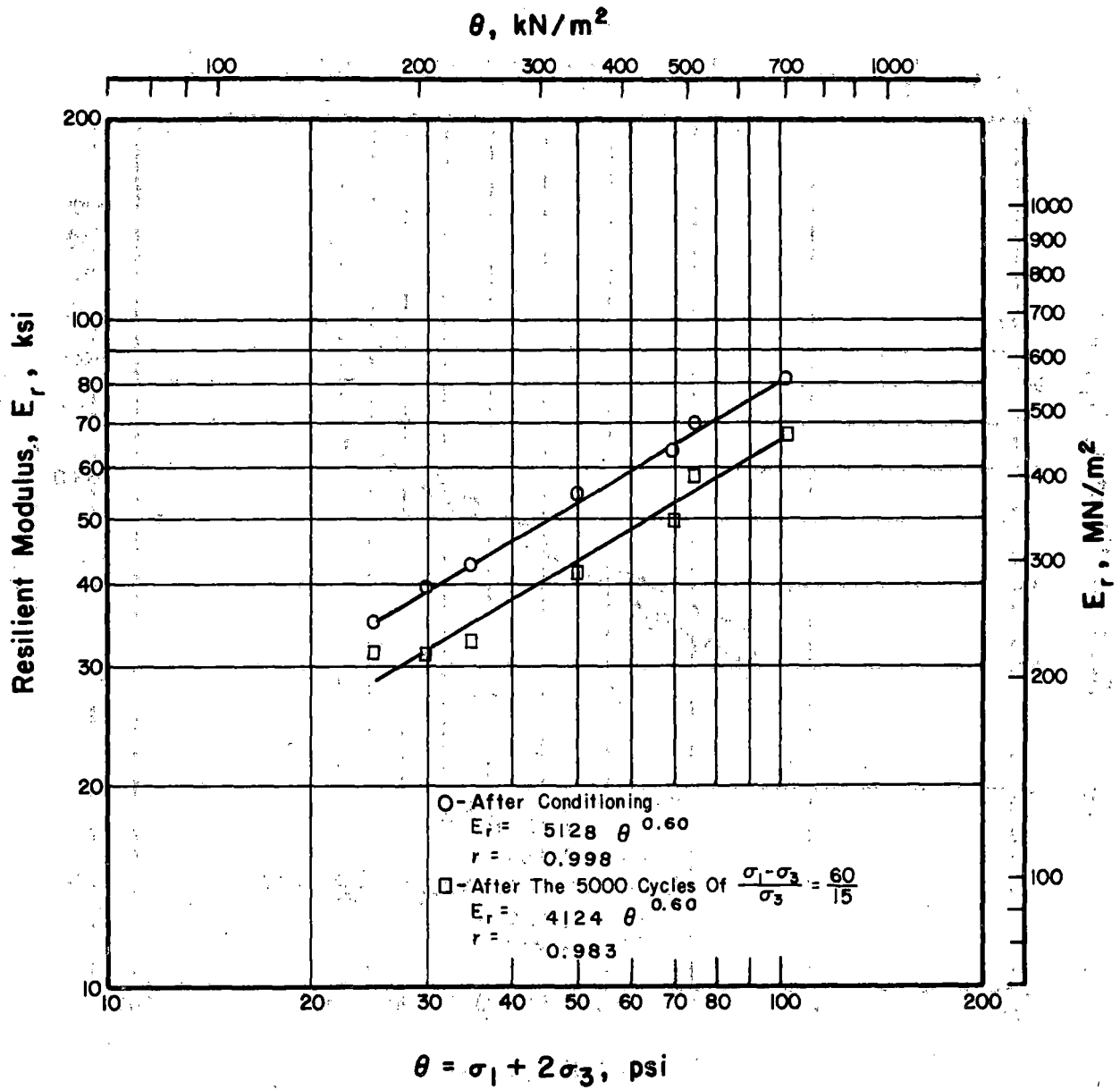


Figure 4.8. Relationship between  $E_r$  and  $\theta$  for No. 4 Gradation Granitic Gneiss, Low Density.

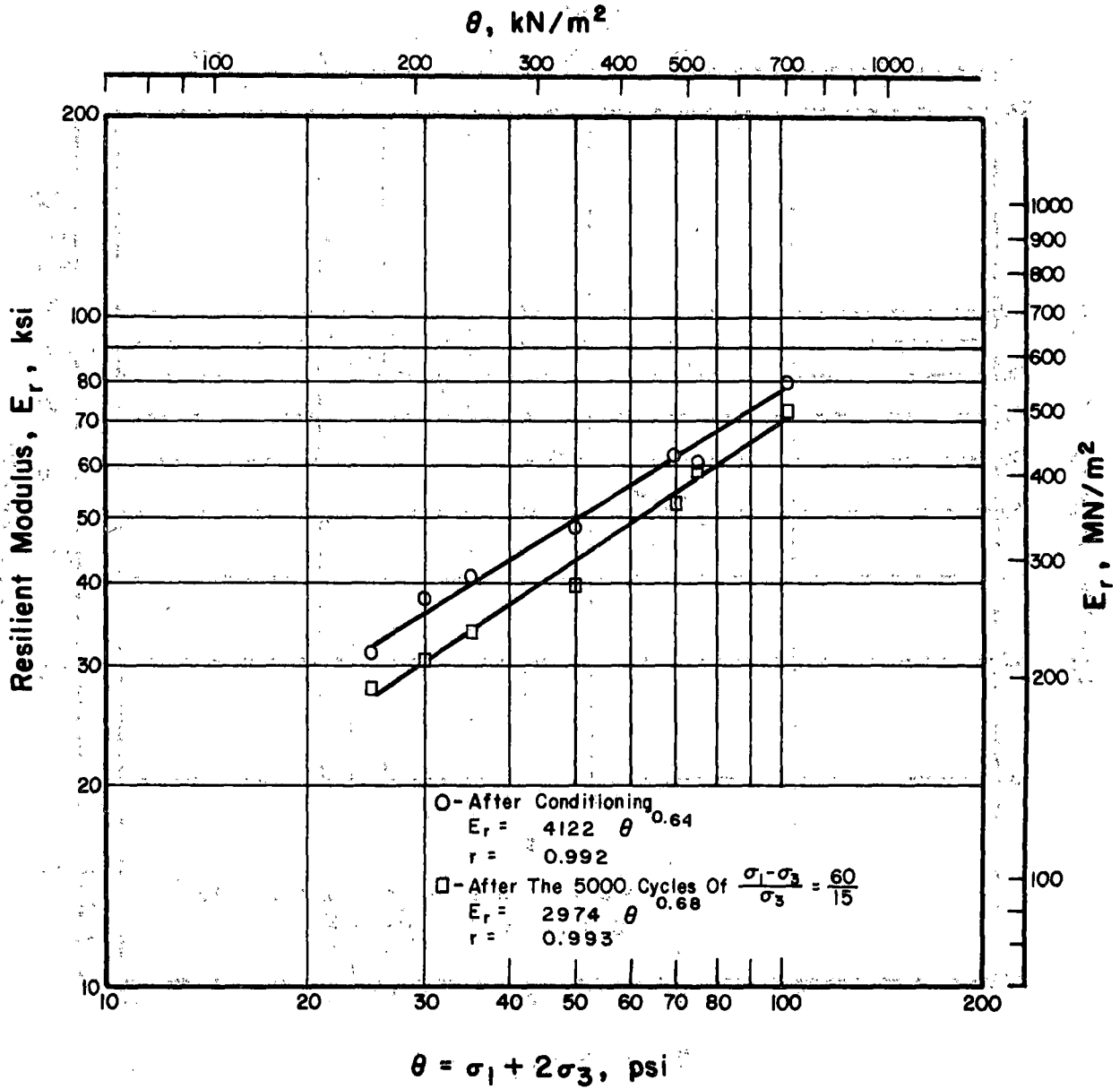
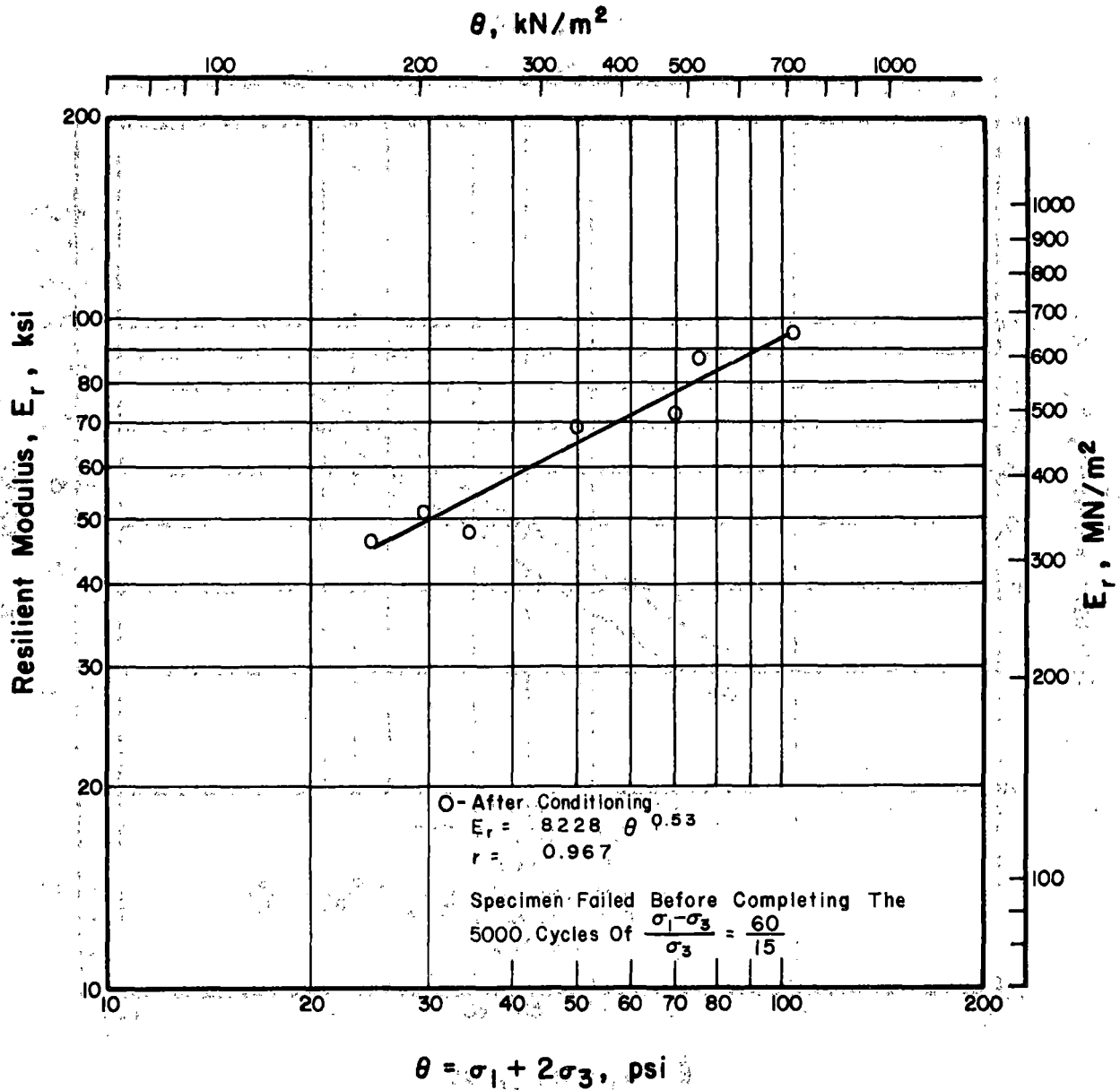


Figure 4.9. Relationship between  $E_r$  and  $\theta$  for No. 4 Gradation Chicago Blast Furnace Slag, Low Density.



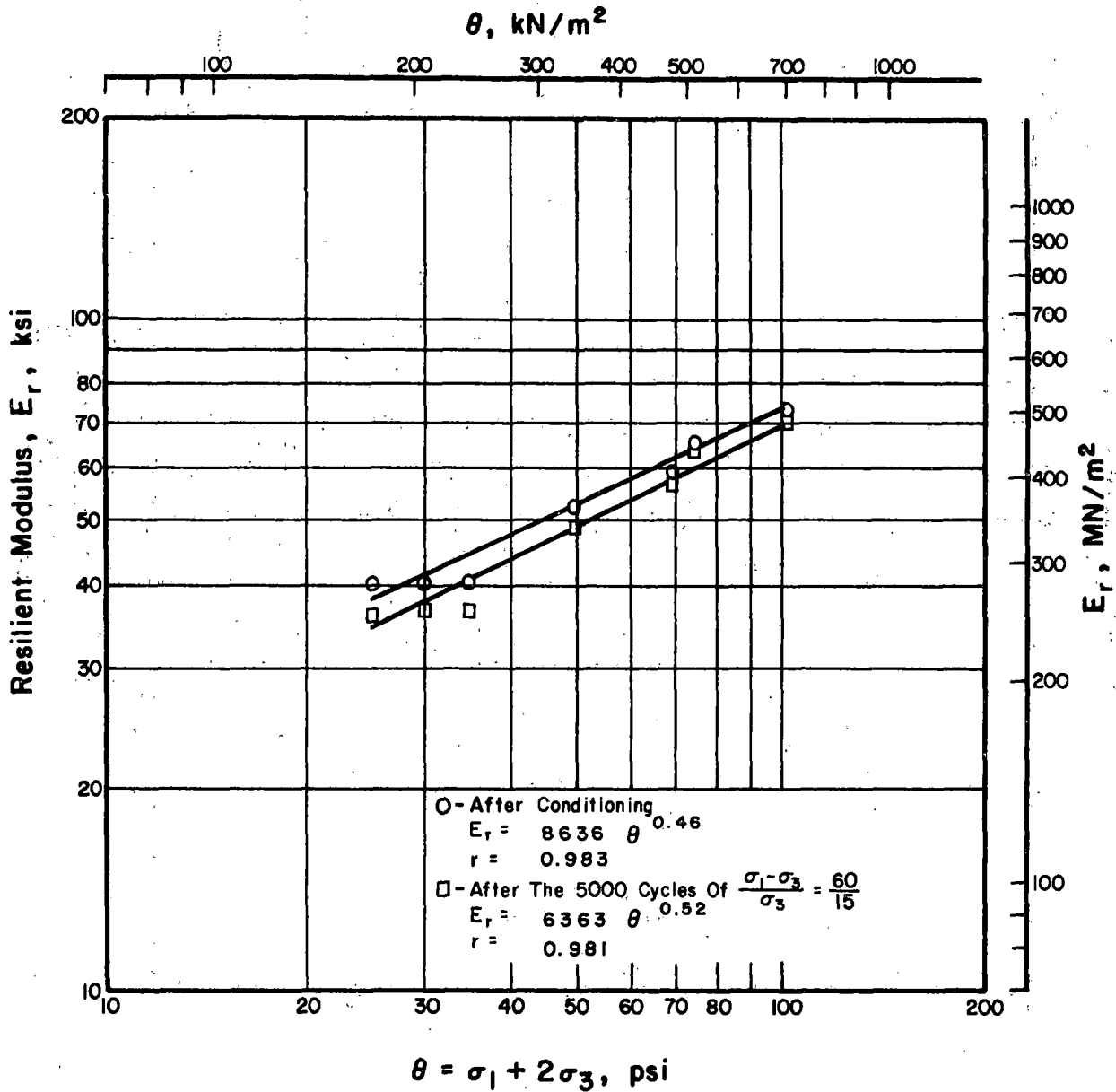


Figure 4.11. Relationship between  $E_r$  and  $\theta$  for No. 4 Gradation Limestone, High Density.

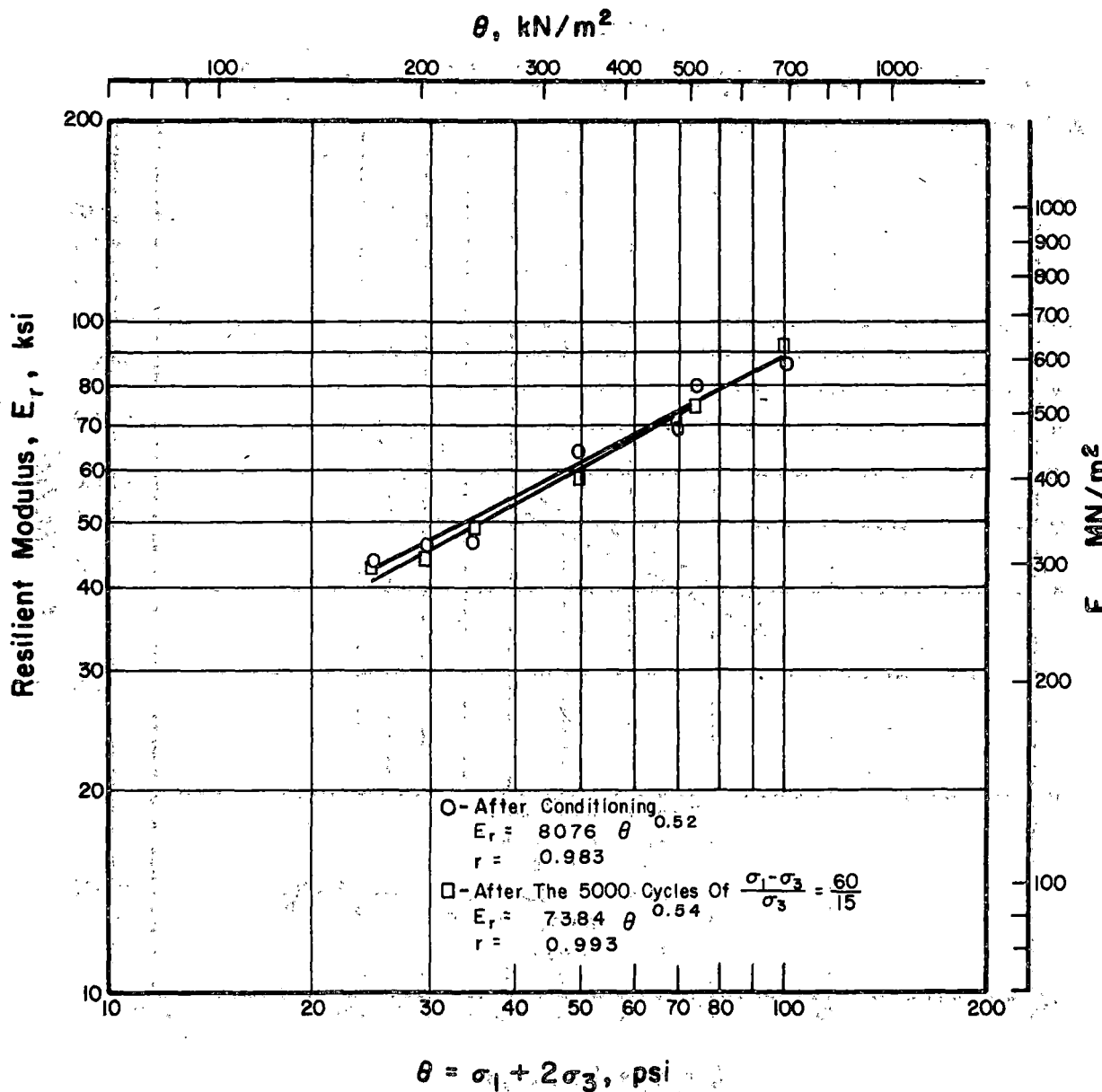


Figure 4.12. Relationship between  $E_r$  and  $\theta$  for No. 4 Gradation Granitic Gneiss, High Density.

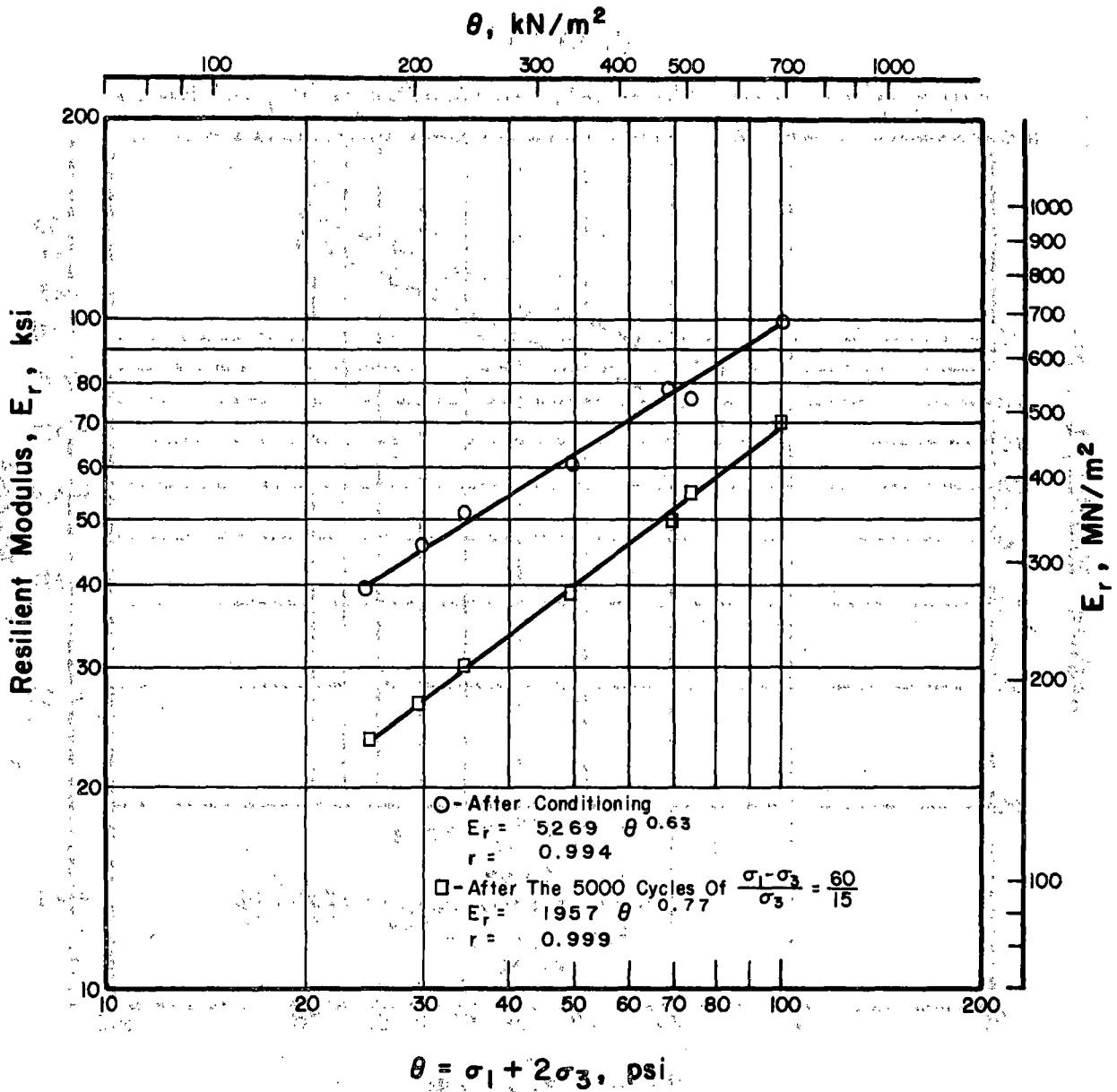


Figure 4.13. Relationship between  $E_r$  and  $\theta$  for No. 4 Gradation Chicago Blast Furnace Slag, High Density.

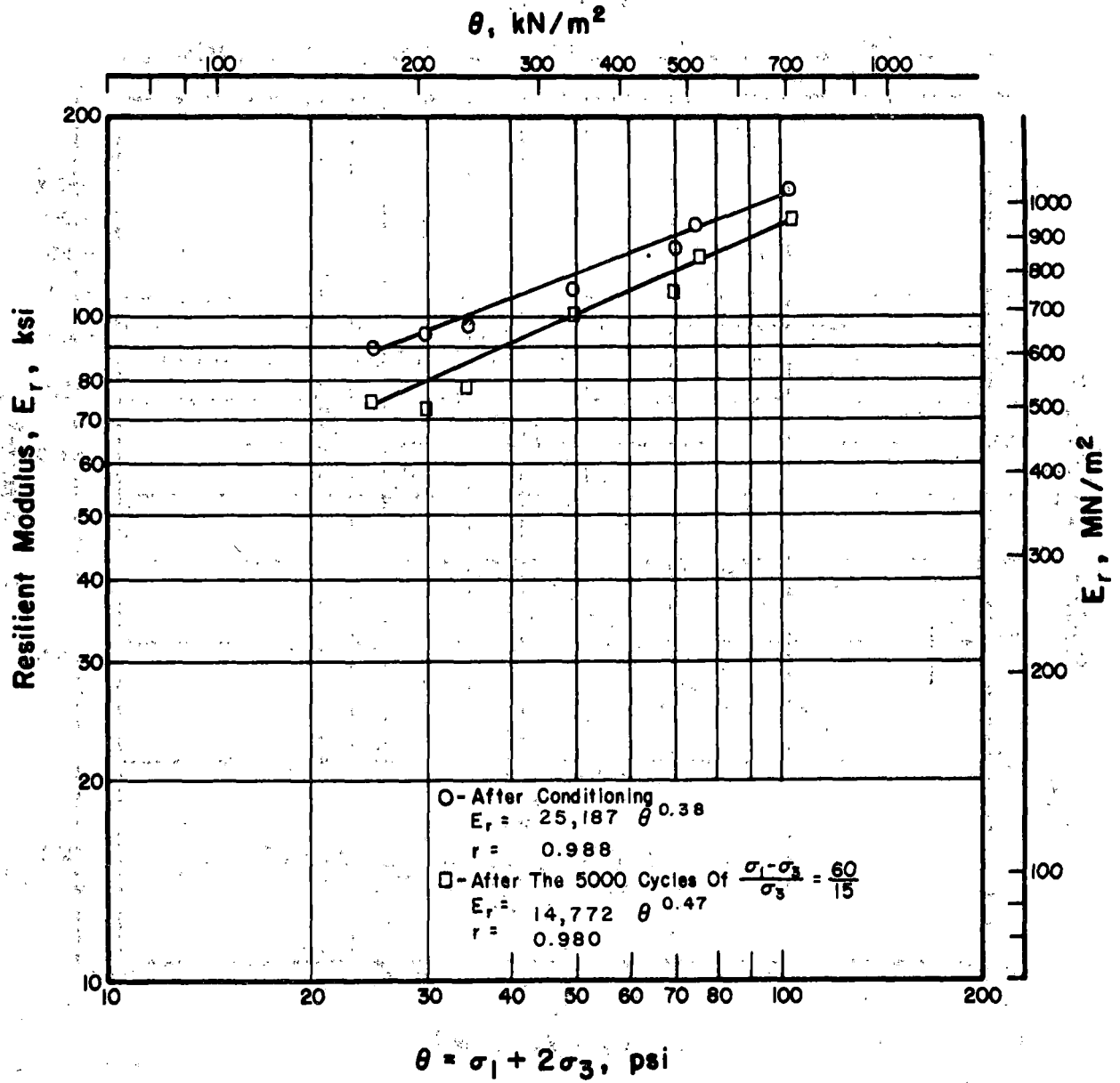


Figure 4.14. Relationship between  $E_r$  and  $\theta$  for No. 4 Gradation Gravel, High Density.

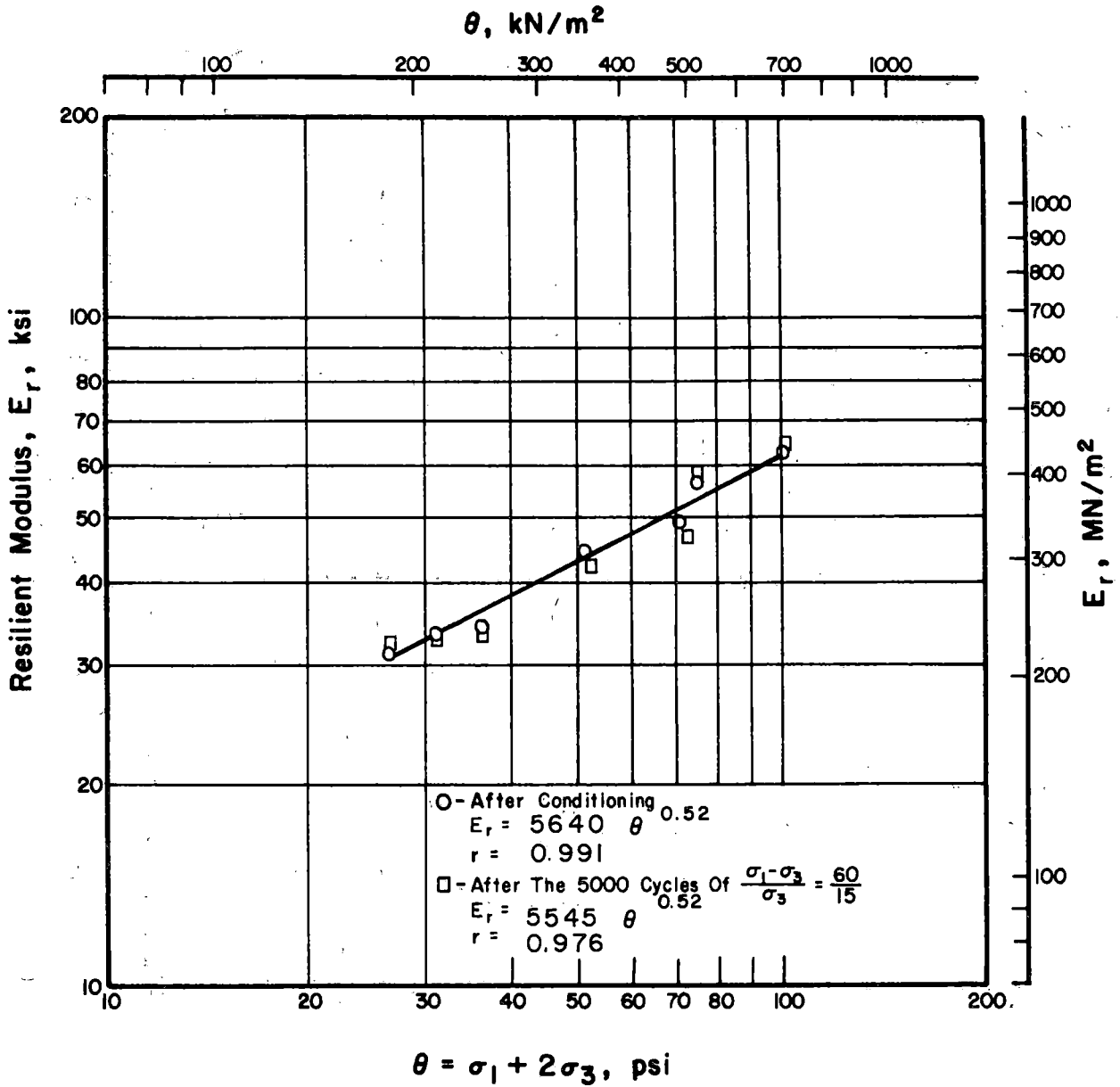


Figure 4.15. Relationship between  $E_r$  and  $\theta$  for No. 5 Gradation Limestone; Medium Density.

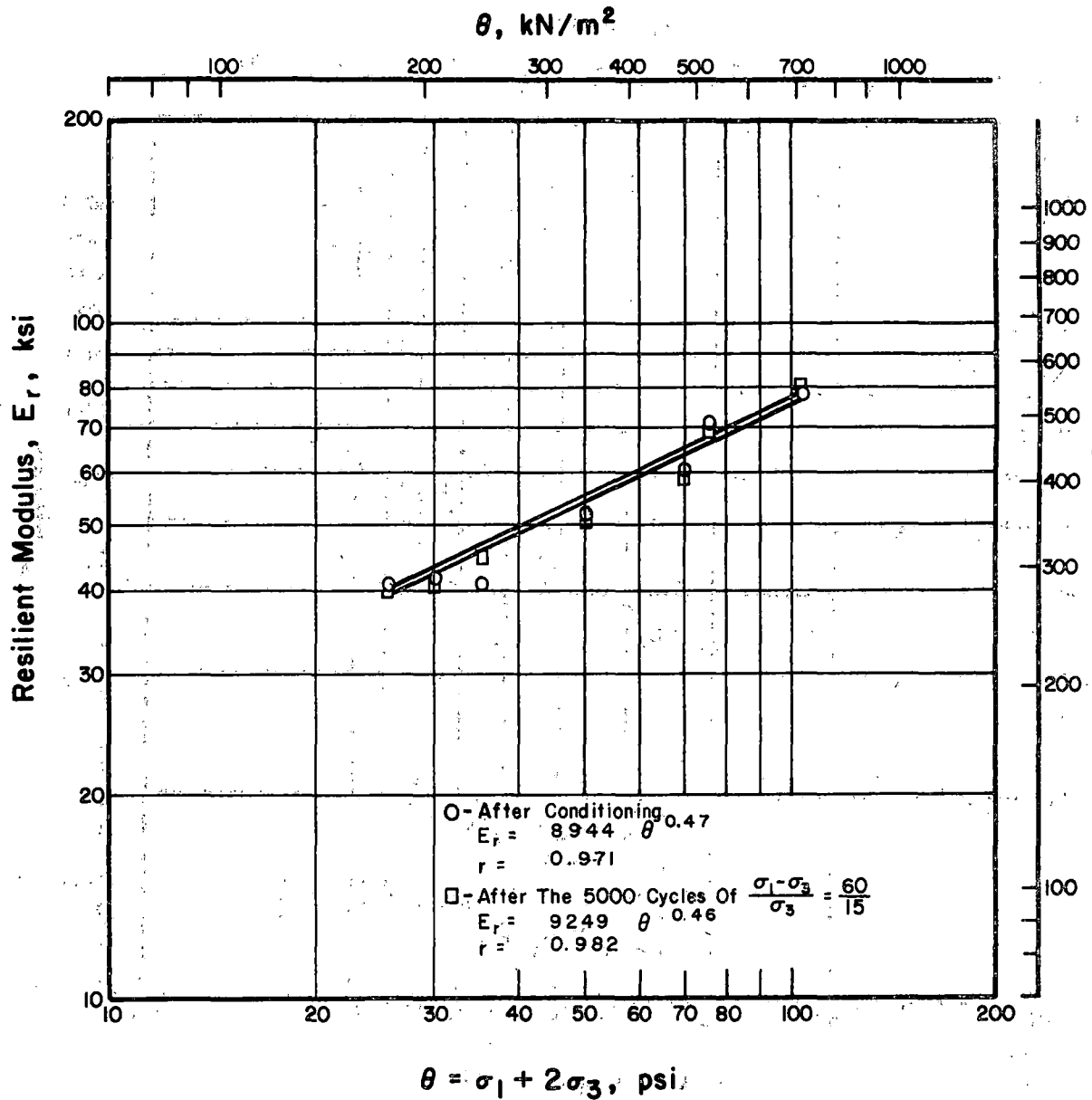


Figure 4.16. Relationship between  $E_r$  and  $\theta$  for No. 5 Gradation Basalt, Medium Density.

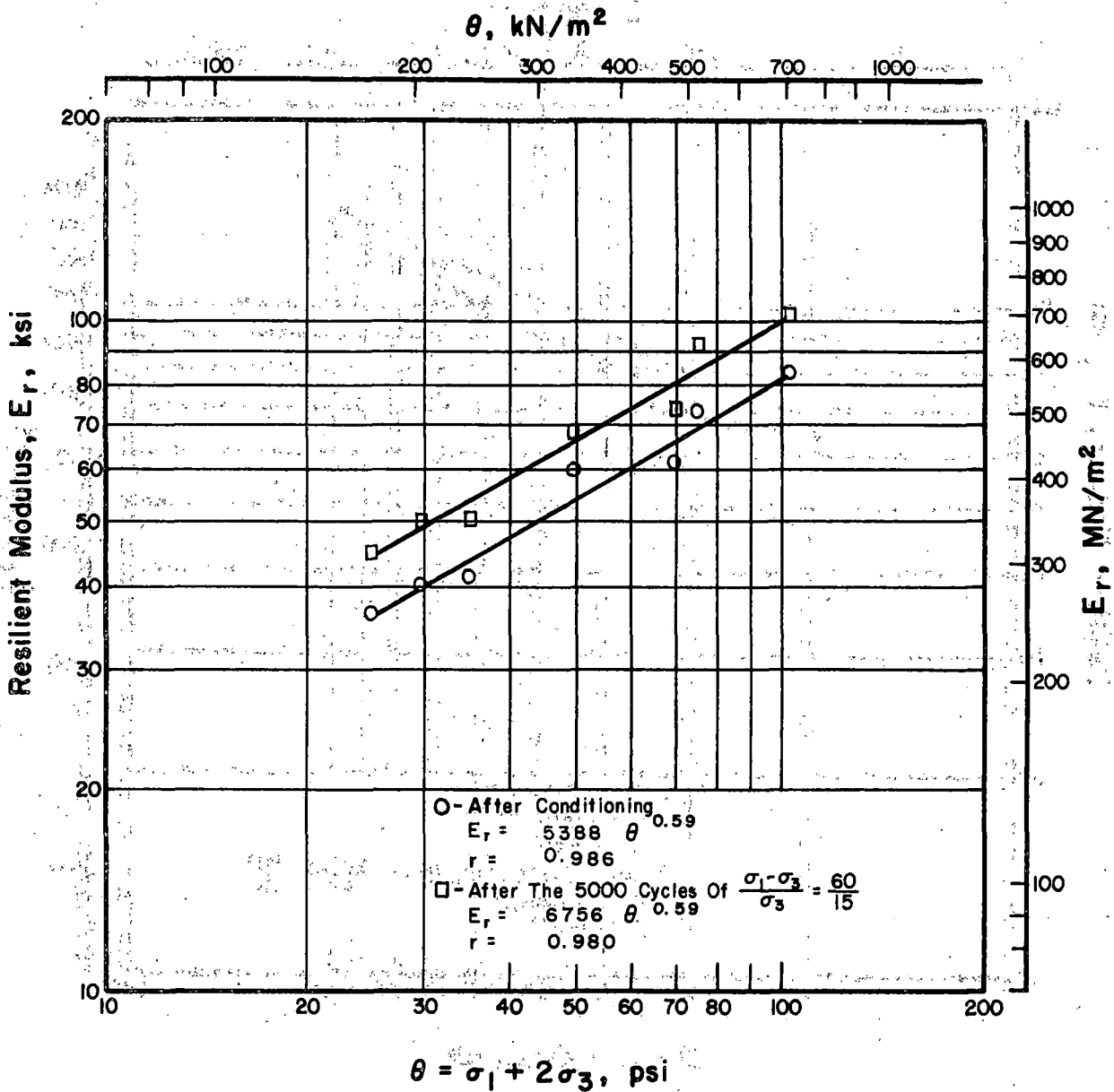


Figure 4.17. Relationship between  $E_r$  and  $\theta$  for No. 5 Gradation Gravel, Medium Density.

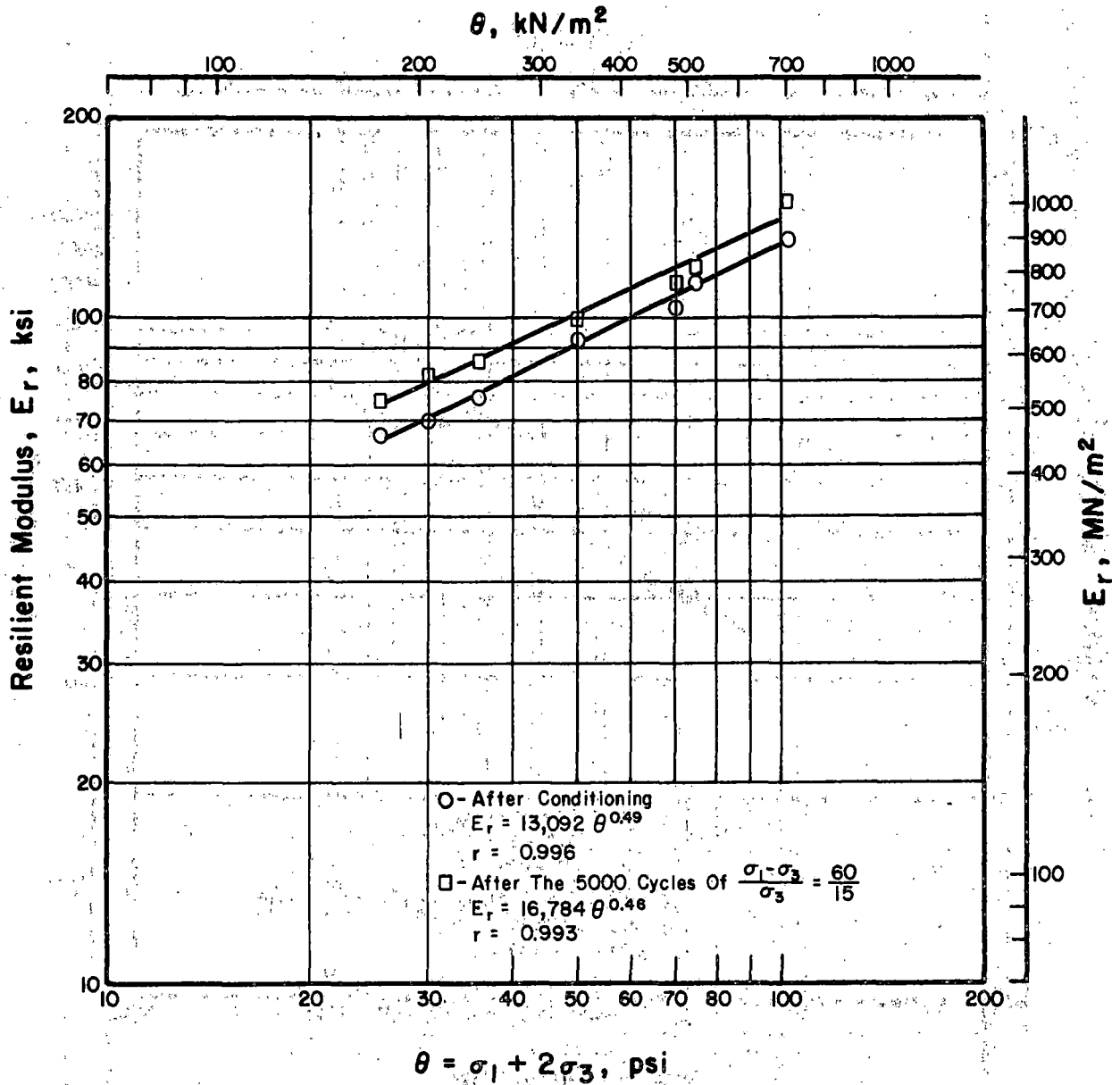


Figure 4.18. Relationship between  $E_r$  and  $\theta$  for No. 5 Gradation Kansas Test Track Slag, Medium Density.

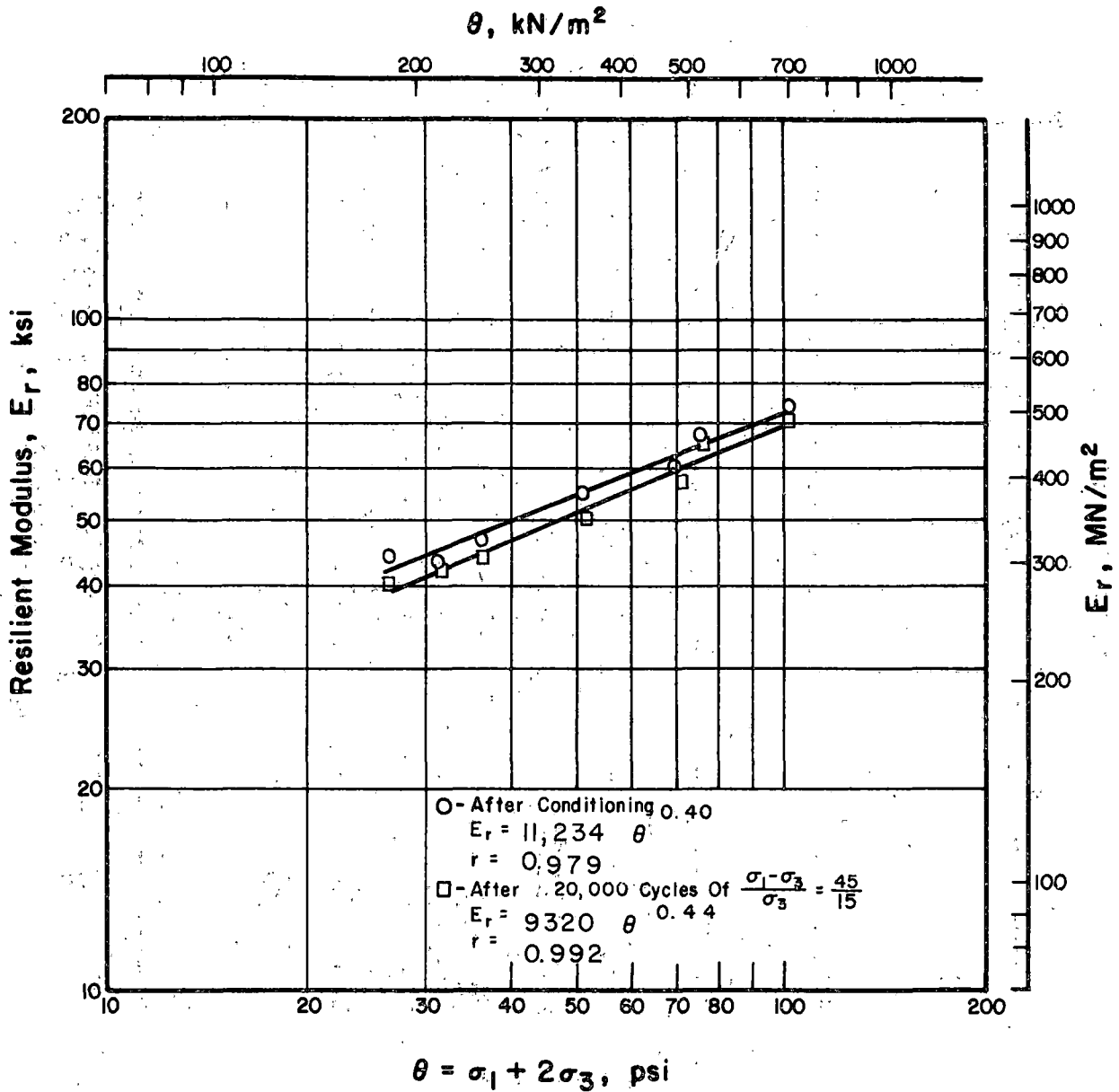


Figure 4.19. Relationship between  $E_r$  and  $\theta$  for No. 5 Gradation Limestone, Low Density.

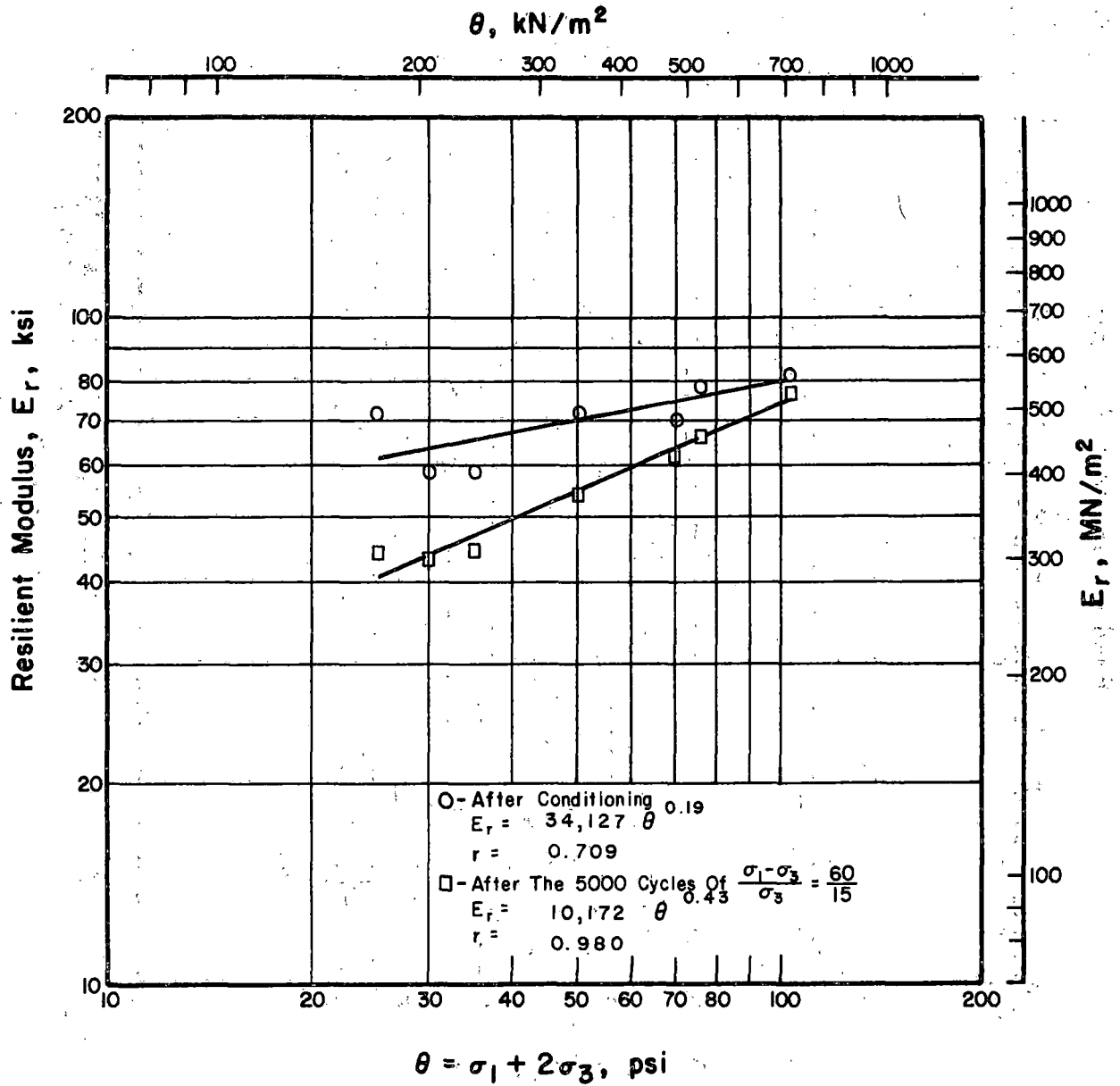


Figure 4.20. Relationship between  $E_r$  and  $\theta$  for No. 5 Gradation Granitic Gneiss, Low Density.

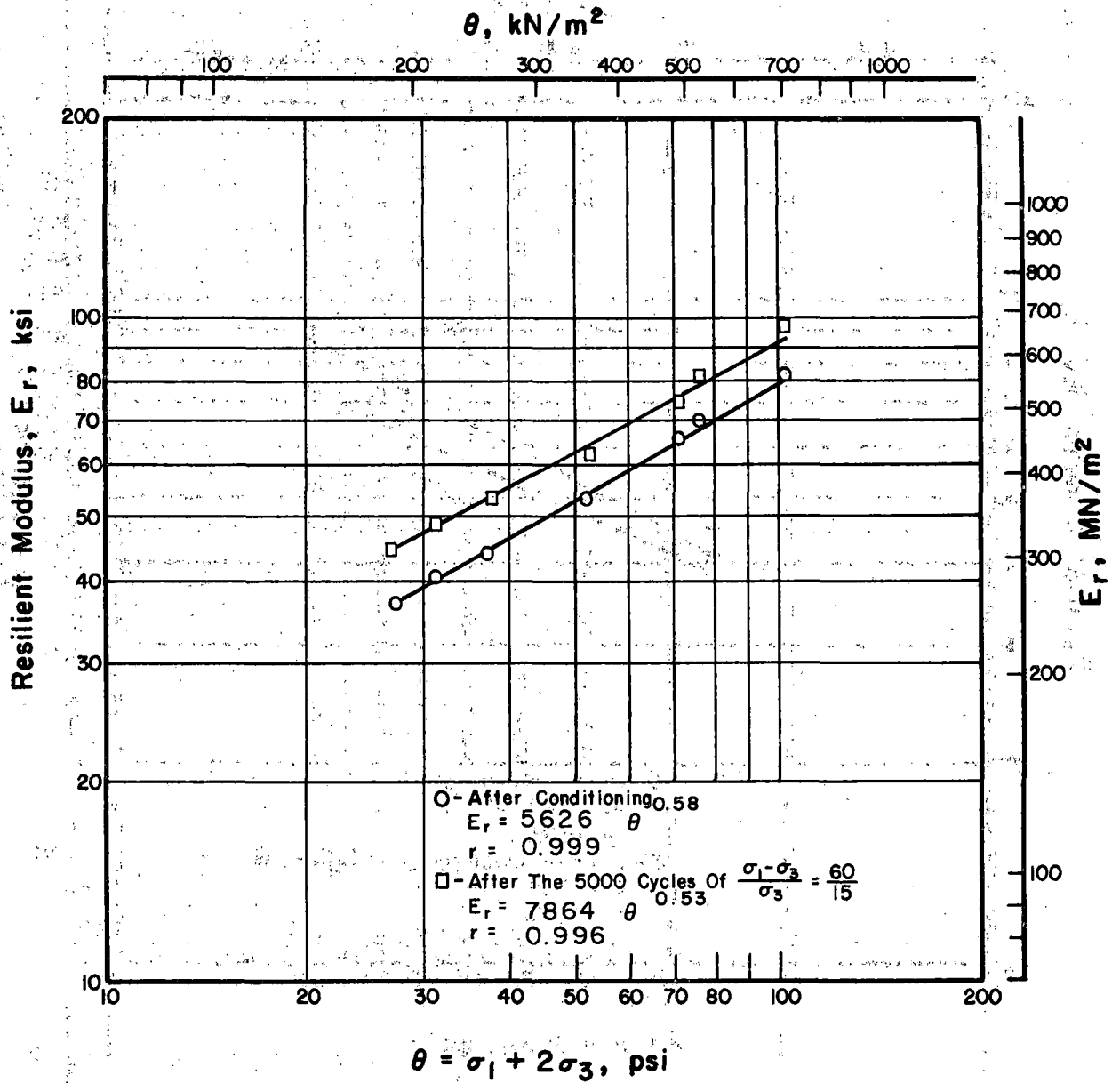


Figure 4.21. Relationship between  $E_r$  and  $\theta$  for No. 5 Gradation Kansas Test Track Slag, Low Density.

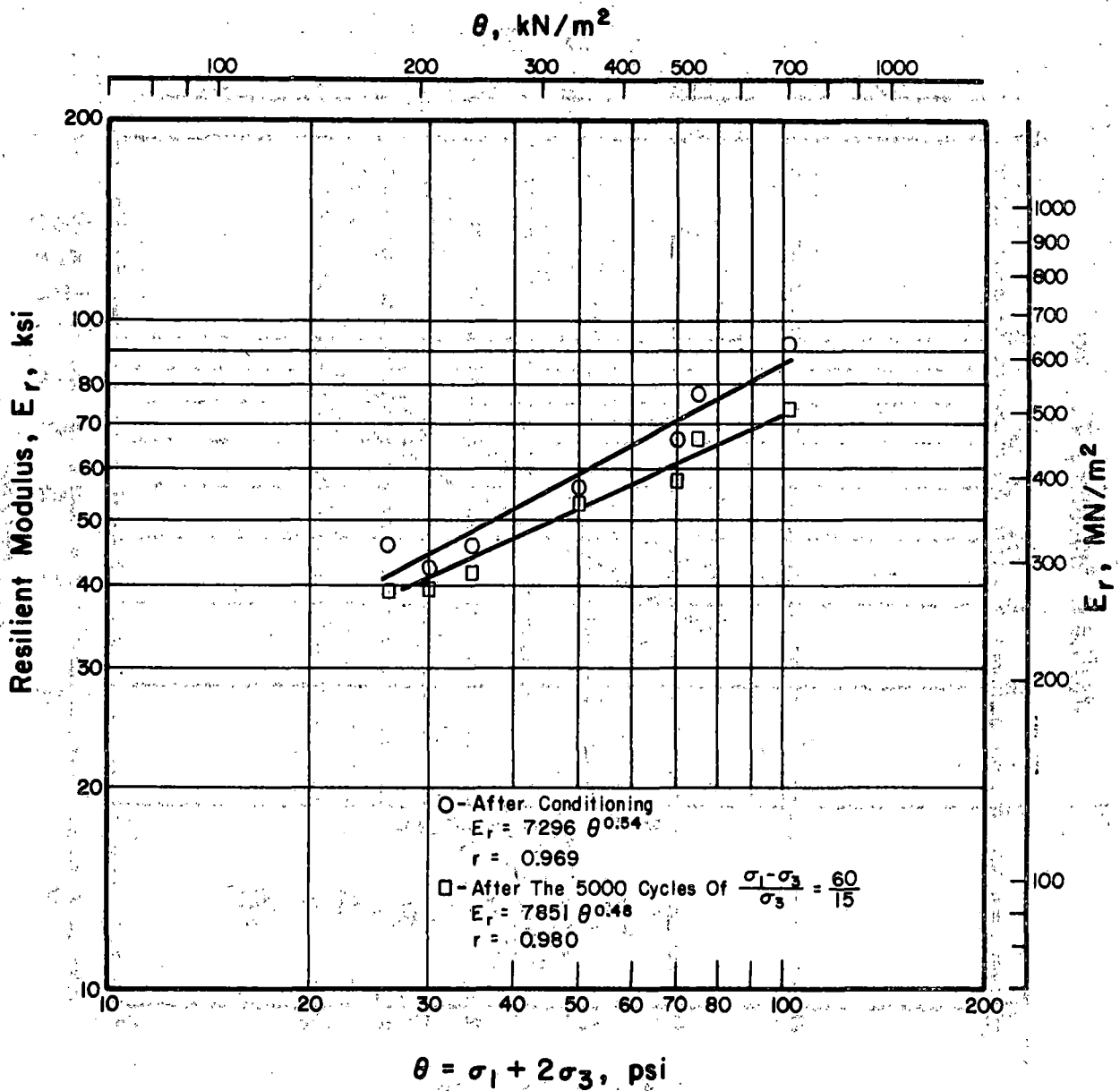


Figure 4.22. Relationship between  $E_r$  and  $\theta$  for No. 5 Gradation Limestone, High Density.

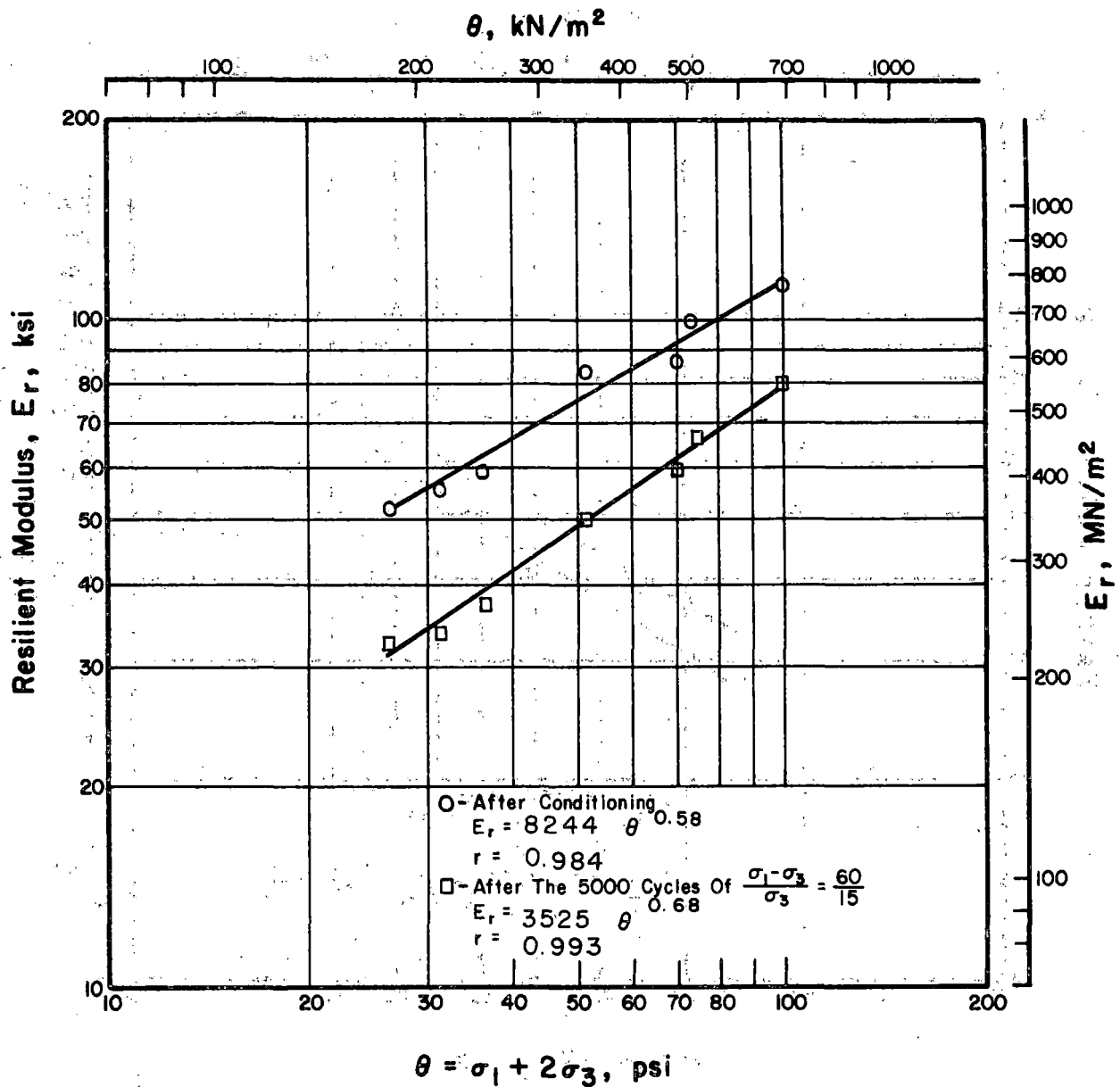


Figure 4.23. Relationship between  $E_r$  and  $\theta$  for No. 5 Gradation Kansas Test Track Slag, High Density.

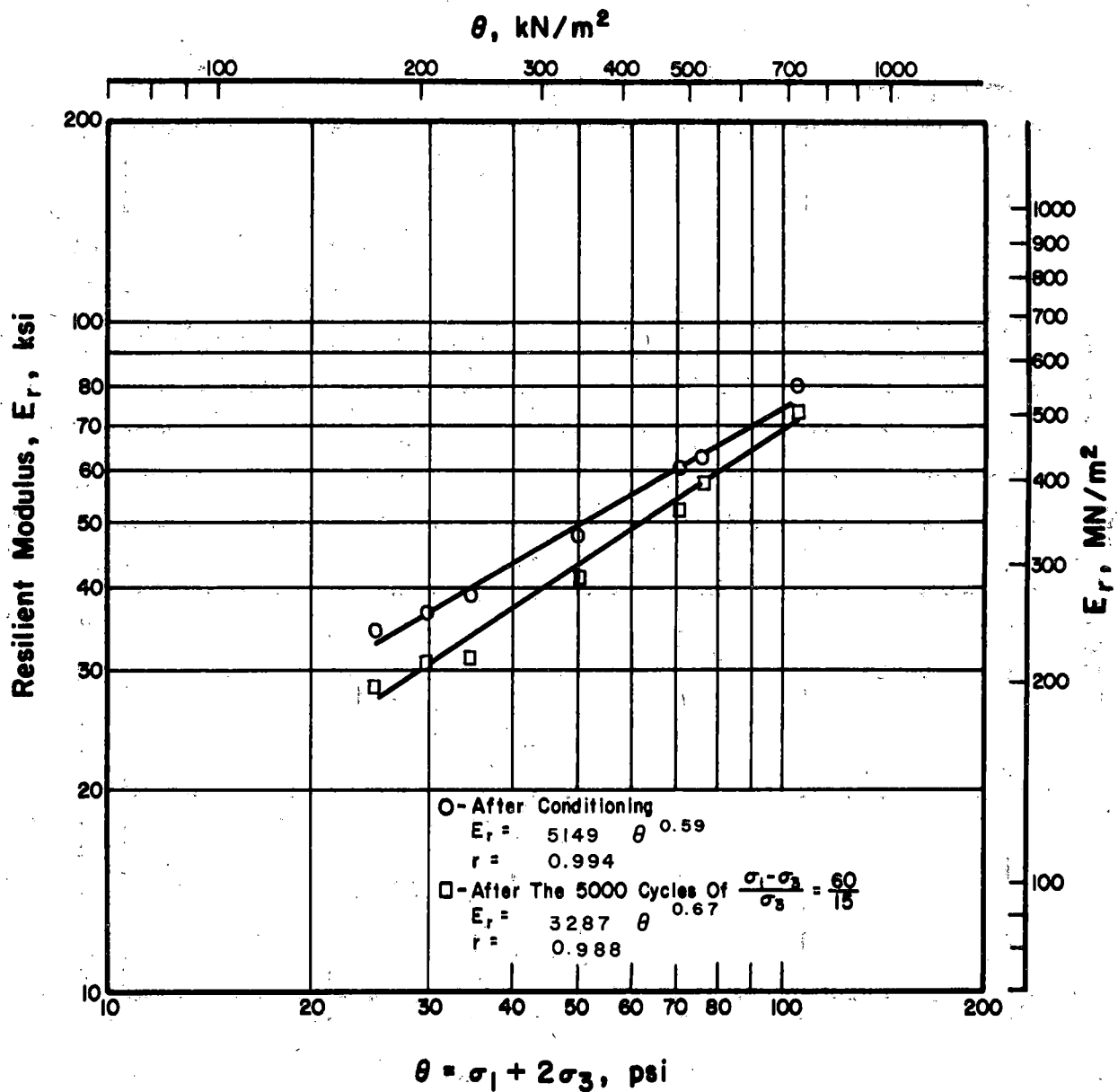


Figure 4.24. Relationship between  $E_r$  and  $\theta$  for Well Graded ( $n = 2/3$ ) Limestone, Medium Density.

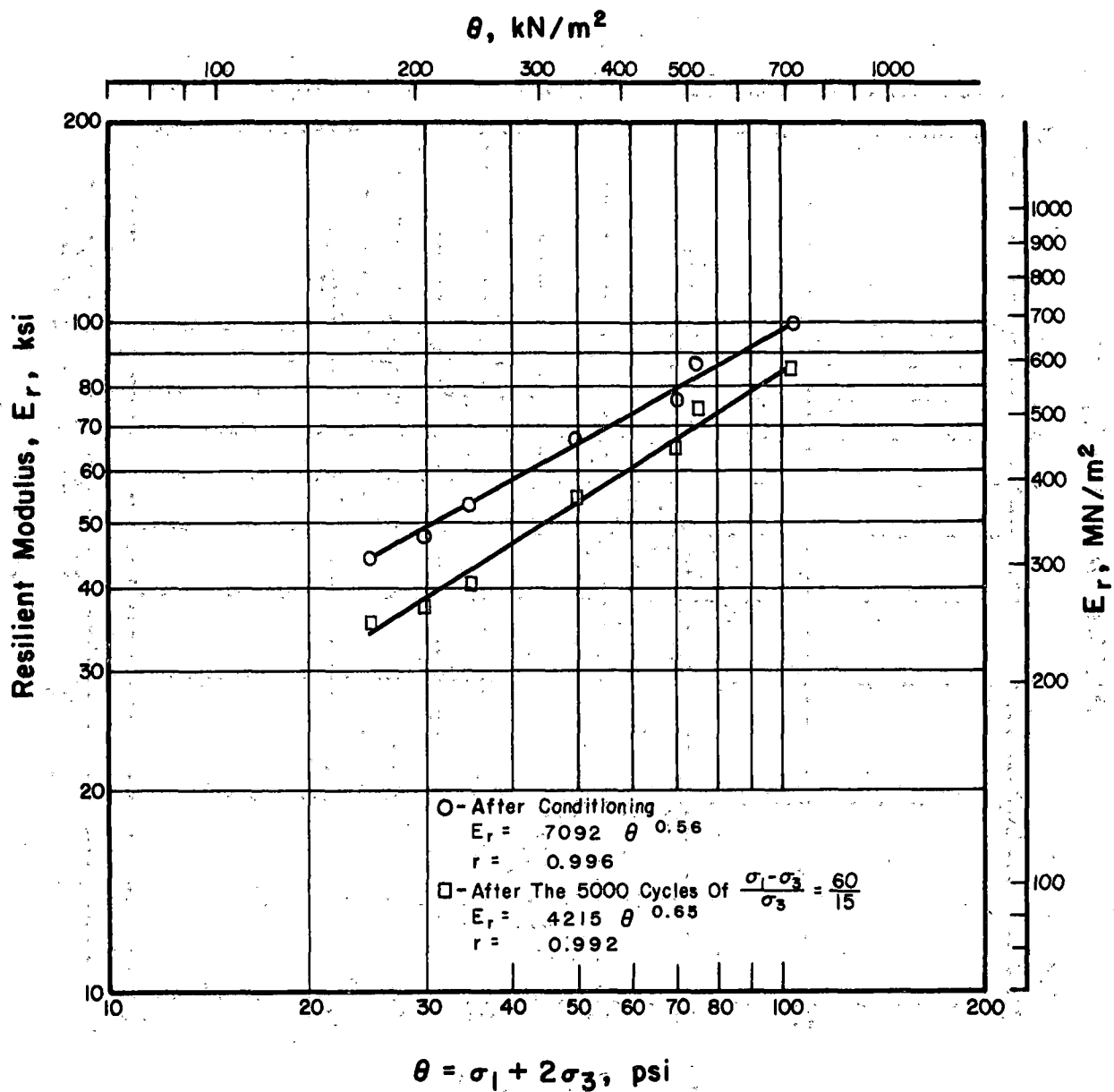


Figure 4.25. Relationship between  $E_r$  and  $\theta$  for Well Graded ( $n = 2/3$ ) Granitic Gneiss, Medium Density.

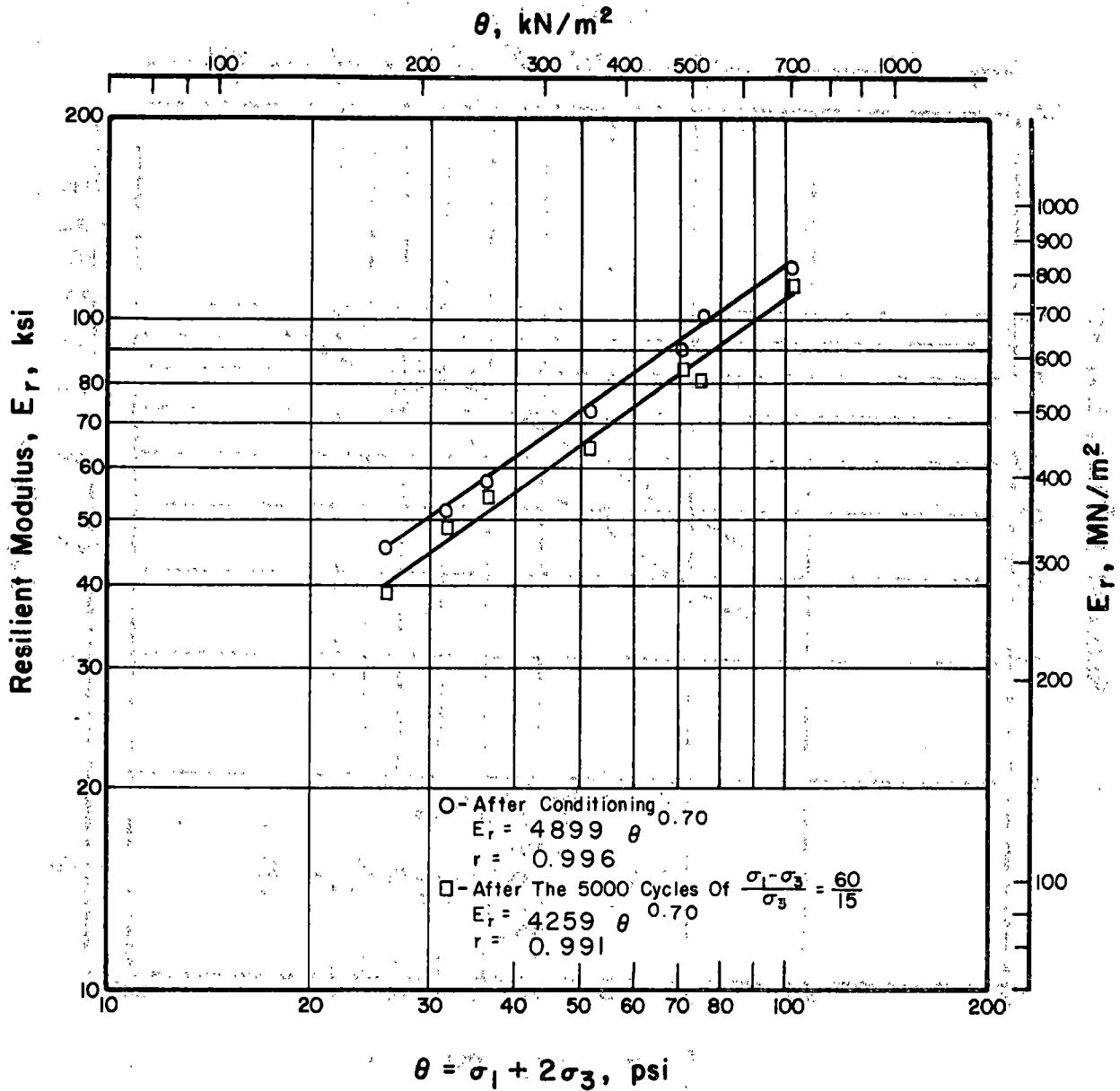


Figure 4.26: Relationship between  $E_r$  and  $\theta$  for Well Graded ( $n = 2/3$ ) Chicago Blast Furnace Slag, Medium Density.

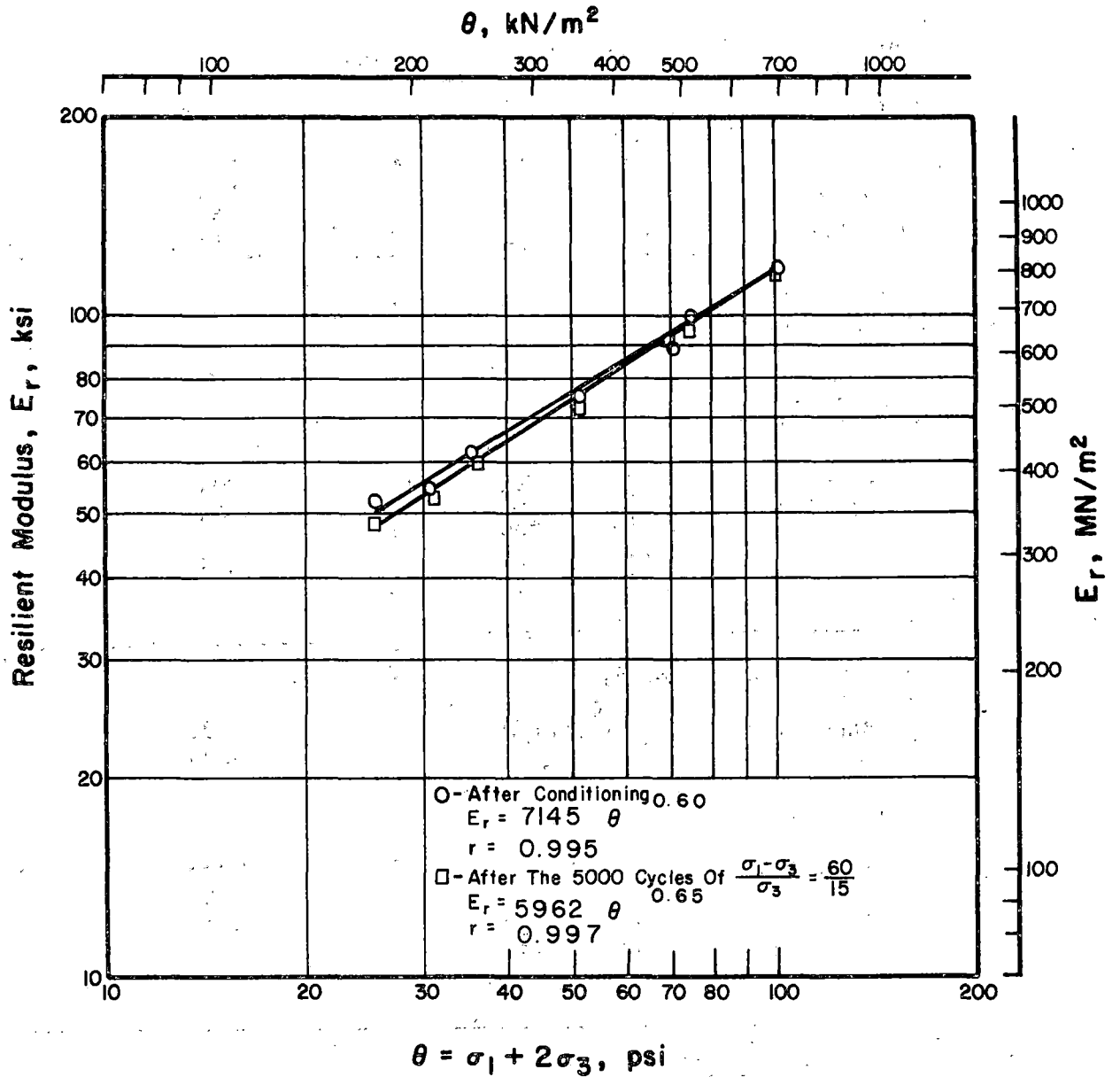


Figure 4.27. Relationship between  $E_r$  and  $\theta$  for Well Graded ( $n = 2/3$ ) Basalt, Medium Density.

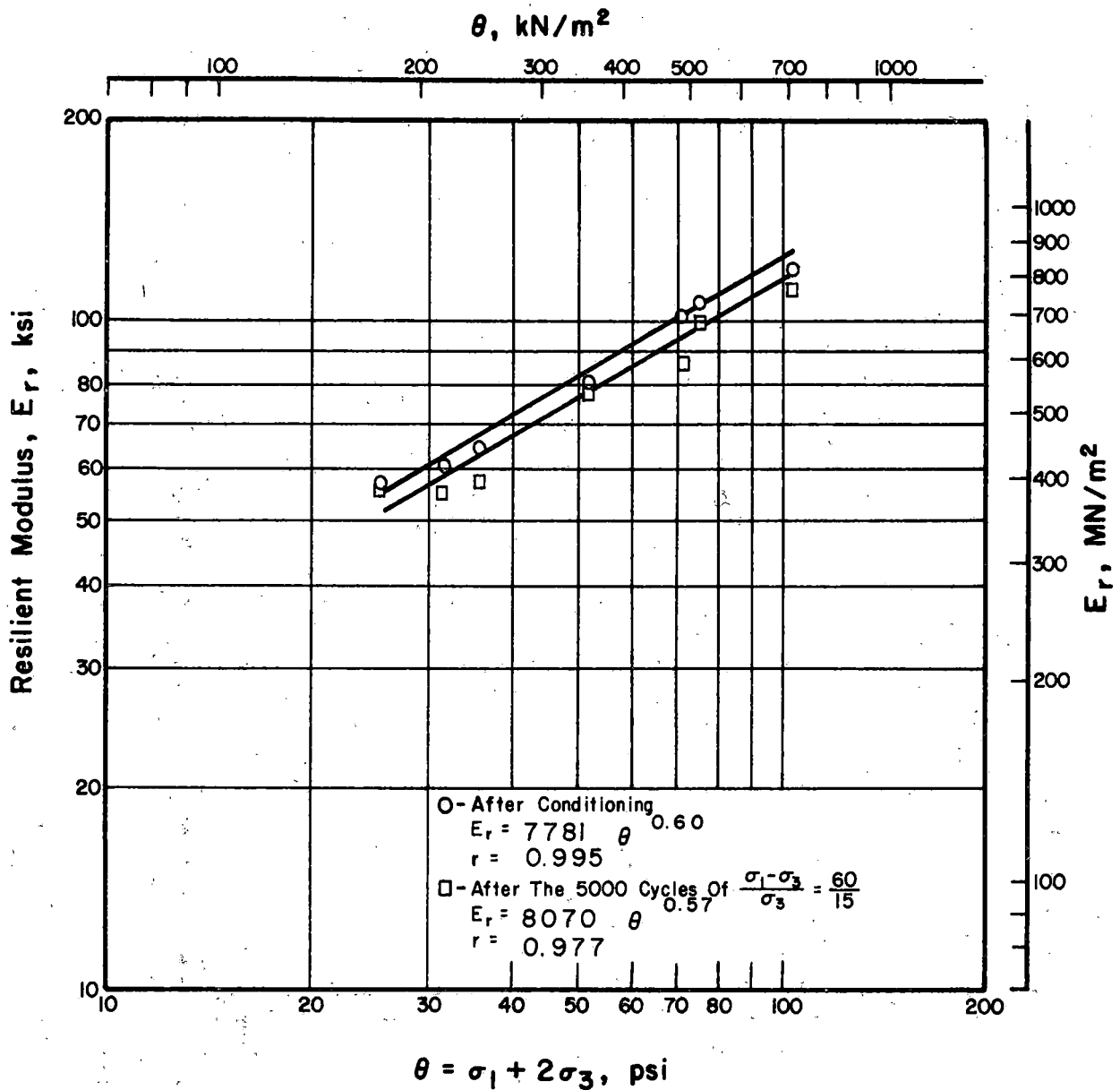


Figure 4.28. Relationship between  $E_r$  and  $\theta$  for Well Graded ( $n = 2/3$ ) Gravel, Medium Density.

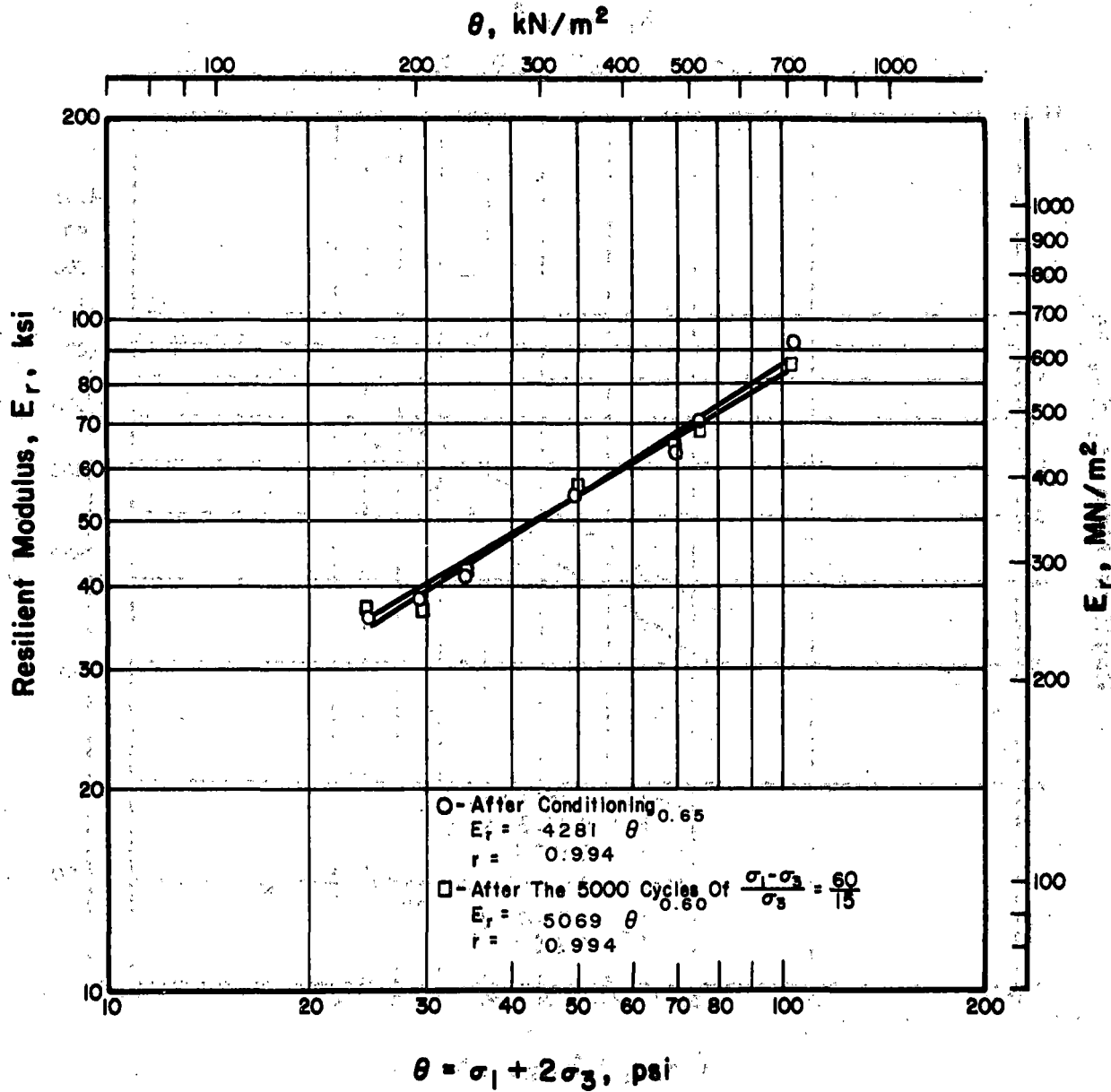


Figure 4.29: Relationship between  $E_r$  and  $\theta$  for Well Graded ( $n = 1/2$ ) Limestone, Medium Density, No. 1.

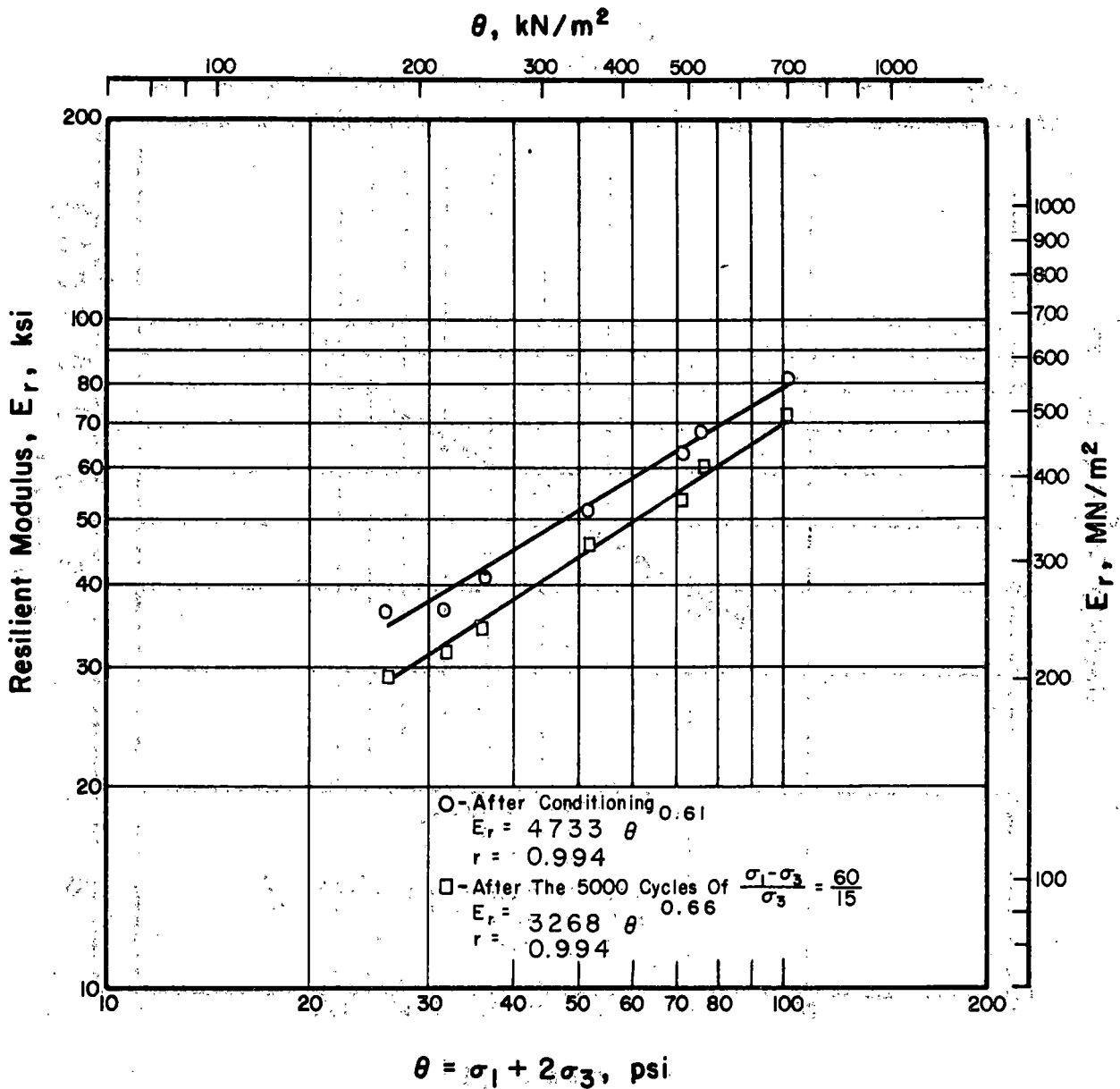


Figure 4.30. Relationship between  $E_r$  and  $\theta$  for Well Graded ( $n = 1/2$ ) Limestone, Medium Density, No. 2.

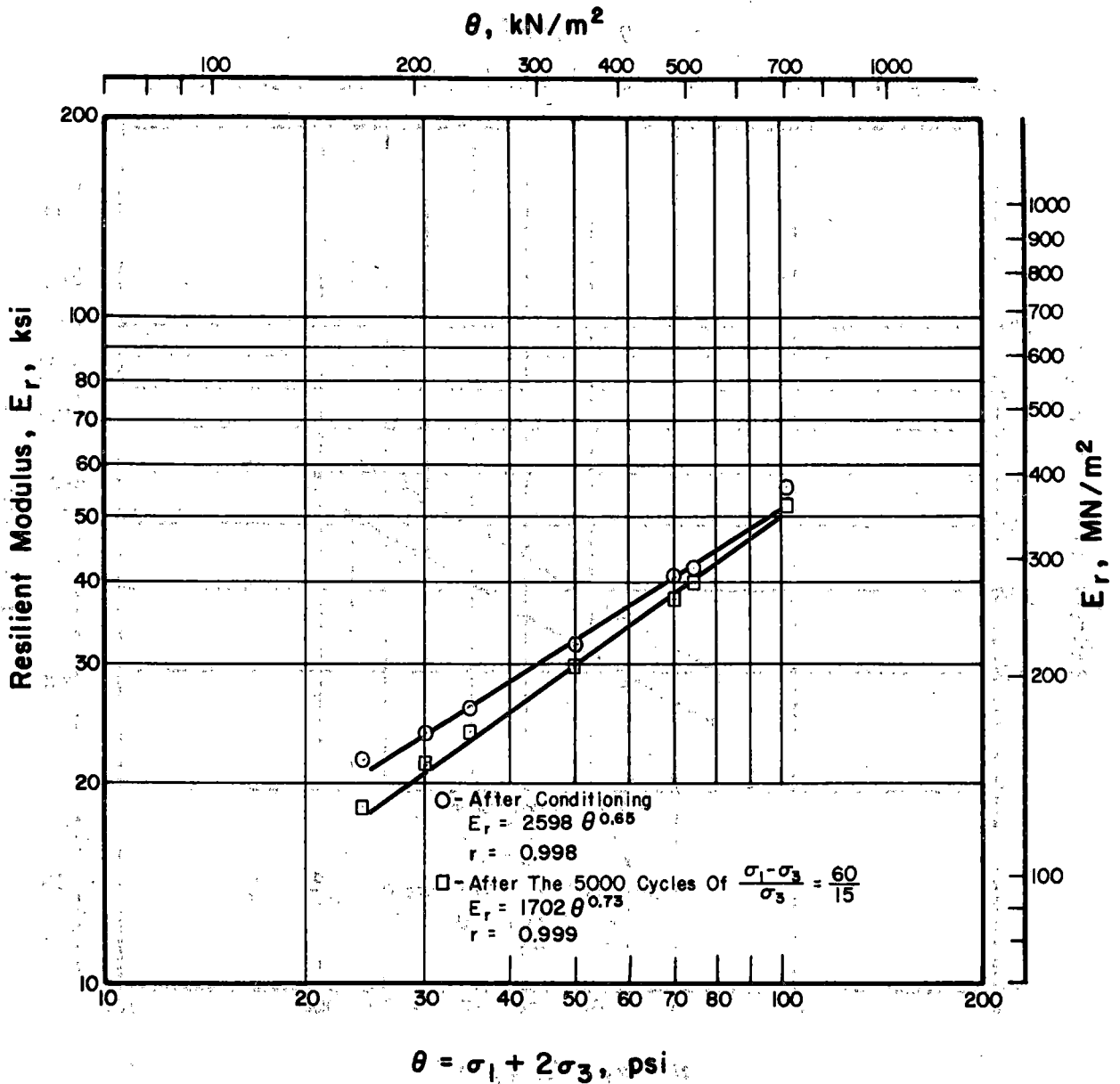


Figure 4.31. Relationship between  $E_r$  and  $\theta$  for CA-10 Gradation Limestone, Medium Density.

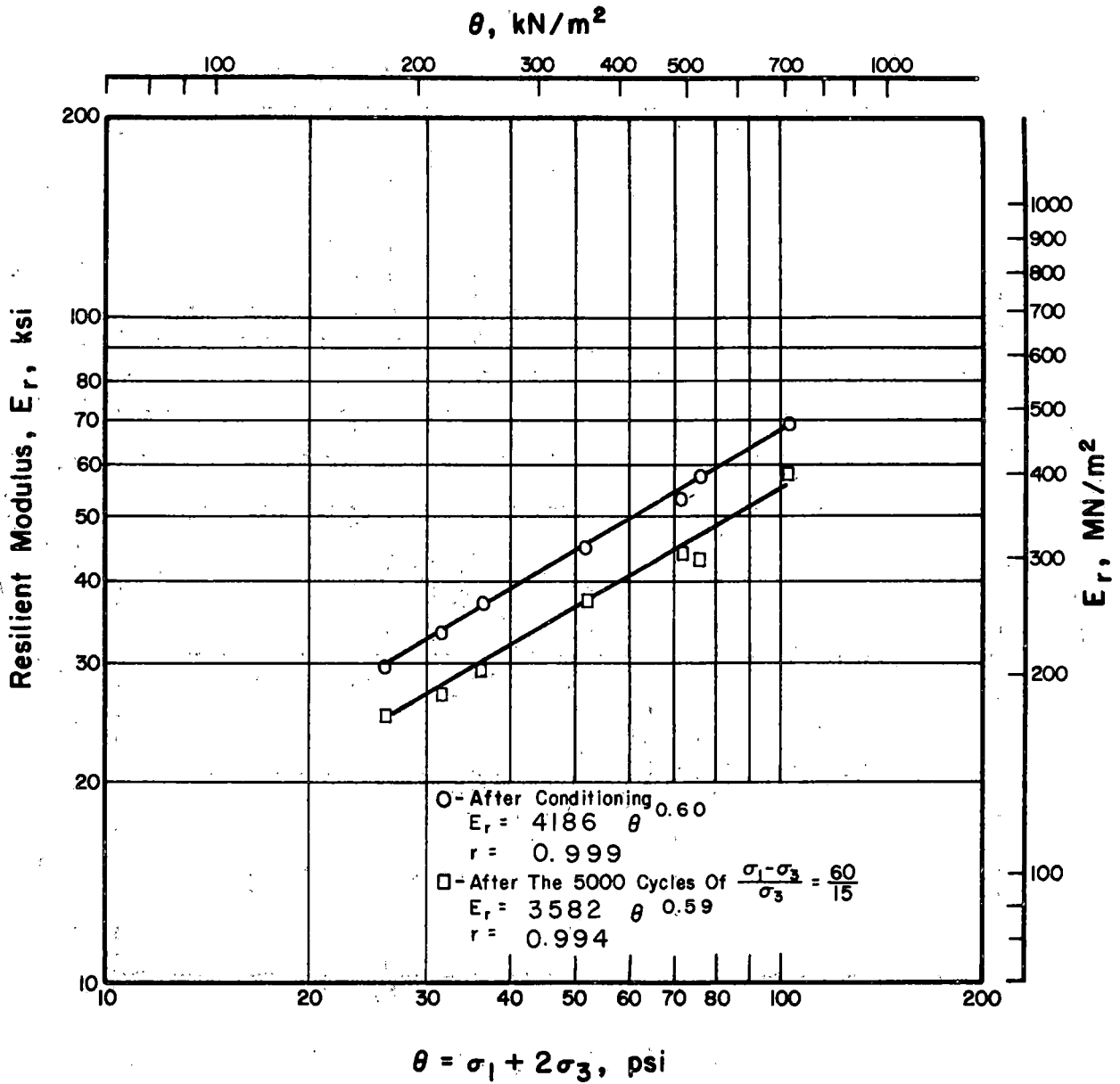


Figure 4.32: Relationship between  $E_r$  and  $\theta$  for CA-10 Gradation Limestone, High Density.

Figures 4.7 through 4.14 depict the results for specimens of the same gradation (No. 4) but prepared at compactive efforts different from the medium density specimens of Figures 4.1 through 4.6. Figures 4.7, 4.8, 4.9, and 4.10 show the results for the specimens that were prepared using the rodding technique only. Figures 4.11, 4.12, 4.13, and 4.14 are the results for No. 4 gradation specimens compacted for 45 seconds per layer (high density).

Figures 4.15 through 4.18 are the results for No. 5 ballast gradation specimens compacted for 5 seconds per layer (medium density) and Figures 4.19, 4.20, and 4.21 show the results for three different No. 5 gradation materials compacted by the rodding method only. All of the linear regression results were significant at  $\alpha = 0.01$  except for the values for the granitic gneiss tested immediately after conditioning. No explanation is known for the erratic behavior of this specimen. Figures 4.22 and 4.23 are the results for two No. 5 ballast gradation specimens prepared by compacting each layer for 45 seconds.

The results for 5 "well graded" specimens are shown in Figures 4.24 through 4.28. All of the well graded specimens were compacted for 5 seconds per layer (medium density).

The results of two additional limestone specimens with gradations only slightly different from well graded are shown in Figures 4.29 and 4.30. The resilient modulus lines for these two specimens are extremely close to those shown in Figure 4.24, the well graded limestone specimen. Because the gradations of these three limestone specimens were extremely close and because the densities and void ratios after compaction were

almost identical, it is believed that the similarity among the results affords a check on the repeatability of the testing procedure in general.

Figures 4.31 and 4.32 show the regression lines for two limestone specimens of CA-10 gradation of medium and high density, respectively. The resilient behavior of both specimens is considerably lower than that of the open graded materials. It should be noted that the results for the CA-10 limestone agree closely with those for similar material tested by Allen (5).

The following sections present the analysis of the resilient modulus results according to gradation, density, stress history, and basic material properties.

#### 4.4 Correlation with Characterization Test Results

Attempts were made to correlate resilient modulus values with the mechanical properties of the aggregate which are presented in Table 3.3. Because of the difficulty in using equations for correlation, the values of intercept, K, and slope, n, obtained from the regression analyses were used. Only the equations developed for the resilient response immediately after conditioning were considered because some of the specimens failed before the second resilient response tests could be conducted. Table 4.2 presents the results of the simple correlation analyses.

For the first correlation analysis all 32 samples were considered. The significant ( $\alpha = 0.05$ ) correlations were:

- (a) intercept with particle index and crushing value (inverse),
- (b) slope with specific gravity (inverse), and
- (c) Slope with crushing value.

Table 4.2. Correlation Coefficients for Regression Analyses of Resilient and Characterization Test Results.

	Particle Index	Specific Gravity	Los Angeles Abrasion Loss	Density	Void Ratio	Gradation Parameter	Flakiness Index	Soundness	Crushing Value
<u>All 32 specimens</u>									
Intercept, K	-.387*	.249	-.301	.100	-.035	-.283	-.137	-.124	-.356*
Slope, n	.355	-.488*	.148	-.078	-.121	.260	-.288	-.188	.393*
<u>14 No. 4 gradation specimens</u>									
Intercept, K	-.689*	.331	-.367	.640*	-.748*	-.108	-.184	.089	-.518
Slope, n	.711*	-.588*	.184	-.781*	.785*	-.254	-.264	-.535*	.589*
<u>6 No. 4 gradation specimens (medium density)</u>									
Intercept, K	-.986*	.514	-.194	.850*	-.986*	-.130	-.183	.114	-.569
Slope, n	.724	-.580	-.086	-.786	.825*	-.513	-.300	-.590	.425
<u>9 specimens (3 gradations of each of 3 types of material)</u>									
Intercept, K	-.217	.162	-.310	.172	-.156	-.061	-.308	-.387	-.447
Slope, n	-.077	.265	-.322	.346	-.237	.271	-.145	-.398	-.309

\* significant at  $\alpha = 0.05$

Another analysis was made in which only the results for the No. 4 ballast gradation were considered. The following significant ( $\alpha = 0.05$ ) correlations were observed:

- (a) intercept with particle index and void ratio (inverse)
- (b) intercept with density,
- (c) slope with specific gravity, density, and soundness (inverse), and
- (d) slope with particle index, void ratio, and crushing value.

Because all 14 of the No. 4 gradation specimens were included in the above analysis, there was some inherent bias, e.g., one basalt specimen but 3 limestone specimens were included. To give equal weighting to each material type, another analysis included only the medium density No. 4 gradation specimens. The significant ( $\alpha = 0.05$ ) correlations were reduced to:

- (a) intercept with particle index and void ratio (inverse),
- (b) intercept with density, and
- (c) slope with void ratio.

To include gradation parameter on an equal basis, 3 levels of gradation of each of 3 material types (limestone, basalt, and gravel) were included in another correlation analysis. Neither intercept nor slope was found to correlate significantly ( $\alpha = 0.05$ ) with any of the material properties for the analysis of these 9 samples.

From the results of the correlation analyses no consistent relations could be established, although in several instances the intercept and particle index values seemed to be related.

Further attempts to determine the effects on resilient response of gradation changes and material type are reported in the following section.

#### 4.5 Analysis of Variance Results

Additional attempts were made to determine the effect on resilient response of material type and gradation through the use of randomized complete block (RCB) analyses. The effects of loading history and relative density were investigated also. The results of the analyses are included in Tables 4.3 and 4.4.

Because previous research (5) has shown that the effect of variations in the slope ( $n$ ) and intercept values ( $K$ ) of the predictive equations for resilient modulus often is to cancel one another, two values of  $E_r$  were calculated at values of the first stress invariant,  $\Theta$ , of 35 psi (241 kN/m<sup>2</sup>) and 90 psi (621 kN/m<sup>2</sup>). Thus the variables included in the analyses were  $K$ ,  $n$ ,  $E_r$  at 35 psi (241 kN/m<sup>2</sup>) and  $E_r$  at 90 psi (621 kN/m<sup>2</sup>).

To determine the effect of maximum particle size, two gradations (No. 4 and No. 5 ballast) each of 5 material types were considered. None of the four variables showed significant ( $\alpha = 0.05$ ) differences due to the change in gradation. The conclusion was that there is no difference in resilient modulus between the No. 4 and No. 5 gradations.

To further examine the effect of gradation 3 levels of gradation (No. 4, No. 5, and well graded) each of 3 material types (limestone, basalt, and gravel) were included in the analysis. Only one of the four variables,  $E_r$  at 90 psi (621 kN/m<sup>2</sup>), proved to have significant ( $\alpha = 0.05$ ) differences due to gradation. The values of  $E_r$  at 90 psi (621 kN/m<sup>2</sup>) were further analyzed using Duncan's multiple range; no differences were found

Table 4.3. Randomized Complete Block Analyses of Resilient Test Results.

	Intercept, K	Slope, n	$E_r$ at 90 psi	$E_r$ at 35 psi
F values for maximum size analysis (No. 4 and No. 5 gradations)	0.081	0.149	0.199	0.014
F values for gradation analysis (No. 4, No. 5, and well graded for 3 material types)	0.021	0.737	10.10*	4.75
F values for density analysis (low, medium, and high density for each of 6 specimen types)	1.229	0.270	3.701	2.810
F values for stress history effects (before and after 5000 cycles at $\sigma_D/\sigma_3$ of 60/15)	3.312	3.727		

\*significant at  $\alpha = 0.05$

Multiple range test of Duncan for  $E_r$  at 90 psi:

	<u>Gradation</u>		
	<u>No. 5</u>	<u>No. 4</u>	<u>Well Graded</u>
Mean value of $E_r$ at 90 psi, ksi	<u>69.8</u>	<u>77.1</u>	98.4

Note: a line beneath values indicates that no significant difference exists.

Table 4.4. Randomized Complete Block Analysis of Resilient Test Results by Material Type.

	Intercept, K	Slope, n	$E_r$ at 90 psi	$E_r$ at 35 psi
F values for material type analysis (limestone, granitic gneiss, Chicago slag, and gravel; 3 gradations of each)	3.62	14.30*	7.66*	5.99*

\*significant at  $\alpha = 0.05$

Multiple range test of Duncan for slope, n:

	<u>Gravel</u>	<u>Limestone</u>	<u>Granitic Gneiss</u>	<u>Chicago Slag</u>
Mean value of slope	0.47	0.48	0.55	0.66

Multiple range test of Duncan for  $E_r$  at 90 psi:

	<u>Limestone</u>	<u>Granitic Gneiss</u>	<u>Chicago Slag</u>	<u>Gravel</u>
Mean value of $E_r$ at 90 psi, ksi	59.6	78.0	82.3	107.7

Multiple range test of Duncan for  $E_r$  at 35 psi:

	<u>Limestone</u>	<u>Chicago Slag</u>	<u>Granitic Gneiss</u>	<u>Gravel</u>
Mean value of $E_r$ at 35 psi, ksi	38.0	44.3	46.5	70.3

Note: a line beneath values indicates that no significant difference exists.

between the values for the No. 4 and No. 5 ballast gradations, but both were significantly lower than the values for the well graded specimens. In general, the effect on resilient modulus of changes in gradation was slight.

The effect of density was included by considering 3 density levels (low, medium, and high) each of 6 different specimen materials. From Table 4.3 it can be seen that there were no differences among the resilient responses.

Also included in Table 4.3 is the analysis of the resilient responses of the specimens to determine the effect of loading history. None of the four variables was significantly ( $\alpha = 0.05$ ) different for the two tests conducted. The conclusion that the resilient response of granular materials remains essentially unchanged throughout a complex loading history thus is reinforced (3, 5, 9).

To include the effect of material type, an analysis was made of low, medium, and high density, No. 4 ballast specimens of limestone, granitic gneiss, gravel, and Chicago slag. The results are shown in Table 4.4.

There was no difference in the values of intercept,  $K$ , among the 4 materials considered, but significant ( $\alpha = 0.05$ ) differences among the material types did exist for slope,  $E_r$  at 90 psi ( $621 \text{ kN/m}^2$ ), and  $E_r$  at 35 psi ( $241 \text{ kN/m}^2$ ). A further analysis (Table 4.3) was made using the multiple range test of Duncan.

Although differences among the values for the various material types are shown, no consistent trends can be noted. The Chicago slag had the highest value of slope,  $n$ , and the value was significantly different from

the other three. For the values of  $E_r$  at 35 psi (241 kN/m<sup>2</sup>) and at 90 psi (621 kN/m<sup>2</sup>), the gravel specimens had the highest mean values and the values were significantly different from those for the other three material types.

Although resilient response depends somewhat on material type, the lack of consistency in the data prevents making any specific conclusions. The differences in resilient behavior were so slight as to be negligible from the CRTSS structural response standpoint.

#### 4.6 Summary

The resilient response of granular materials cannot readily be linked to material properties. In addition the resilient response is almost totally independent of gradation, loading history, and density. Although some dependence of resilient response on material type can be shown, the effects are not consistent. None of the other variables is nearly so important a parameter in determining the resilient response of granular materials as is the stress level.

## CHAPTER 5 PRESENTATION AND ANALYSIS OF RESULTS FOR PLASTIC BEHAVIOR

### 5.1 Introduction

Permanent deformation is a major factor contributing to the deterioration of the CRTSS. Some research has been done on the permanent deformation behavior of dense graded aggregates, but little research has been done concerning the repeated load characteristics of open graded materials such as ballast. This chapter presents the accumulated plastic strain results of the repeated load tests conducted on a variety of material types of open graded nature and also the results for two dense graded specimens.

All of the primary test specimens were conditioned for 5000 cycles at a deviator stress of 45 psi ( $310 \text{ kN/m}^2$ ) and a confining pressure of 15 psi ( $103 \text{ kN/m}^2$ ). The permanent deformations recorded by the LVDT method were divided by the specimen height to obtain the strains at 10, 100, 1000, and 5000 cycles. It should be noted that the plastic strain data obtained during the conditioning phase have not been influenced by any stress history effects and are probably the most representative results for making direct comparisons.

After the conditioning phase the stress ratio was increased; 5000 load cycles were applied at the new stress level. The process was repeated until the sample failed. The entire test sequence is included in Table 3.8. Whenever 5 percent strain was attained at any given stress level, testing was discontinued.

The sample height at the start of each 5000 load cycles was taken as the gauge length for strain determination.

## 5.2 Plastic Strain Results

The purpose of this part of the research was to determine the effects of material type and gradation on the plastic strain behavior under repeated load conditions of a variety of aggregate types. The effects of stress history, degree of compaction, and stress level were considered also.

Before the primary tests were started, preliminary samples were tested to determine the effects of stress history on the plastic strain behavior of open graded materials such as ballast. The results are included in Section 3.2.4.

After careful consideration of the preliminary test results, the primary testing program was started. Figures 5.1 through 5.9 are plots of permanent strain versus logarithm of the number of cycles for the data obtained during the conditioning phase of testing. As previously noted the data collected during the conditioning phase have not been influenced by the effects of other stress levels (no stress history). The results obtained at stress levels other than conditioning are included in Figures 5.10 through 5.40. The following sections include the analyses of the data collected during the permanent deformation portion of the testing program.

## 5.3 Linear Regression Analysis

Linear regression analysis was used to develop relationships between the plastic strain and the corresponding number of loading cycles.

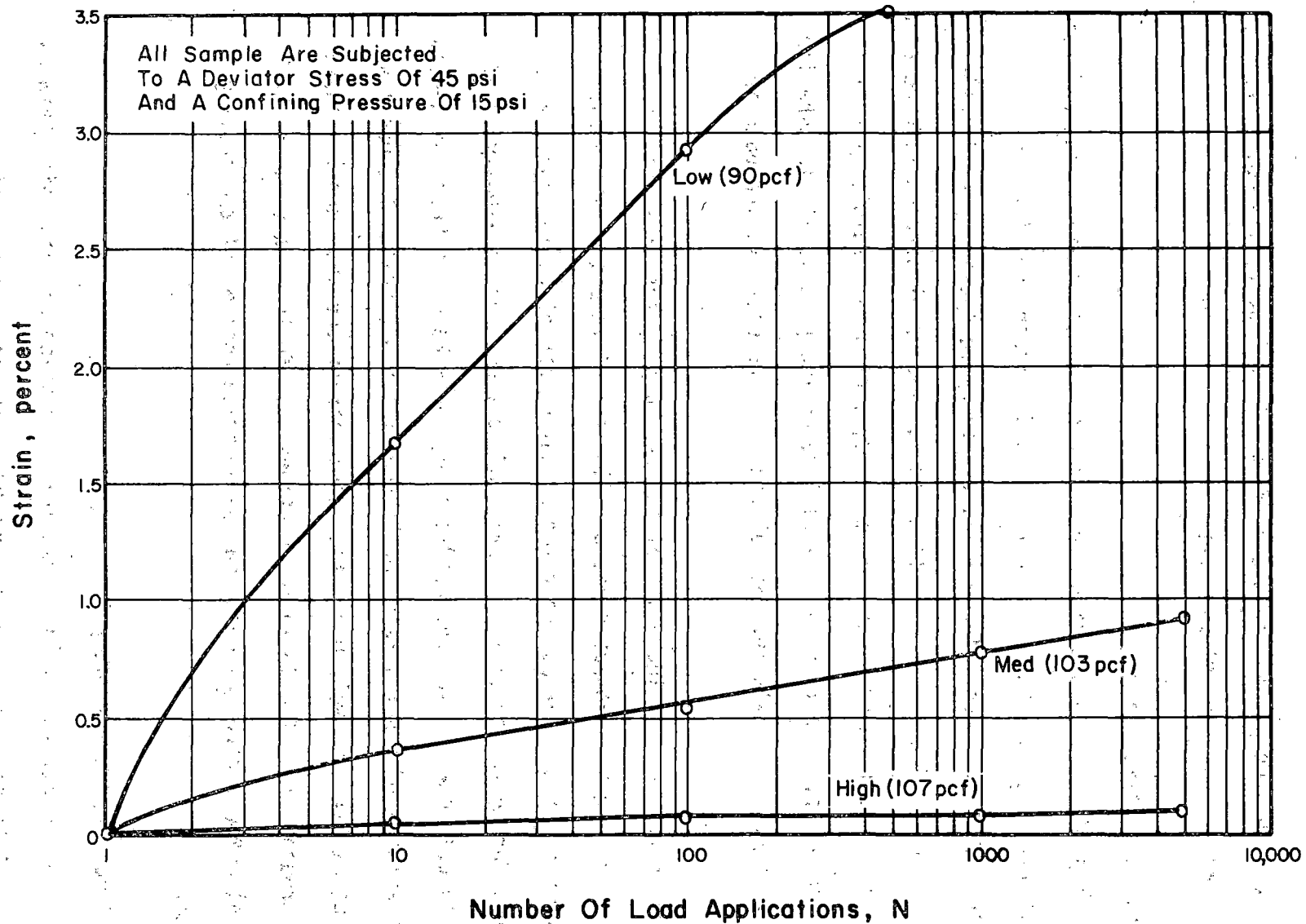


Figure 5.1. Effect of Density on Plastic Strain Response for No. 5 Gradation Limestone.

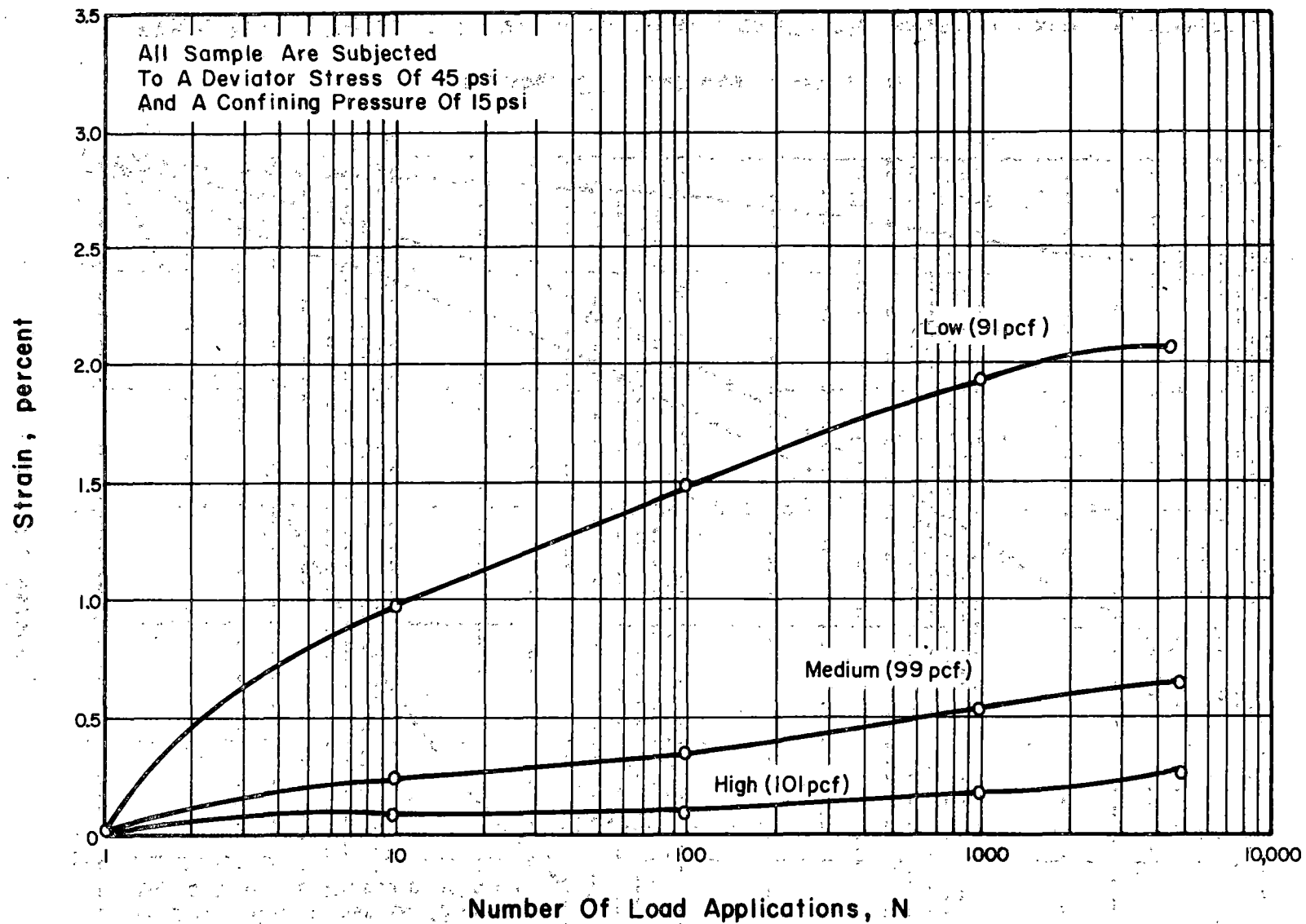


Figure 5.2. Effect of Density on Plastic Strain Response for No. 5 Gradation Kansas Test Track Slag.

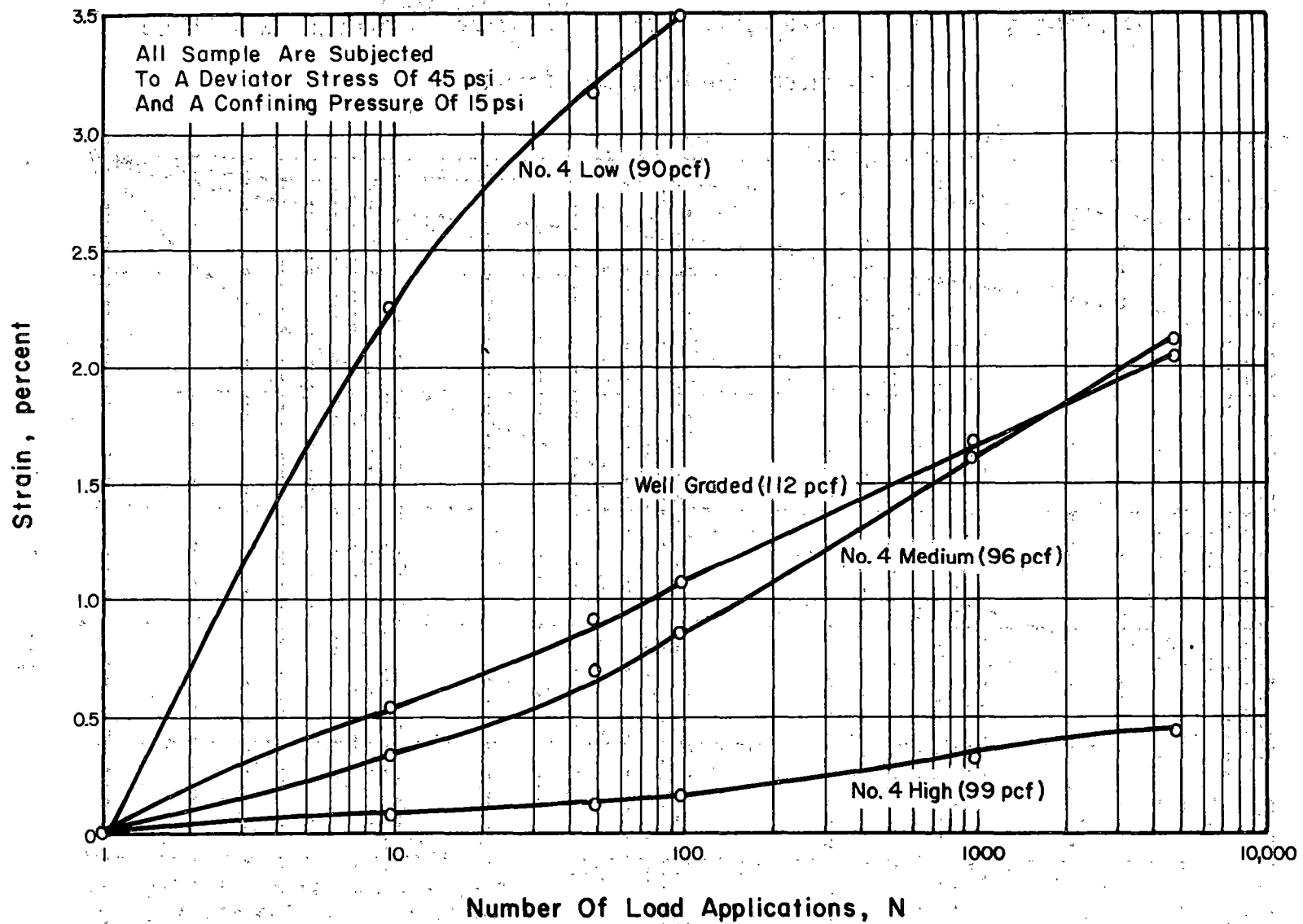


Figure 5.3. Effects of Gradation and Density on Plastic Strain Response for Limestone.

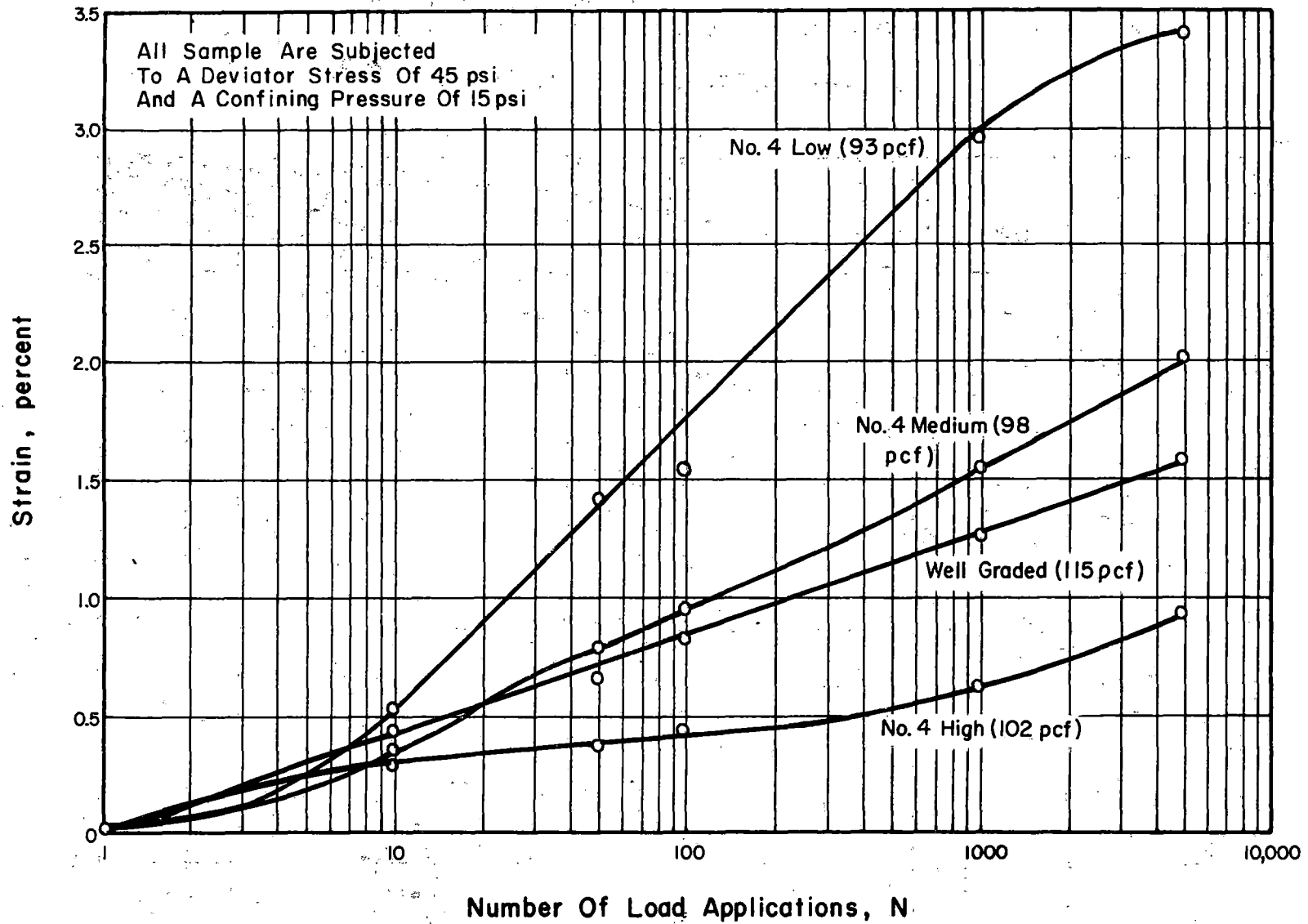


Figure 5.4. Effects of Gradation and Density on Plastic Strain Response for Granitic Gneiss.

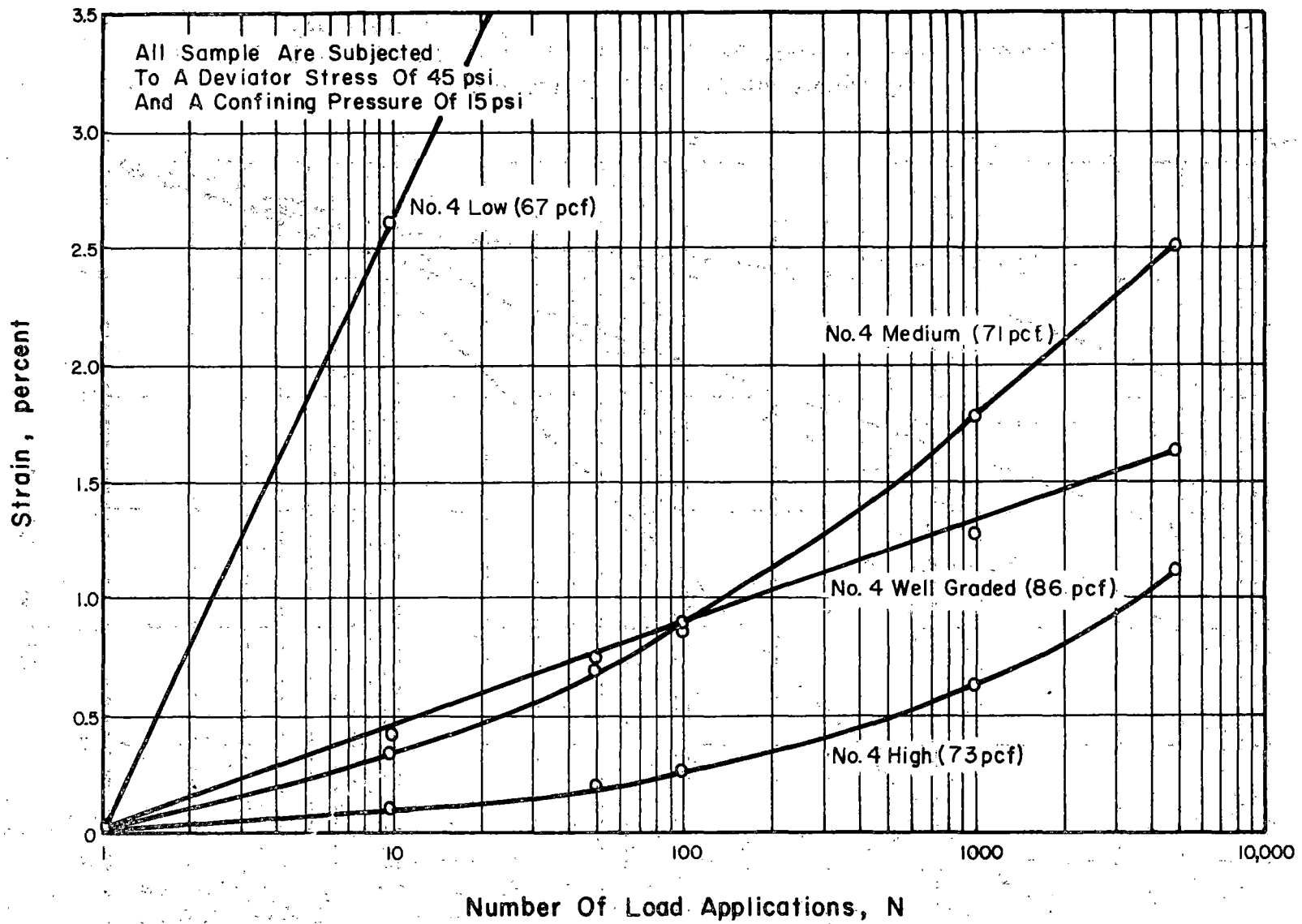


Figure 5.5. Effects of Gradation and Density on Plastic Strain Response for Chicago Blast Furnace Slag.

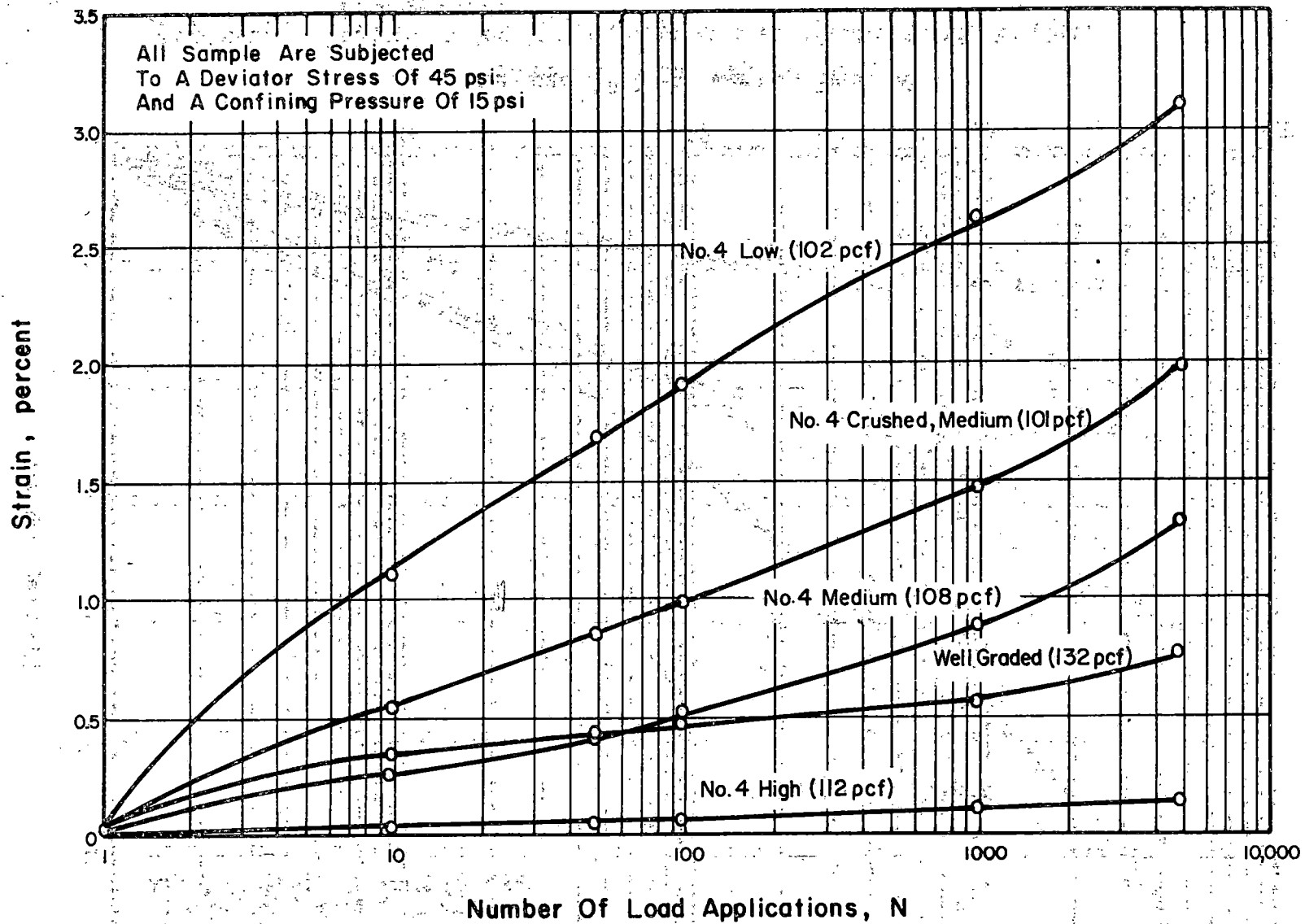


Figure 5.6. Effects of Crushing, Density, and Gradation on Plastic Strain Response for Gravel.

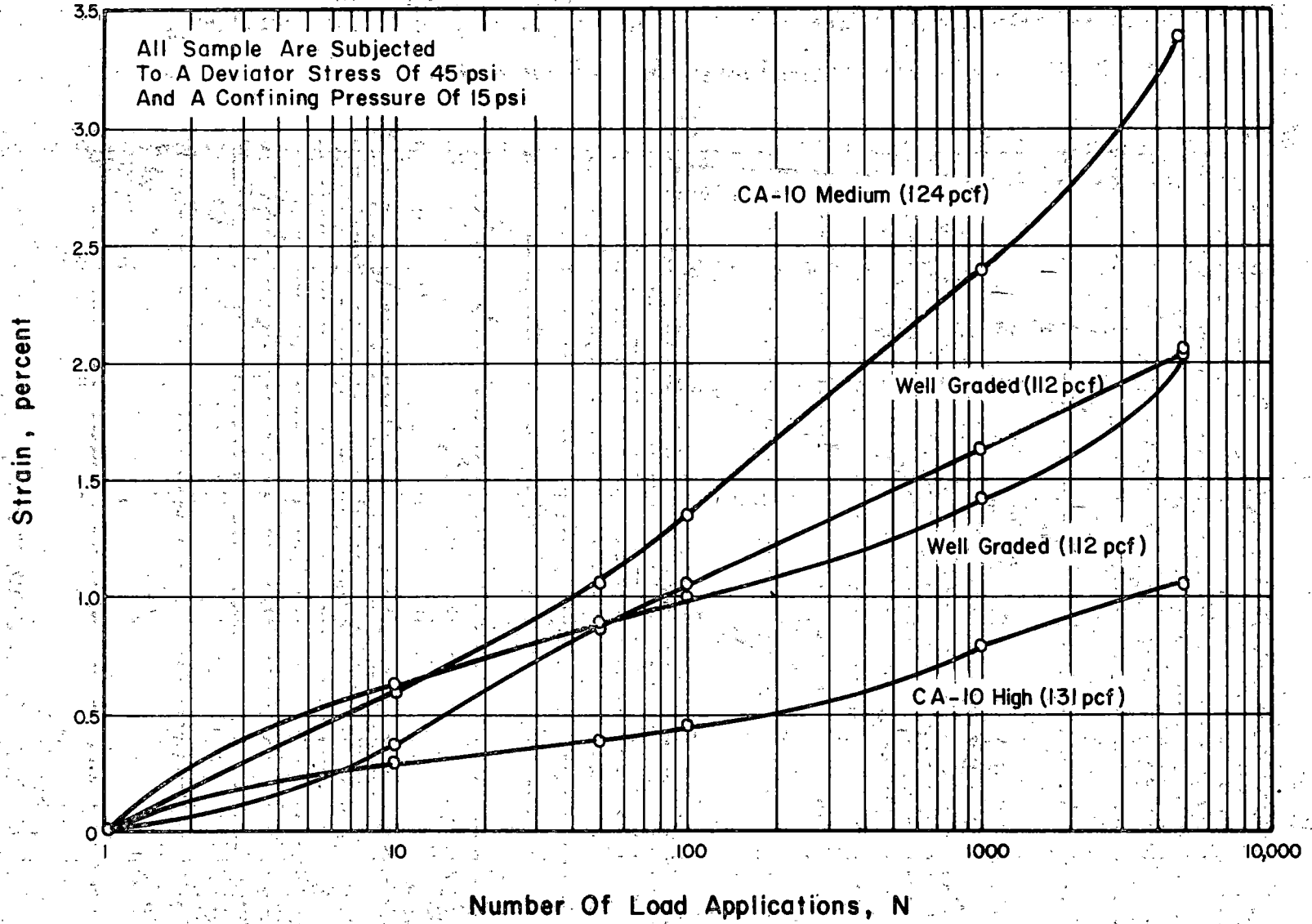


Figure 5.7. Effects of Density and Gradation on Plastic Strain Response for Limestone.

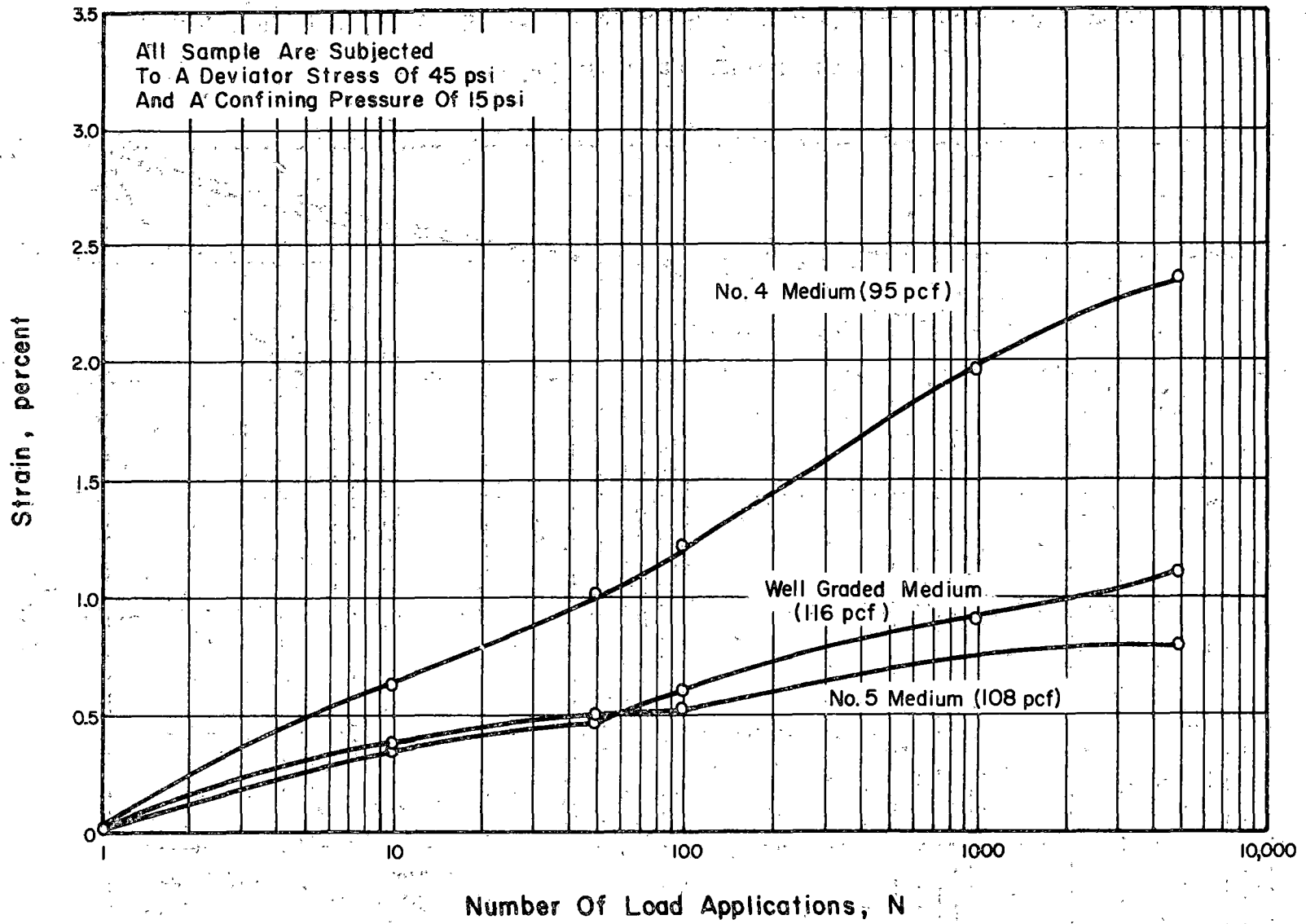


Figure 5.8. Effects of Gradation on Plastic Strain Response for Basalt.

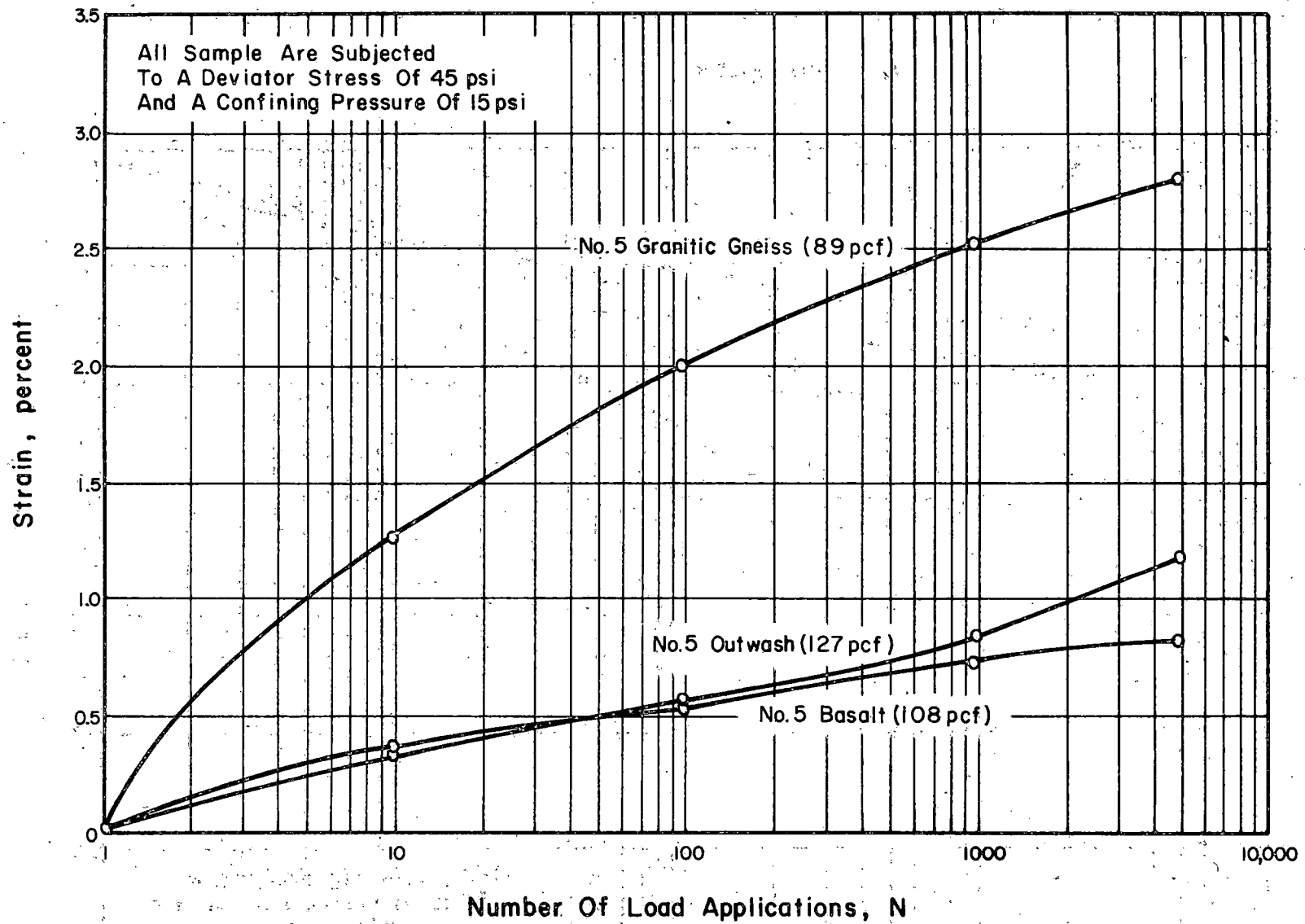


Figure 5.9. Effects of Material Type and Density on Plastic Strain Response.

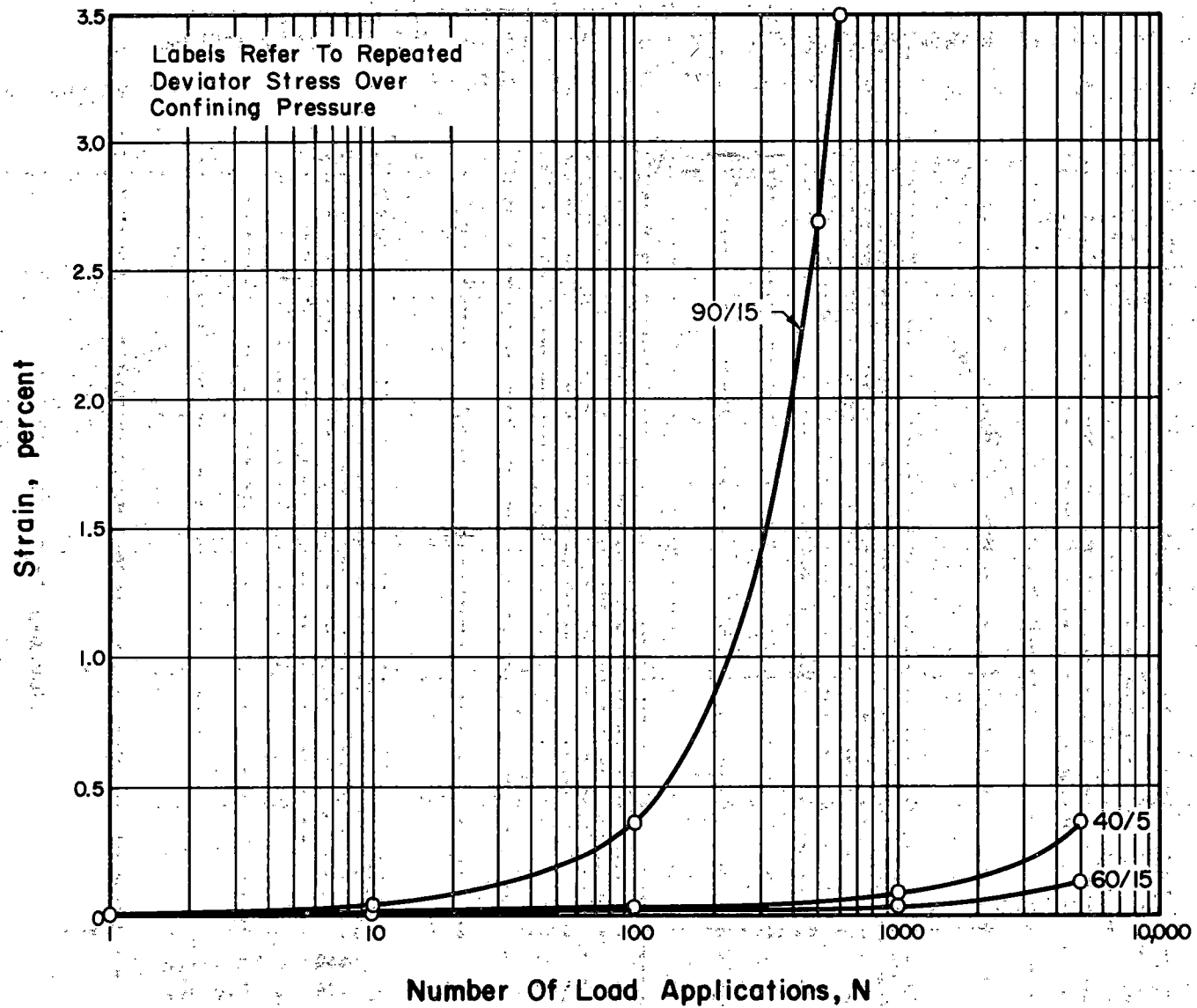


Figure 5.10. Effect of Stress Level on Plastic Strain Response of No. 5 Gradation Limestone, Medium Density.

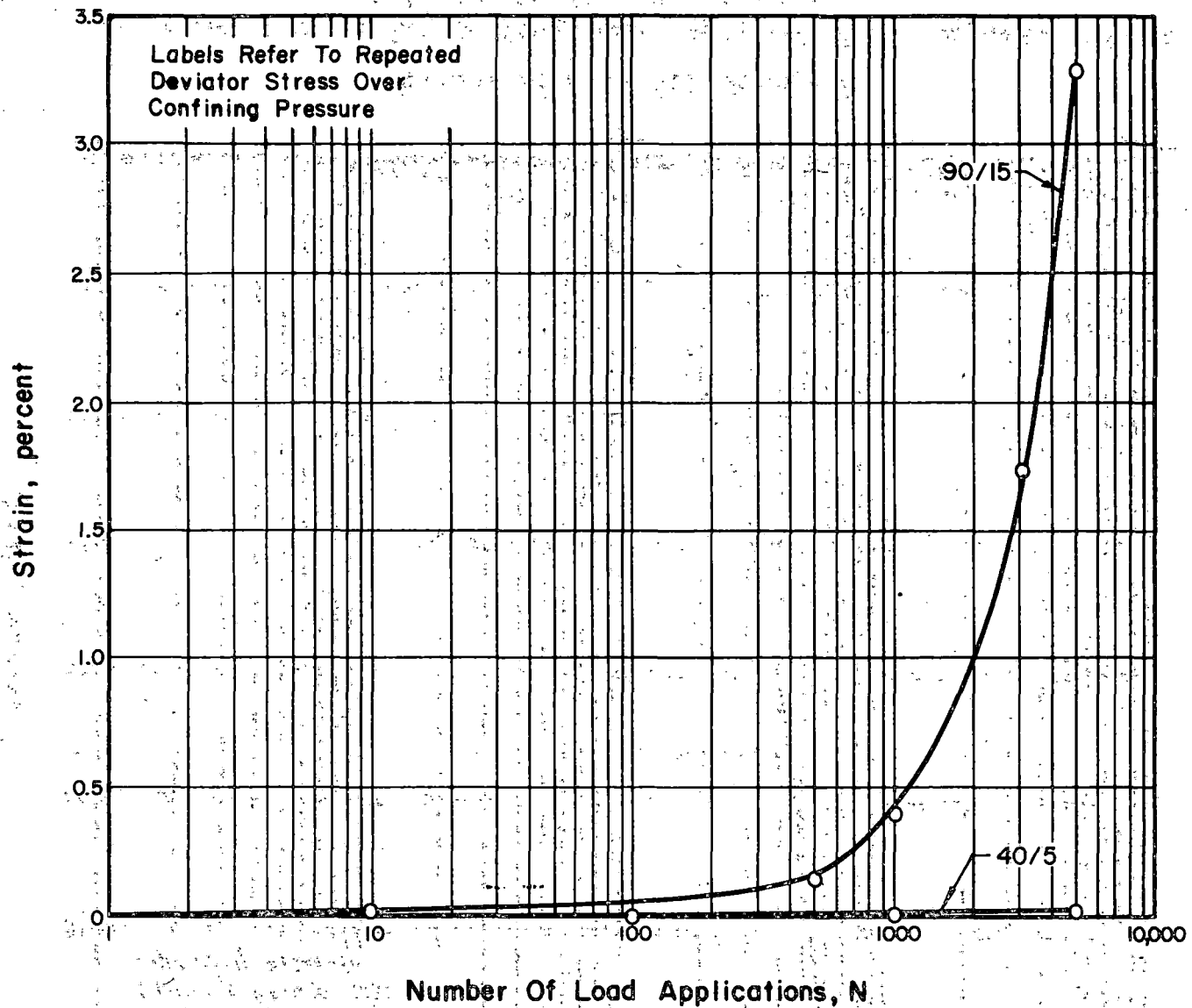


Figure 5.11. Effect of Stress Level on Plastic Strain Response of No. 5 Gradation Limestone, High Density.

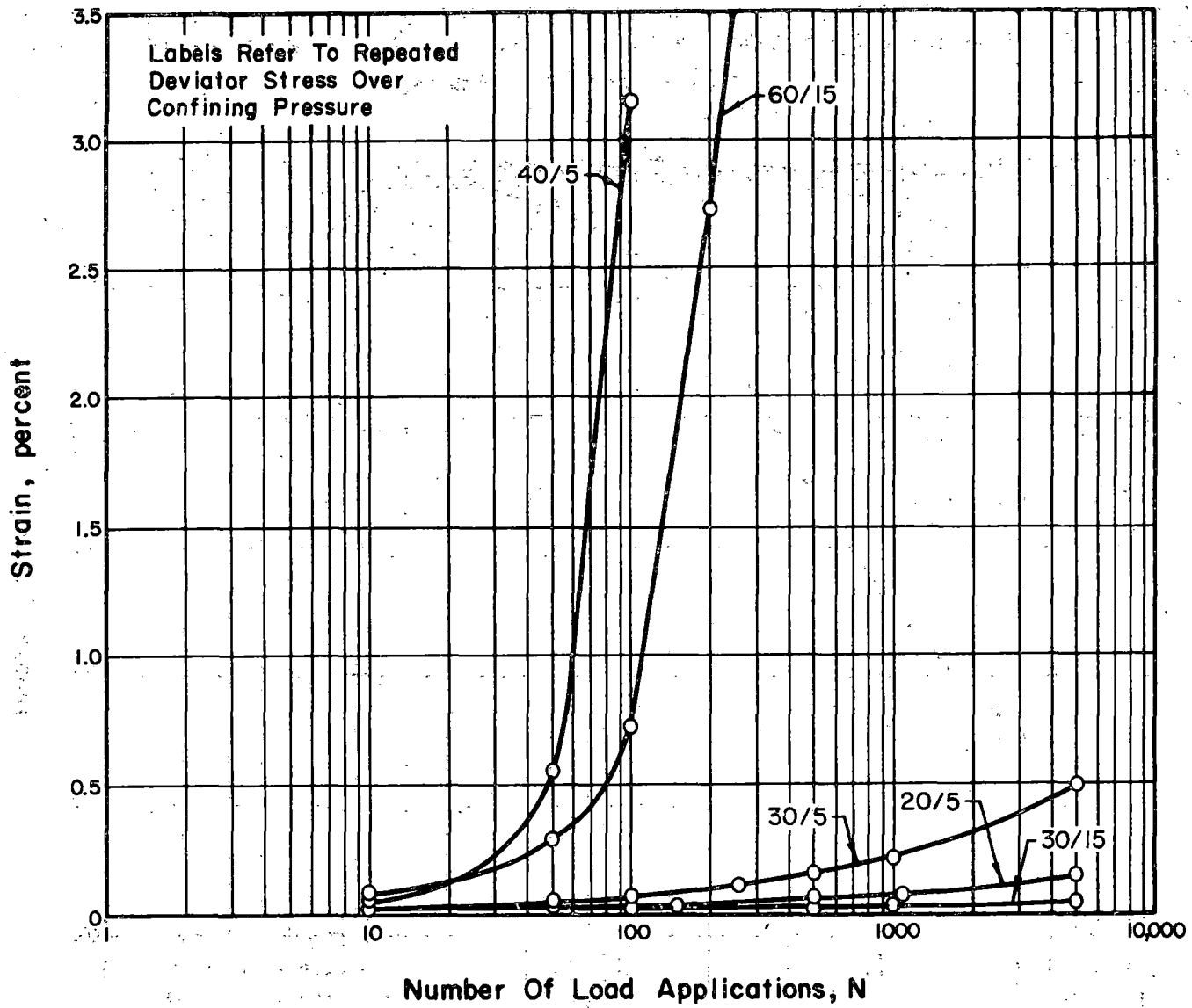


Figure 5.12. Effect of Stress Level on Plastic Strain Response of No. 4 Gradation Limestone, Low Density.

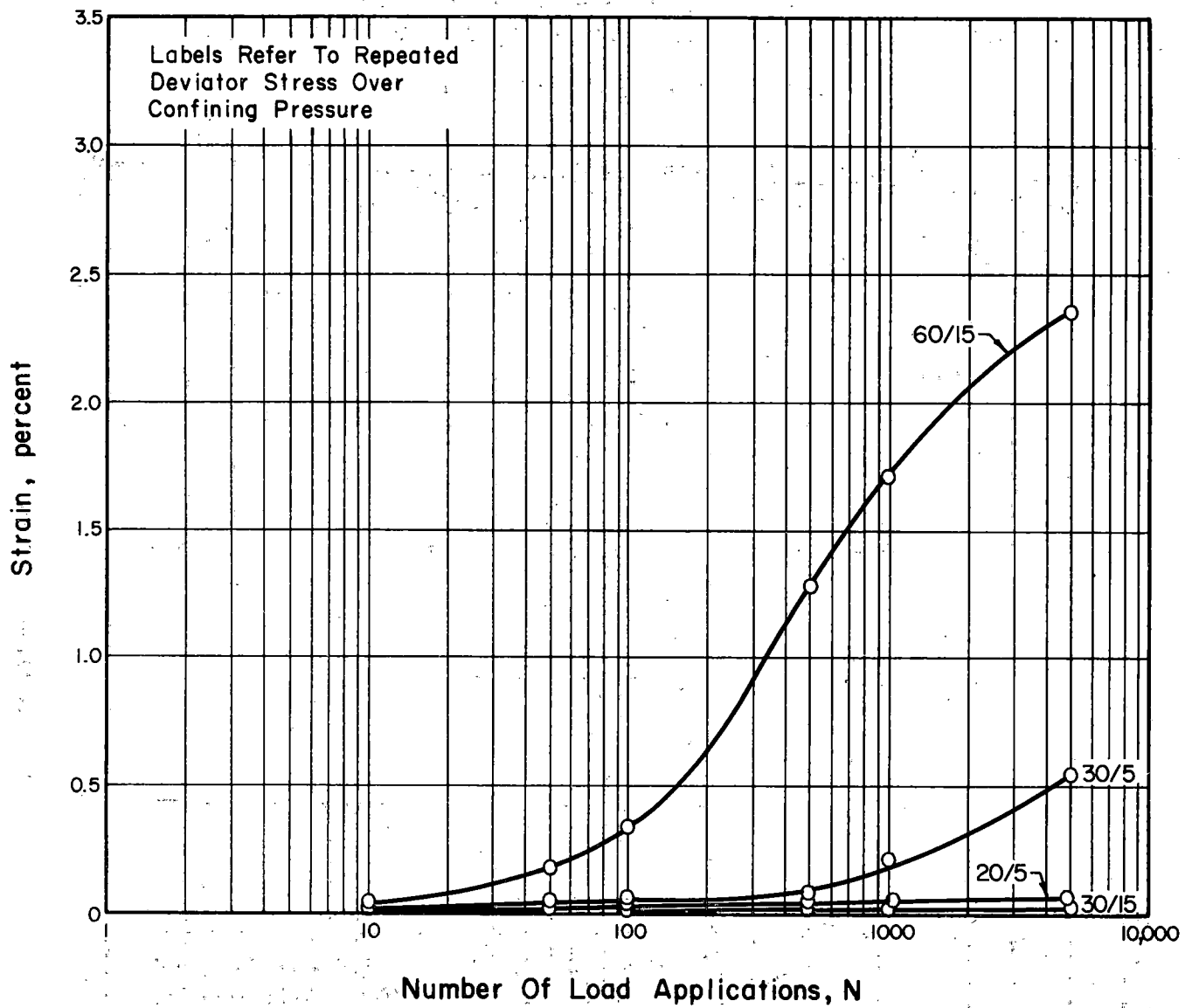


Figure 5.13. Effect of Stress Level on Plastic Strain Response of No. 4 Gradation Limestone, Medium Density.

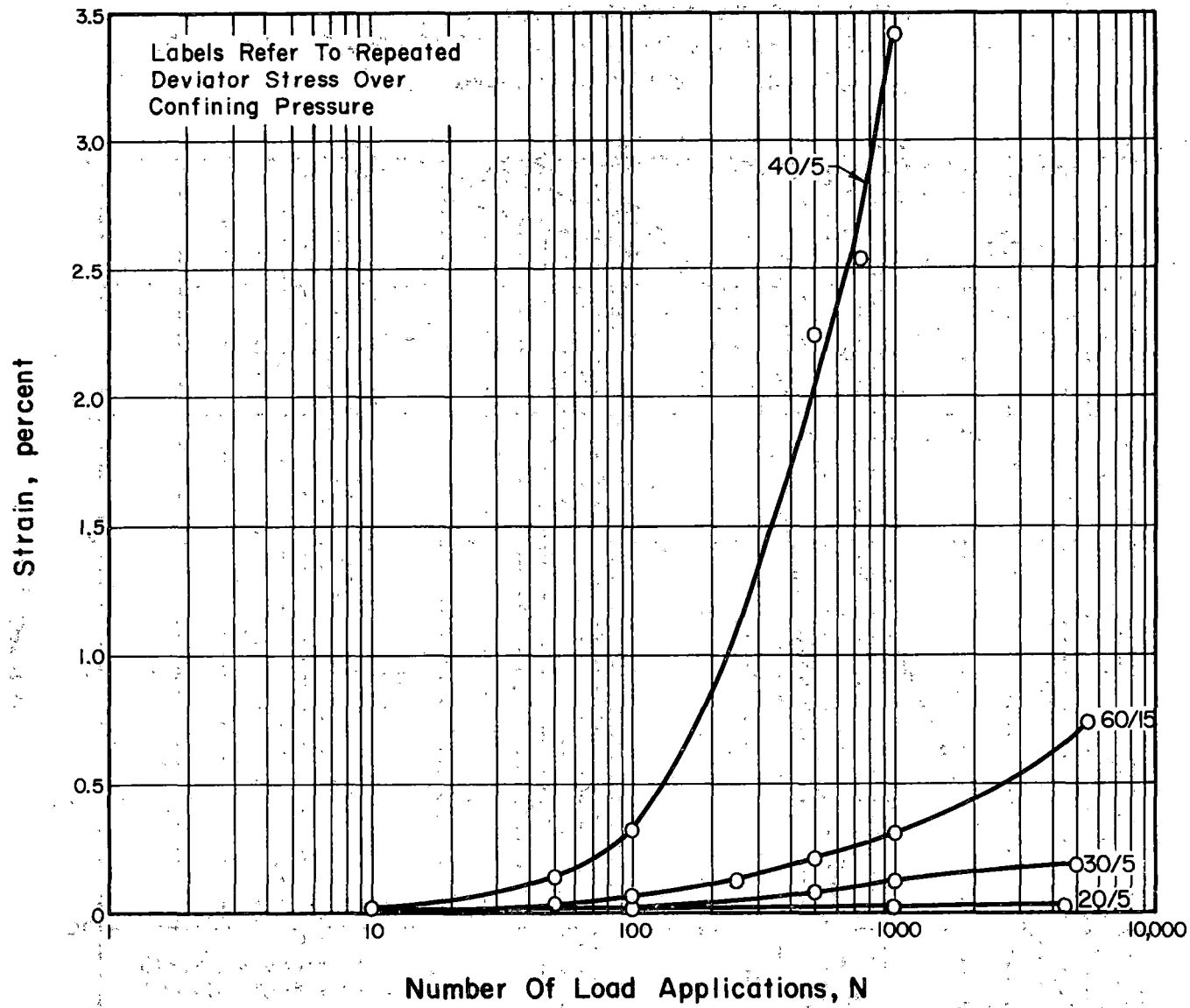


Figure 5.14. Effect of Stress Level on Plastic Strain Response of No. 4 Gradation Limestone, High Density.

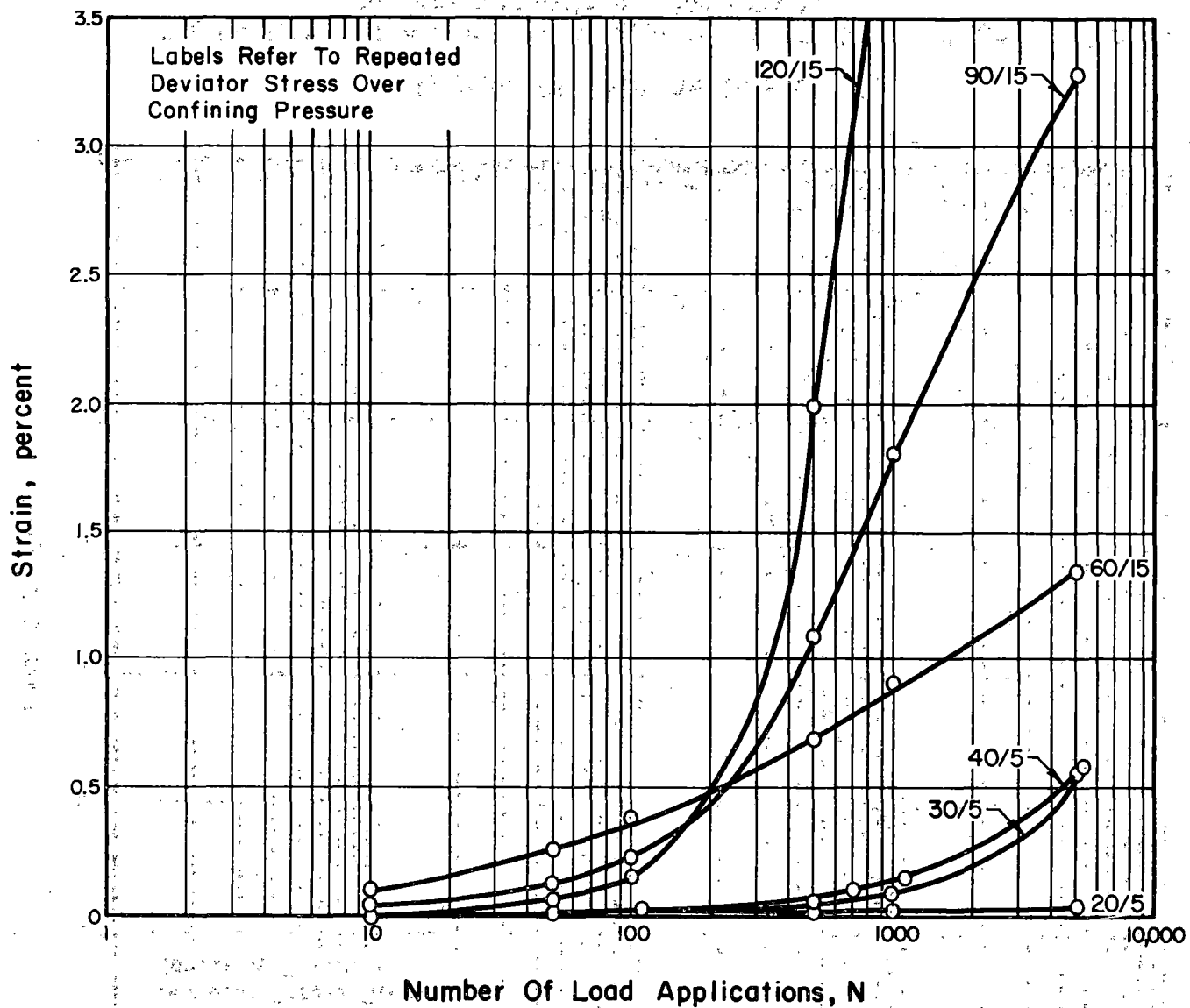


Figure 5.15. Effect of Stress Level on Plastic Strain Response of Well Graded ( $n = 2/3$ ) Limestone, Medium Density.

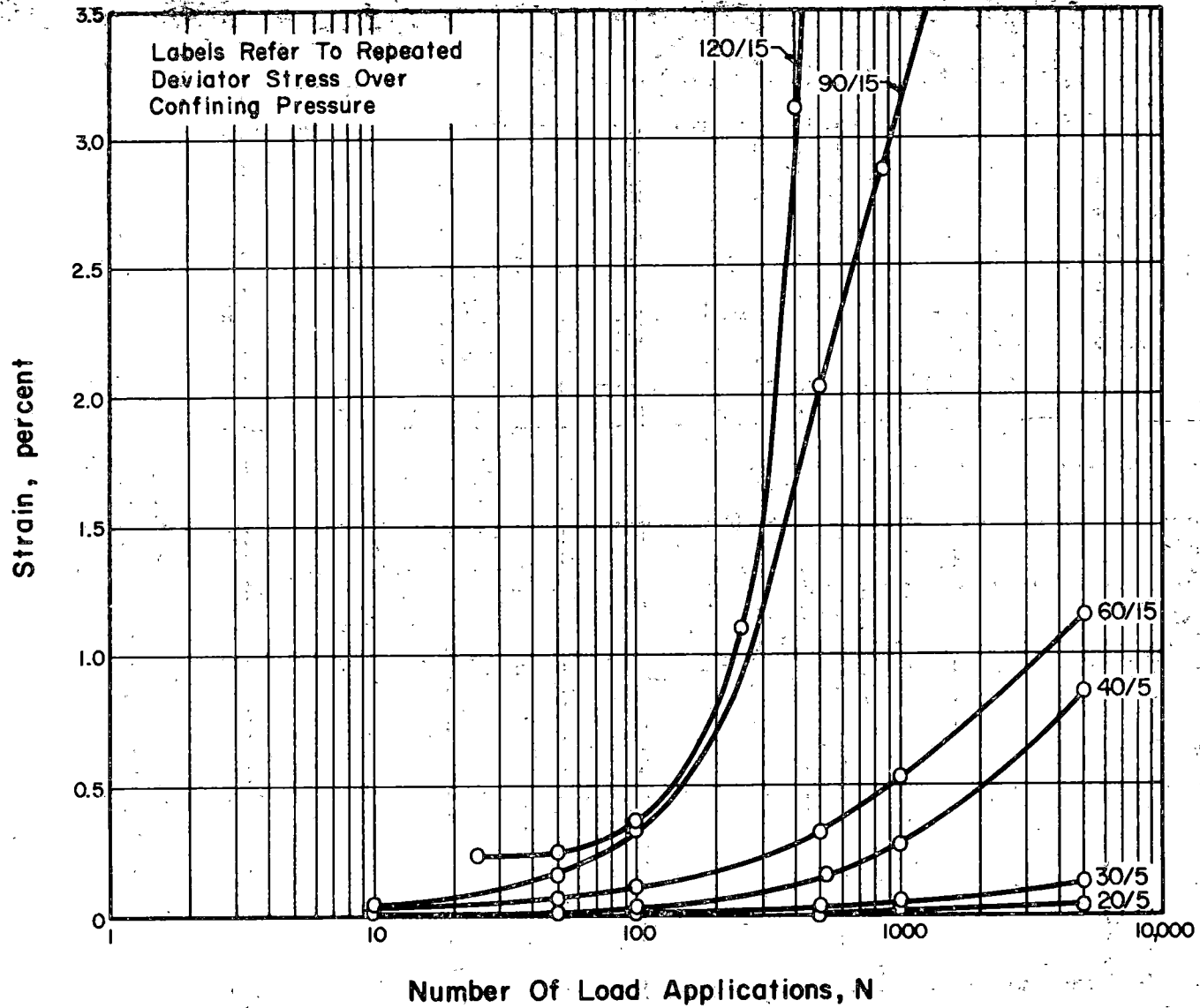


Figure 5.16. Effect of Stress Level on Plastic Strain Response of Well Graded. ( $n = 1/2$ ) Limestone, Medium Density, No. 1.

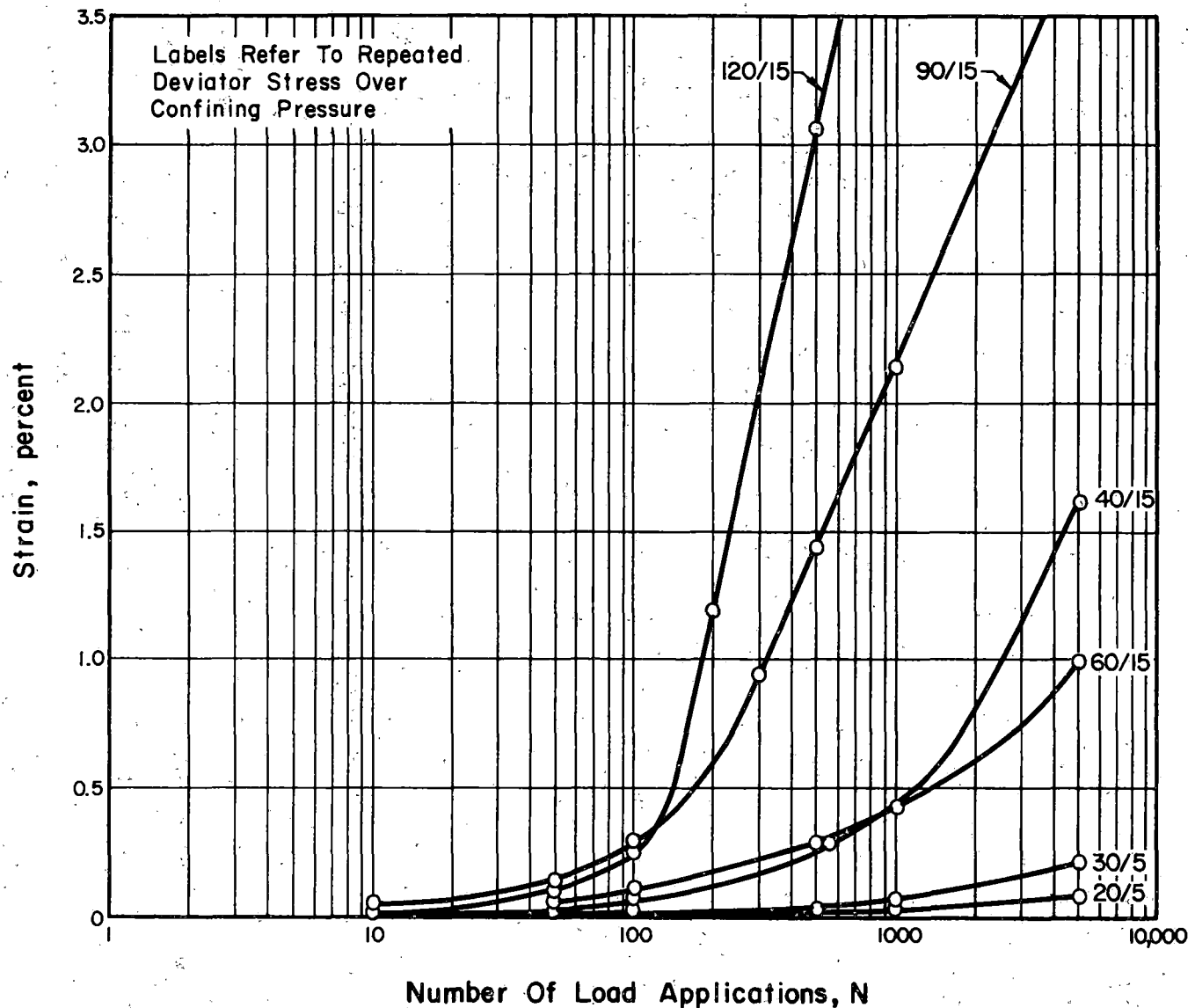


Figure 5.17. Effect of Stress Level on Plastic Strain Response of Well Graded ( $n = 1/2$ ) Limestone, Medium Density, No. 2.

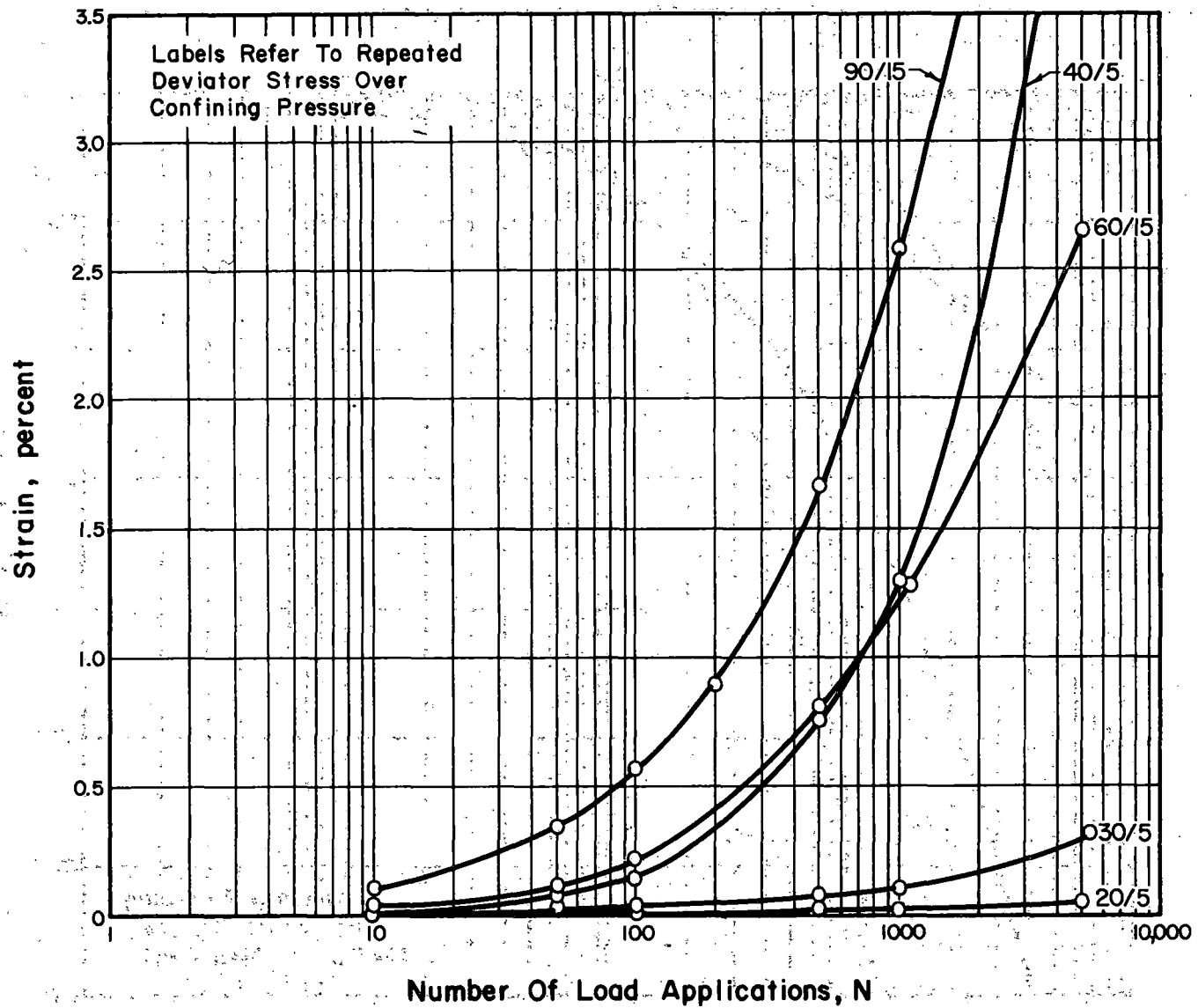


Figure 5.18. Effect of Stress Level on Plastic Strain Response of CA-10 Gradation Limestone, Medium Density.

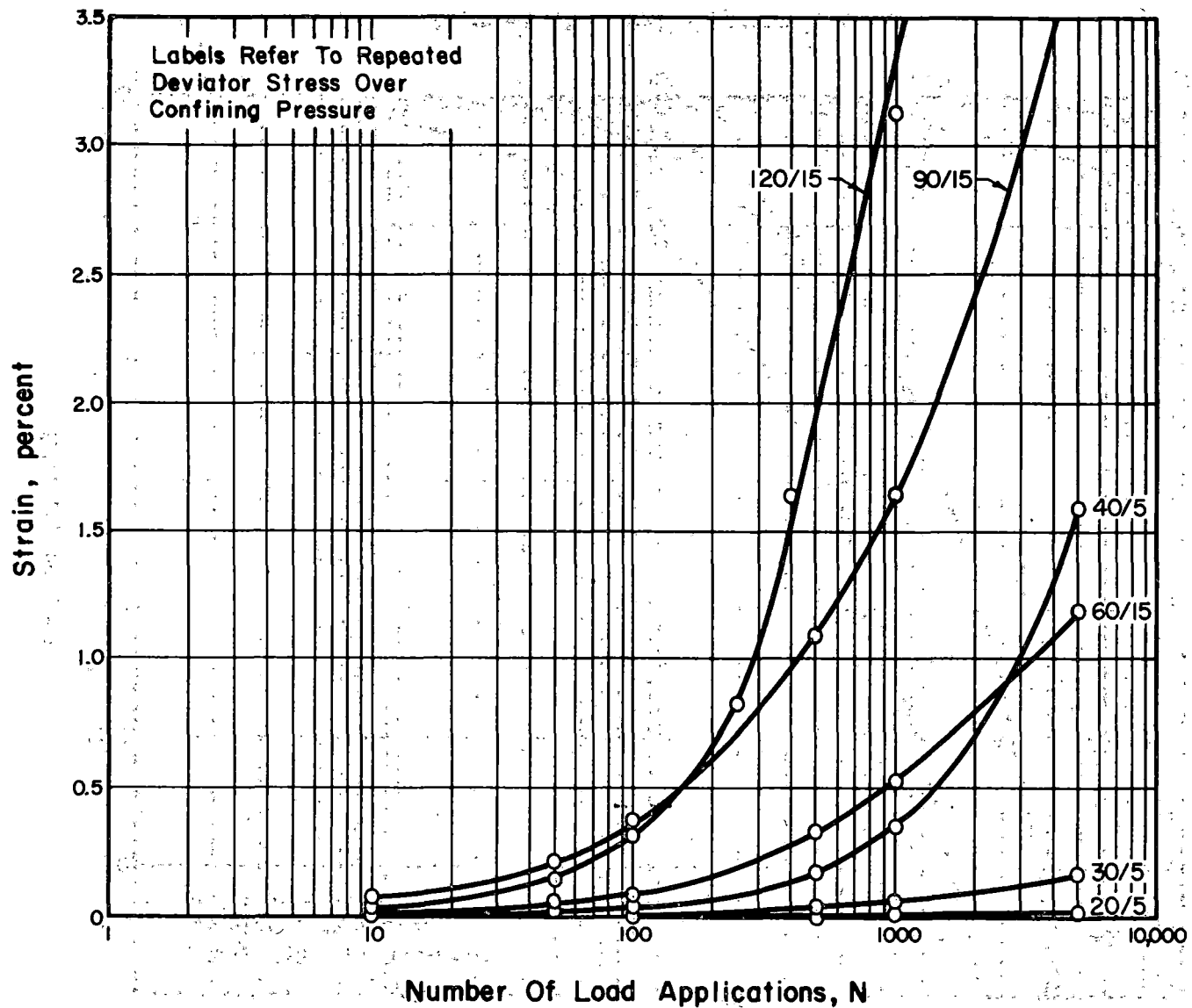


Figure 5.19. Effect of Stress Level on Plastic Strain Response of CA-10 Gradation Limestone, High Density.

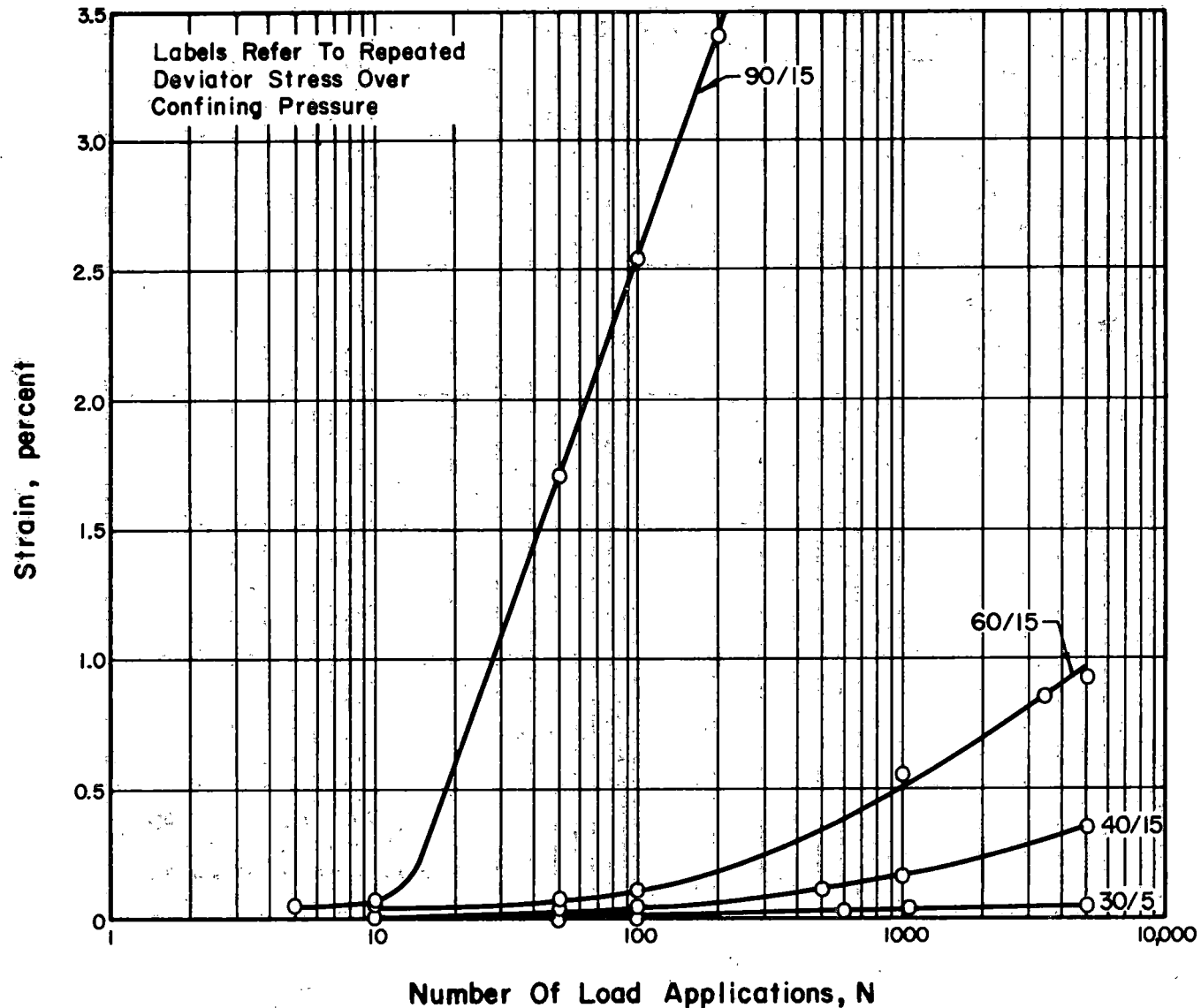


Figure 5.20. Effect of Stress Level on Plastic Strain Response of No. 5 Gradation Granitic Gneiss, Low Density.

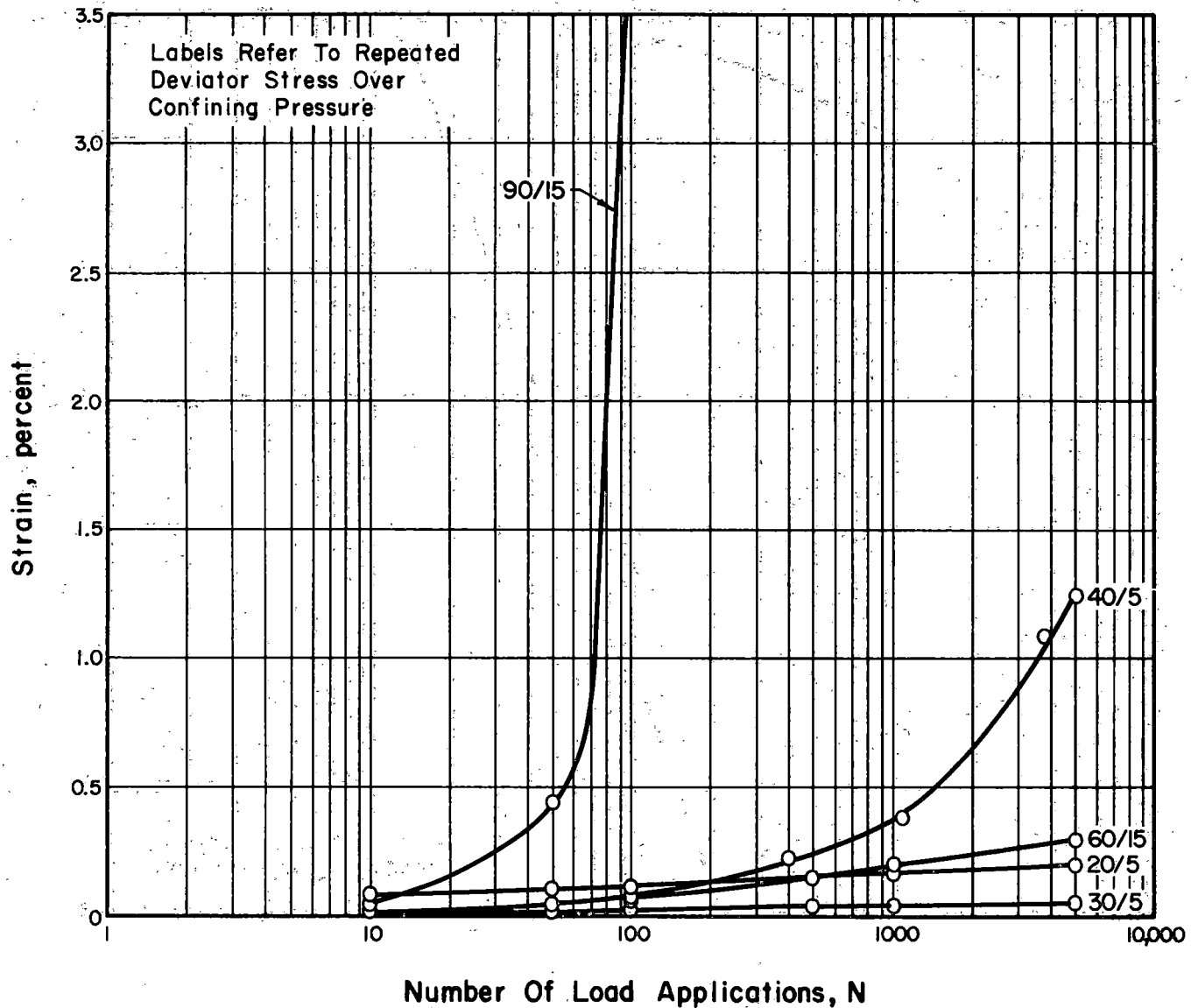


Figure 5.21. Effect of Stress Level on Plastic Strain Response of No. 4 Gradation Granitic Gneiss, Low Density.

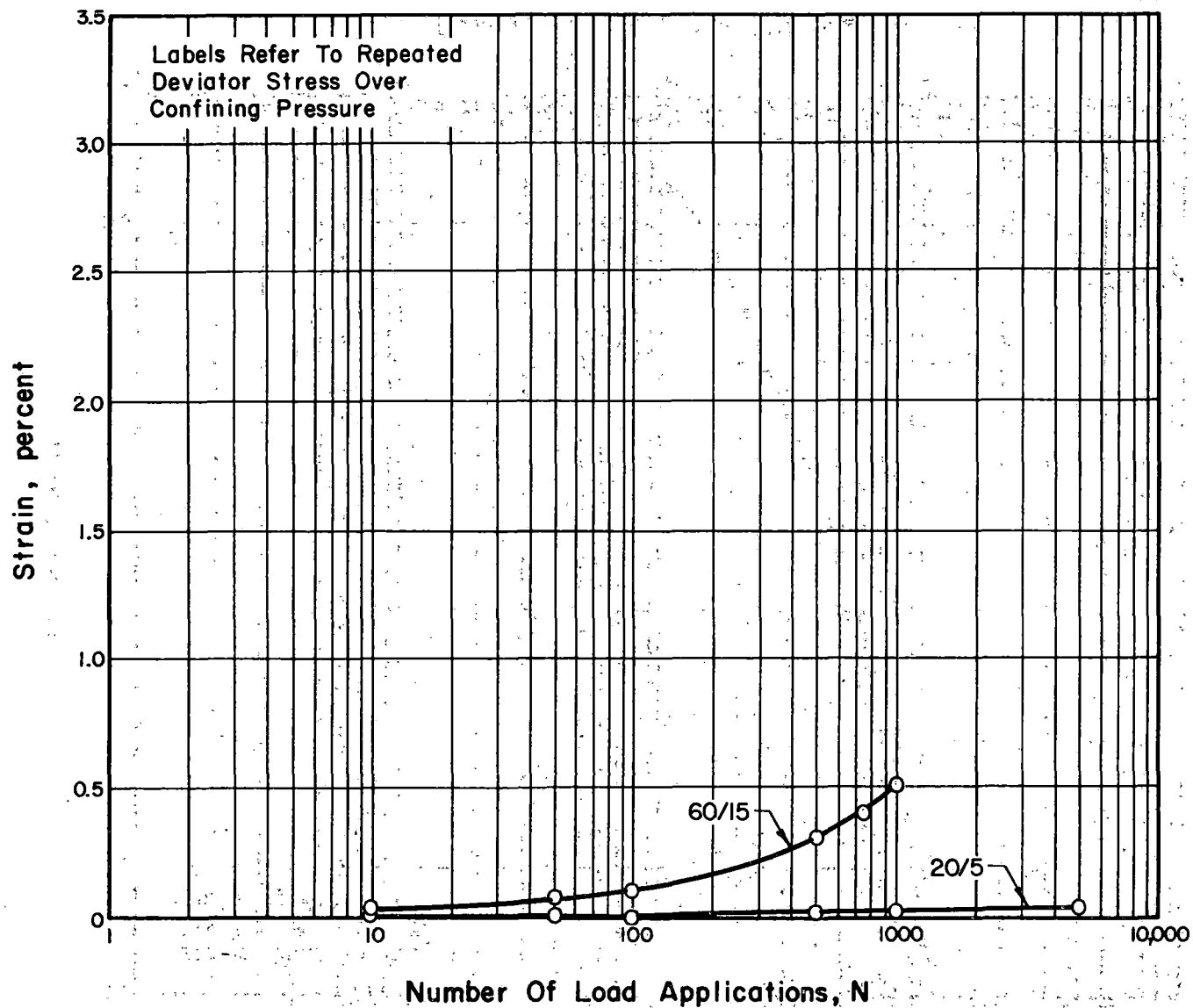


Figure 5.22. Effect of Stress Level on Plastic Strain Response of No. 4 Gradation Gneiss, Medium Density.

CLASSIFICATION: CONFIDENTIAL  
DATE: 10/10/84

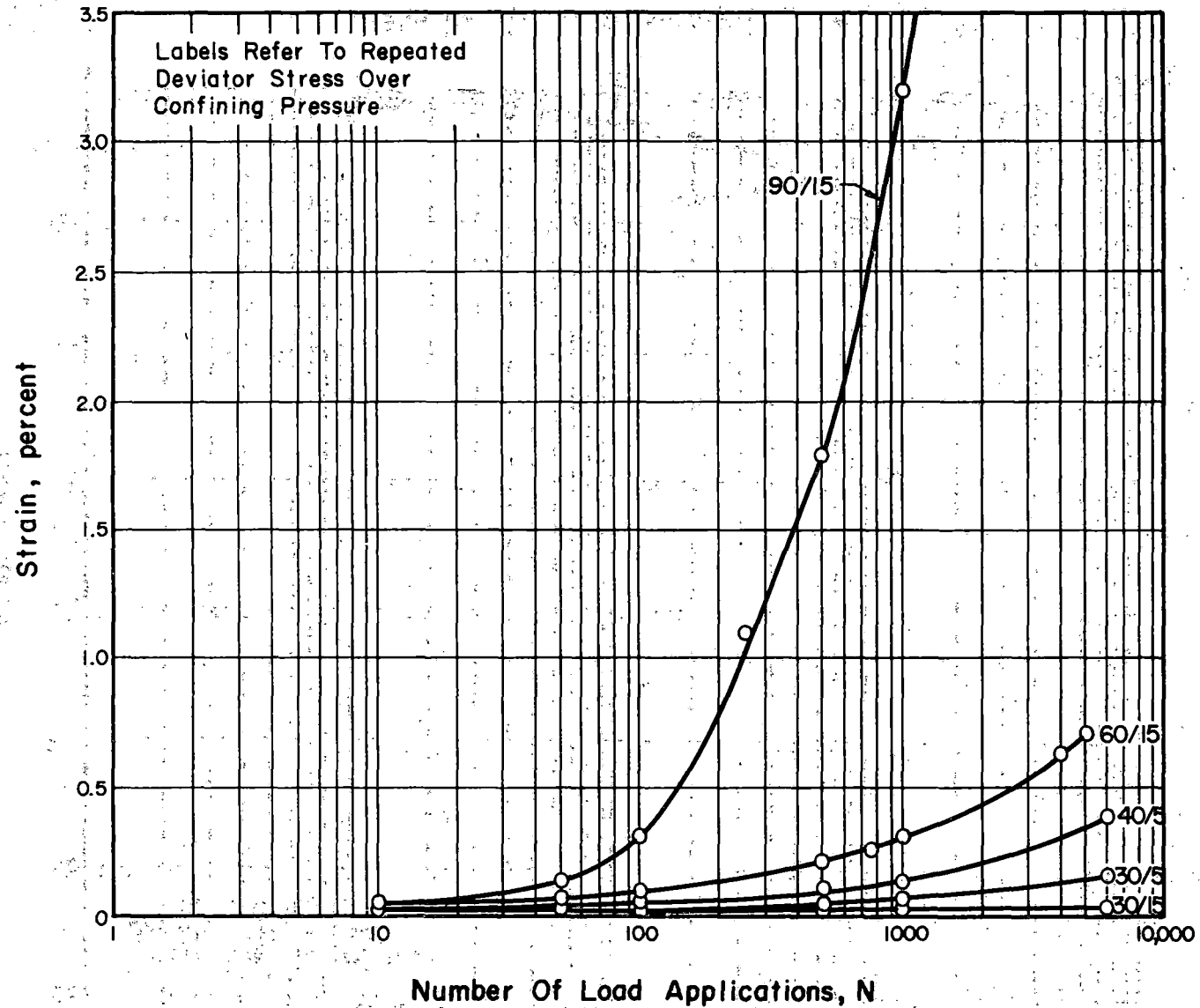


Figure 5.23. Effect of Stress Level on Plastic Strain Response of No. 4 Gradation Granitic Gneiss, High Density.

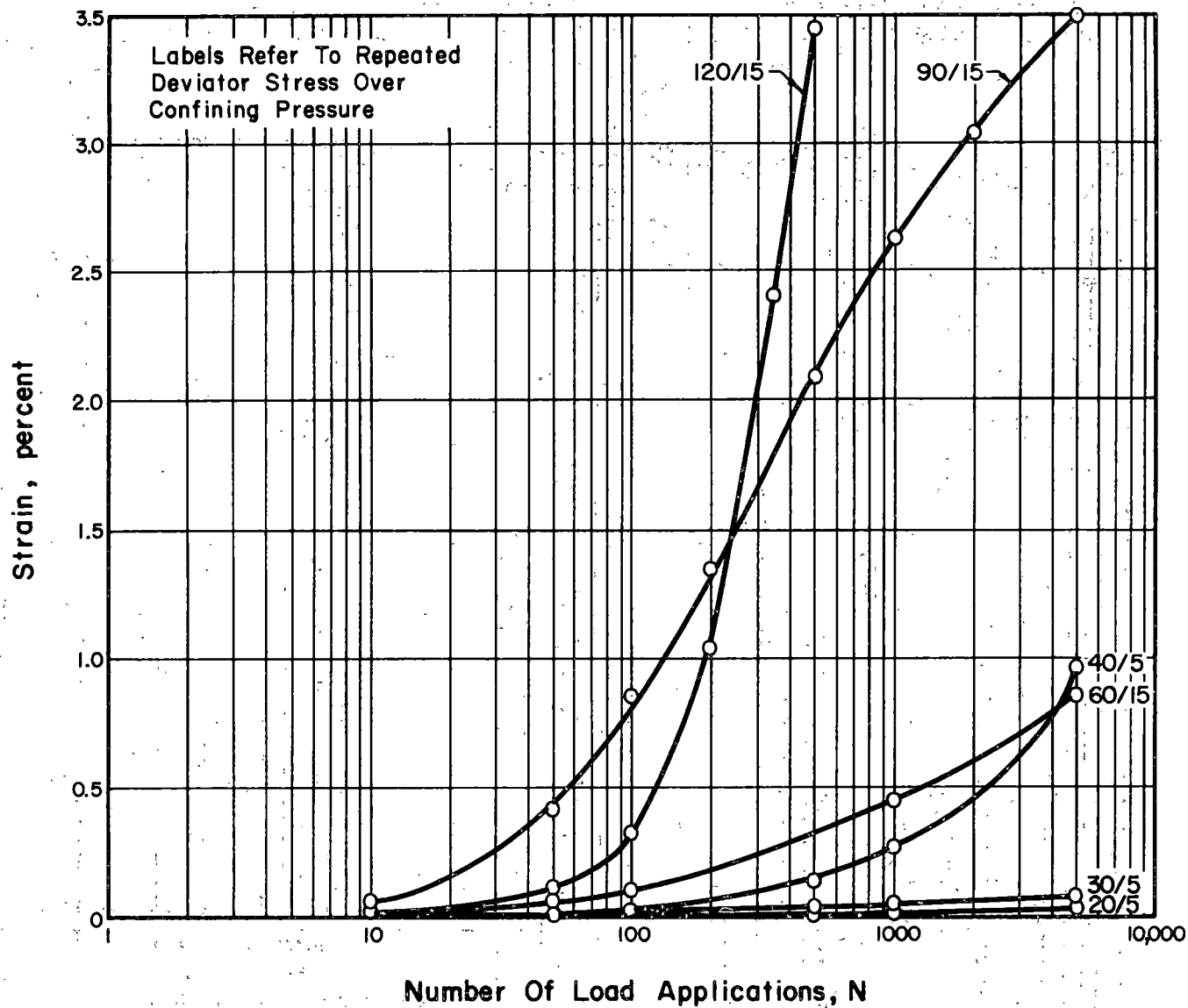


Figure 5.24. Effect of Stress Level on Plastic Strain Response of Well Graded ( $n = 2/3$ ) Granitic Gneiss, Medium Density.

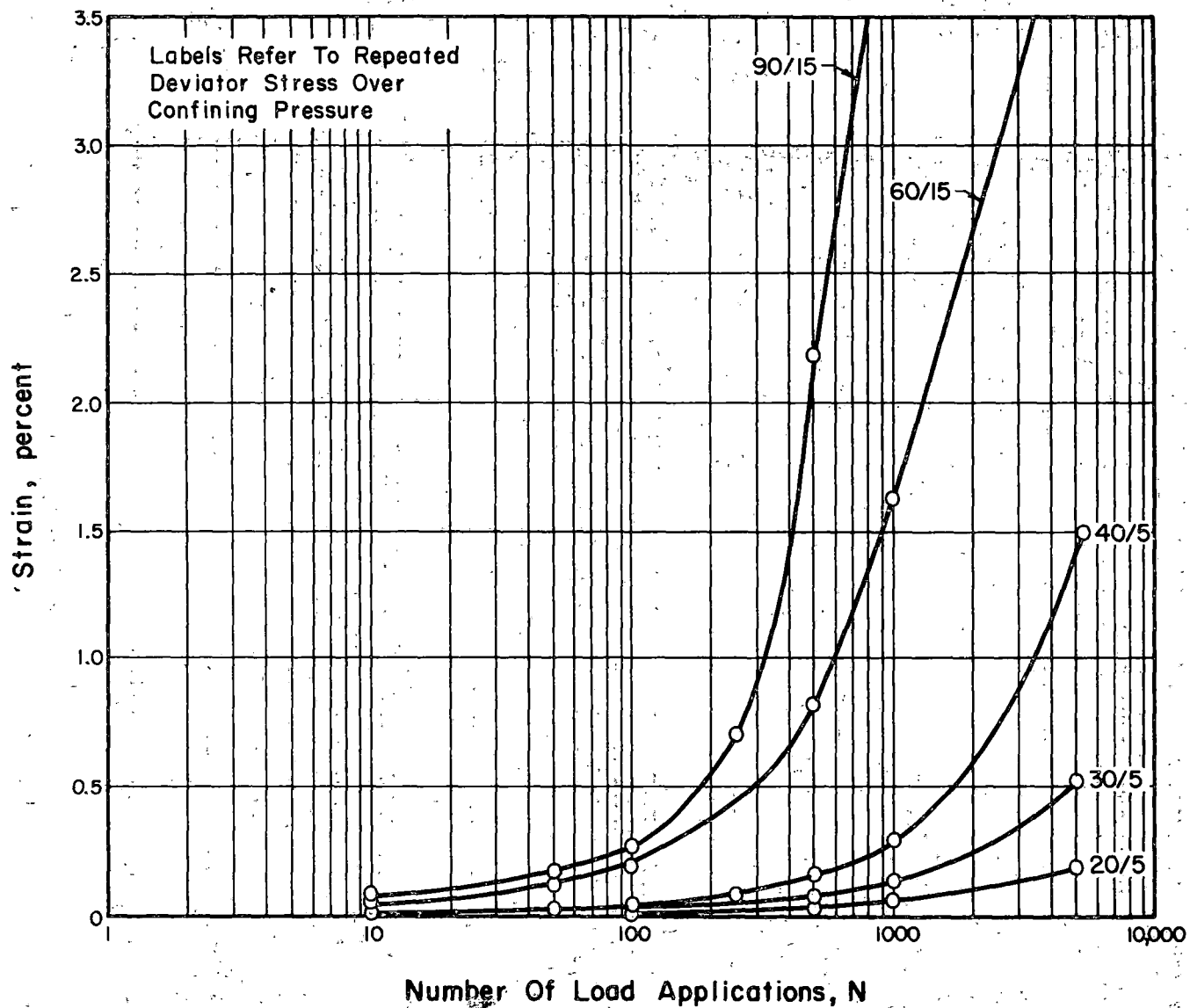


Figure 5.25. Effect of Stress Level on Plastic Strain Response of the No. 4 Gradation Chicago Blast Furnace Slag, Low Density.

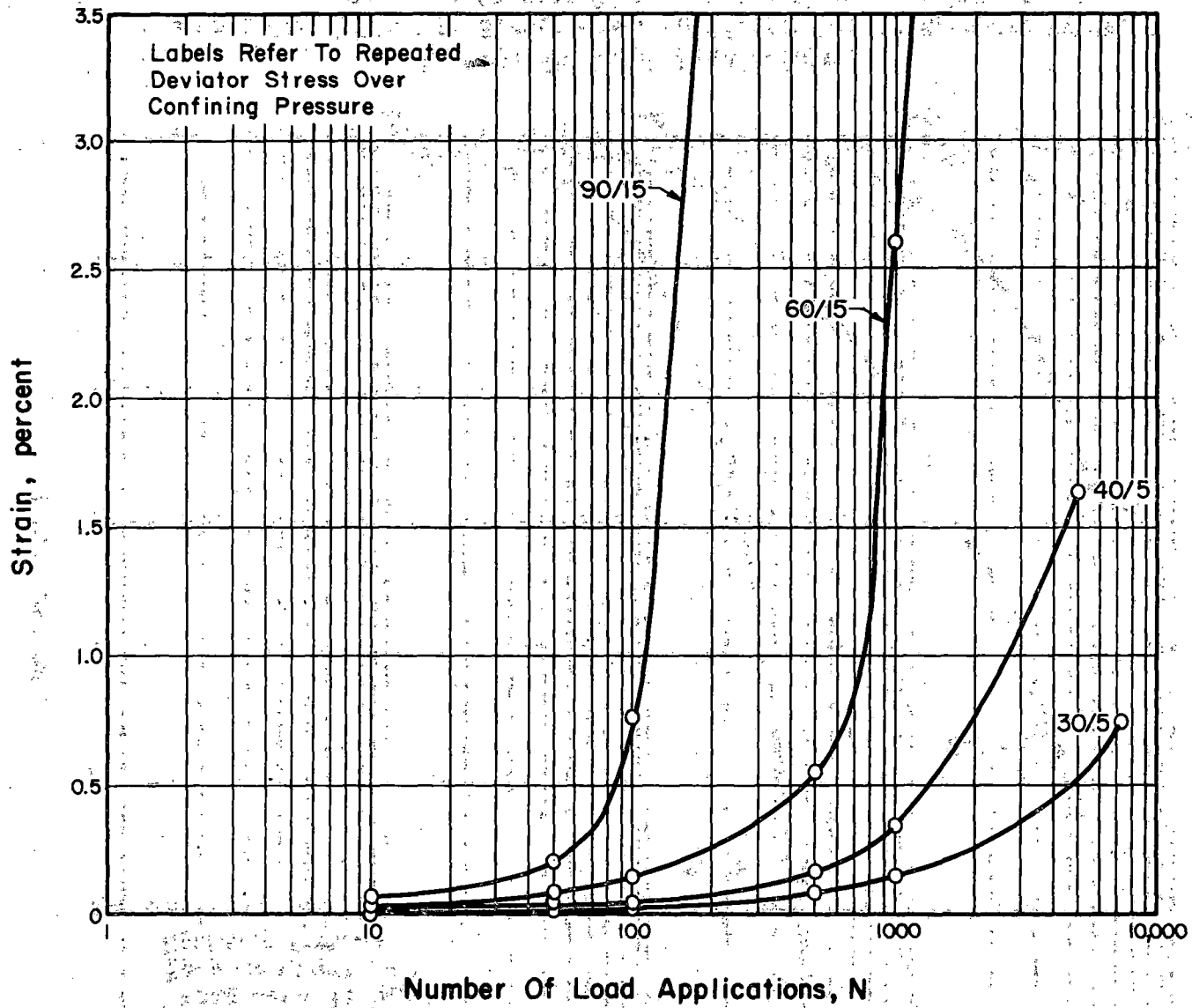


Figure 5.26. Effect of Stress Level on Plastic Strain Response of No. 4 Gradation Chicago Blast Furnace Slag, Medium Density.

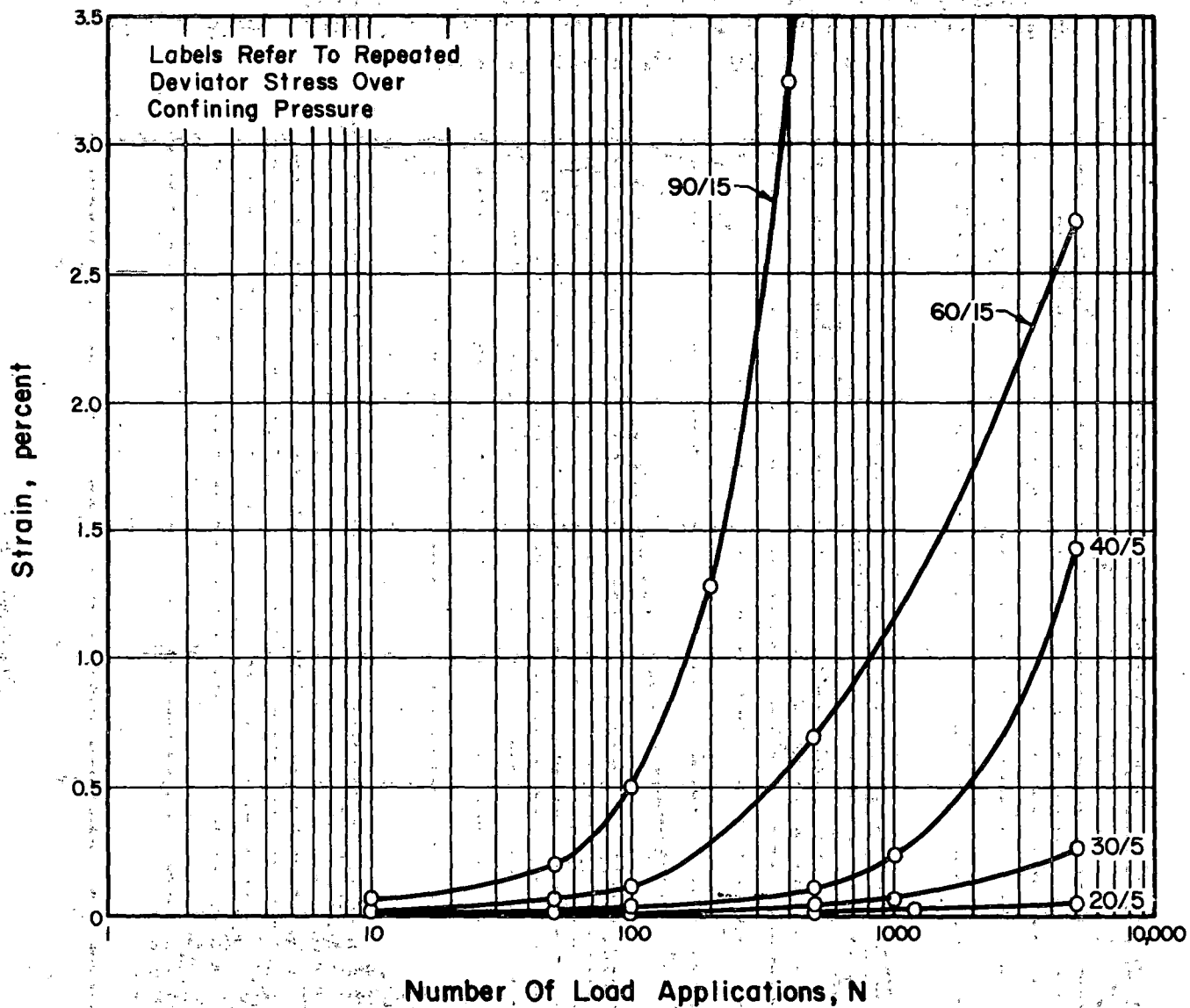


Figure 5.27. Effect of Stress Level on Plastic Strain Response of No. 4 Gradation Chicago Blast Furnace Slag, High Density.

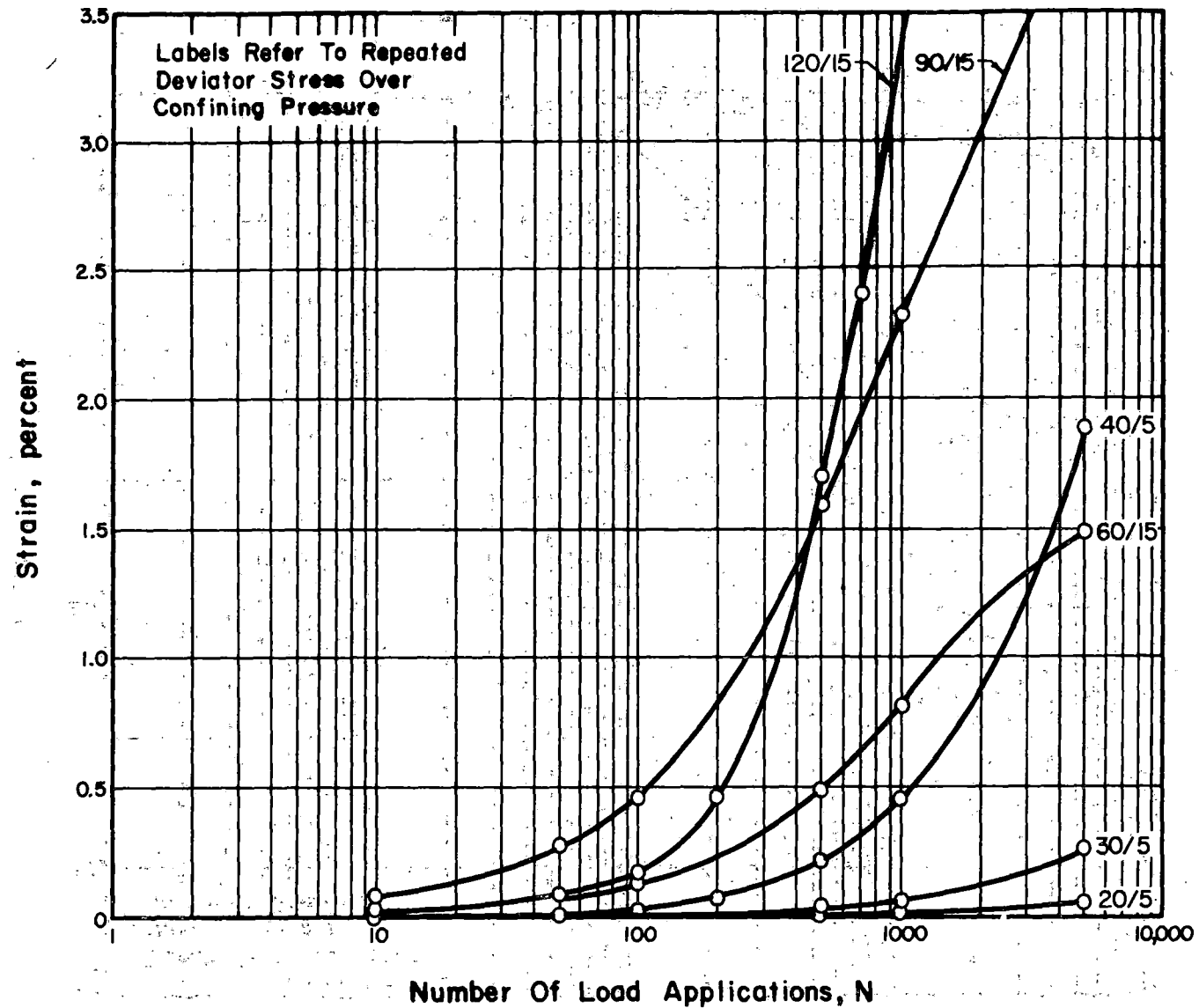


Figure 5.28. Effect of Stress Level on Plastic Strain Response of Well Graded ( $n = 2/3$ ) Chicago Blast Furnace Slag, Medium Density.

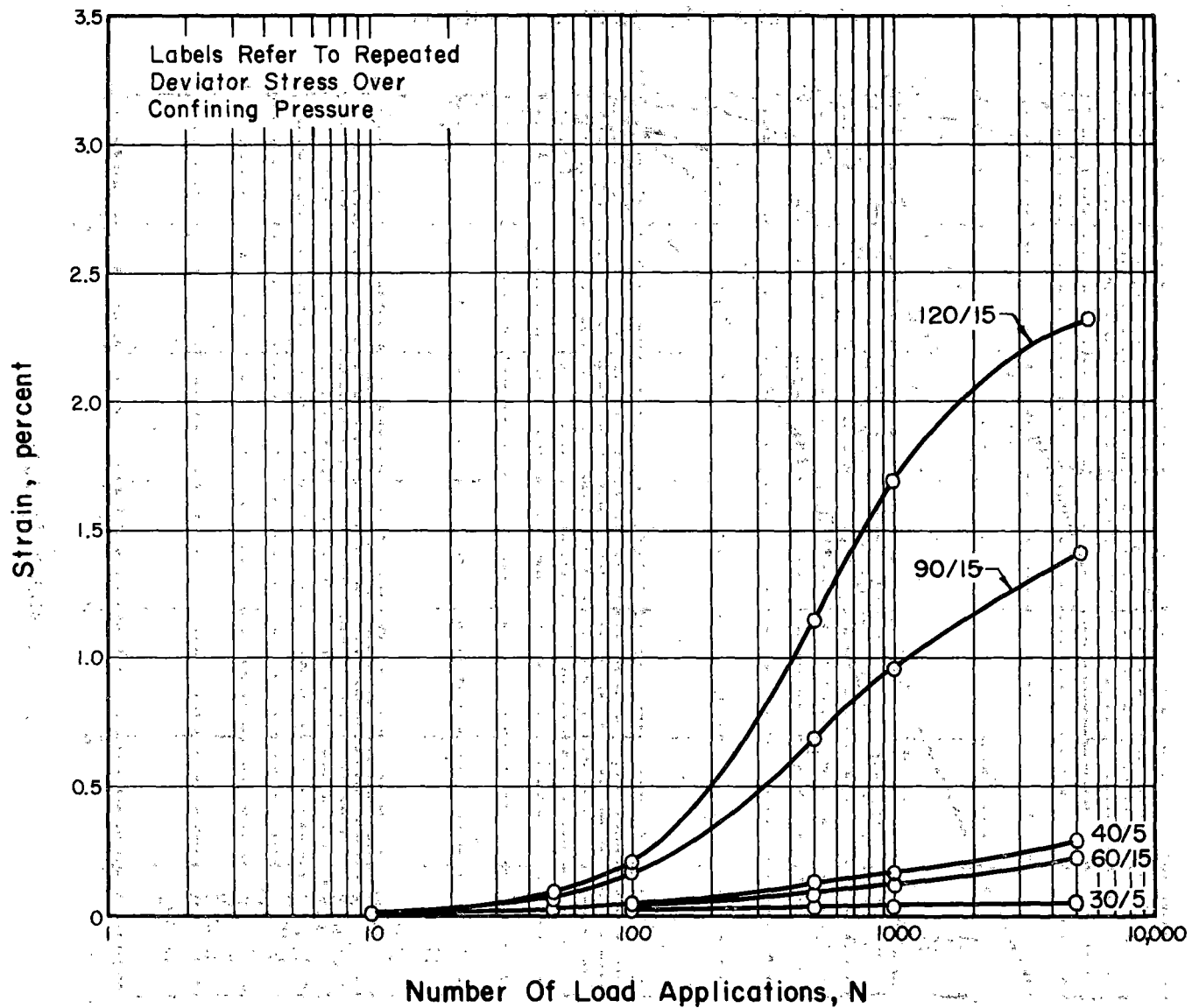


Figure 5.29. Effect of Stress Level on Plastic Strain Response of No. 5 Gradation Basalt, Medium Density.

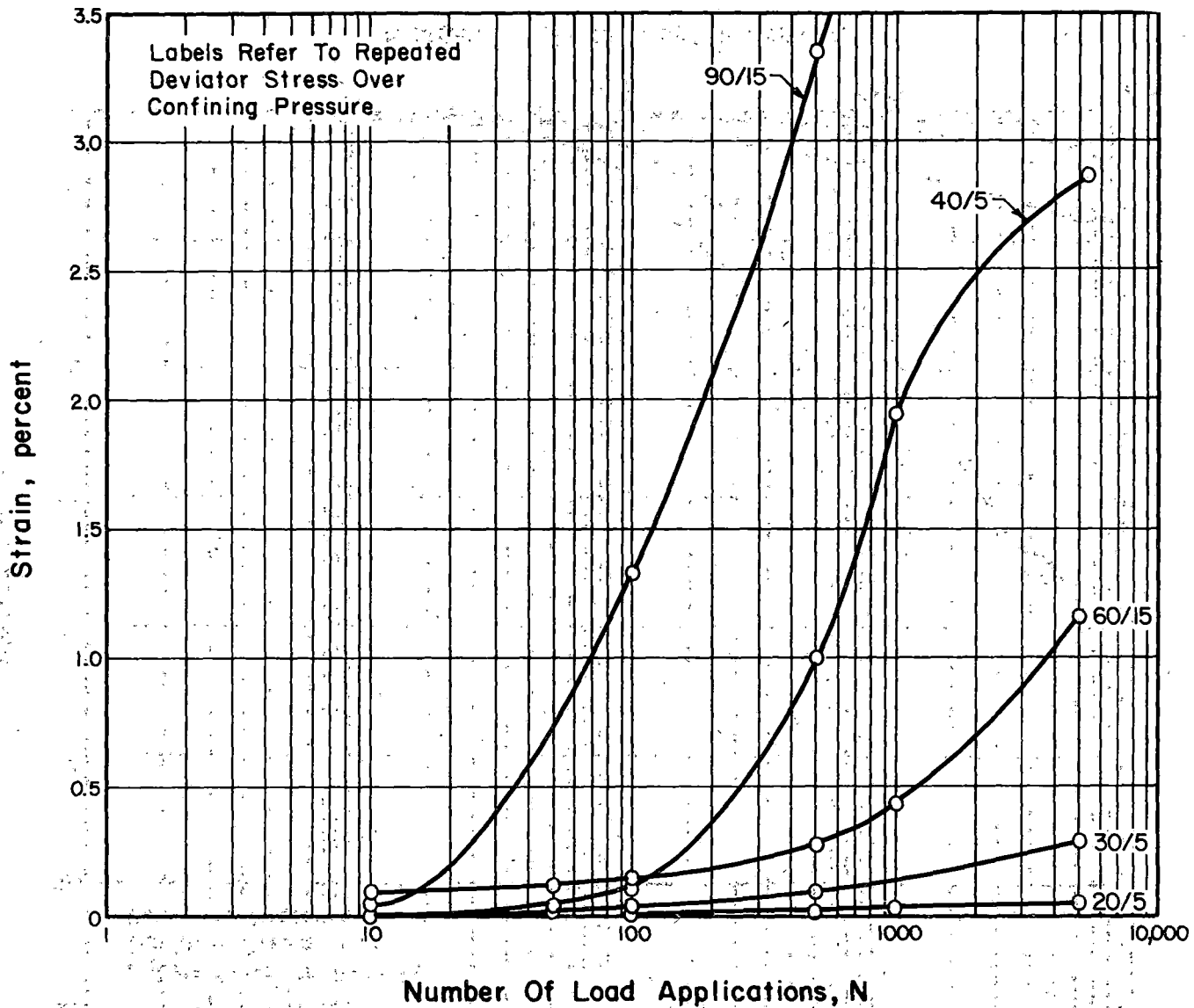


Figure 5.30. Effect of Stress Level on Plastic Strain Response of No. 4 Gradation Basalt, Medium Density.

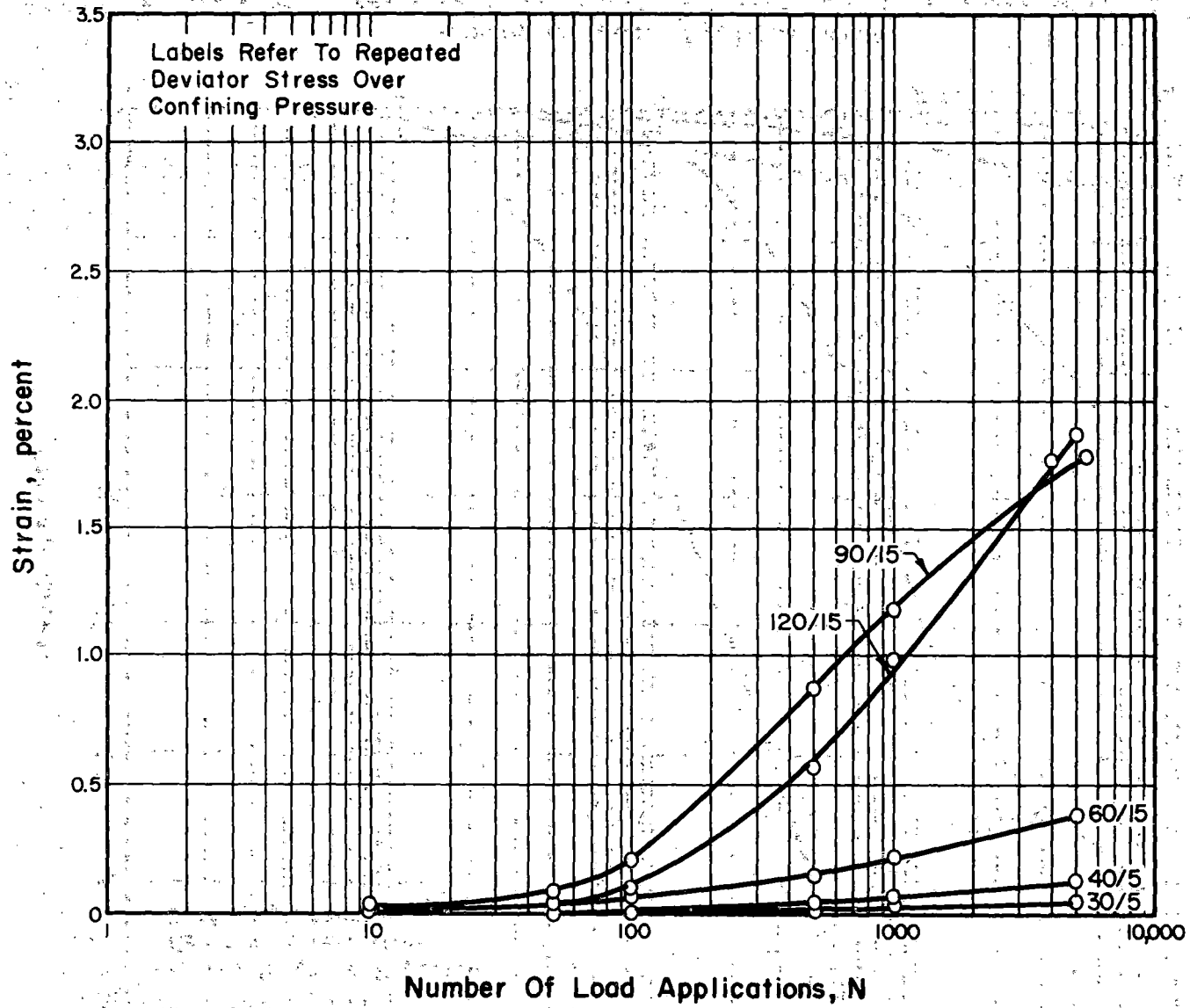


Figure 5.31. Effect of Stress Level on Plastic Strain Response of Well Graded ( $n = 2/3$ ) Basalt, Medium Density.

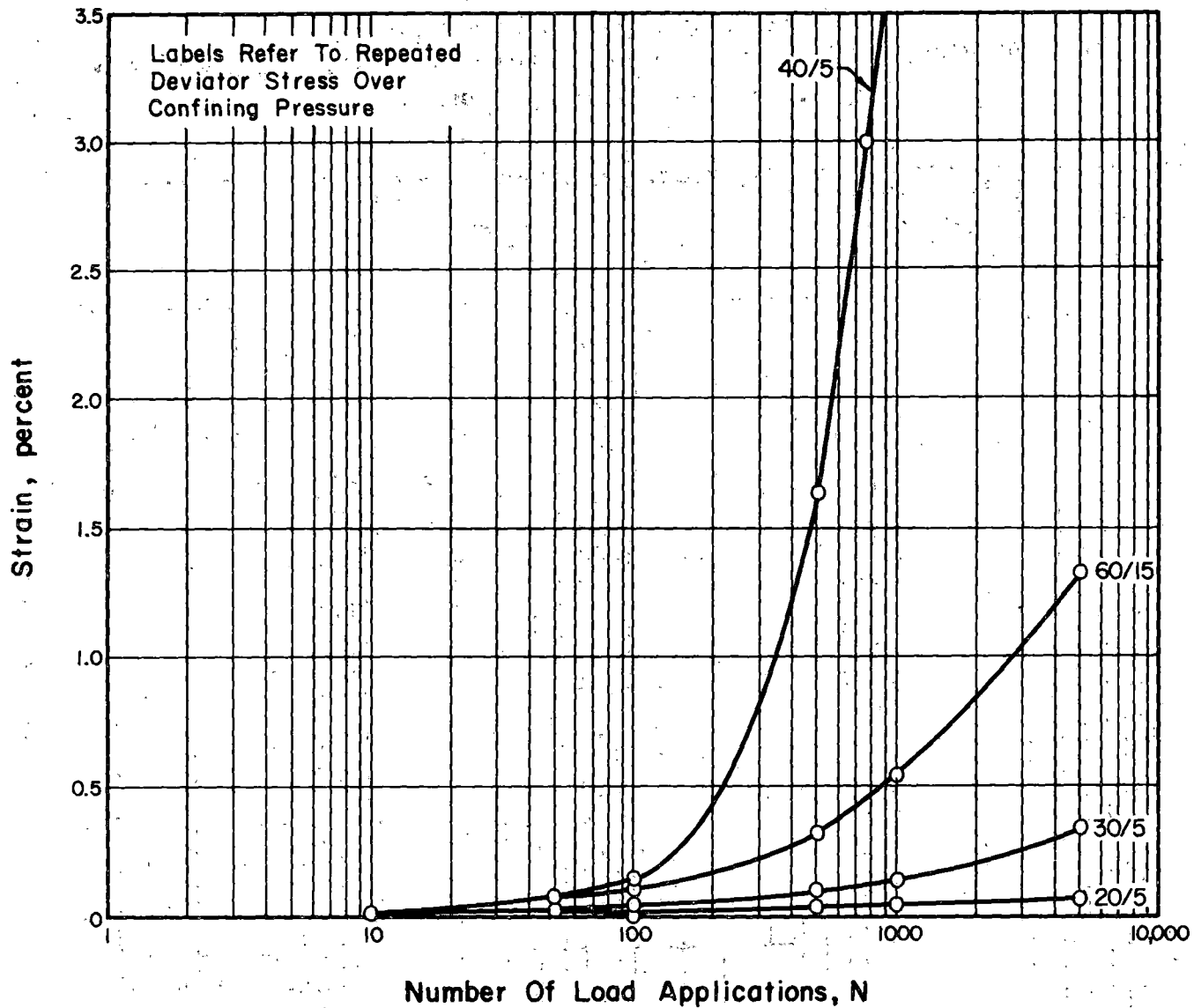


Figure 5.32. Effect of Stress Level on Plastic Strain Response of No. 4 Gradation Crushed Gravel, Medium Density.

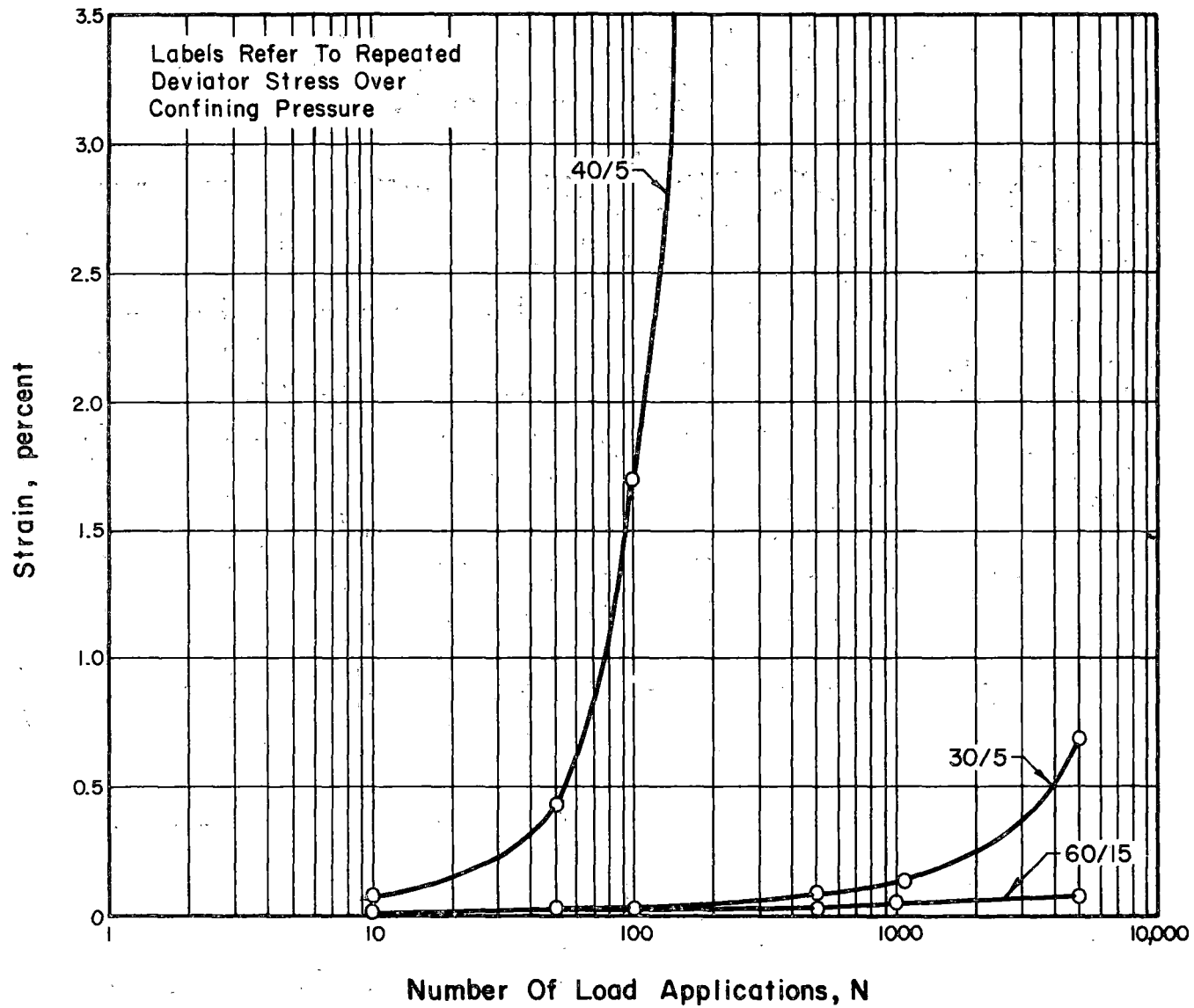


Figure 5.33. Effect of Stress Level on Plastic Strain Response of No. 5 Gradation Gravel, Medium Density.

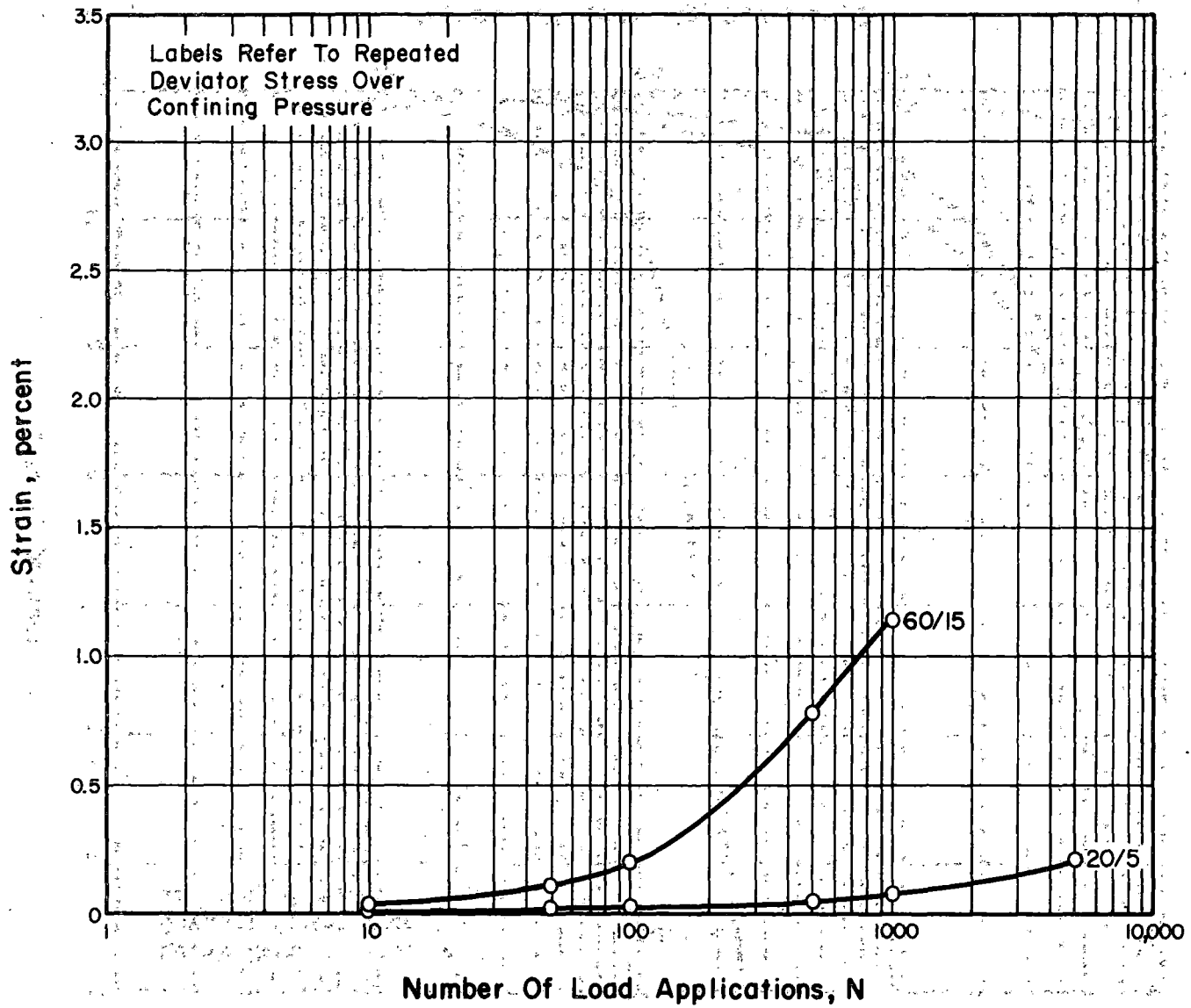


Figure 5.34. Effect of Stress Level on Plastic Strain Response of No. 4 Gradation Gravel, Low Density.

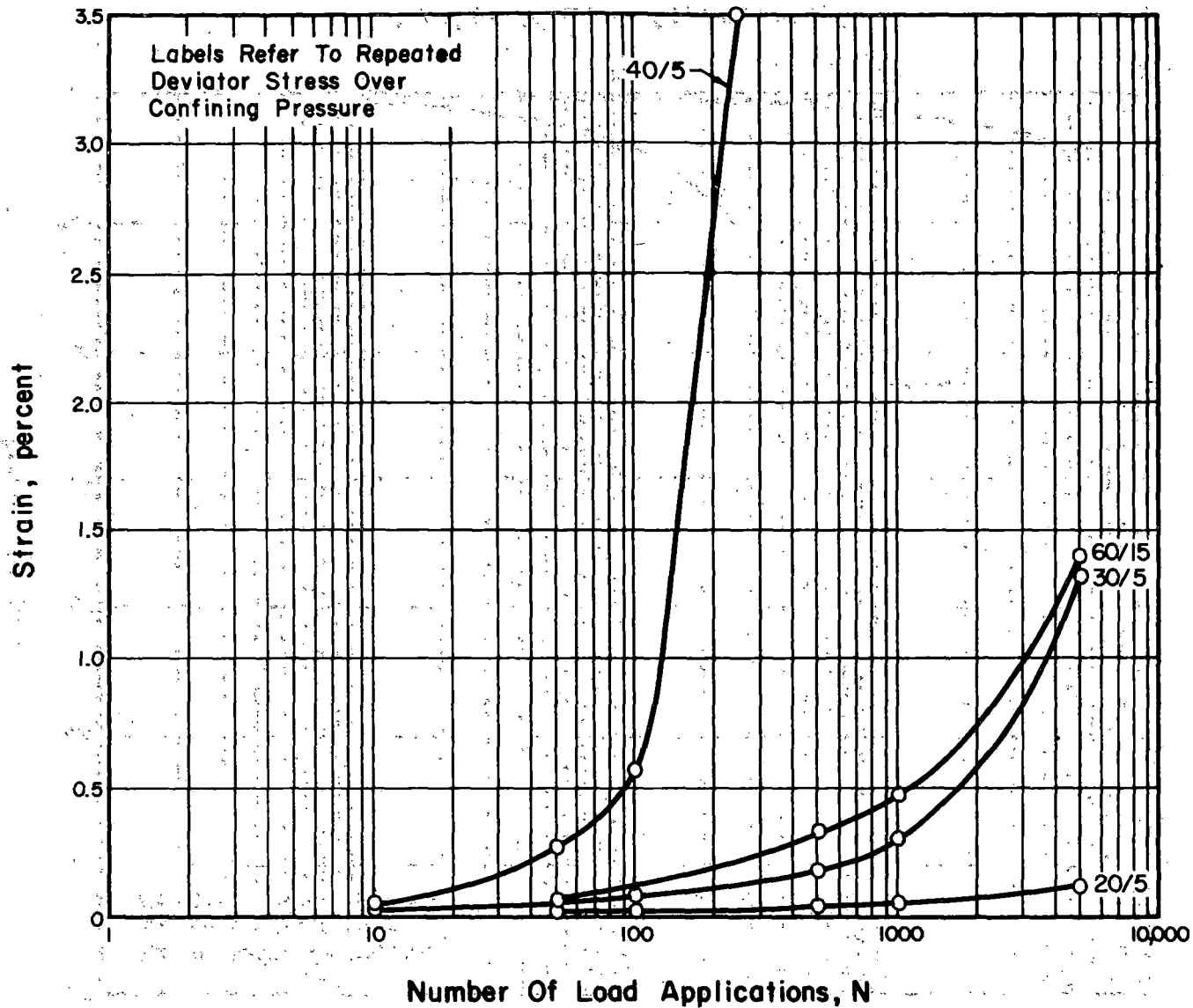


Figure 5.35. Effect of Stress Level on Plastic Strain Response of No. 4 Gradation Gravel, Medium Density.

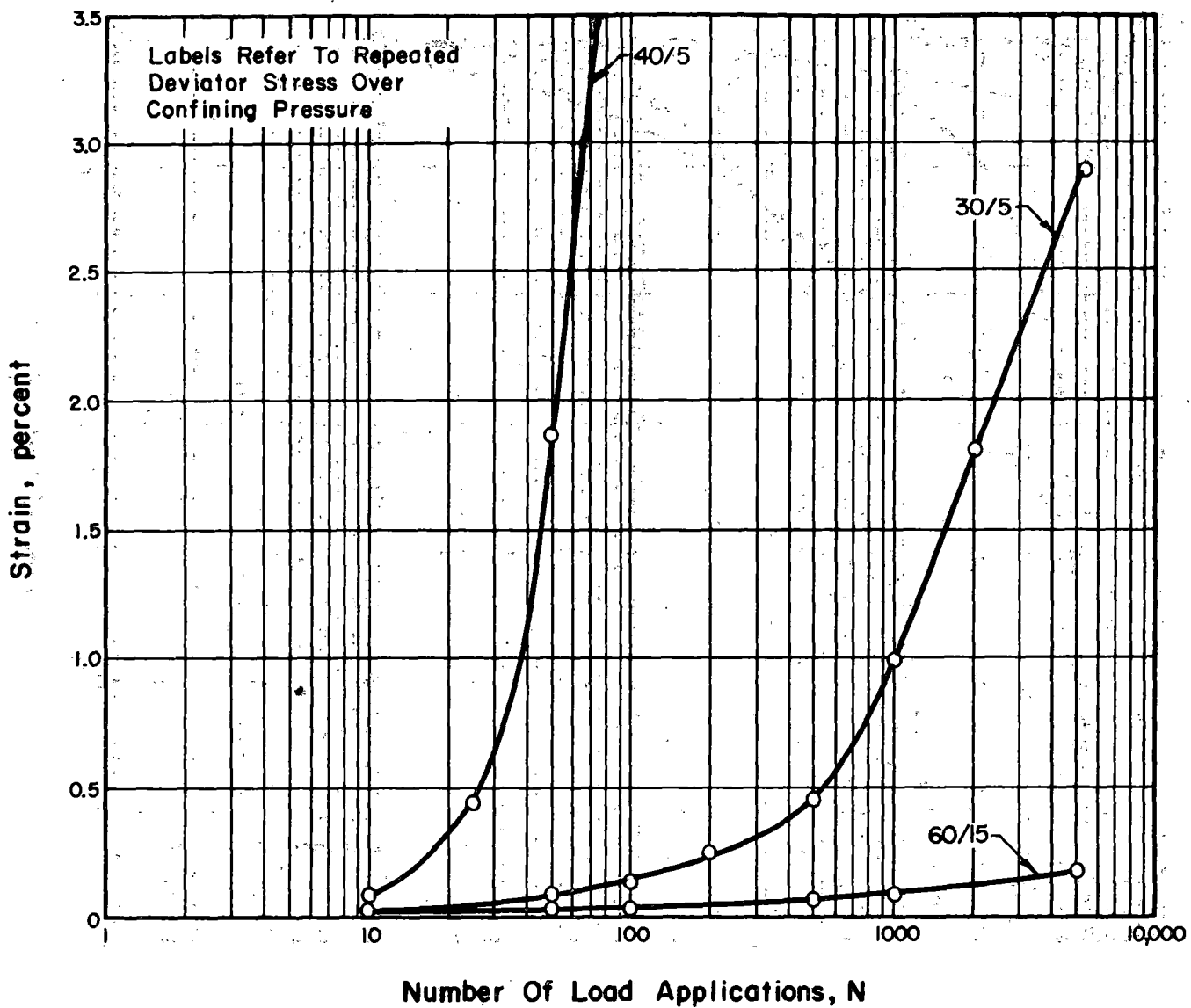


Figure 5.36. Effect of Stress Level on Plastic Strain Response of No. 4 Gradation Gravel, High Density.

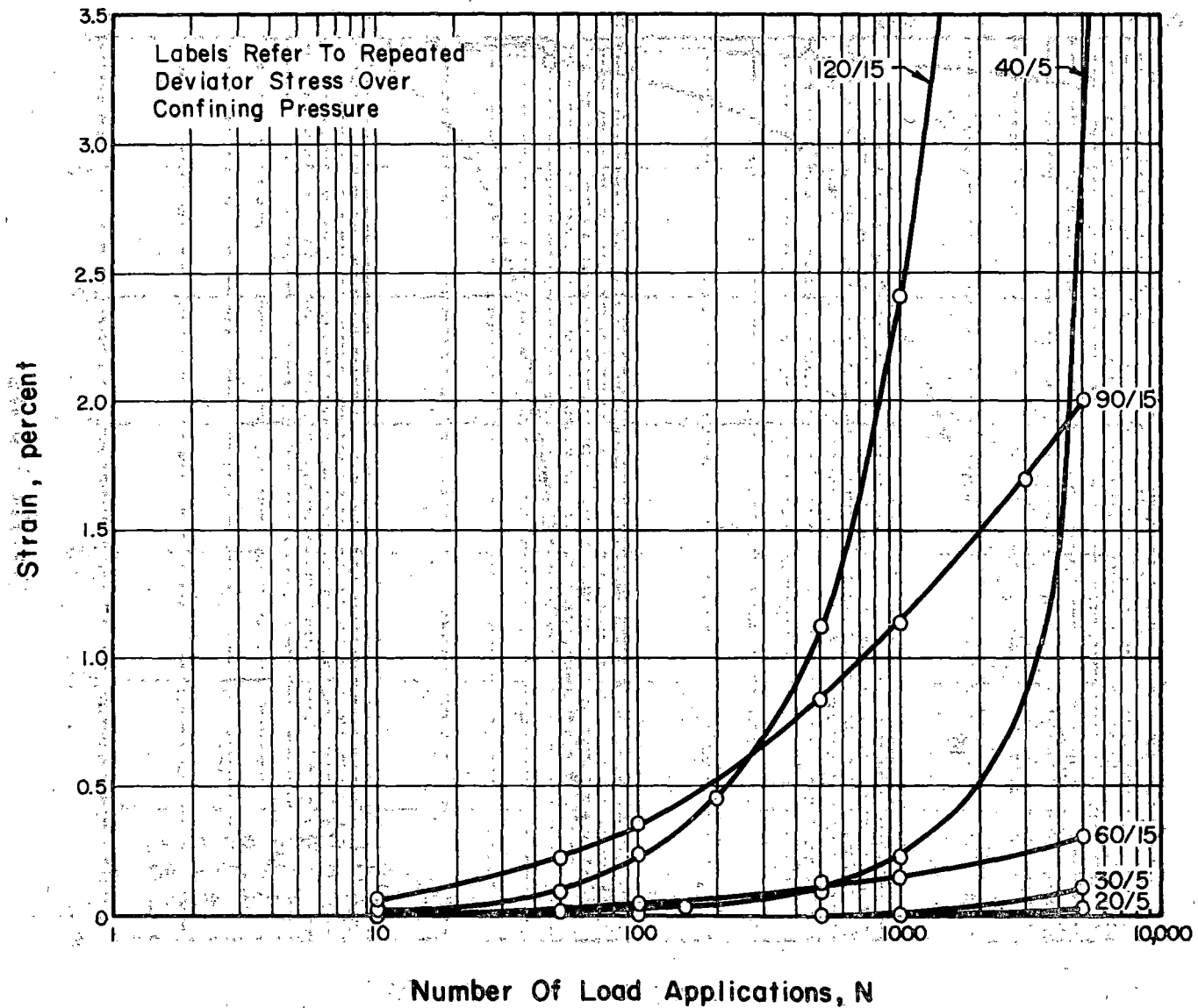


Figure 5.37. Effect of Stress Level on Plastic Strain Response of Well Graded ( $n = 2/3$ ) Gravel, Medium Density.

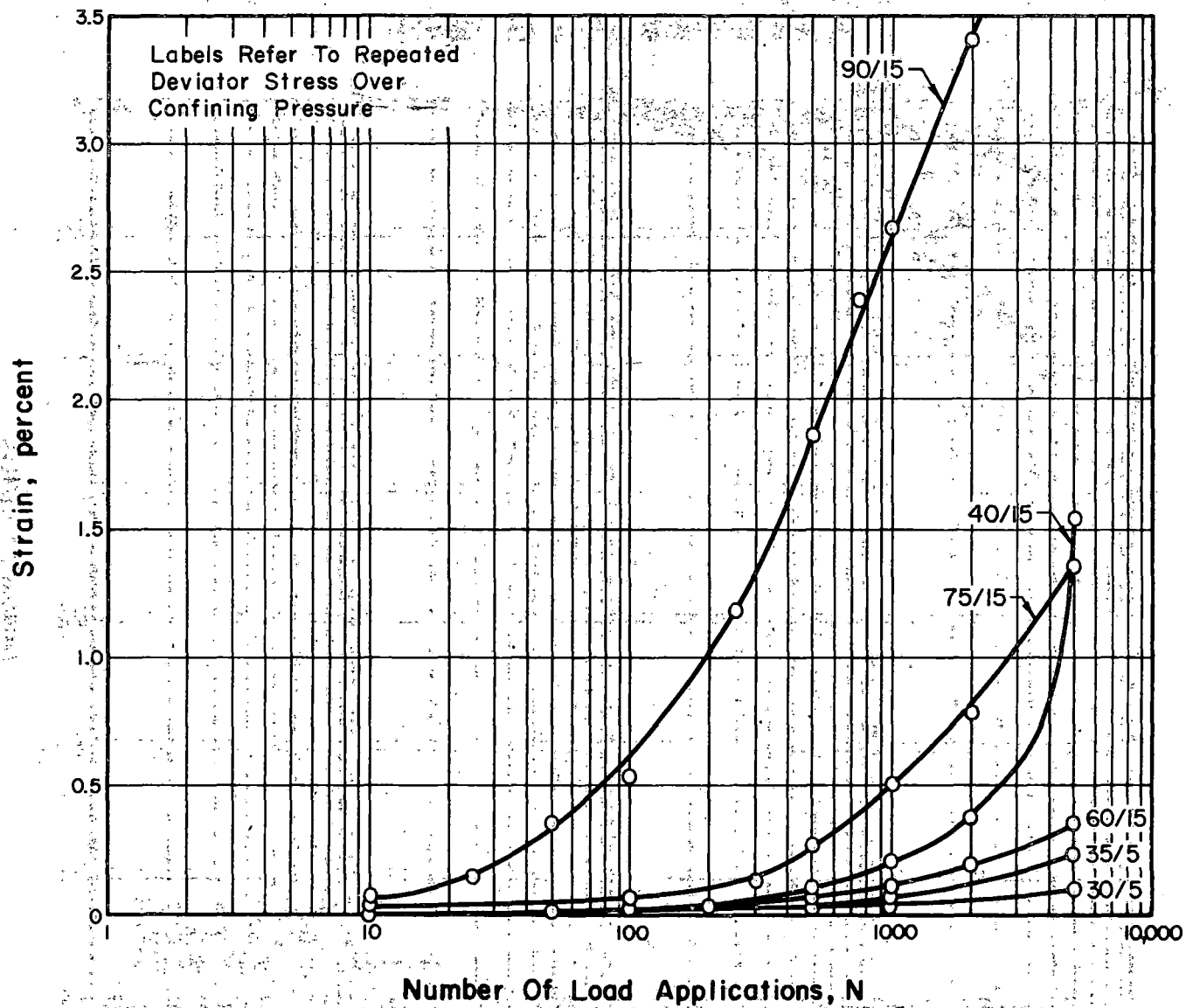


Figure 5.38. Effect of Stress Level on Plastic Strain Response of No. 5 Gradation Kansas Test Track Slag, Low Density.

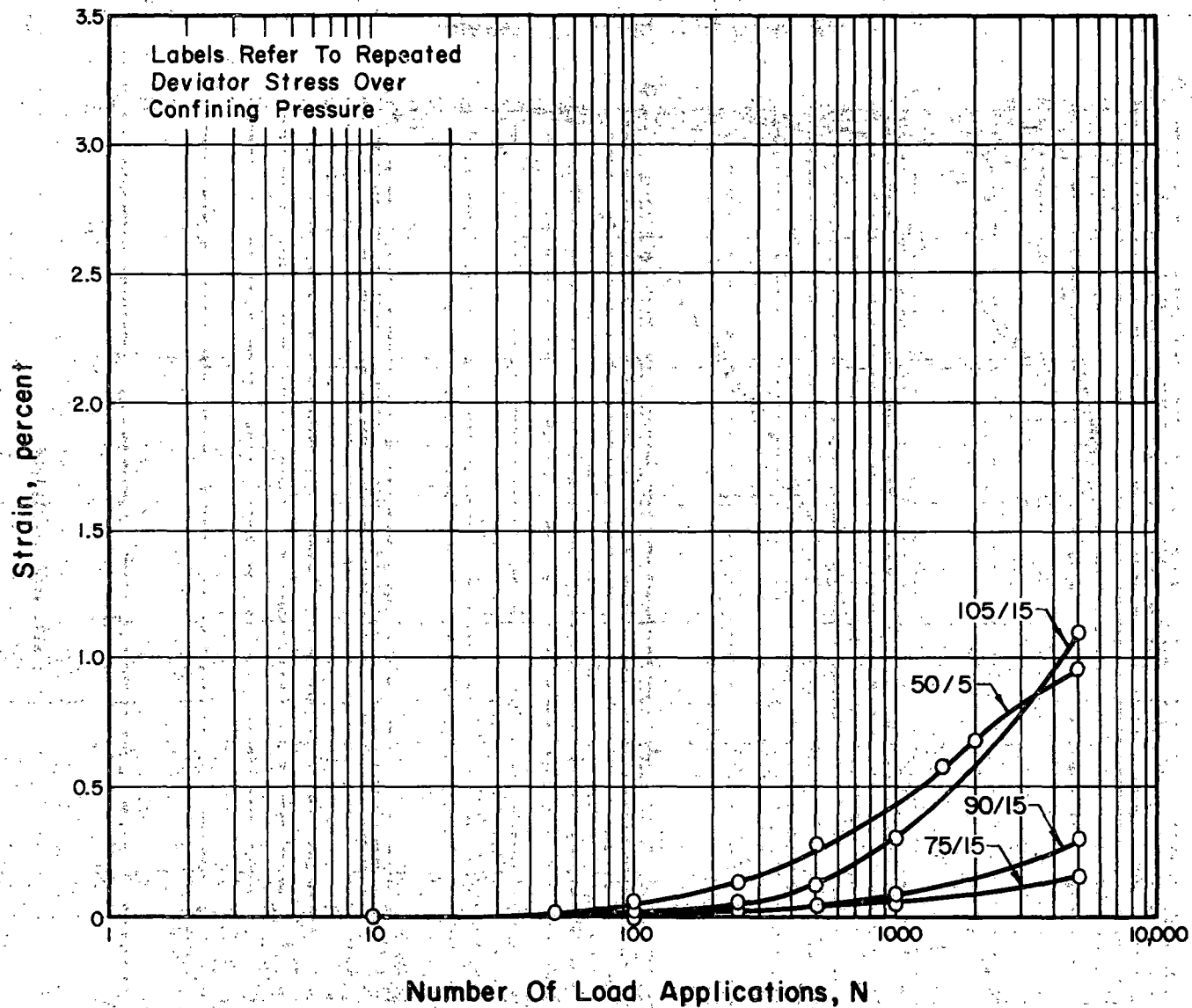


Figure 5.39. Effect of Stress Level on Plastic Strain Response of No. 5 Gradation Kansas Test Track Slag, Medium Density.

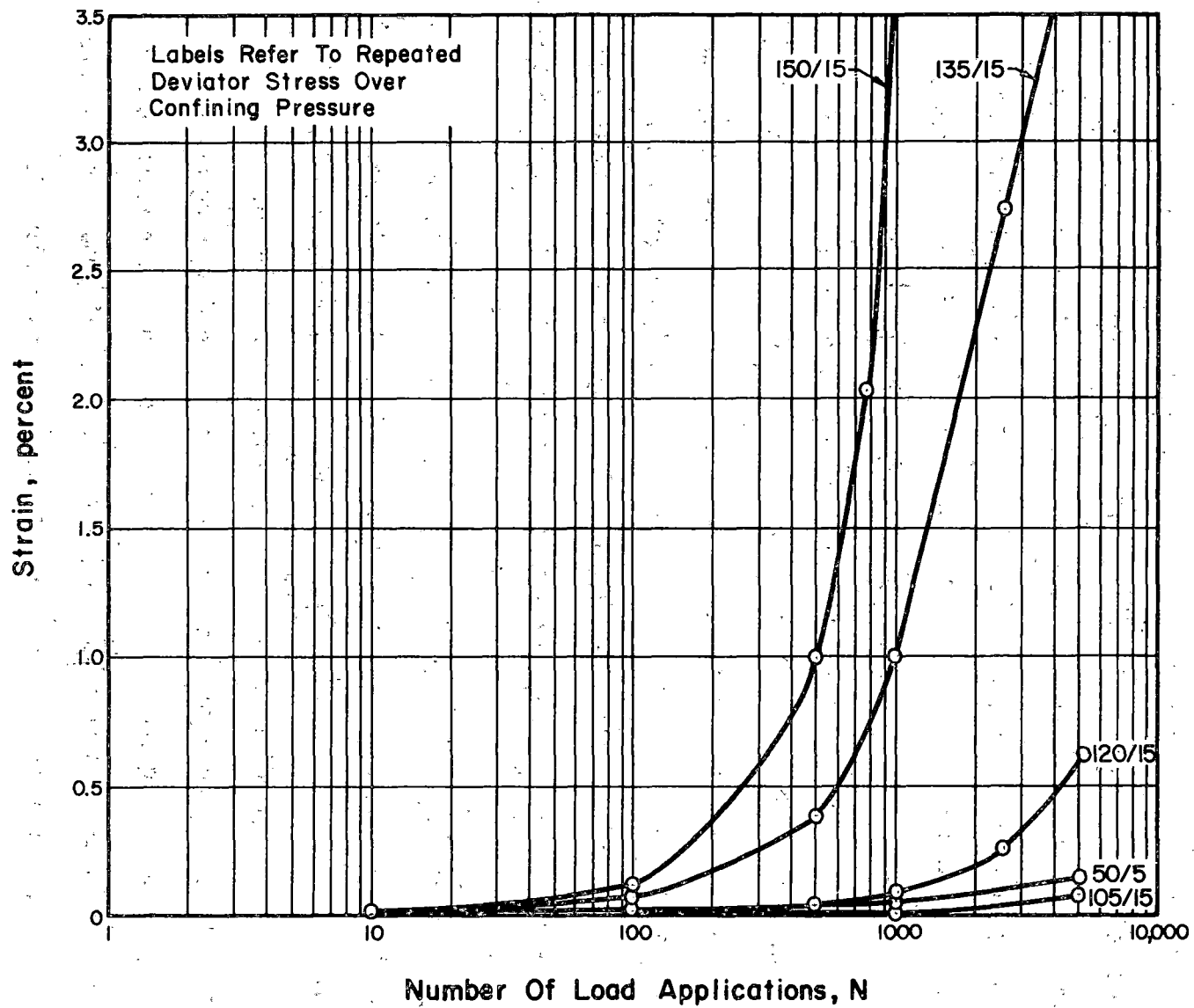


Figure 5.40. Effect of Stress Level on Plastic Strain Response of No. 5 Gradation Kansas Test Track Slag, High Density.

Three types of regression analyses were used: arithmetic, semi-log, and log-log (strain versus number of cycles, strain versus logarithm of number of cycles, and logarithm of strain versus logarithm of number of cycles, respectively). In general the best results were obtained for plastic strain versus the logarithm of the number of cycles. The slopes obtained from the linear regression equations were used in attempts to further analyze plastic strain behavior. Because strain is zero at the start of testing and because only the trend of plastic strain is of practical importance, the equation intercepts were not included in the analyses.

Table 5.1 is a summary of the slopes and correlation coefficients for the data obtained at a repeated deviator stress of 45 psi ( $310 \text{ kN/m}^2$ ) and a confining pressure of 15 psi ( $103 \text{ kN/m}^2$ ). The analysis of the data obtained at the other stress levels is included in Table 5.2. Because the semi-logarithmic analyses proved to provide the best results, they are the only ones included in Table 5.2.

In all cases an increase in stress ratio (repeated deviator stress divided by confining pressure) resulted in additional plastic strain accumulation during the 5000 cycles. However, stress ratio by itself cannot be used to predict adequately the plastic strain behavior of ballast materials. Both repeated deviator stress and confining pressure must be considered together because the application of a stress ratio of 4 and a confining pressure of 5 psi ( $34 \text{ kN/m}^2$ ) is usually much less severe than the same stress ratio in conjunction with a 15 psi ( $103 \text{ kN/m}^2$ ) confining pressure. For example, in Figure 5.12, the results for low density, No. 4 gradation limestone, a stress ratio of 4 and a confining

Table 5.1. Regression Analyses of Plastic Strain during Conditioning Phase.

Material	Gradation	Compaction Level (a)	Type of Regression Analysis						
			$\epsilon_p - N$		$\epsilon_p - \log N$			$\log \epsilon_p - \log N$	
			Slope	Correlation Coefficient	Slope	Correlation Coefficient	Standard error of estimate	Slope	Correlation Coefficient
Limestone	No. 5	Low	.0004	.644	1.07	.986*	.196	.194	.934*
	No. 5	Med	.0001	.999*	.219	.943*	.042	.209	.977*
	No. 5	High	.0000	.907*	.022	.970*	.007	.348	.998*
	No. 4	Low	.0008	.612	1.47	.981*	.382	.372	.874*
	No. 4	Med	.0003	.845*	.678	.995*	.075	.304	.984*
	No. 4	High	.0000	.902*	.088	.967*	.028	.162	.996*
	well graded	Med	.0002	.803	.555	.999*	.021	.208	.985*
	well graded	Med	.0002	.767	.619	.996*	.057	.284	.932*
	well graded	Med	.0002	.897*	.507	.980*	.112	.188	.998*
	CA-10	Med	.0004	.830*	1.06	.995*	.119	.282	.987*
CA-10	High	.0001	.882*	.309	.985*	.060	.240	.998*	
Granitic Gneiss	No. 5	Low	.0002	.613	.609	.981*	.133	.152	.942*
	No. 4	Low	.0004	.715	1.12	.982*	.210	.296	.942*
	No. 4	Med	.0002	.800*	.632	.999*	.029	.276	.969*
	No. 4	High	.0001	.942*	.218	.952*	.077	.177	.991*
	well graded	Med	.0002	.755	.417	.996*	.043	.203	.981*
Chicago Blast Furnace Slag	No. 4	Low	.0005	.727	1.26	.964*	.348	.127	.930*
	No. 4	Med	.0004	.876*	.797	.985*	.153	.304	.994*
	No. 4	High	.0005	.936*	.936	.879*	.557	.501	.957*
	well graded	Med	.0002	.838*	.439	.996*	.041	.203	.993*
Basalt	No. 5	Med	.0001	.657	.171	.988*	.107	.168	.938*
	No. 4	Med	.0003	.791	.668	.999*	.028	.221	.981*
	well graded	Med	.0001	.773*	.327	.997*	.029	.224	.979*
Crushed Gravel	No. 4	Med	.0002	.846*	.513	.995*	.058	.202	.995*
Gravel	No. 5	Med	.0001	.795	.297	.995*	.033	.248	.984*
	No. 4	Low	.0003	.796*	.727	.998*	.045	.160	.988*
	No. 4	Med	.0002	.923*	.391	.984*	.089	.265	.997*
	No. 4	High	.0000	.854*	.023	.994*	.003	.111	.999*
	well graded	Med	.0000	.840*	.152	.994*	.018	.128	.999*
Kansas Test Track Blast Furnace Slag	No. 5	Low	.0001	.725	.422	.994*	.051	.124	.978*
	No. 5	Med	.0001	.732*	.151	.999*	.066	.205	.969*
	No. 5	High	.0000	.953*	.047	.954*	.021	.098	.975*

(a) Low - rodded 10 blows per layer  
 Med - 5 seconds per layer vibration  
 High - 45 seconds per layer vibration

\* Significant at  $\alpha = 0.05$

Table 5.2. Regression Analysis of Plastic Strain at Stress Levels Other Than Conditioning.

Material Type	Gradation	Compaction Level	Stress Level $\sigma_D/\sigma_3$ (psi/psi)	$\epsilon_p$ -log N Regression Results			
				Slope	Correlation Coefficient	Standard Error of Estimate	
Limestone	No. 5	Med	60/15	.044	.832	.042	
			30/5	.021	.901	.014	
			40/5	.123	.875*	.090	
			90/15	2.876	.860*	1.716	
		High	60/15	.014	.929	.003	
			40/5	.007	.929	.004	
			90/15	1.026	.747	.966	
	No. 4	Low	30/15	.010	.945*	.004	
			20/5	.045	.931*	.019	
			60/15	2.207	.935*	.969	
			30/5	.164	.908*	.083	
		Med	30/15	.005	.984*	.001	
			20/5	.020	.997*	.002	
			60/15	.776	.970*	.232	
			30/5	.150	.837*	.117	
		High	20/5	.005	.977*	.001	
			60/15	.256	.895*	.126	
			30/5	.068	.976*	.017	
			40/5	3.436	.826*	1.985	
		Well Graded	Med	20/5	.011	.895*	.006
				60/15	.466	.981*	.100
				30/5	.175	.765	.161
				40/5	.177	.815*	.138
90/15	1.216			.933*	.511		
120/15	2.203			.848*	1.267		
Med	20/5		.014	.932	.006		
	60/15		.399	.907*	.202		
	30/5		.043	.893*	.024		
	40/5		.288	.856*	.190		
	90/15		1.911	.947*	.698		
	120/15		3.169	.804	1.537		
Med	20/5	.026	.885*	.015			
	60/15	.334	.908*	.169			
	30/5	.069	.855*	.046			
	40/5	.524	.839*	.374			
	90/15	1.384	.933*	.519			
	120/15	2.583	.860*	1.232			

Table 5.2. (continued).

Material Type	Gradation	Compaction Level	Stress Level $\sigma_D/\sigma_3$ (psi/psi)	$\epsilon_p$ -log N Regression Results			
				Slope	Correlation Coefficient	Standard Error of Estimate	
Limestone	CA-10	Med	20/5	.016	.894*	.009	
			60/15	.947	.920*	.441	
			30/5	.104	.849*	.071	
			40/5	1.410	.850*	.948	
			90/15	1.692	.906*	.708	
		High	20/5	.005	.938*	.006	
			60/15	.422	.912*	.206	
			30/5	.054	.845*	.037	
			40/5	.505	.806*	.406	
			90/15	1.389	.896*	.750	
			120/15	1.923	.845*	.833	
	Granitic Gneiss	No. 5	Low	20/5	.006	.979*	.001
				60/15	.287	.942*	.141
				30/5	.021	.952*	.006
40/5				.124	.933*	.052	
90/15				2.294	.965*	.576	
No. 4		Low	20/5	.052	.998*	.004	
			60/15	.107	.967*	.031	
			30/5	.016	.993*	.002	
			40/5	.452	.883*	.264	
			90/15	7.500	.777	3.924	
		Med	20/5	.016	.962*	.005	
			60/15	.233	.933*	.079	
			High	30/15	.028	.984*	.004
		20/5		.036	.937	.020	
		60/15		.243	.902*	.118	
		30/5		.051	.897*	.027	
		40/5		.125	.892*	.070	
				90/15	2.478	.930*	.942
Well Graded	Med	20/5	.011	.955*	.004		
		60/15	.302	.928*	.132		
		30/5	.027	.970*	.007		
		40/5	.319	.835*	.229		
		90/15	1.403	.985*	.233		
		120/15	1.881	.837*	.860		

Table 5.2. (continued).

Material Type	Gradation	Compaction Level	Stress Level $\sigma_D/\sigma_3$ (psi/psi)	$\epsilon_p$ - log N Regression Results		
				Slope	Correlation Coefficient	Standard Error of Estimate
Chicago Blast Furnace Slag	No. 4	Low	20/5	.061	.842*	.043
			60/15	1.444	.872*	.881
			30/5	.163	.811*	.128
			40/5	.461	.778*	.365
			90/15	2.706	.849	1.458
		Med	20/5	.036	.821*	.027
			60/15	2.091	.848	1.421
			30/5	.231	.819*	.185
			40/5	.514	.792	.430
			90/15	5.878	.828*	2.742
		High	20/5	.020	.915*	.010
			60/15	.956	.897*	.512
			30/5	.088	.830*	.064
			40/5	.441	.778	.390
			90/15	3.298	.876*	1.397
	Well Graded	Med	20/5	.017	.879*	.010
			60/15	.535	.935*	.233
			30/5	.078	.809*	.062
40/5			.615	.798*	.452	
90/15			1.476	.951*	.522	
120/15			1.726	.848*	.858	
Basalt	No. 5	Med	60/15	.076	.921*	.035
			30/5	.015	.996*	.001
			40/5	.104	.958*	.034
			90/15	.547	.962*	.169
			120/15	.936	.959*	.303
	No. 4	Med	20/5	.019	.947*	.008
			60/15	.361	.858*	.235
			30/5	.104	.930*	.049
			40/5	1.118	.932*	.478
			90/15	2.157	.990*	.313
	Well Graded	Med	20/5	.010	.939*	.004
			60/15	.135	.948*	.049
			30/5	.018	.945*	.007
			40/5	.048	.910*	.024
			90/15	.691	.965*	.205
			120/15	.745	.940*	.299

Table 5.2. (continued).

Material Type	Gradation	Compaction Level	Stress Level $\sigma_D/\sigma_3$ (psi/psi)	$\epsilon_p$ -log N Regression Results		
				Slope	Correlation Coefficient	Standard Error of Estimate
Crushed Gravel	No. 4	Med	20/5	.023	.934*	.010
			60/15	.451	.890*	.252
			30/5	.116	.903*	.061
			40/5	2.064	.850*	1.223
Gravel	No. 5	Med	60/15	.019	.920*	.009
			30/5	.210	.788	.180
			40/5	3.075	.793	1.501
	No. 4	Low	30/15	.005	.989*	.001
			20/5	.068	.882*	.039
			60/15	.557	.930*	.203
		Med	30/15	.004	.960*	.001
			20/5	.039	.930*	.017
			60/15	.467	.871*	.286
	Well Graded	Med	30/5	.415	.811*	.326
			40/5	2.156	.788	1.217
			20/5	.011	.974*	.003
			60/15	.058	.941*	.023
			30/5	.992	.866*	.552
Kansas Test Track Slag	No. 5	Low	40/5	5.063	.946	1.098
			20/5	.008	.915*	.005
			60/15	.102	.907*	.052
			30/5	.034	.912*	.017
			40/5	1.244	.700	1.368
			90/15	.739	.965*	.216
Kansas Test Track Slag	No. 5	Low	120/15	1.963	.845*	1.141
			60/15	.111	.836*	.079
			75/15	.458	.850*	.279
			30/5	.034	.881*	.020
			35/5	.080	.844*	.056
			40/5	.419	.713*	.396
			90/15	1.588	.962*	.395

Table 5.2. (continued).

Material Type	Gradation	Compaction Level	Stress Level $\sigma_D/\sigma_3$ (psi/psi)	$\epsilon_p$ - log N Regression Results		
				Slope	Correlation Coefficient	Standard Error of Estimate
Kansas Test Track Slag	No. 5	Med	60/15	.015	.910*	.007
			30/5	.035	.957*	.010
			35/5	.057	.864*	.036
			40/5	.046	.822*	.035
			50/5	.306	.895*	.169
			75/15	.036	.838*	.031
			90/15	.081	.794*	.068
		105/15	.361	.804*	.260	
		High	20/5	.003	.923	.002
			60/15	.012	.766	.012
			30/5	.013	.904	.009
			40/5	.005	.963*	.002
			90/15	.012	.896	.008
			105/15	.023	.829	.019
			120/15	.177	.741	.178
50/5	.047		.915	.030		
135/15	1.301	.822*	.993			
150/15	3.111	.682	3.072			

\* Significant at  $\alpha = 0.05$ .

pressure of 5 psi ( $34 \text{ kN/m}^2$ ) produced only 0.5 percent strain, but application of the same stress ratio and a confining pressure of 15 psi ( $103 \text{ kN/m}^2$ ) resulted in more than 3.5 percent strain. Similar results were observed for almost all of the specimens tested. In general for a given stress ratio the specimen deformed significantly more at high confining pressures than at low confining pressures.

Because both stress ratio and deviator stress must be considered in analyses of plastic strain, attempts were made to eliminate stress state as a variable. Regression analysis was used to develop improved relationships between the semi-log slopes presented in Tables 5.1 and 5.2 and various combinations of stress ratio and deviator stress. The results of two of the attempts are shown in Table 5.3. The regression equation slopes generated from this type of modeling will be referred to as "stress factors". A low stress factor means the sample is less sensitive to high stress levels than is a specimen having a high stress factor.

In general, the model which used deviator stress squared times stress ratio cubed proved slightly better than any of the others. Although the majority of the regression equations showed significant ( $\alpha = 0.05$ ) correlations, the standard errors of estimate were too large to enable successful prediction of plastic strain.

Attempts were made to further analyze the significant ( $\alpha = 0.05$ ) correlations of the above results. Because of the varied effects of stress level the analyses are included in the following sections.

Table 5.3. Stress Factor Results.

Material Type	Gradation	Compaction Level	Stress Factors Obtained from Regression Analysis Using	
			$\sigma_D^2$ ( $\times 10^{-6}$ )	$\sigma_D^5/\sigma_3^3$ ( $\times 10^{-6}$ )
Limestone	No. 5	Med	406	1.80
		High	163*	.59
	No. 4	Low	758*	5.30
		Med	283*	2.02
	Well Graded	High	15	4.34*
		Med	154*	.28*
		Med	229*	.41*
	CA-10	Med	176*	.33*
		High	178	.77
			170	.71
Granitic Gneiss	No. 5	Low	294*	1.11*
		High	951*	3.85*
	No. 4	Low	99	.58
		Med	304*	1.26*
		High	38*	.24*
Chicago Blast Furnace Slag	No. 4	Low	341*	1.08
		Med	786*	2.86*
	Well Graded	High	422*	1.55*
		Med	122*	.20*
Basalt	No. 5	Low	68*	.12*
	No. 4	Med	243*	1.14*
	Well Graded	High	57*	.09*
Crushed Gravel	No. 4	Med	167	2.43*
Gravel	No. 5	Med	391	4.11*
		Low	192	1.97
	No. 4	Med	130	2.57*
		High	-203	6.57*
		Med	116*	.25*
Kansas Test Track Slag	No. 5	Low	168*	.83*
		Med	17	.09*
		High	100*	.13*

\*Significant at  $\alpha = 0.05$

#### 5.4 Correlations with Characterization Test Results

To determine possible links between plastic strain behavior and material properties, correlation analyses between various plastic strain parameters and the material characterization test results presented in Chapter 3 were accomplished. The results of the analyses are presented in this section.

The results for the correlation analysis of the plastic strains recorded at a stress ratio of 45/15 for all 32 samples are shown in Table 5.4.

Significant ( $\alpha = 0.05$ ) correlations resulted between the 4 plastic strain values and both the initial density (inverse) and the void ratio. The strain value recorded after 5000 cycles also showed a significant correlation with the crushing value test results. None of the other variables achieved a significant level of correlation. The dependency of plastic strain on initial void ratio or density (or porosity) reported by ORE (25) thus is reinforced.

To eliminate gradation effects a correlation analysis was performed using only the results for the 14 No. 4 ballast gradation specimens. The plastic strain values for two additional stress ratios were included in the analysis. As shown in Table 5.5 the significant correlations were much the same as in the previous analysis. None of the correlations for the higher stress levels was significant except for soundness value with the plastic strain after 100 cycles of a stress ratio equal to 20/5. Furthermore, the significant correlations with density were reduced to the two strain values recorded after 1000 and 5000 cycles of a 45/15 stress ratio.

Table 5.4. Correlation of Plastic Strain Results for 32 Specimens.

Stress Level, $\sigma_D/\sigma_3$	Number of Cycles	Particle Index	Specific Gravity	Los Angeles Abrasion Number	Density	Void Ratio	Gradation Parameter	Flakiness Index	Soundness	Crushing Value
45/15	10	.150	-.214	.175	-.475*	.564*	-.141	-.033	.041	.211
	100	.178	-.223	.217	-.484*	.571*	-.128	-.010	.049	.242
	1000	.227	-.250	.287	-.521*	.597*	-.136	.016	.038	.309
	5000	.252	-.331	.330	-.536*	.578*	-.098	-.046	.009	.371*

\* Significant at  $\alpha = 0.05$

Table 5.5. Correlation of Plastic Strain Results for 14 No. 4 Gradation Specimens.

Stress Level, $\sigma_D/\sigma_3$	Number of Cycles	Particle Index	Specific Gravity	Los Angeles Abrasion Number	Density	Void Ratio	Gradation Parameter	Flakiness Index	Soundness	Crushing Value
45/15	10	.228	-.268	.170	-.462	.619*	-.136	-.082	.100	.221
	100	.227	-.277	.199	-.501*	.671*	-.097	-.063	.035	.265
	1000	.376	-.328	.268	-.593*	.754*	.028	-.034	.030	.346
	5000	.436	-.451	.308	-.690	.807	-.055	-.153	-.086	.445
20/5	10	-.049	.269	.148	.094	.008	.043	.311	-.085	-.009
	100	-.109	.299	.121	.113	.002	.096	.315	-.010	-.065
	1000	-.077	.182	.156	-.022	.140	-.003	.180	-.125	.022
	5000	.298	-.260	.391	-.426	.494	-.098	-.041	-.255	.419
60/15	10	.312	-.155	-.316	-.158	.445	-.023	.353	.101*	-.154
	100	.278	-.031	.244	-.254	.416	.308	.368	.567*	.115
	1000	.294	-.299	.331	-.450	.508	.112	.051	.412	.276

\*Significant at  $\alpha = 0.05$

In the above analysis not all of the material types were weighted equally; another analysis therefore was conducted using only the 6 medium density No. 4 gradation specimens. The results are shown in Table 5.6. Although particle index correlated significantly with two of the strain readings, the results were not consistent. The results of the analysis in general were too erratic to draw any conclusions.

To include the gradation parameter, three gradation levels of each of three material types (limestone, basalt, and gravel) were used in another correlation analysis. The results, presented in Table 5.7, show significant ( $\alpha = 0.05$ ) correlations between gradation parameter and 5 of the recorded strain values. The relationship is inverse which means that the strains were highest for the more uniformly graded (No. 4) specimens. A further analysis of gradation effects will be presented in a latter section.

Table 5.8 presents the results for two additional correlation analyses. The  $\epsilon_p - \log N$  slope values for all 32 specimens (for a stress ratio of 45/15) correlated significantly ( $\alpha = 0.05$ ) with Los Angeles Abrasion Number, density, void ratio, and crushing value. When the two dense graded (CA-10) specimens were left out of the analysis the results were unchanged except gradation parameter was an additional significant correlation.

Table 5.9 presents similar analyses for the "stress factors" derived previously. The significant correlations were density, void ratio, and gradation parameter with the stress factor derived using the deviator stress squared model. The other analysis presented in

Table 5.6. Correlation of Plastic Strain Results for 6 No. 4 Gradation Specimens.

Stress Level, $\sigma_D/\sigma_3$	Number of Cycles	Particle Index	Specific Gravity	Los Angeles Abrasion Number	Density	Void Ratio	Gradation Parameter	Flakiness Index	Soundness	Crushing Value
45/15	10	.420	.243	-.514	-.101	.475	-.330	.348	-.155	-.220
	100	.706	.182	-.288	-.271	.701	-.113	.591	-.136	.001
	1000	.814*	-.100	.136	-.473	.740	.567	.622	.379	.282
	5000	.968*	-.443	.193	-.803	.975*	.101	.242	-.120	.552
20/5	10	-.386	.171	.135	.364	-.490	.833*	.164	.862*	-.235
	100	-.437	.270	.056	.458	-.551	.795	.212	.840*	-.328
	1000	-.742	.158	-.025	.524	-.779	.397	-.244	.560	-.378
	5000	-.301	-.594	.155	-.226	-.219	-.163	-.878*	-.119	.199
60/15	10	.624	.302	-.696	-.106	.559	-.074	.581	-.064	-.374
	100	.287	-.029	.285	-.125	.174	.977*	.476	.851*	.120
	1000	.541	-.891*	.655	-.857*	.573	.363	-.376	.113	.814*

\* Significant at  $\alpha = 0.005$ .

Table 5.7. Correlation of Plastic Strain Results for 9 No. 4 Gradation Specimens.

Stress Level, $\sigma_D/\sigma_3$	Number of Cycles	Particle Index	Specific Gravity	Los Angeles Abrasion Number	Density	Void Ratio	Gradation Parameter	Flakiness Index	Soundness	Crushing Value
45/15	10	.288	.371	-.322	-.115	.220	-.138	.224	-.049	-.217
	100	.336	.240	-.155	-.316	.374	-.349	.255	.151	-.029
	1000	.343	.069	.041	-.477	.490	-.541	.281	.395	.170
	5000	.272	.076	-.001	-.433	.443	-.559	.175	.284	.091
20/5	10	-.137	-.420	.379	-.138	.052	-.484	-.187	.433	.275
	100	-.087	-.366	.335	-.301	.214	-.664	-.163	.425	.249
	1000	-.060	-.236	.184	-.357	.280	-.746*	-.208	.231	.094
	5000	-.073	-.197	.127	-.341	.260	-.722*	-.248	.112	.023
60/15	10	.335	-.004	.109	-.261	.242	-.145	.287	.288	.224
	100	.319	-.358	.506	-.383	.267	-.258	.337	.769*	.616
	1000	.262	-.370	.496	-.504	.394	-.507	.272	.785*	.580
	5000	.244	-.293	.380	-.597	.496	-.710*	.181	.625	.435
30/5	10	.076	.167	-.176	.001	.024	-.199	-.018	.102	-.162
	100	-.260	-.127	.005	-.274	.226	-.794*	-.398	.004	-.147
	1000	-.326	-.289	.166	-.280	.198	-.813*	-.448	.098	-.009
	5000	-.451	-.396	.243	-.071	-.054	-.549	-.554	.045	.020

\* Significant at  $\alpha = 0.05$ .

Table 5.8. Correlation of Regression Results.

	Particle Index	Specific Gravity	Los Angeles Abrasion Number	Density	Void Ratio	Gradation Parameter	Flakiness Index	Soundness	Crushing Value
Slopes of $\epsilon_p - \log N$ at $\sigma_D/\sigma_3 =$ 45/15 for all 32 samples	.267	-.292	.361*	.498*	.532*	-.070	.019	.069	.366*
Slopes of $\epsilon_p - \log N$ at $\sigma_D/\sigma_3 =$ 45/15 for open graded samples only	.271	-.311	.362*	-.609*	.664*	-.373*	.013	.039	.381*

\* significant at  $\alpha = 0.05$

Table 5.9: Correlation of Stress Factor Results.

	Particle Index	Specific Gravity	Los Angeles Abrasion Number	Density	Void Ratio	Gradation Parameter	Flakiness Index	Soundness	Crushing Value
Stress factor obtained with $\sigma_{D_n}^2$	.081	-.247	.422	-.547*	.590*	-.694*	-.114	-.049	.388
Stress factor obtained with $\sigma_D^5/\sigma_3^3$	-.472*	.026	.058	-.052	.100	-.672*	-.246	.092	-.136

\*significant at  $\alpha = 0.05$

Table 5.9 is for the stress factors derived using the deviator stress squared times the stress ratio cubed (or  $\sigma_D^5/\sigma_3^3$ ). Particle index and gradation parameter were the only observed significant correlations for this analysis. Of the four factors considered in Tables 5.8 and 5.9, no variable afforded consistent significant correlation values.

In general, none of the analyses considered in Section 5.4 resulted in consistent significant ( $\alpha = 0.05$ ) correlations between the various strain parameters and the specimen properties. However an inverse relationship between plastic strain and the initial void was present in several of the analyses. Because of the lack of consistent results and because of the difficulty in establishing causal relationships through correlation studies, analysis of variance was used to determine possible differences among the plastic strain responses of the samples due to gradation, compaction, and material effects.

## 5.5 Analysis of Variance

The effects of material type, compaction effort, and gradational changes on the plastic strain behavior of aggregate are presented in this section.

### 5.5.1 Effects of Gradation

Because changes in gradation affect the compaction characteristics and the maximum theoretical density of aggregate, gradation effects on plastic strain behavior are difficult to demonstrate quantitatively. Figures 5.3 through 5.8 show some of the effects, although the differences in density make direct comparisons difficult.

For example, in Figure 5.3 the two plastic strain curves representing the well graded and the medium density No. 4 gradation limestone specimens are extremely close, but the density of the well graded specimen was 16 pcf ( $256 \text{ kg/m}^2$ ) greater than the density of the No. 4 gradation sample, although the same compactive effort was used for both specimens. Figures 5.4 and 5.5 show similar results for granitic gneiss specimens and for blast furnace slag specimens, respectively. In both cases the well graded materials attained higher densities than did the No. 4 gradation, although the plastic strain curves were similar. Figures 5.6 and 5.8 show similar trends for gravel and for basalt, respectively. Figure 5.7 includes the plastic strain results for the CA-10 gradation specimens and two well graded specimens. Although the well graded specimens attained densities appreciably less than those of the CA-10, the plastic strain results for all 4 samples were of the same order of magnitude.

To show quantitatively the effects of gradation, randomized complete block (RCB) analysis was used to consider the plastic strain data recorded at 10, 100, 1000 and 5000 cycles for several stress levels. Three material types and 3 gradation levels of each were included. The results are included in Table 5.10. In only two cases were the strains different.

A completely randomized design (CRD) analysis also was used to evaluate the effects of gradation on plastic strain behavior. The significant ( $\alpha = 0.05$ ) results obtained in the stress factor analysis of Section 5.3 were divided into two groups on the basis of numerical ranking. As previously mentioned a material showing a low stress factor will better resist permanent deformation than one with a high stress factor. The CRB

Table 5.10. RCB Analysis of Plastic Strain Results by Gradation.

Stress Level(a)	Number of Cycles	Mean Strain, %, for 3 levels of gradation <sup>(b)</sup>			F Value
		No. 5	No. 4	Well Graded	
45/15	10	.213	.380	.390	0.795
	100	.367	.850	.707	1.328
	1000	.523	1.653	1.077	2.642
	5000	.647	1.947	1.300	2.787
60/15	10	.014	.049	.052	0.921
	100	.024	.195	.168	2.207
	1000	.066	.877	.430	3.366
	5000	.146	1.640	.686	12.693*
30/5	10	.008	.014	.014	1.241
	100	.025	.067	.025	6.625
	1000	.070	.224	.065	11.355*
	5000	.284	.725	.243	1.707

\*significant at  $\alpha = 0.05$

(a) Repeated deviator stress over confining pressure: psi/psi

(b) Based on three material types, limestone, basalt, and gravel

analysis considered the stress factor and gradation parameter as variables; the results are shown in Table 5.11. Both of the variables (stress factor and gradation parameter) were found to differ significantly ( $\alpha = 0.05$ ). The No. 4 gradation specimens were in general among those in the lower half of the ranking. The CRD analysis indicates that the No. 5 gradation ballast and the well graded ballast better resist permanent deformation than does the No. 4 gradation material.

### 5.5.2 Effects of Material Type

Because of economic considerations a ranking of ballast according to material type (slag, granite, etc.) is desirable. This section includes the analysis of plastic strain behavior according to material type. Some information is available from the plots of plastic strain versus logarithm of the number of cycles. For example, Figure 5.6 presents the plastic strain results of two No. 4 gradation gravel specimens compacted with the same effort. As shown one specimen contained rounded material and the other was made from crushed particles. The material for the two samples was obtained from a single source. The crushed gravel sample accumulated more plastic strain, but for the same compactive effort the uncrushed gravel attained a density 7 pcf ( $112 \text{ kg/m}^3$ ) greater than did the crushed material.

Randomized complete block analysis was used to determine the effect of the material properties on the plastic strain after 10, 100, 1000, and 5000 cycles for various stress levels. Three materials (limestone, basalt, and gravel) and 3 gradations of each were considered in the analysis. The results of the analysis are shown in Table 5.12. No significant

Table 5.11. CRD Analysis of Stress Factor Results by Gradation.

Analysis Using Stress Factor Based on  $\sigma_D^5 / \sigma_D^3$ 

Number of Repetitions	Mean Stress Factor ( $\times 10^{-6}$ )	Mean Gradation Parameter, $\bar{A}$
11	.27	2.00
11	2.90	1.21
F value	25.9*	57.5*

Analysis Using Stress Factor Based on  $\sigma_D^2$ 

Number of Repetitions	Mean Stress Factor ( $10^{-6}$ )	Mean Gradation Parameter, $\bar{A}$
10	126	1.98
10	461	1.27
F value	15.5*	24.4*

\*Significant at  $\alpha = 0.05$ .

Table 5.12. RCB Analysis of Plastic Strain Results by Material Type.

Stress Level (a)	Number of Cycles	Mean strain, %, for 3 types of material (b)			F Value
		Limestone	Basalt	Gravel	
45/15	10	.418	.414	.281	0.479
	100	.860	.776	.499	0.413
	1000	1.333	1.210	.771	0.622
	5000	1.696	1.413	1.059	0.288
60/15	10	.050	.041	.024	0.372
	100	.266	.083	.055	2.857
	1000	.888	.261	.233	2.853
	5000	1.282	.594	.596	3.485
30/5	10	.012	.013	.012	0.103
	100	.032	.032	.052	1.553
	1000	.111	.075	.172	3.390
	5000	.389	.153	.711	1.875

(a) Repeated deviator stress over confining pressure; psi/psi

(b) Based on three gradations, No. 5, No. 4, and Well Graded.

( $\alpha = 0.05$ ) differences were found among the strain readings with regard to material type.

Completely randomized design analysis was used to determine the effect of various material properties on plastic strain behavior. The stress factor values and the material properties (particle index, specific gravity, Los Angeles abrasion number, flakiness index, soundness loss, and crushing value) were included as the variables. The results (Table 5.13) show there were no significant differences for any of the material properties between the two stress factor groups.

### 5.5.3 Effects of Degree of Compaction

The effect on plastic strain behavior of various levels of compaction is shown in Figures 5.1 through 5.6. All of the data were recorded during the conditioning phase of testing. In every case the permanent strain after 5000 cycles was appreciably less for the specimens compacted to the highest levels of density. The results of randomized complete block analysis of the  $\epsilon_p - \log N$  regression equation slopes (at 45/15) for 5 sample types and 3 levels each of compactive effort (Table 5.14) show there were significant ( $\alpha = 0.05$ ) differences among the slopes for the three levels of compaction. Further analysis using Duncan's multiple range test revealed there was no significant ( $\alpha = 0.05$ ) difference in slope between the high and medium compactive effort samples, but both were significantly different from the low compactive effort samples. The lowest slope values were those obtained for the high density samples.

Although the effect of initial void ratio is pronounced no conclusions should be drawn with respect to density among material types because of the

Table 5.13. CRD Analysis of Stress Factor Results.

Analysis Using Stress Factor Based on  $\sigma_D^5 / \sigma_D^3$

Number of Repetitions	Mean Stress Factor (x 10 <sup>-6</sup> )	Mean Particle Index	Mean Specific Gravity	Mean Los Angeles Abrasion Number	Mean Flakiness Index	Mean Soundness Loss	Mean Crushing Value
11	.27	14.0	2.59	27.5	11.8	5.90	22.3
11	2.90	12.8	2.58	29.4	10.1	4.52	22.7
F Value	25.9*	1.43	.01	.27	.41	.32	.00

Analysis Using Stress Factor Based on  $\sigma_D^2$

Number of Repetitions	Mean Stress Factor (X 10 <sup>-6</sup> )	Mean Particle Index	Mean Specific Gravity	Mean Los Angeles Abrasion Number	Mean Flakiness Index	Mean Soundness Loss	Mean Crushing Value
10	126	13.9	2.59	27.6	12.5	6.18	22.1
10	461	14.5	2.51	33.2	12.3	5.94	27.1
F value	15.5*	.56	.70	2.21	.00	.01	2.03

\*Significant at  $\alpha = 0.05$

**Table 5.14. RCB Analysis of Regression Results by  
Compaction Level.**

Stress Level, $\sigma_D/\sigma_3$ , (psi/psi)	Mean Slope for 3 Compaction Levels <sup>(a)</sup>			F* Value
	Low	Medium	High	
45/15	1.00	.528	.265	13.363*

\* Significant at  $\alpha = 0.05$

(a) Based on 5 material types each, limestone, granitic gneiss, Chicago blast furnace slag, outwash and Kansas test track blast furnace slag.

differences in the ease with which some types of materials, especially the gravels, were compacted. For example the behavior of the No. 5 gradation Kansas Test Track slag (Figure 5.2) was comparable to that of the No. 4 gradation gravel (Figure 5.6) although for all three levels of compaction the density for the gravel was approximately 10 pcf ( $160 \text{ kg/m}^3$ ) greater than for the slag.

A completely randomized design analysis of the stress factors and void ratios (Table 5.15) indicates there is a significant ( $\alpha = 0.05$ ) difference between the void ratios of the specimens with low stress factors and those in the group with high stress factor values.

The results of the above analyses indicate that no other specimen parameter is as important in influencing the permanent strain behavior as is the degree of compaction.

#### 5.6 Comparisons with Hyperbolic Stress-Strain Law

The equation that Barksdale used for predicting permanent strain after 100,000 cycles of loading was presented in Section 2.3. For cohesionless materials for which the deviator stress value at failure is known the equation simplifies to:

$$\epsilon_p = \frac{\sigma_D}{E_i \left[ 1 - \frac{\sigma_D}{(\sigma_1 - \sigma_3)_{ult}} \right]} \quad (5.1)$$

where  $\epsilon_p$  = permanent axial strain,  
 $E_i$  = initial tangent modulus, psi,  
 $\sigma_D$  = deviator stress, psi, and

Table 5.15. CRD Analysis of Stress Factor Results by Void Ratio.

Analysis Using Stress Factor Based on  $\sigma_D^5/\sigma_3^3$

Number of Repetitions	Mean Stress Factor ( $\times 10^{-6}$ )	Mean Void Ratio
11	.27	.514
11	2.90	.674
F value	25.9*	6.16*

Analysis Using Stress Factor Based on  $\sigma_D^2$

Number of Repetitions	Mean Stress Factor ( $\times 10^{-6}$ )	Mean Void Ratio
10	126	.515
10	461	.778
F value	15.5*	18.4*

\*Significant at  $\alpha = 0.05$

$(\sigma_1 - \sigma_3)_{ult}$  = the stress difference the stress-strain curve approaches at infinite strain, psi

Equation 5.1 and the results of the static triaxial tests presented in Table 3.4 were used to calculate permanent strain values for 6 No. 4 ballast gradation specimens of medium density. The results and the strain values recorded after 10 and 100 cycles of loading for the corresponding repeated load samples are presented in Table 5.16. The correlation coefficients are 0.50 and 0.43 for the comparisons between the predicted values and the 10 and 100 cycles recorded values, respectively. Neither is significant ( $\alpha = 0.05$ ).

Although the data available are limited, there appears to be no relation between the strains obtained through repeated load testing of open graded materials and the values predicted by the hyperbolic stress-strain law.

## 5.7 Summary

The analyses presented in this chapter have shown that the most important factors influencing the permanent deformation behavior of ballast are the number of repetitions, the degree of compaction, and the stress level. As previous studies also have shown, the increase in plastic strain in general is inversely proportional to the number of loading cycles. In every case the permanent deformation was least for the specimens compacted with the greatest effort. The stress level effects are more difficult to discern because both the deviator stress and the confining pressure and not merely the ratio of the two must be considered. In addition, the permanent strain results are very much in accordance with the concepts of

Table 5.16. Comparisons with Hyperbolic Stress-Strain Law Results.

Material Type	Strain, %		
	Recorded after		Calculated from Hyperbolic Stress-Strain Law
	10 cycles	100 cycles	
Limestone	0.308	0.837	0.406
Granitic Gneiss	0.347	0.953	0.508
Chicago Blast Furnace Slag	0.376	0.882	1.023
Basalt	0.589	1.213	0.593
Crushed Gravel	0.542	0.980	0.829
Gravel	0.240	0.503	0.297

Lade and Duncan (31) in that large strains accumulated during primary loading but practically zero strain resulted during reloading or during loading at reduced stress levels.

The effects on permanent deformation of gradation are important to a lesser extent than the above parameters. In general, the No. 4 gradation tended to resist permanent deformation less than did the No. 5 or the "well graded" materials.

The effects of material properties, such as particle index, flakiness index, etc., are not consistent and therefore no conclusions are made with respect to such properties.

## CHAPTER 6

### SUMMARY AND CONCLUSIONS

#### 6.1 Summary

Ballast type materials from several sources were tested in the triaxial apparatus. In service conditions were simulated by utilization of a repeated deviator stress and constant confining pressure. Permanent strain and resilient modulus characteristics were determined; the variables considered included material type and gradation, density, and stress level. Equations relating resilient modulus to the first stress invariant were developed, and the results were analyzed with respect to the variables. The permanent strain results were analyzed with respect to stress level, and comparisons were made between the results according to material characteristics, gradation, and density.

#### 6.2 Conclusions

During this investigation the following conclusions were reached:

1. The resilient response of a specimen of open graded granular material is independent of stress history so long as the specimen has not been subjected to a stress level which would cause failure.
2. The resilient modulus of open graded materials is appreciably higher than that of dense graded aggregate for a given stress level.
3. The resilient modulus of open graded materials is virtually insensitive to changes in gradation and compaction level. The dependence of resilient response on material type is weak and inconsistent, and therefore no conclusion is drawn with respect to material type.

4. Stress level is the variable most directly influencing the resilient modulus of granular materials. The stress dependent nature of ballast type materials can be characterized by the predictive equation:

$$E_r = K \sigma^n \quad (2.1)$$

5. In sharp contrast to the resilient behavior, plastic strain is affected by stress history. The effect can be explained in terms of primary loading, unloading, and reloading. Large plastic strain results during primary loading. During unloading and reloading elastic strain develops which is accompanied by a small amount of plastic strain.

6. For low stress levels plastic strain is proportional to the logarithm of the number of cycles. As the stress level is increased a "critical value" is reached and the rate of plastic strain accumulation then increases.

7. Plastic strain accumulation is not solely a function of the repeated deviator stress but depends on both the deviator stress and the confining pressure.

8. In general, the No. 5 ballast and the "well graded" specimens tended to resist permanent deformation better than did the No. 4 gradation material.

9. There is a definite dependence of permanent strain behavior on compaction level. In every case the accumulated permanent strain was least for specimens compacted to the highest densities.

10. No definite conclusion can be made with respect to the effects on plastic strain behavior of material properties such as particle index, soundness, Los Angeles abrasion loss, and flakiness index.

PART B  
CHAPTER 7

## INTRODUCTION

## 7.1 Statement of the Problem

Because railway ballast is subjected in the field to large numbers of repeated loadings and because only recently have solutions to the states of stress in ballast become available the characterization of the repeated load permanent deformation has not been addressed readily. It is desirable to determine the response, both plastic and elastic, of various types and gradations of ballast subjected to simulated field stress conditions. Also because ballast necessarily will suffer some breakdown due to repeated mechanical loading, characterization of its degradation\* is required before intelligent choices involving ballast selection can be made.

Modern investigations (25, 32, 44, 45) have used large diameter triaxial cells and repeated loading techniques to determine the behavior of ballast, but additional testing is needed to define the effects of long term ( $10^5$  or more cycles) loading on ballast materials. As an outgrowth of long term testing valuable degradation information also may be obtained.

Because of the success of other investigations, the repeated load triaxial procedure is a logical choice of test method. Information on the elastic and permanent deformation response of ballast materials can be gained easily through the use of repeated load triaxial investigations.

## 7.2 Objective and Scope

The objective of this research was to determine the effects of  $10^5$  to  $10^6$  cycles of loading on the permanent deformation behavior of six ballast

---

\*Degradation as used in this report refers to breakdown due to loading only.

material types. Also studied was the mechanical breakdown of the aggregate after  $10^6$  loading cycles.

It was the intent of the study that the results be used to correlate field performance with laboratory results of permanent deformation behavior, although a study of the field performance of ballast was beyond the scope of this investigation.

The work was divided into four phases. Phase I involved a literature survey of laboratory studies and in service evaluations of both the permanent deformation behavior of ballast and the breakdown of ballast and is presented in Chapter 8.

Phase II involved establishing a standard test sequence. Six types (limestone, basalt, etc.) of materials were selected and were tested in a large diameter triaxial cell under conditions of repeated deviator stress and constant confining pressure. The results are included in Chapter 9.

Chapter 10 (Phase III) presents the permanent deformation data obtained during the long term testing program and the analyses of the results with regard to material characteristics previously determined (1). Also included in Chapter 10 are the results of two specimens tested at low confining pressure.

Phase IV involved establishing meaningful measures of degradation and analyzing the gradations of the samples before and after testing. Phase IV is included in Chapter 11.

The summary and the conclusions are presented in Chapter 12.

## CHAPTER 8

### LITERATURE SURVEY

#### 8.1 General

The primary factors influencing the repeated load, permanent strain behavior are the stress history, the stress level, including both deviator stress and confining pressure, the degree of compaction, and the number of loading cycles. The type of ballast (limestone, basalt, etc.) and the gradation are important but to a lesser extent. An amplified discussion of the factors is included in References 39 and 44. This report therefore will be limited to the findings of other long term tests of ballast, to the results of degradation studies, and to field studies of ballast deformation and degradation.

#### 8.2 Permanent Deformation

##### 8.2.1 Laboratory Investigations of Permanent Deformation Behavior

Heath and Shenton (45) tested three gradations of Meldon Stone ballast in a triaxial apparatus (9 in. by 9 in.) and measured the permanent deformation due to repeated loading. Three levels of compaction were investigated. The important conclusions were:

1. The first load application causes as much as 35 to 45 percent of the total deformation produced by  $10^7$  cycles.

2. The permanent deformation resulting from the first load cycle is greatly dependent on the degree of compaction.

3. The initial deformation and the rate of permanent deformation accumulation both depend on the applied stress.

Studies by ORE (32) were based in part on that of Heath and Shenton, and therefore the conclusions were similar. One important additional conclusion was that the larger of two different loads, such as would result

from wheel flats, causes the preponderance of the deformation.

Wong (28) tested ten types of ballast in a one dimensional (rigidly confined) repeated load apparatus for 100,000 cycles at a stress of 100 psi (690 kN/m<sup>2</sup>). The permanent strain was proportional to the logarithm of the number of cycles and was least for samples compacted to the highest density. An average of 50 percent of the total strain occurred on the first cycle. Wong found no correlations between permanent strain and the mechanical or physical properties of the aggregate.

Triaxial testing of ballast was accomplished by Chung (46). The tests were not repeated load tests but were static triaxial tests in which the effects of gradation, density, and confining pressure were investigated. The maximum deviator stress values were obtained for samples of high density when tested at high confining pressures. The effect of gradation was slight. Although the tests were static tests another series of tests was conducted on specimens which had been "preloaded". The preloaded specimens were subjected to as many as 10,000 cycles of a repeated axial pressure, to simulate field loading, before they were tested statically. The differences between the two types of tests were minimal.

Olowokere (24) extended the study by Chung to include repeated load triaxial testing of ballast. The material tested was described as Coteau dolomite; the variables investigated included the magnitude of the cycled deviator stress. The first cycle vertical strain resulted in about 50 percent of the strain accumulated during 100,000 cycles, and the total strain increased with increasing repeated deviator stress.

Bishop (29) extended the one dimensional tests of Wong to include three other types of ballast: St. Marc limestone, Nouvelle igneous, and Sudbury slag. The important conclusions of the study showed differences in the permanent deformation behavior by ballast type. On the average the St.

Marc limestone accumulated more permanent strain than did the other materials.

Lau (23) conducted repeated load triaxial tests on sand and concluded that the permanent axial strain increased as the number of cycles increased but at a decreasing rate. Lau also found that the critical value for the repeated deviator stress was between 50 and 62.5 percent of the static triaxial value.

### 8.2.2 Field Correlations

Literature on permanent deformation studies in the field is extremely limited. Perhaps most noteworthy is the study by Heath and Shenton (45). In addition to the laboratory testing previously discussed, observations of permanent deformation at field sites were also made. Plates were installed beneath each of ten consecutive ties, and the level of each plate was monitored after various amounts of loading. The conclusions were:

1. There is a large deformation during early loading.
2. The permanent deformation tends to be proportional to the logarithm of the number of axle loads.
3. The magnitude of the field deformations tended to "correspond to those observed in the laboratory..." The field deformations were slightly greater than the laboratory results suggested.

Again the ORE (32) results were based in part on the above investigation although some additional variables were included. The conclusions therefore are much the same as those of Heath and Shenton. It is interesting to note that the field investigation of the effect of ballast thickness resulted in more total settlement for the sections using 30 cm (12 in.) of ballast than for the section with only 20 cm (8 in.) of ballast.

### 8.3 Degradation

Before a meaningful specification can be written for ballast resistance

to degradation due to repeated loading, testing of many types of materials and analysis of the results must be accomplished. A method of measuring the repeated load degradation of ballast through sieve analysis and observation of change in gradation is possible. For example, No. 4 ballast should have no material passing the No. 4 sieve; thus the amount of material passing the No. 4 sieve after in service loading might serve as a measure of degradation. However the ballast gradation in place prior to loading must be known before comparisons can be made. The problem therefore is twofold: a measure of degradation must be defined, and a method must be developed for sampling in place ballast.

Two problems common to both laboratory and field degradation studies are those of variability (or repeatability) of the sieve analyses and the resultant problem of sample size determination.

NCHRP Report 34 (49) presented statistical concepts and nomographs for sample weight and the required number of samples. Various sampling methods were tested and standard deviations that could be expected for the various sieve sizes were determined. For example, for amounts of material passing the No. 4 sieve ranging from 5 to 8 percent, the standard deviation expected is approximately 3 percent.

NCHRP Report 46 (50) continued the above study and included degradation due to construction operations. Several sections were constructed of well graded materials; the degradation due to construction was much less than expected. For amounts of material passing the No. 4 sieve ranging from 1.3 to 7.5 percent, the standard deviation varied from 0.4 to 2.9 percent.

### 8.3.1 Laboratory Degradation Studies

Laboratory investigations of aggregate degradation can be divided into two groups: those that deal with breakdown due to repeated loading and those

that are concerned with predicting degradation caused by weathering. The latter subject has been covered in Reference 39; this section will cover only studies involving degradation of ballast due to repeated loading.

In addition to the measurements of permanent deformation previously discussed, Wong (28) determined the breakdown of the ballast materials tested. No material passed the No. 4 sieve in the initial grading. Breakdown was defined as any material passing the No. 4 sieve after testing and the breakdown was subdivided into the amount passing the No. 200 sieve. The results of the study indicated that breakdown was independent of initial void ratio for ballasts placed in a loose state and that particle shape did not affect the breakdown. Furthermore, degradation increased both as the number of loading cycles and as the cycled pressure increased. The amount of material passing the No. 200 sieve was small and was "independent of initial density and pressure." Significant correlations were obtained between breakdown and both Los Angeles abrasion loss and crushing value. Wong's results were based on the rigidly confined test - a procedure resulting in higher stresses than would normally occur in the field.

Chung (46) evaluated degradation following his triaxial tests. He concluded that breakdown increased as both initial density and cell pressure increased but was independent of stress-strain curve results. The repeated load triaxial test results of Olowekere (24) indicated that breakdown increased as the cell confining pressure increased. Bishop (29) concluded that ballast breakdown increased as the cycled pressure increased but was independent of initial density; the amount of material passing the No. 200 sieve was shown to be independent of both initial density and cycled pressure.

Eske and Morris (51) modified the Los Angeles abrasion test to produce a greater percentage of fines and fines of a more plastic nature. In the

modified test, the aggregate was subjected to abrasion in the standard machine without the use of the steel balls. A four hour run was used instead of the standard 500 revolutions. The fines produced tended to be more plastic, and the amount of material passing the No. 200 sieve increased as compared with the standard test. For example, in the standard test on basalt the amount of material passing the No. 200 sieve was 7.5 percent; the fines were nonplastic; and the Los Angeles abrasion loss was 16.2 percent. The same material subjected to the modified test produced material with 8.3 percent passing the No. 200 sieve and a plasticity index of 6.8, but the Los Angeles abrasion loss decreased to 12.2 percent.

A series of tests was conducted by AREA (47) in an attempt to correlate laboratory test results with field performance. Los Angeles abrasion loss, sieve analysis, and soundness (magnesium sulfate) were determined for field samples of 36 ballast types. "Generally . . . no correlation was found between the evaluation of field performance . . . and the tests performed on those samples . . ." (47). In another AREA study (34, 48, 52) 17 types of ballast were subjected to repeated loading in a full scale oscillation device and the degradation of each type of ballast was compared to the physical properties of the material. No significant results were reported although "good correlation" was found between results of a Los Angeles test (conducted without a surcharge) and the degradation from the oscillator test.

### 8.3.2 Field Degradation Studies

Several studies of the in service degradation of highway aggregates have been made, but few field investigations of ballast breakdown are available. The most significant research is probably Dalton's (53) study of the in service degradation of 10 types of crushed ballast. Adjoining

quarter mile sections of track were ballasted with materials from different sources. Polyethylene sheeting was installed at the top of the subgrade so that any fines generated by degradation could be recovered and the ballast would not foul from beneath. Samples were taken at the time of construction and after each of the three following years. The samples were tested for flakiness, absorption, Los Angeles abrasion, and soundness; sieve analysis was also accomplished so that comparisons could be made with the original gradation. After three years, three ballasts (two limestones and an intrusive igneous) had broken down enough so that drainage was affected. The conclusions of the study were that the absorption, soundness, and Los Angeles abrasion tests do not adequately evaluate aggregate resistance to freeze-thaw and mechanical breakdown.

It is interesting to note that the materials used in the field study by Dalton (53) were the same ones tested in the aforementioned laboratory investigation of Wong (28). Table 8.1 is a comparison of the results of the breakdown obtained in Wong's laboratory research with the evaluations of the same materials used in the in service tests reported by Dalton. Total breakdown was defined as any material passing the No. 4 sieve. Although there appears to be some relationship between the qualitative evaluations and the total breakdown, it is difficult to find any correlation between the minus 200 (passing the No. 200 sieve) breakdown and either the qualitative evaluations or the total breakdown results.

#### 8.4 Summary

Although no well established methods have been developed for characterizing laboratory or in service degradation of ballast due to either mechanical mechanisms or weathering, the studies of Dalton (53) and Wong (28) appear promising, especially for establishing criteria for measuring the amount of breakdown.

Table 8.1. Comparison of Field and Laboratory Ballast Degradation (References 28 and 53).

BALLAST	CANADIAN NATIONAL RAILWAYS FIELD EVALUATION	BREAKDOWN DUE TO REPEATED LOADING	
		TOTAL (%)	MINUS 200 (%)
Dulude Shale	Breakdown is minimal and the quantity of fines is not significant	0.69	0.08
Joliette Limestone	Some breakdown, but ballast remains free draining	1.85	0.23
Montreal Limestone	Noticeable breakdown; not seriously affecting drainage	2.23	0.05
St. Marc Limestone	Excessive breakdown; drainage is impeded	3.71	0.17
Coteau Dolomite	Slight breakdown; not impeding drainage	1.09	0.07
St. Isidore Limestone	Significant breakdown; drainage impeded	1.04	0.09
Marmóna Traprock	Minimal breakdown, not impeding drainage	1.21	0.08
Noranda Slag	No noticeable breakdown; free draining though excess minus 200 breakdown	0.89	0.06
Nouvelle Igneous	Major chemical breakdown	1.27	0.06
Sudbury Slag	No noticeable breakdown; free draining	0.71	0.03

## CHAPTER 9

## LABORATORY TESTING PROGRAM

## 9.1 Ballast

Six types of ballast were selected for testing under conditions of repeated loading. Because the American Railway Engineering Association (AREA) No. 4 ballast gradation is used most often the approximate center of the recommended gradation limits was selected for testing. Both the gradation of the samples tested and the AREA No. 4 limits are shown in Figure 9.1.

## 9.1.1 Description of Materials

The materials selected for testing were dolomitic limestone from Kankakee, Illinois; granitic gneiss from Columbus, Georgia, blast furnace slag from Chicago; basalt from New Jersey; and crushed and uncrushed gravels from McHenry, Illinois. The materials were sieved into various size fractions and were recombined as needed to conform to the standard testing gradation.

## 9.1.2 Characterization Tests

Because there is interest in relating mechanical breakdown to the physical properties of ballast, the following standard tests were performed: particle index, specific gravity, Los Angeles abrasion, flakiness, soundness, and crushing value. The standard tests and references are included in Table 3.3. An amplified discussion of the tests is available in Reference 39.

The results of the tests are summarized in Table 9.1.

## 9.2 Testing Program

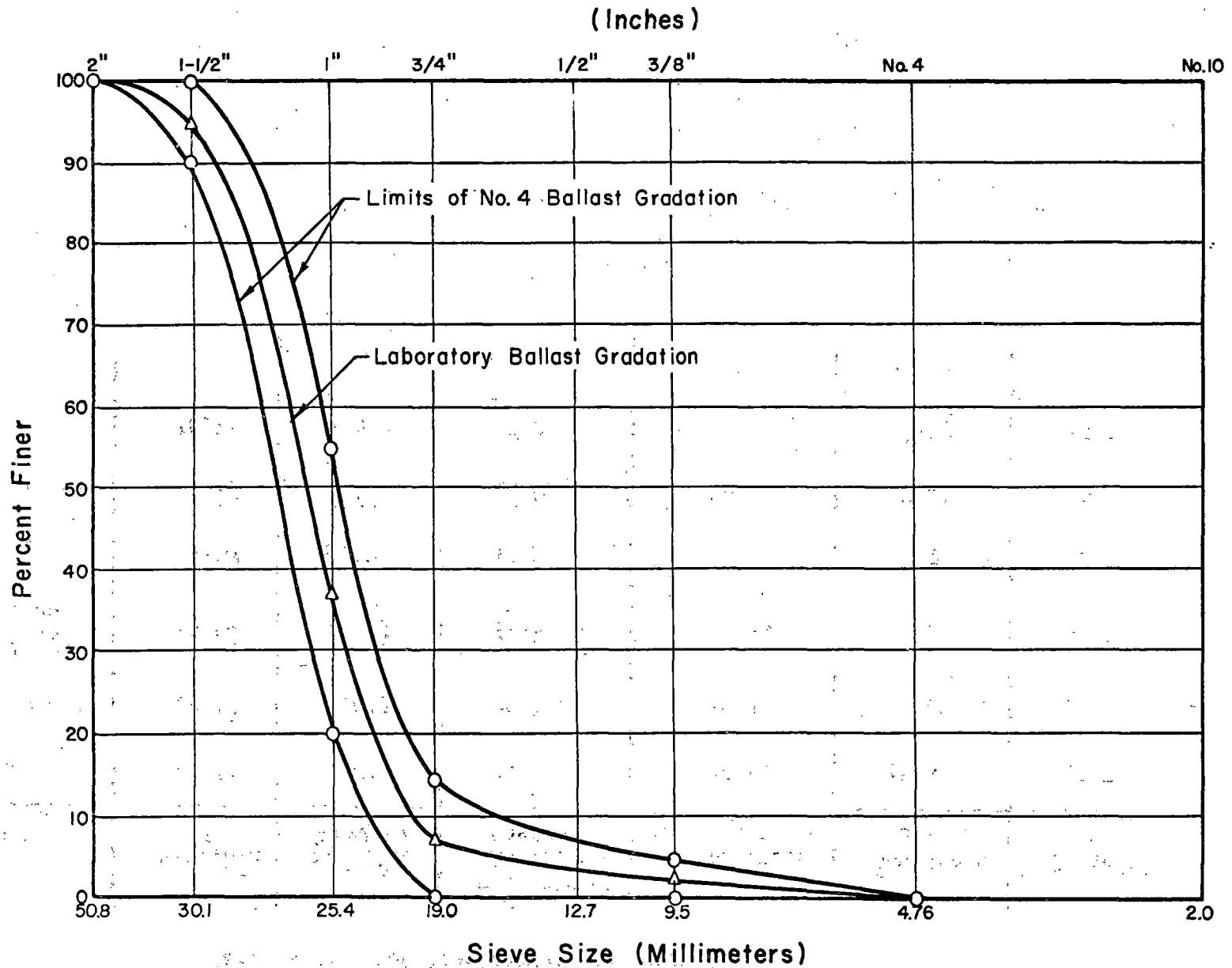


Figure 9.1. Ballast Gradation Tested and Limits for No. 4 Ballast.

Table 9.1. Characterization Test Results.

Material	Particle Index	Specific Gravity	Los Angeles Abrasion Loss, %	Flakiness Index	Soundness Loss, %	Crushing Value
Limestone	13.75	2.626	34.2	16.78	18.5	22.7
Granitic Gneiss	13.45	2.679	34.7	14.39	0.25	26.1
Chicago Blast Furnace Slag	15.68	2.133	37.8	3.59	0.75	37.3
Basalt	15.40	2.775	12.3	17.33	4.93	12.4
Crushed Gravel	11.85	2.678	28.0	10.12	7.45	20.0
Gravel	10.17	2.658	23.2	5.79	5.78	13.8

### 9.2.1 Triaxial Equipment

See Section 3.2.1

### 9.2.2 Instrumentation

See Section 3.2.2

### 9.2.3 Specimen Preparation

See Section 3.2.3

### 9.2.4 Testing Sequence

Two series of tests were chosen. The first involved the application of one million loading cycles at a repeated deviator stress of 45 psi ( $310 \text{ kN/m}^2$ ) and 15 psi ( $103 \text{ kN/m}^2$ ) confining pressure. The stresses were selected as representative of those predicted by finite element technique (6) to occur in an element of ballast located immediately beneath a tie. During the testing program and deformations were measured at least as often as  $10^n$  cycle, where n is an integer. The deformations were converted to strains by dividing by the sample height.

To characterize the permanent deformation characteristics of ballast at a low confining pressure, or that existing near the ballast-subgrade interface, a second series of tests was run. The specimens for this series were prepared in the same manner as for the first tests, although only two specimens (limestone and gravel) were tested. A deviator stress of 12 psi ( $83 \text{ kN/m}^2$ ) was selected as typical of the in service stress, and the testing procedure started using a confining pressure of 3 psi ( $21 \text{ kN/m}^2$ ). Each specimen was subjected to 100,000 loading cycles at the 3 psi ( $21 \text{ kN/m}^2$ ) confining pressure; the confining pressure was then reduced to 2 psi ( $12 \text{ kN/m}^2$ ) and another 100,000 cycles applied. The confining pressure was reduced further to 1 psi ( $7 \text{ kN/m}^2$ ) and a third set of 100,000 cycles was applied.

### 9.2.5 Degradation Measurement

After the application of one million load cycles, the six primary test specimens were removed from the triaxial cell, and sieve analyses were accomplished. The specimens tested, their material types, gradations, densities and void ratios are included in Table 9.2. A detailed description of the testing equipment and procedures is contained in Reference 44.

Table 9.2. Test Specimen Properties.

Test Sequence	Material	Density (pcf)	Void Ratio
Long Term	Limestone	93.4	0.75
	Granitic Gneiss	96.4	.73
	Chicago Blast Furnace Slag	71.0	.87
	Basalt	96.0	.80
	Crushed Gravel	99.8	.67
	Gravel	104.4	.59
Low Confining Pressure	Limestone	96.3	0.70
	Gravel	105.2	0.58

## CHAPTER 10

## PRESENTATION AND ANALYSIS OF PERMANENT DEFORMATION BEHAVIOR

## 10.1 Introduction

This chapter presents the plastic strain results of the primary series tests and also the results of the two specimens tested at multiple stress levels and low confining pressures.

## 10.2 Plastic Strain Results for Primary Testing Series

One of the objectives of the research was to characterize the long term permanent deformation behavior of ballast materials. The only variable involved in the primary testing series was material type. Compaction level, gradation, and stress level were the same for all specimens.

Figures 10.1 through 10.6 present the results of the tests. In addition, to facilitate direct comparisons by material type, Table 10.1 is a summary of the plastic strain data for all six specimens and for the linear regression analysis results.

## 10.2.1 Regression Analysis

To determine the trend of permanent deformation as the number of loading cycles increased, linear regression between the plastic strains and the logarithm of the corresponding number of cycles was accomplished. Previous research (44) has shown that the semi-log analysis is appropriate for determining the trend of deformation behavior. Because the trend with tonnage (or time) is of most practical significance for ballast, the intercepts are not included. As noted the linear regression results are included in Table 10.1.

## 10.2.2 Relationship of Plastic Strain to Material Properties

Table 10.2 presents the correlation coefficients of the analysis for

Table 10.1. Permanent Strain and Regression Results for Long Term Testing.

Ballast Type	Permanent Strain at Number of Cycles of Loading Equal to						Regression Results ( $\epsilon_p$ -Log N)	
	10	$10^2$	$10^3$	$10^4$	$10^5$	$10^6$	Slope	Correlation Coefficient
Limestone	0.58	1.69	2.96	4.50	5.90	6.05	1.17	.997*
Granitic Gneiss	.60	1.44	2.74	3.43	3.66	3.92	.75	.962*
Chicago Blast Furnace Slag	.35	.89	1.99	3.54	6.67	8.30	1.48	.655*
Basalt	.20	.62	1.14	1.57	2.02	2.15	.40	.982*
Crushed Gravel	.23	.57	1.29	1.88	2.27	2.45	.46	.987*
Gravel	.42	.71	1.05	1.47	1.92	2.39	.37	.993*

\*Significant at  $\alpha = 0.05$ .

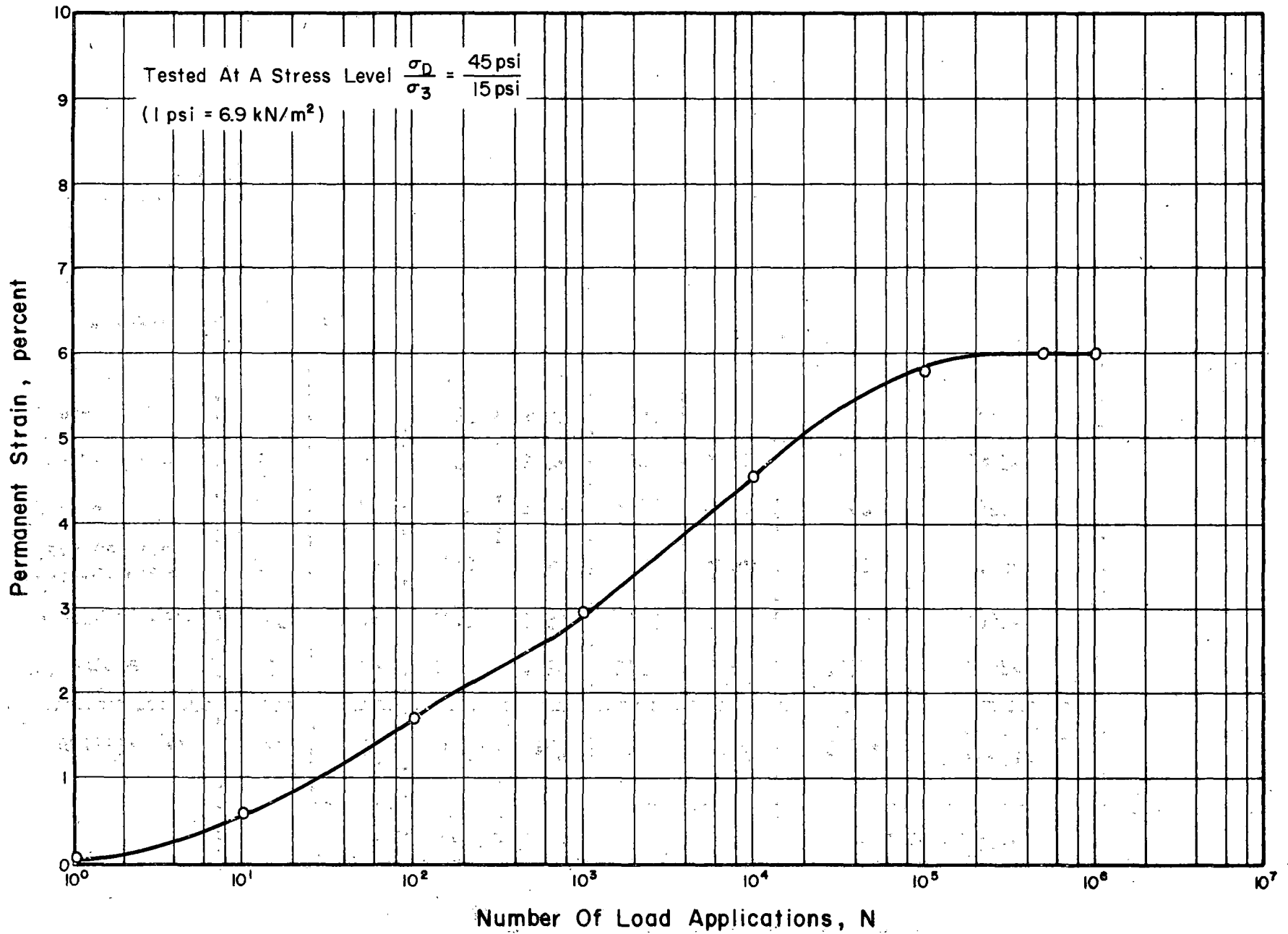


Figure 10.1. Effect of Number of Loading Cycles on Plastic Strain for Limestone.

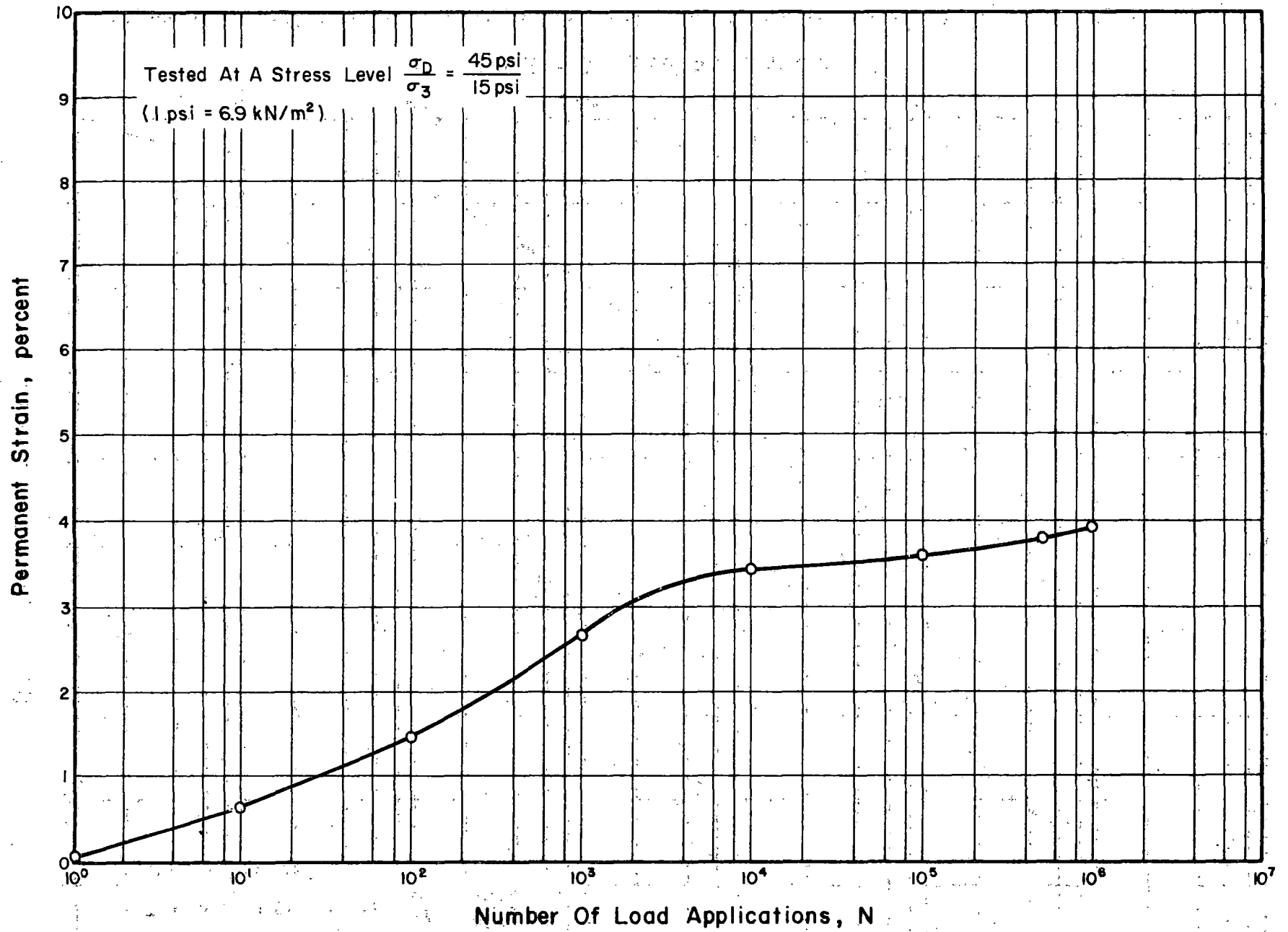


Figure 10.2. Effect of Number of Loading Cycles on Plastic Strain for Granitic Gneiss.

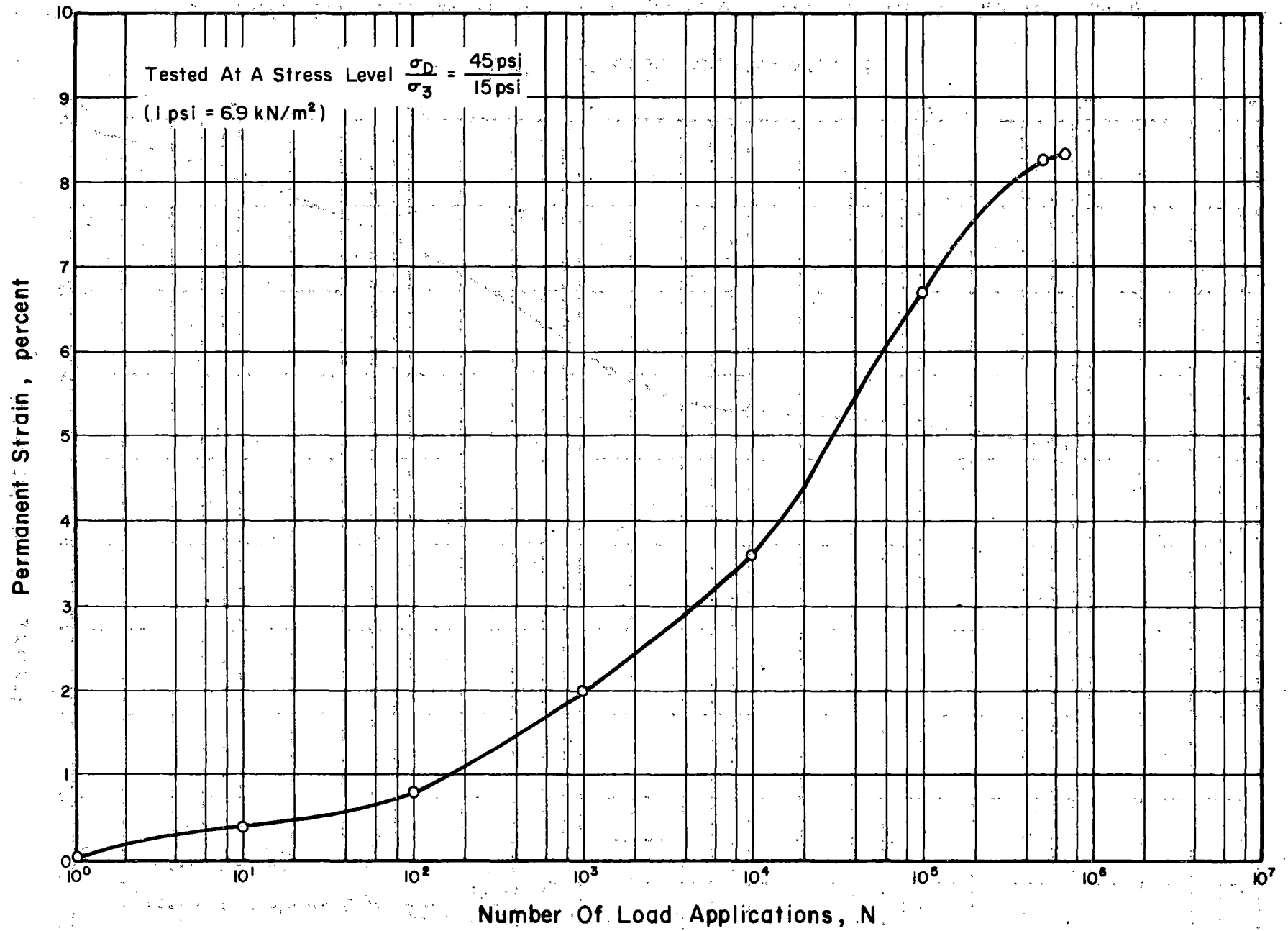


Figure 10.3... Effect of Number of Loading Cycles on Plastic Strain for Chicago Blast Furnace Slag.

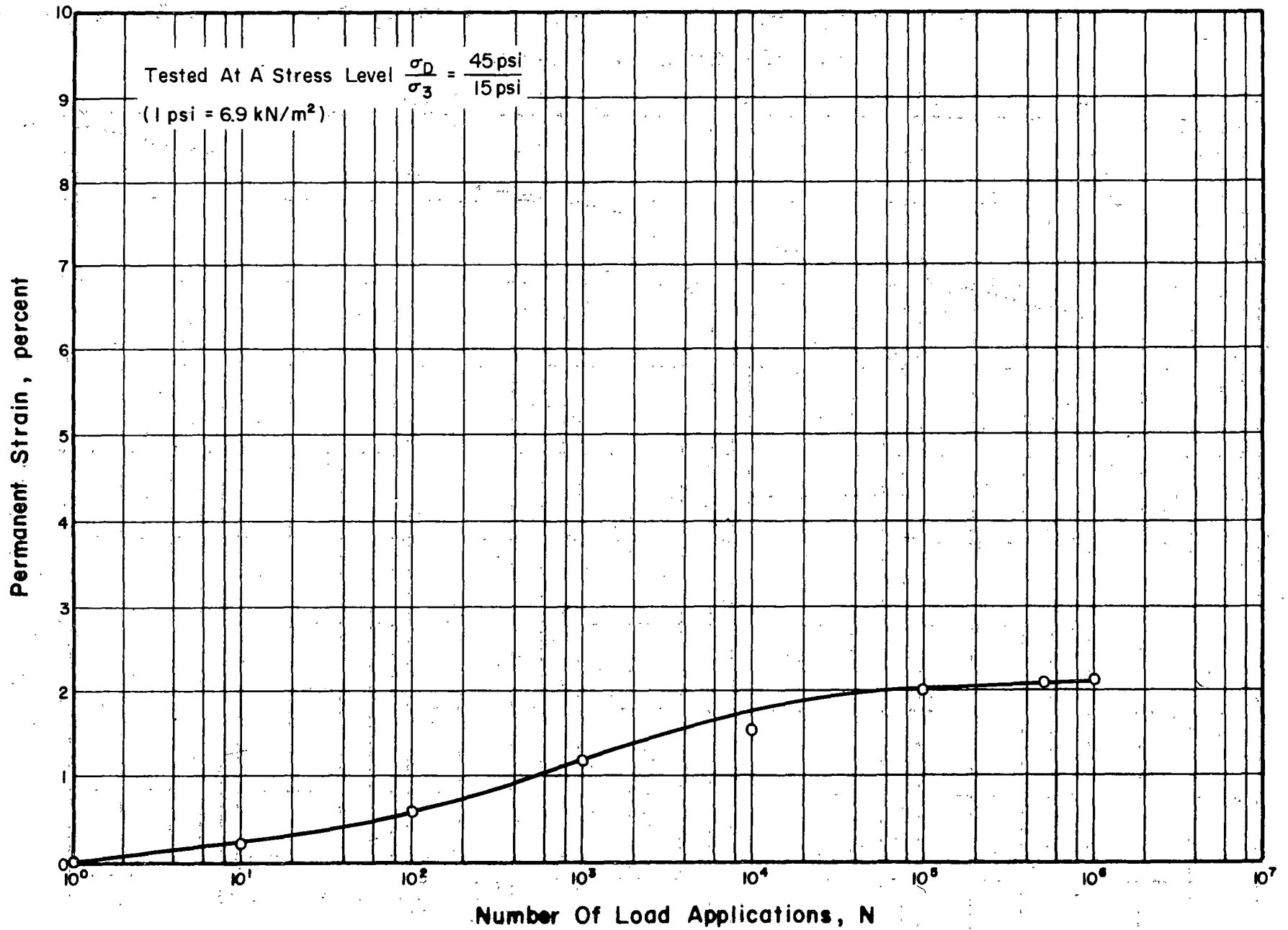


Figure 10.4. Effect of Number of Loading Cycles on Plastic Strain for Basalt.

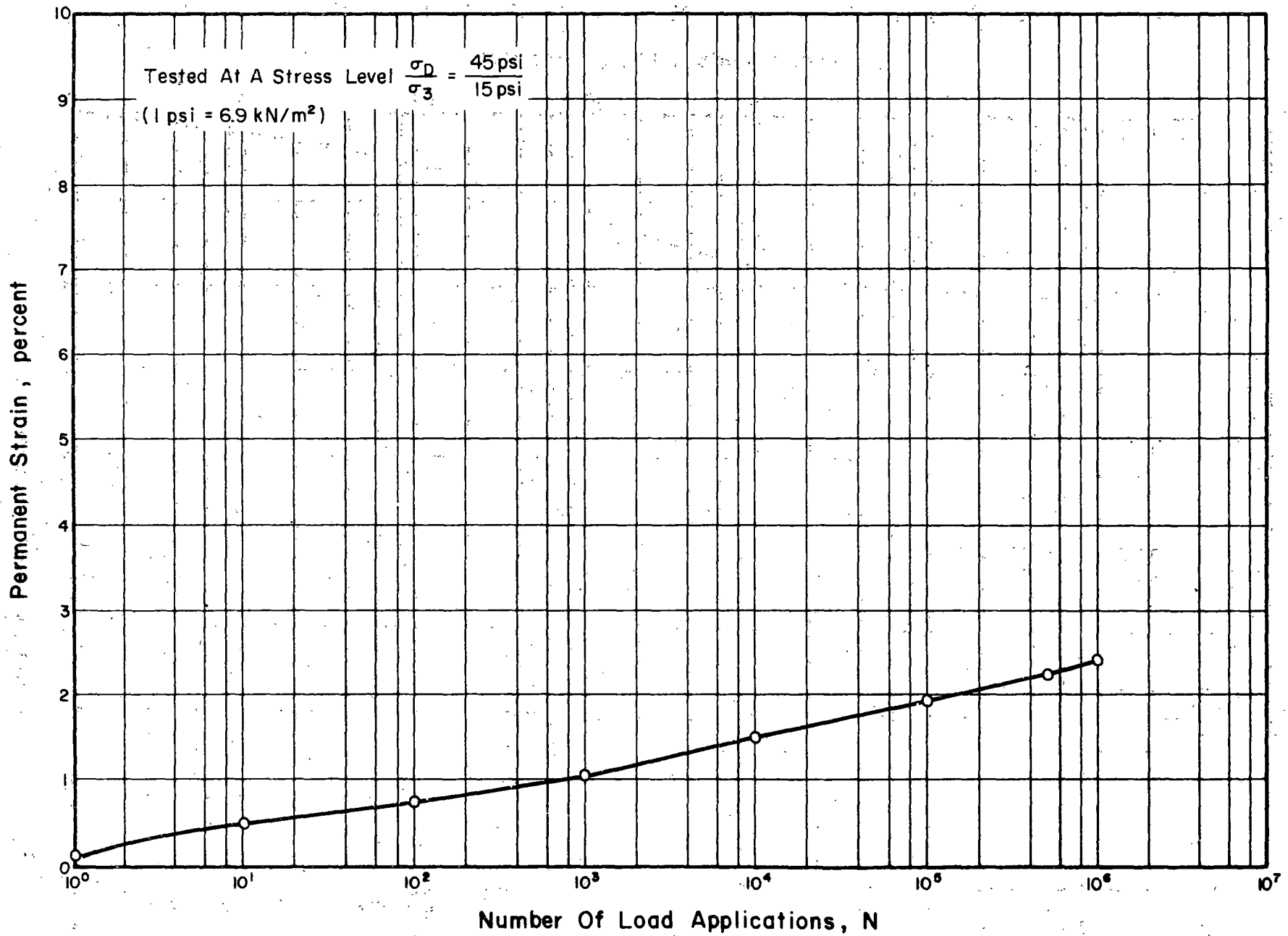


Figure 10.5. Effect of Number of Loading Cycles on Plastic Strain for Gravel.

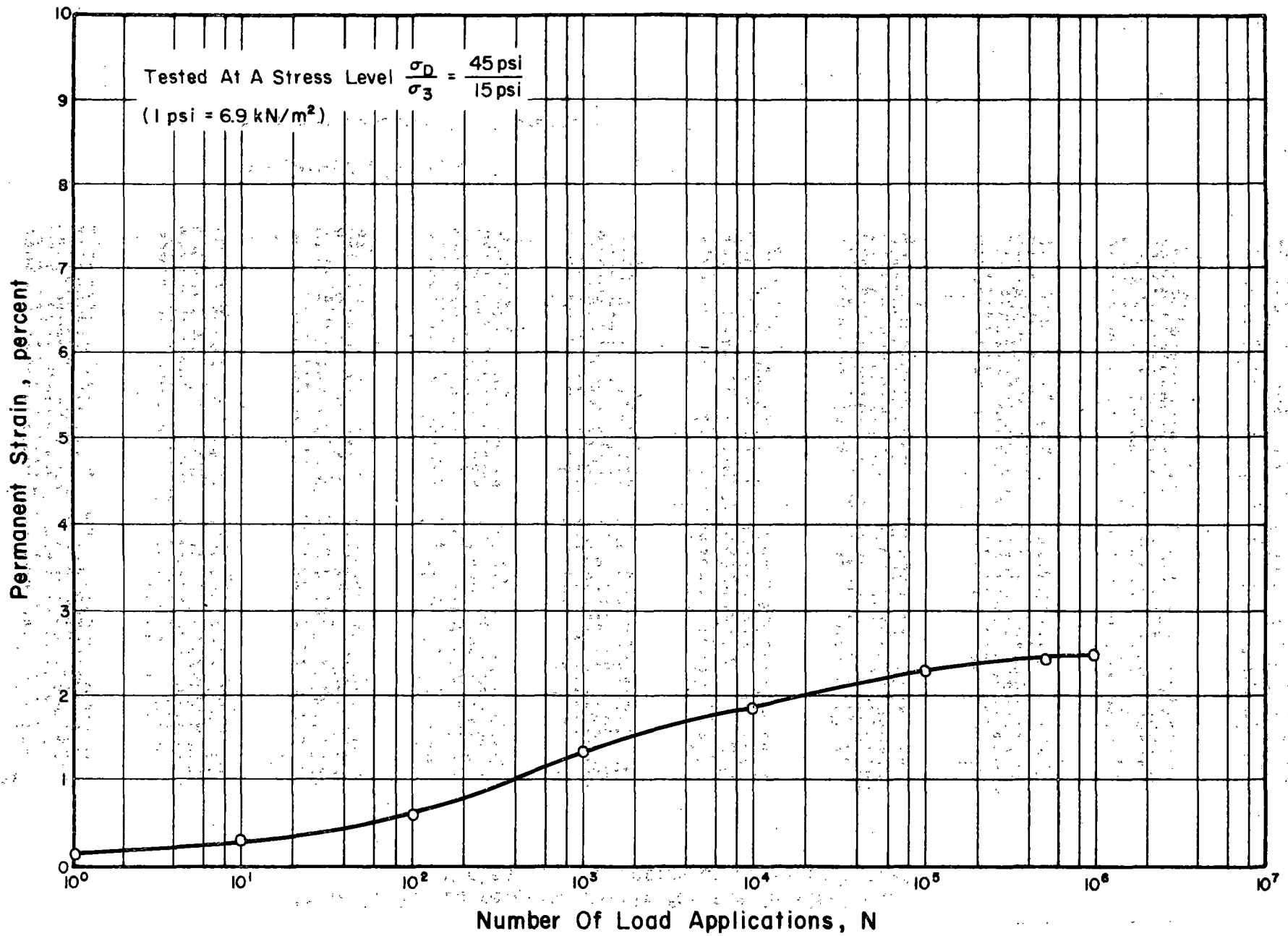


Figure 10.6. Effect of Number of Loading Cycles on Plastic Strain for Crushed Gravel.

Table 10.2. Correlation Matrix for the Physical and Mechanical Properties of Ballasts Tested.

DATA FIELD 1.	2	3	4	5	6	7	8	9	10	
1	1.00000	-0.41742	0.09022	-0.74300	0.98172*	0.26567	-0.16528	0.47697	-0.54359	-0.12562
2	-0.41742	1.00000	-0.63301	0.91692*	-0.57839	0.69573	0.29503	-0.86972*	-0.23980	-0.02934
3	0.09022	-0.63301	1.00000	-0.53150	0.22825	-0.32355	0.01521	0.86223*	0.32891	0.63702
4	-0.74300	0.91692*	-0.53150	1.00000	-0.85516*	0.38369	0.26985	-0.86353*	0.07280	0.02023
5	0.98172*	-0.57839	0.22825	-0.85516*	1.00000	0.10359	-0.19237	0.61675	-0.45533	-0.10719
6	0.26567	0.69573	-0.32355	0.38369	0.10359	1.00000	0.44054	-0.42333	-0.49709	0.17811
7	-0.16528	0.29503	0.01521	0.26985	-0.19237	0.44054	1.00000	-0.28507	0.18376	0.23216
8	0.47697	-0.86972*	0.86223*	-0.86353*	0.61675	-0.42333	-0.28507	1.00000	0.06639	0.31049
9	-0.54359	-0.23980	0.32891	0.07280	-0.45533	-0.49709	0.18376	0.06639	1.00000	0.53752
10	-0.12562	-0.02934	0.63702	0.02023	-0.10719	0.17811	0.23216	0.31049	0.53752	1.00000
11	0.16803	-0.02177	0.61163	-0.11042	0.16302	0.43229	0.42411	0.34934	0.26198	0.91259*
12	0.31638	-0.18714	0.73688	-0.30167	0.33538	0.35545	0.29234	0.55301	0.11800	0.84175*
13	0.45594	-0.42193	0.79332	-0.53530	0.51070	0.20842	0.32909	0.69802	0.10653	0.69900
14	0.54727	-0.76924	0.79162	-0.82103*	0.65823	-0.16196	0.18559	0.85174*	0.18930	0.44282
15	0.54596	-0.87778*	0.77910	-0.89526*	0.67582	-0.32632	0.39920	0.90045*	0.21419	0.34585
16	0.56998	-0.87551*	0.74327	-0.90736*	0.70176	-0.31939	0.07920	0.88742*	0.10703	0.21928
17	0.55919	-0.94521*	0.72485	-0.94928*	0.70291	-0.45166	-0.08709	0.92104*	0.11334	0.14335
18	0.52150	-0.93929*	0.77571	-0.93063*	0.66936	-0.45770	-0.09318	0.94389*	0.13220	0.19338
19	0.23653	-0.62006	0.80043	-0.58523	0.35900	-0.16758	0.48005	0.69407	0.30040	0.44081
20	0.57546	-0.82086*	0.78478	-0.86853*	0.69188	-0.22315	0.09135	0.88514*	0.18083	0.40397
DATA FIELD 11	12	13	14	15	16	17	18	19	20	
1	0.16803	0.31638	0.45594	0.54727	0.54596	0.56998	0.55919	0.52150	0.23653	0.57546
2	-0.02177	-0.18714	-0.42193	-0.76924	-0.87778*	-0.87551*	-0.94521*	-0.93929*	-0.62006	-0.82086*
3	0.61163	0.73688	0.79332	0.79162	0.77910	0.74327	0.72485	0.77571	0.80043	0.78478
4	-0.11042	-0.30167	-0.53530	-0.82103*	-0.89526*	-0.90736*	-0.94928*	-0.93063*	-0.58523	-0.86853*
5	0.16302	0.33538	0.51070	0.65823	0.67582	0.70176	0.70291	0.66936	0.35900	0.69188
6	0.43229	0.35545	0.20842	-0.16196	-0.32632	-0.31939	-0.45166	-0.45770	-0.16758	-0.22315
7	0.42411	0.29234	0.32909	0.18559	0.03920	0.07920	-0.08709	-0.09318	0.48005	0.09135
8	0.34934	0.55301	0.69802	0.85174*	0.90045*	0.88742*	0.92104*	0.94389*	0.69407	0.88514*
9	0.26198	0.11800	0.10653	0.18930	0.21419	0.10703	0.11334	0.13220	0.30040	0.18083
10	0.91259*	0.84175*	0.69900	0.44282	0.34585	0.21928	0.14335	0.19338	0.44081	0.40397
11	1.00000	0.96284*	0.87286*	0.59368	0.45539	0.37029	0.24779	0.28393	0.58193	0.53842
12	0.96284*	1.00000	0.94903*	0.71175	0.59275	0.52796	0.42343	0.46227	0.65852	0.66940
13	0.87286*	0.94903*	1.00000	0.88749*	0.79286	0.75714	0.65846	0.68366	0.83186*	0.85209*
14	0.59368	0.71175	0.88749*	1.00000	0.98098*	0.96565*	0.91837*	0.92355*	0.90629*	0.99479*
15	0.45539	0.59275	0.79286	0.98098*	1.00000	0.98507*	0.97173*	0.97334*	0.85720*	0.99372*
16	0.37029	0.52796	0.75714	0.96565*	0.98507*	1.00000	0.98307*	0.98073*	0.87164*	0.97571*
17	0.24779	0.42343	0.65846	0.91837*	0.97173*	0.98307*	1.00000	0.99683*	0.78897	0.94605*
18	0.28393	0.46227	0.68366	0.92355*	0.97334*	0.98073*	0.99683*	1.00000	0.80432	0.94941*
19	0.58193	0.65852	0.83186*	0.90629*	0.85720*	0.87164*	0.78897	0.80432	1.00000	0.86994*
20	0.53842	0.66940	0.85209*	0.99479*	0.99372*	0.97571*	0.94605*	0.94941*	0.86994*	1.00000

\* significant at  $\alpha = 0.05$

\*\* see text for explanation of data fields

the mechanical and physical properties of the materials tested, for strain readings at various cycles of loading, for degradation of the samples after one million loading cycles, and for the slope from the permanent strain-logarithm of numbers of loading cycles regression. A complete listing of the data fields represented in Table 10.2 is as follows:

1. Particle Index
2. Specific Gravity
3. Los Angeles Abrasion Value
4. Density
5. Void Ratio
6. Flakiness Index
7. Soundness Value
8. Crushing Value
9. Permanent Strain at 1 cycle
10. Permanent Strain at 10 cycles
11. Permanent Strain at  $10^2$  cycles
12. Permanent Strain at  $10^3$  cycles
13. Permanent Strain at  $10^4$  cycles
14. Permanent Strain at  $10^5$  cycles
15. Permanent Strain at  $10^6$  cycles
16. Degradation, percent passing No. 4
17. Degradation, percent passing No. 10
18. Degradation, percent passing No. 40
19. Degradation, percent passing No. 200
20. Slope of  $\epsilon_p - \log N$

Significant ( $\alpha = 0.05$ ) correlations for permanent strain were observed for density with the strains at  $10^5$  and  $10^6$  loading cycles (inverse), for specific

gravity with the strain at  $10^6$  cycles of loading (inverse), for crushing value with the strains at  $10^5$  and  $10^6$  loading cycles, and for the  $\epsilon_p$ -log N slope with specific gravity (inverse), with density (inverse) and with crushing value. Thus crushing value is the simplest test result related to long term permanent strain. The remainder of the significant correlation coefficient values will be considered in Chapter 11.

### 10.3 Results for Low Confining Pressure Specimens

Because research (44) has shown large variations in the permanent deformation behavior of rounded versus angular materials at low confining pressure (5 psi/ 34 kN/m<sup>2</sup> or less) but little difference in that behavior at higher confining pressures (15 psi or 103 kN/m<sup>2</sup>) the need existed for characterization of such materials at reduced stress levels. In addition finite element analysis (6) has shown that the minor principal stress,  $\sigma_3$ , can decrease to near or less than 1 psi (7 kN/m<sup>2</sup>) at the ballast-subgrade interface. For these reasons two specimens were included in the program for testing at low stresses. Because the focus was on characterizing the behavior of angular versus rounded materials the series was limited to two samples, a limestone and a gravel. Because the McHenry gravel is predominantly limestone, there was little difference, except in particle index\*, between the two materials.

Although research (9, 30, 31, 44) has shown that the magnitude of plastic strain is affected by stress history, it is believed that valuable information on the relative behavior of materials can be gained by subjecting specimens to mixed loading states, especially if the mixed loading involves

---

\*Particle index as defined by Haung (10) includes shape, angularity, and surface texture.

only successive increases in the deviator stress to confining pressure ratio.

The results of the tests are shown in Figures 10.7 and 10.8. There was little difference between the behavior of the specimens at 3 psi (21 kN/m<sup>2</sup>) confining pressure, but at the lower levels of confining pressure more plastic strain was observed for the gravel specimens. It is interesting that the curve for the gravel specimen at 1 psi (7 kN/m<sup>2</sup>) confining pressure is more irregular than that of the limestone and shows an increase in rate of strain accumulation while that of the limestone appears to be leveling off.

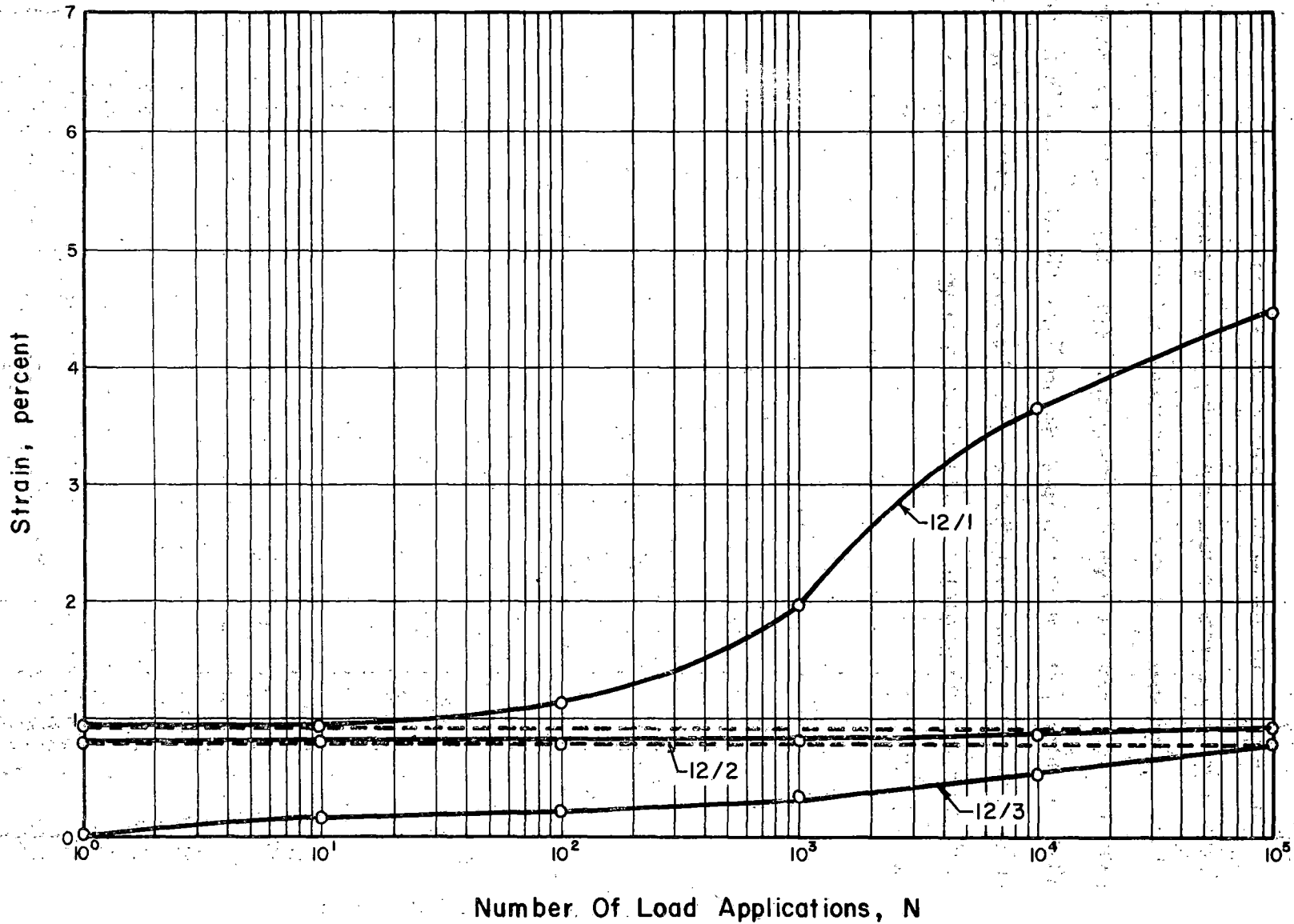


Figure 10.7. Low Confining Pressure Results for Limestone.

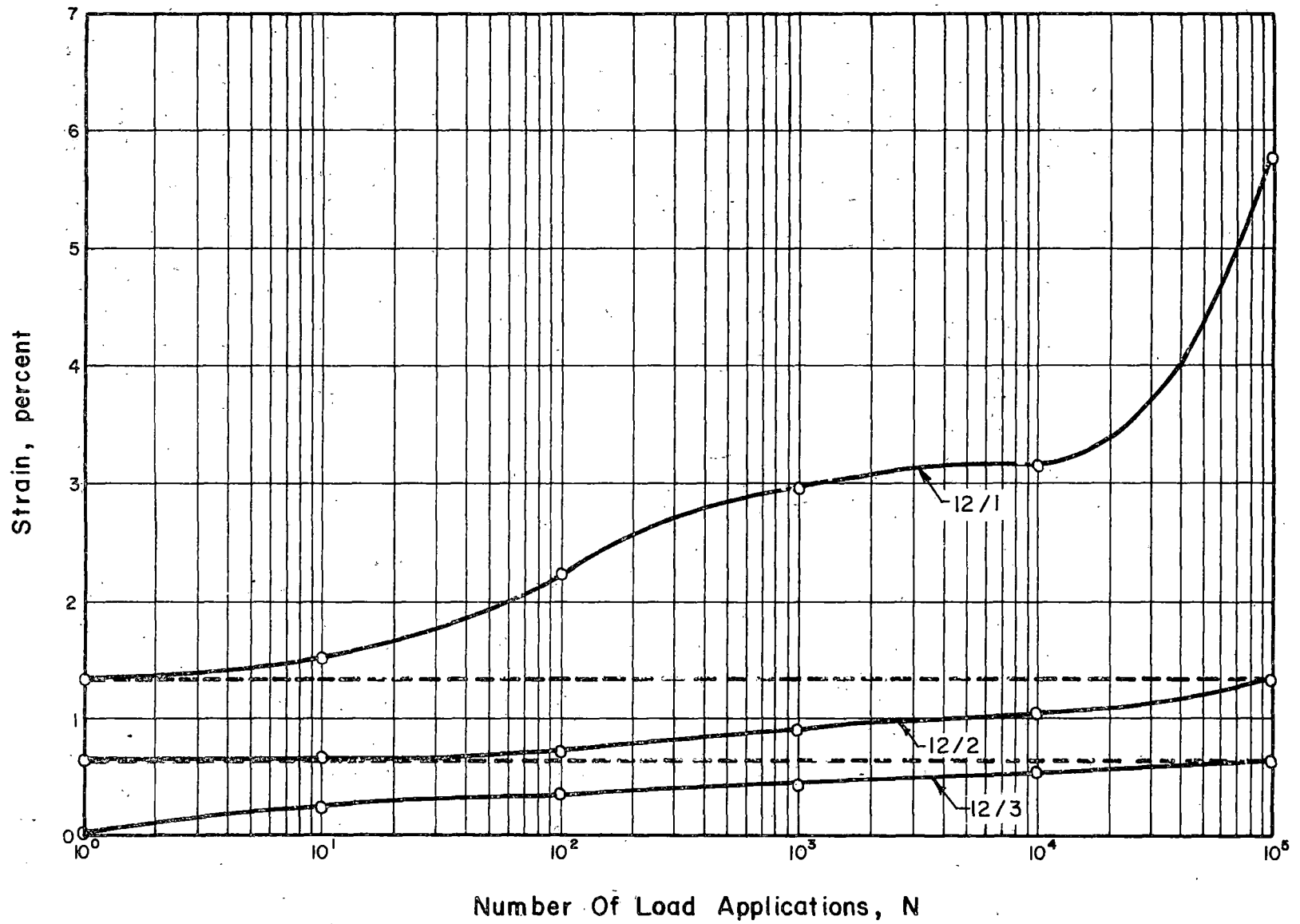


Figure 10.8. Low Confining Pressure Results for Gravel.

## CHAPTER 11

## PRESENTATION AND ANALYSIS OF DEGRADATION RESULTS

## 11.1 Introduction

Excessive breakdown of ballast results in decreased drainage, increased saturation, and possibly decreased load carrying capacity. Therefore, it is desirable to determine the relative susceptibility of ballast materials to both mechanical breakdown and weathering action. The following sections relate the repeated loading breakdown of ballast to the physical properties of the materials and to plastic strain characteristics.

## 11.2 Criteria

Because the ballast gradation tested (AREA No. 4) contained no material passing the No. 4 sieve, it was decided that the amount of passing the No. 4 sieve after testing would define the "total degradation" of the ballast. The total degradation was subdivided into the amounts passing the No. 10, No. 40, and No. 200 sieves. Results are shown in Table 11.1.

## 11.3 Correlations with Material Properties

To determine the relevancy of the various standard tests, the test results and the amounts passing the No. 4, No. 10, No. 40, and No. 200 sieves were used in simple correlation analyses. The results are shown in Table 10.2. The most consistently significant ( $\alpha = 0.05$ ) correlations were between degradation and specific gravity (inverse), degradation and density (inverse), and degradation and crushing value. It is interesting that none of the standard test results achieved a significant correlation with the amount passing the No. 200 sieve.

## 11.4 Correlations with Plastic Strain

Several interesting significant ( $\alpha = 0.05$ ) correlations were noted

Table 11.1. Degradation Results for Long Term Testing.

Sieve Size	Percent Passing						
	Original	Gravel	Granite Gneiss	Crushed Gravel	Limestone	Chicago Slag	Basalt
1 1/2"	95	95.83	97.60	95.00	96.70	96.40	95.51
1"	40	40.07	42.60	41.20	47.56	49.45	41.40
3/4"	7.5	9.37	11.90	11.93	15.22	16.62	12.48
3/8"	2.5	2.78	3.29	3.35	4.69	5.60	3.08
No. 4	0	0.33	0.75	0.74	1.52	2.22	0.43
No. 10	0	0.26	0.50	0.48	0.83	1.56	0.27
No. 40	0	0.23	0.40	0.37	0.56	0.97	0.20
No. 200	0	0.19	0.22	0.26	0.44	0.39	0.12

Note: Gradations are for the material following the application of one million loading cycles ( $\sigma_D/\sigma_3 = 45$  psi/15 psi).

between the degradation and permanent strain results. The total degradation (amount passing No. 4 sieve) the No. 10 degradation, the No. 40 degradation and the No. 200 degradation all correlated significantly with the permanent strain at  $10^5$  and  $10^6$  loading cycles. In addition, there was a significant correlation between the No. 200 degradation and the permanent strain at  $10^4$  loading cycles. One other permanent strain variable, the slope of  $\epsilon_p - \log N$  regression, achieved significant correlations with all four of the degradation measures.

### 11.5 Nature of Fines

In addition to the sieve analysis conducted on the long term loading specimens, the fine material (minus No. 40 sieve) was checked for plasticity (ASTM D 423, ASTM D 424). All of the fines, with the exception of the limestone material, were nonplastic. The limestone fines had a plastic index of 3.

## CHAPTER 12

## SUMMARY AND CONCLUSIONS

## 12.1 Summary

Six types of ballast were tested in the repeated load triaxial apparatus for one million loading cycles each. The compactive effort and gradation for each specimen were the same. The permanent strain behavior and gradation characteristics of the materials were determined. In addition, two specimens were tested at low confining pressure to determine the behavior of rounded versus angular particles.

## 12.2 Conclusions

1. Permanent strain observed at  $10^5$  and at  $10^6$  loading cycles correlated significantly with crushing value. Crushing value appears to be a promising test for predicting resistance to long term, permanent deformation in ballast.
2. Angular materials offer better resistance to permanent deformation at low confining pressures than do rounded materials.
3. The significant correlations for degradation were observed with crushing value, specific gravity (inverse), and density (inverse). No material property correlated significantly with the No. 200 degradation.
4. Long term permanent strain ( $10^5$  and  $10^6$  loading cycles) correlated significantly with the degradation results.

PART C  
CHAPTER 13

## FOUNDATION MATERIAL TESTING PROGRAM AND PROCEDURES

## 13.1 General

This report discusses the subgrade soils evaluation investigation and forms part of the Phase IV - Materials Evaluation Study. A series of laboratory tests have been conducted with selected foundation soils to determine their pertinent engineering properties. For this study the engineering properties that were evaluated can be broadly categorized as:

1. Resilient Response
2. Permanent Deformation

The above properties were determined using repeated load triaxial tests. Extensive work has already been done in repeated load testing of fine-grained soils and a literature review has been presented in the earlier phases of this research program (39, 54).

## 13.2 Soils

The soils selected for investigation are listed in Table 13.1, which also summarizes basic engineering properties of the soils. The soil selection was carried out such that it would include soils ranging in anticipated engineering behavior from good to bad and ranging in texture from clay to sand. Four of the soils were obtained from Illinois locations, two came from Georgia, one came from the Kansas Test Track site in Kansas, and three came from South Carolina.

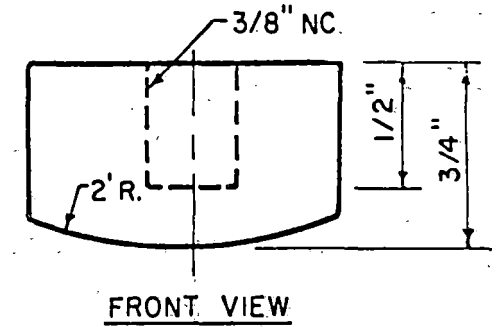
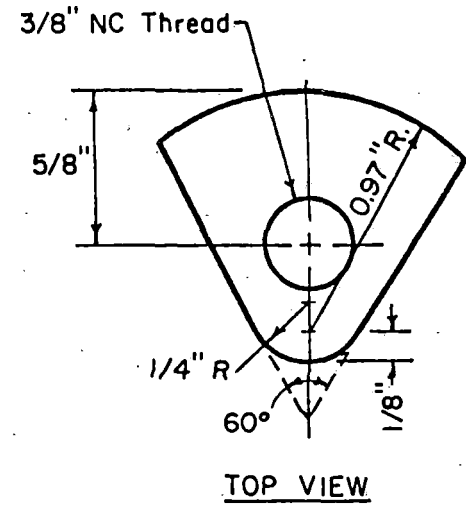
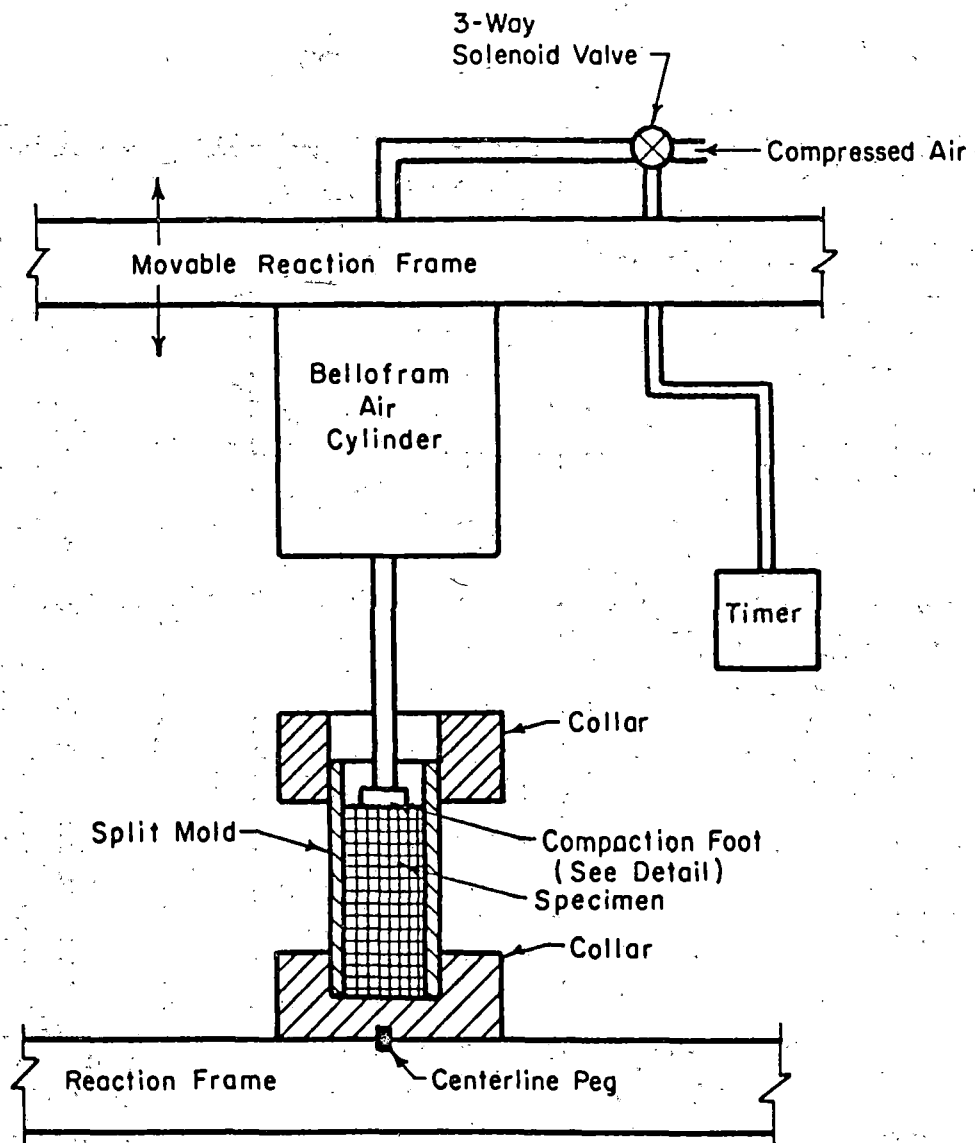
## 13.3 Testing Program and Procedures

The procedure for the resilience testing is described in detail in Reference 55 and therefore only the major aspects of the procedure will be discussed here.

Table 13.1. Soils Used.

<u>Foundation Sample Number</u>	<u>Pedological Name &amp; Horizon</u>	<u>Parent Material</u>	<u>Sampling Location</u>	<u>Unified Soil Classifica- tion</u>
1	Appling	Predominantly residuum from granite	Greenville County South Carolina	CH
2	Cecil	Residuum from acidic rock (granite gneiss and granite)	Catawba County, South Carolina	CH
3	Davidson B <sub>2</sub>	Residuum developed over basic igneous and meta- morphitic rock	Spartanburg County, South Carolina	MH
4	Dickinson C	Fine sandy loam	Whiteside County, IL	SM
5	Drummer B	3-5 ft. of loess on Wisconsinan Till	Champaign Co, IL	CH
6	Fayette B	> 4-5 ft. of Peorian Loess	Henry County, IL	CL
7	Fayette C	> 4-5 ft. of Peorian Loess	Henry County, IL	ML
8	Greenville	Residuum from moderately fine and fine textured costal plain materials	Peach County, Georgia	CL
9	(Kansas Test Track Soil)	Not available	Kansas Test Track	CH
10	Norfolk B <sub>2</sub>	Residuum from thick beds of unconsolidated sandy loams and sandy clays of the costal plain	Peach County, Georgia	SC

<u>Liquid Limit</u>	<u>Plasticity Index</u>	<u>% Clay (&lt;0.002 mm)</u>	<u>Resilient Response Testing</u>	<u>Permanent Deformation Testing</u>
71	38	50	Yes	
53	27	41	Yes	
70	34	54	Yes	Yes
Non Plastic		8		Yes
52	28	38	Yes	Yes
43	21	31	Yes	Yes
32	9	18	Yes	Yes
35	23	39	Yes	
58	38	—		Yes
28	18	27	Yes	Yes



Compaction Foot Detail

Figure 13.1. Schematic Diagram of Kneading Compaction Apparatus.

### 13.3.1 Specimen Preparation

Specimens measuring 2 in. (5.1 cm) in diameter by 4 in. (10.2 cm) in height were prepared using a miniature kneading type compactor as shown in Figure 13.1. The specimens were prepared in sets of at least three at moisture and density conditions representative of expected field conditions (using the AASHTO T-99 procedure). The specimens were wrapped in plastic paper and placed in a constant temperature room at 77°F to cure for a minimum of 7 days prior to the repeated load testing.

### 13.3.2 Specimen Testing

The repeated load test equipment used is shown in Figure 13.2. The pneumatic loading apparatus is capable of applying repeated dynamic loads of controlled magnitude and duration.

In the resilience testing sequence, specimens were tested with no lateral confining pressure, i.e.,  $\sigma_3 = 0$ . It has been shown (55) that the effect of small magnitudes of confining pressure, as normally encountered in a subgrade soil, on the resilient response of the subgrade soils (fine-grained cohesive) is not significant. The specimens were placed in the testing device and conditioned with 1000 axial stress applications of a predetermined magnitude. Following specimen conditioning, the resilient behavior of a set of specimens was determined at various levels of axial stress,  $\sigma_1$ . At each incremental stress level, approximately 10 stress applications were applied to the specimen and the resilient deformation was recorded. The stress level was incrementally increased, approximately 3-5 psi (20-35 kN/m<sup>2</sup>) per increment, until a substantial amount of permanent deformation developed, making it impossible to further record the resilient behavior.

For the permanent deformation testing sequence, the specimens were subjected to approximately 10,000 load applications and the permanent deformations

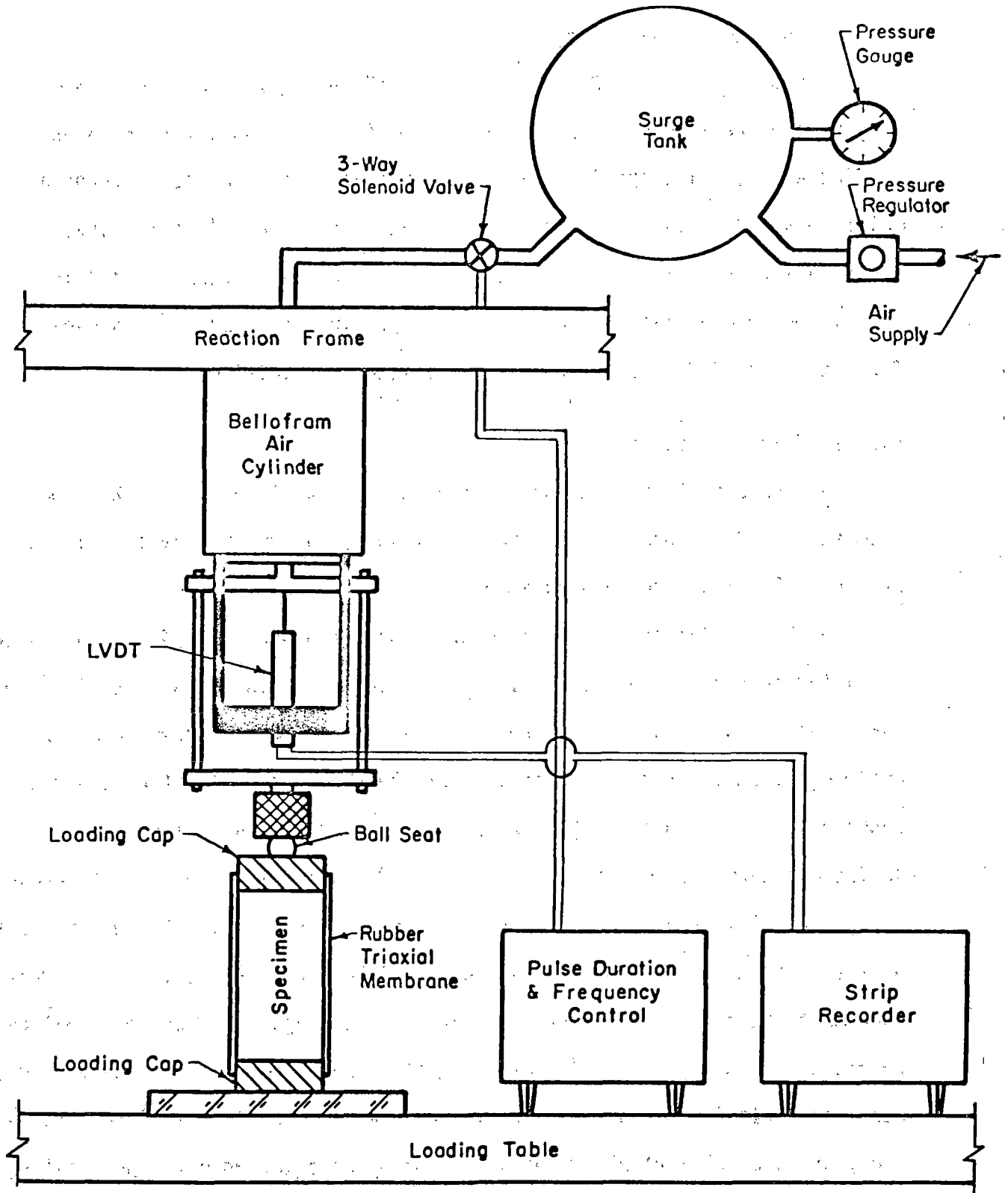


Figure 13.2. Schematic Diagram of Resilience Testing Equipment Used with Fine-Grained Soils

were recorded at various intervals. Usually four specimens were tested for each set of preparation conditions, with each of the specimens being tested at a different stress level. The range of stress levels used depended on the type of soil and preparation conditions and generally ranged from about 3 psi ( $21 \text{ kN/m}^2$ ) to about 50 psi ( $345 \text{ kN/m}^2$ ). Deformations corresponding to approximately the first 1 percent of permanent strain were measured by an LVDT (Linear Variable Differential Transformer) and thereafter the strains were measured by a dial gage attached to the loading apparatus.

## CHAPTER 14

## FOUNDATION MATERIAL TEST RESULTS

## 14.1 Resilience Test Results

The resilient response is determined by the resilient modulus,  $E_R$ , which is calculated by dividing the repeated deviator stress,  $\sigma_D = \sigma_1 - \sigma_3$  by the resilient or recoverable strain,  $\epsilon_R$ , i.e.

$$E_R = \frac{\sigma_D}{\epsilon_R} = \frac{\sigma_1 - \sigma_3}{\epsilon_R}$$

The five soils included in the Resilient Response Testing are listed in Table 13.1. For each soil, two sets of specimens were tested - one at optimum moisture content (AASHTO T-99) and one at optimum plus 2 percent moisture content. For fine-grained soils, the resilient modulus has been shown to be a function of the repeated deviator stress, and generally decreases with an increase in deviator stress. Plots of resilient modulus versus repeated deviator stress for the five soils are given in Figures 14.1 to 14.8. The plots typically display a "break point" deviator stress where there was a substantial change in the slope of  $E_R - \sigma_D$  relation. Linear regression analyses were conducted using data for deviator stresses less than and greater than the break point deviator stress. From the two linear regression equations, it was possible to determine their point of intersection.

In Figures 14.1 to 14.8 it should be noted that:

1. Moisture contents are expressed relative to the optimum moisture content for the soils
2.  $K_1$  is the slope, ksi/psi, for the left part of the plot
3.  $K_2$  is the slope, ksi/psi, for the right part of the plot
4.  $K_3$  is  $E_{Ri}$ , the resilient modulus in ksi at the intersection point, and
5.  $K_4$  is  $\sigma_{Di}$ , the deviator stress in psi at the intersection point.

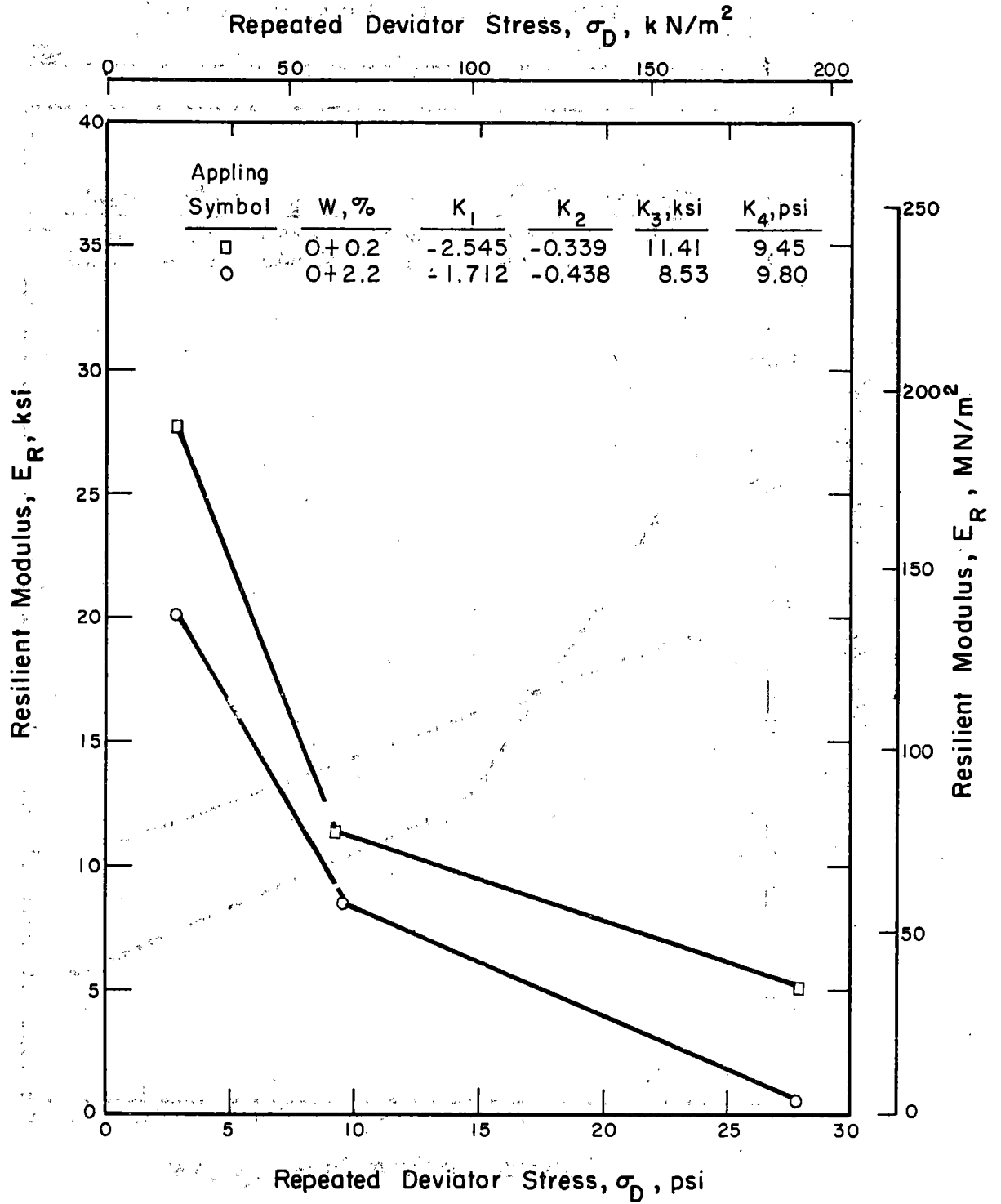


Figure 14.1. Resilient Modulus-Repeated Deviator Stress Relation for Appling

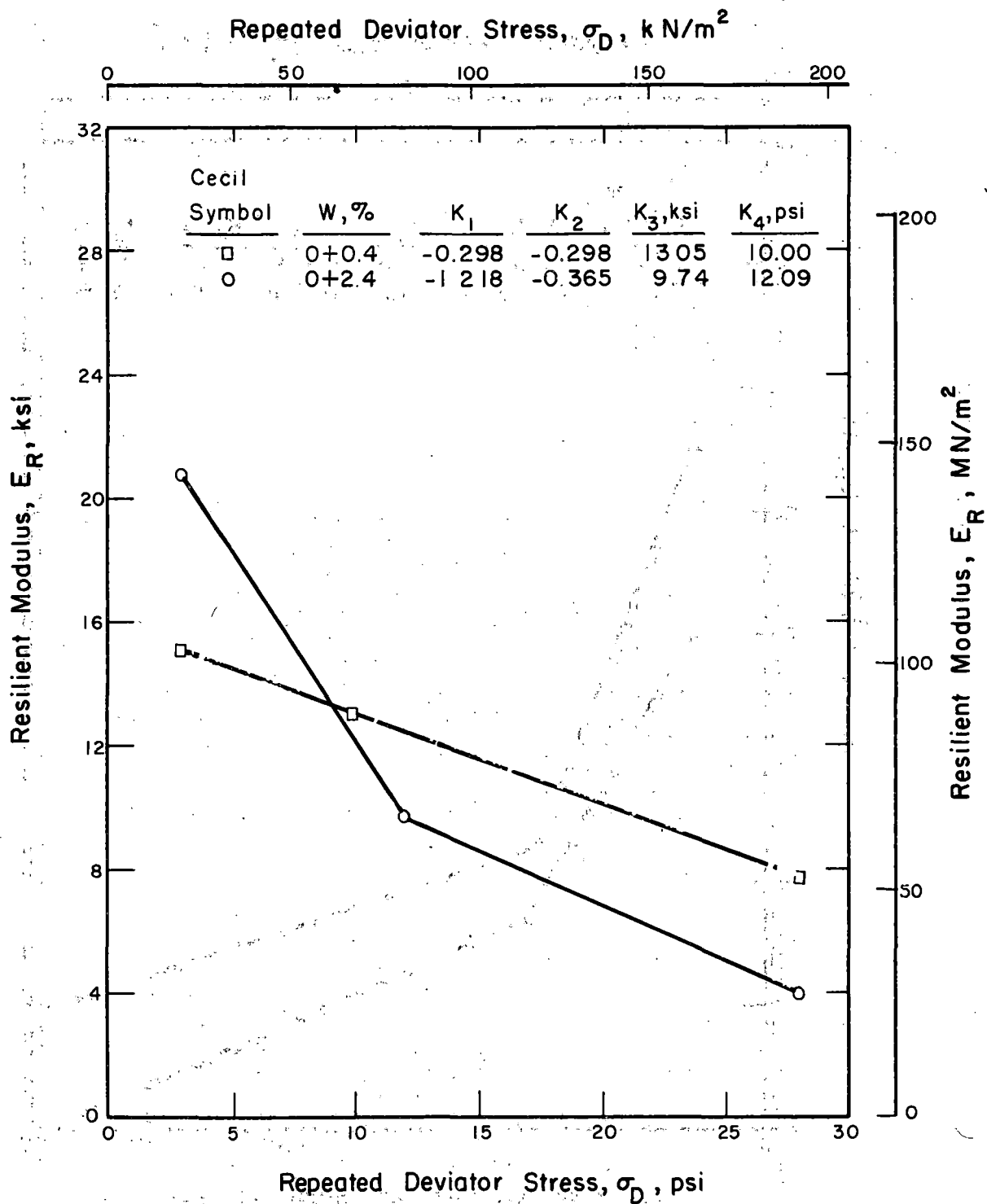


Figure 14.2. Resilient Modulus-Repeated Deviator Stress Relation for Cecil

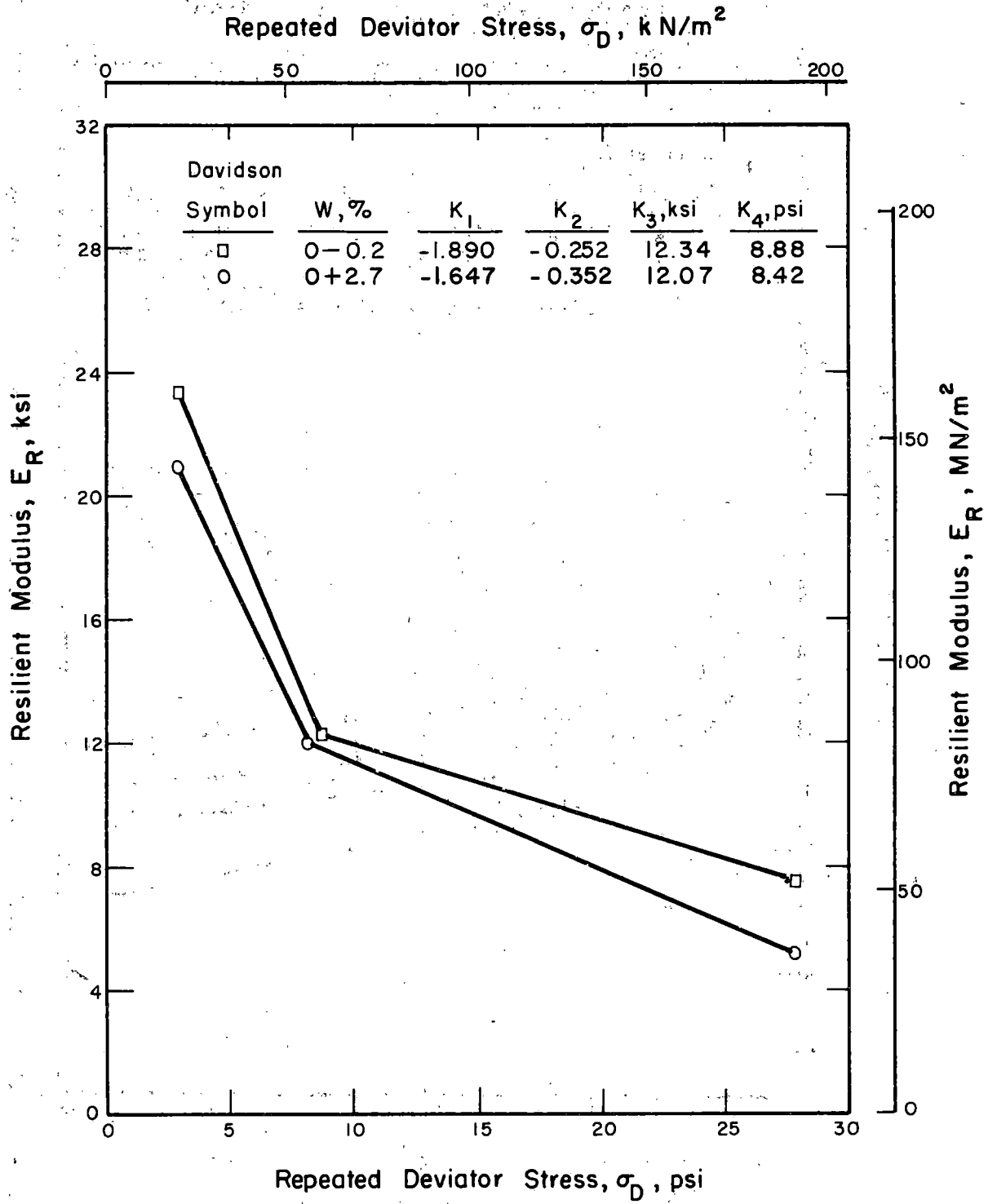


Figure 14.3. Resilient Modulus-Repeated Deviator Stress Relation for Davidson

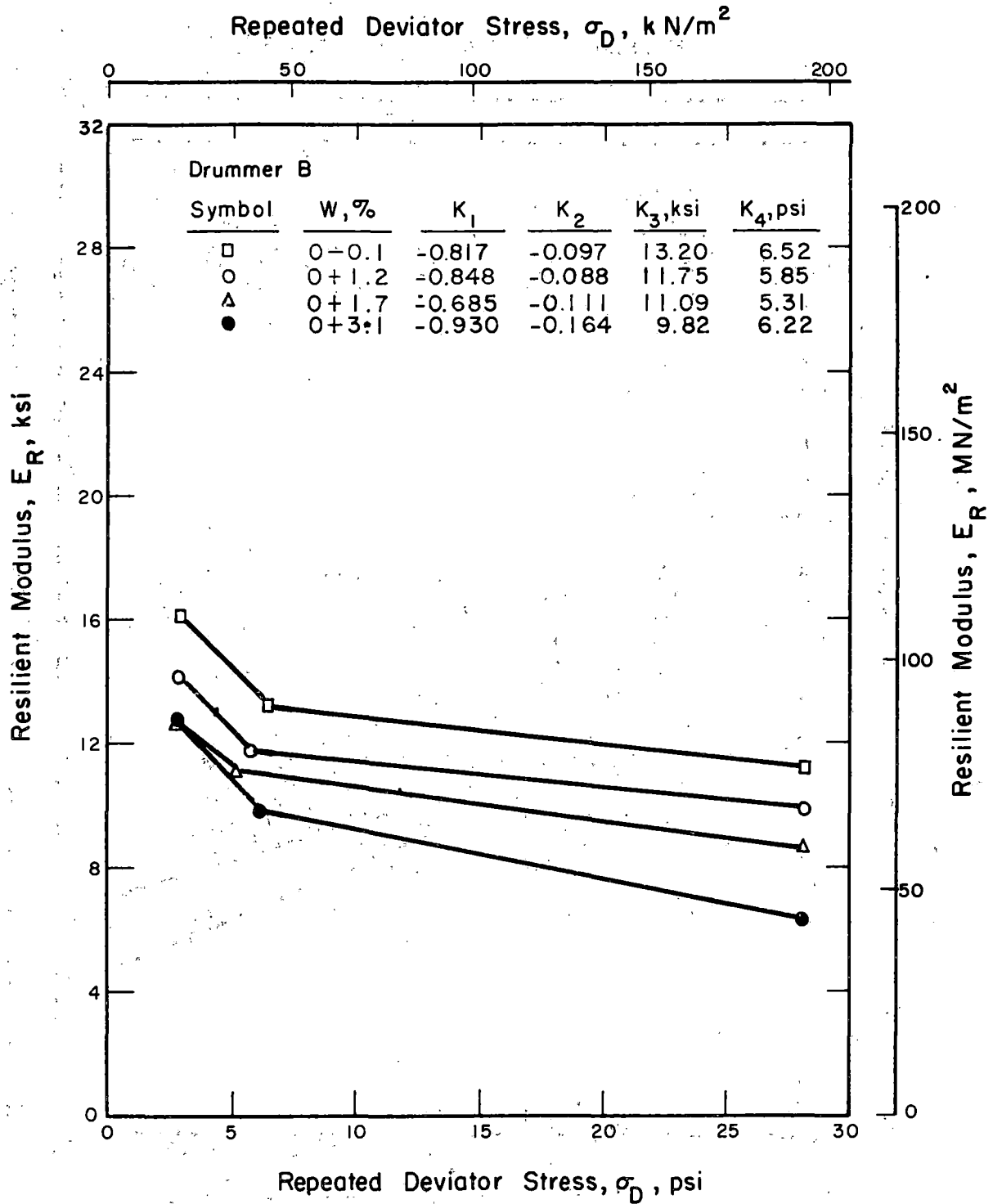


Figure 14.4. Resilient Modulus-Repeated Deviator Stress Relation for Drummer B

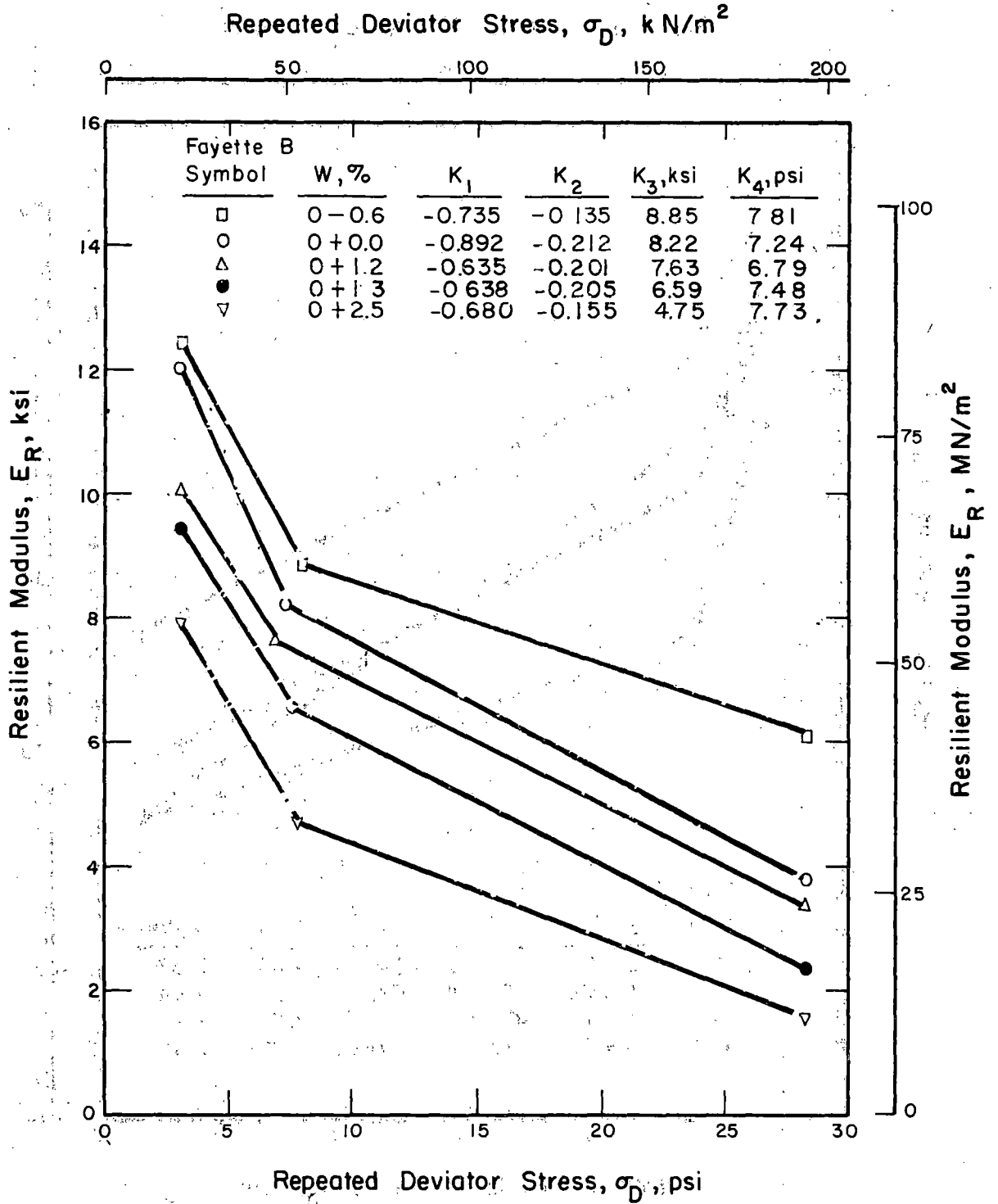


Figure 14.5. Resilient Modulus-Repeated Deviator Stress Relation for Fayette B.

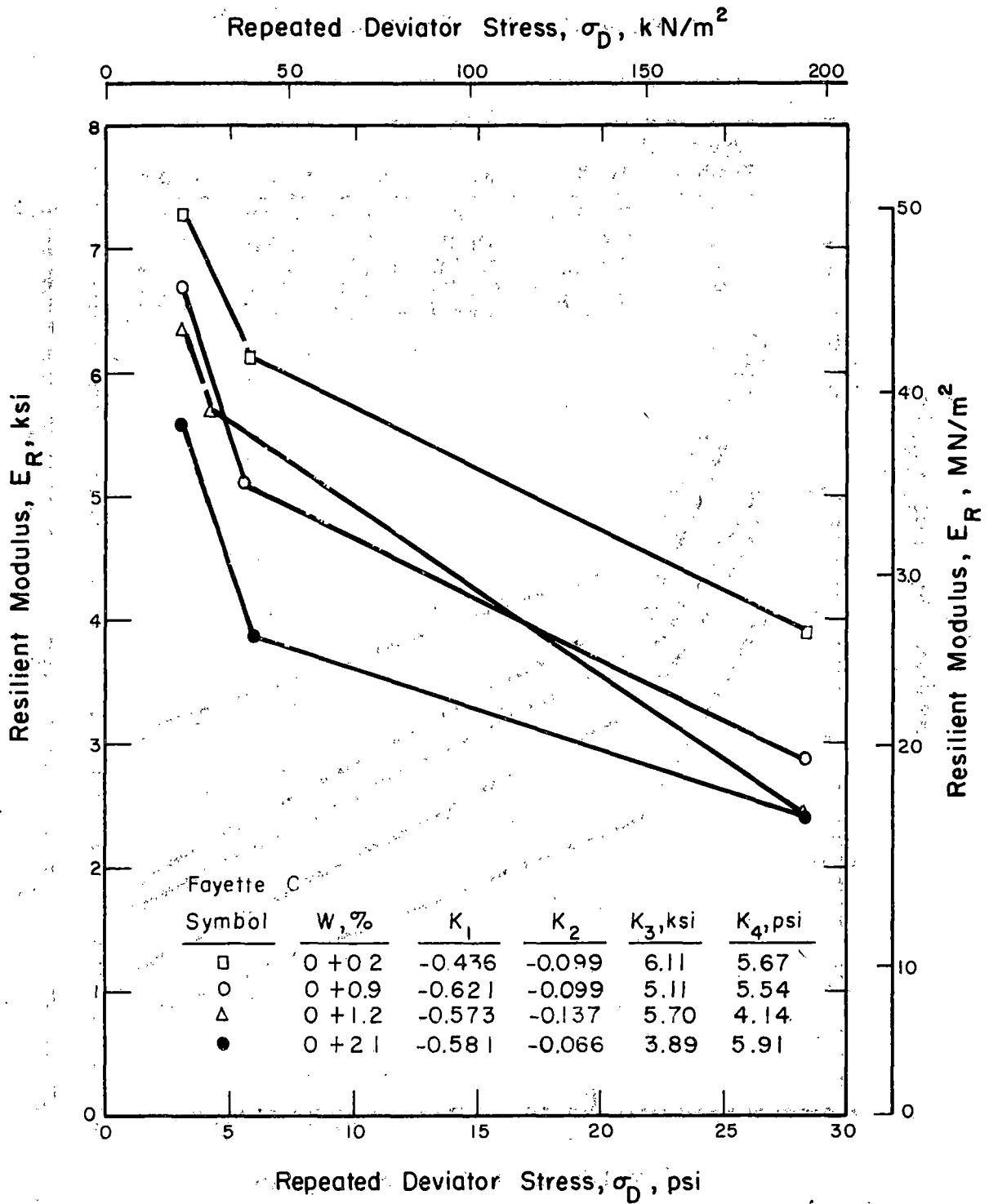


Figure 14.6. Resilient Modulus-Repeated Deviator Stress Relation for Fayette C

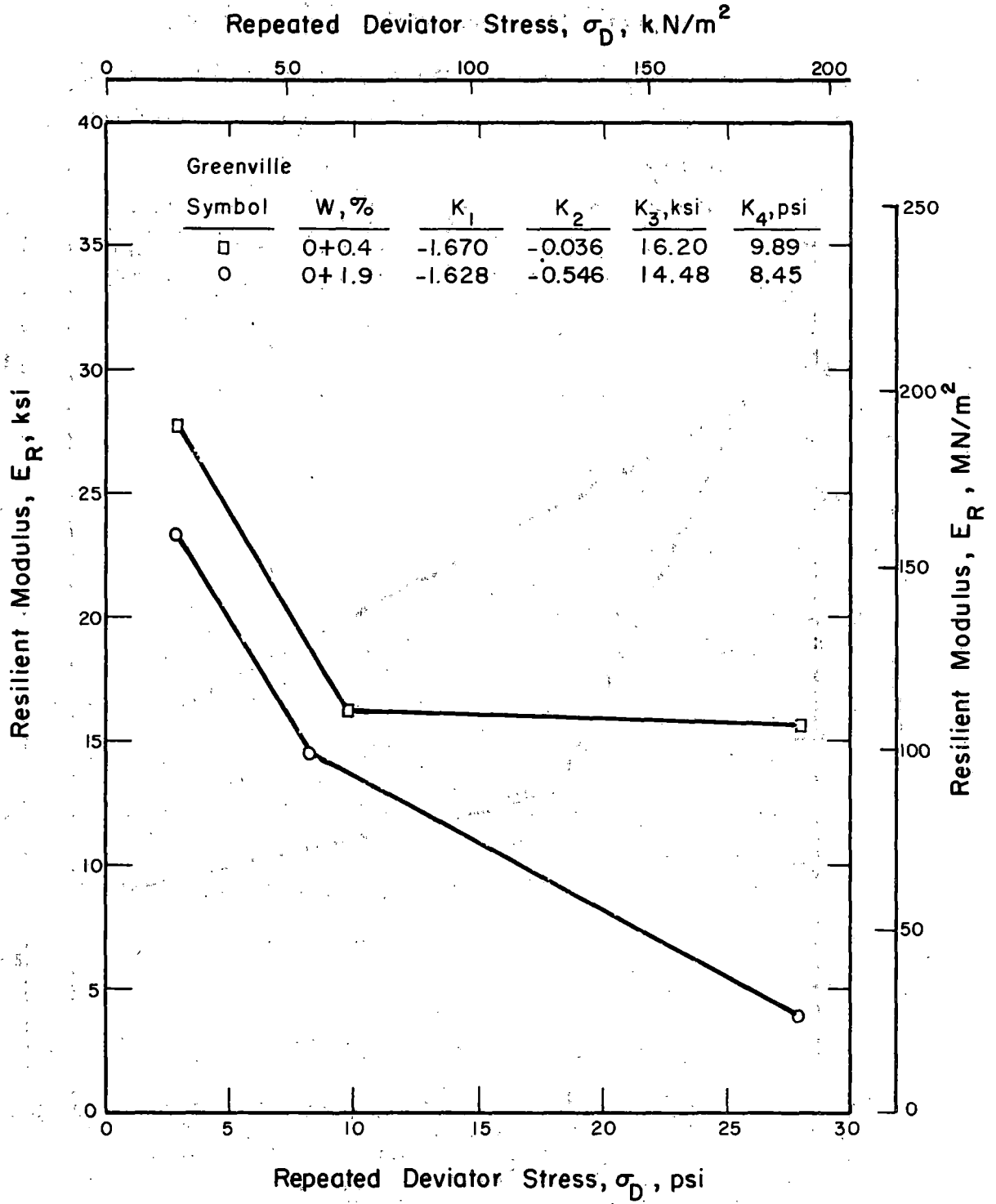


Figure 14.7. Resilient Modulus-Repeated Deviator Stress Relation for Greenville

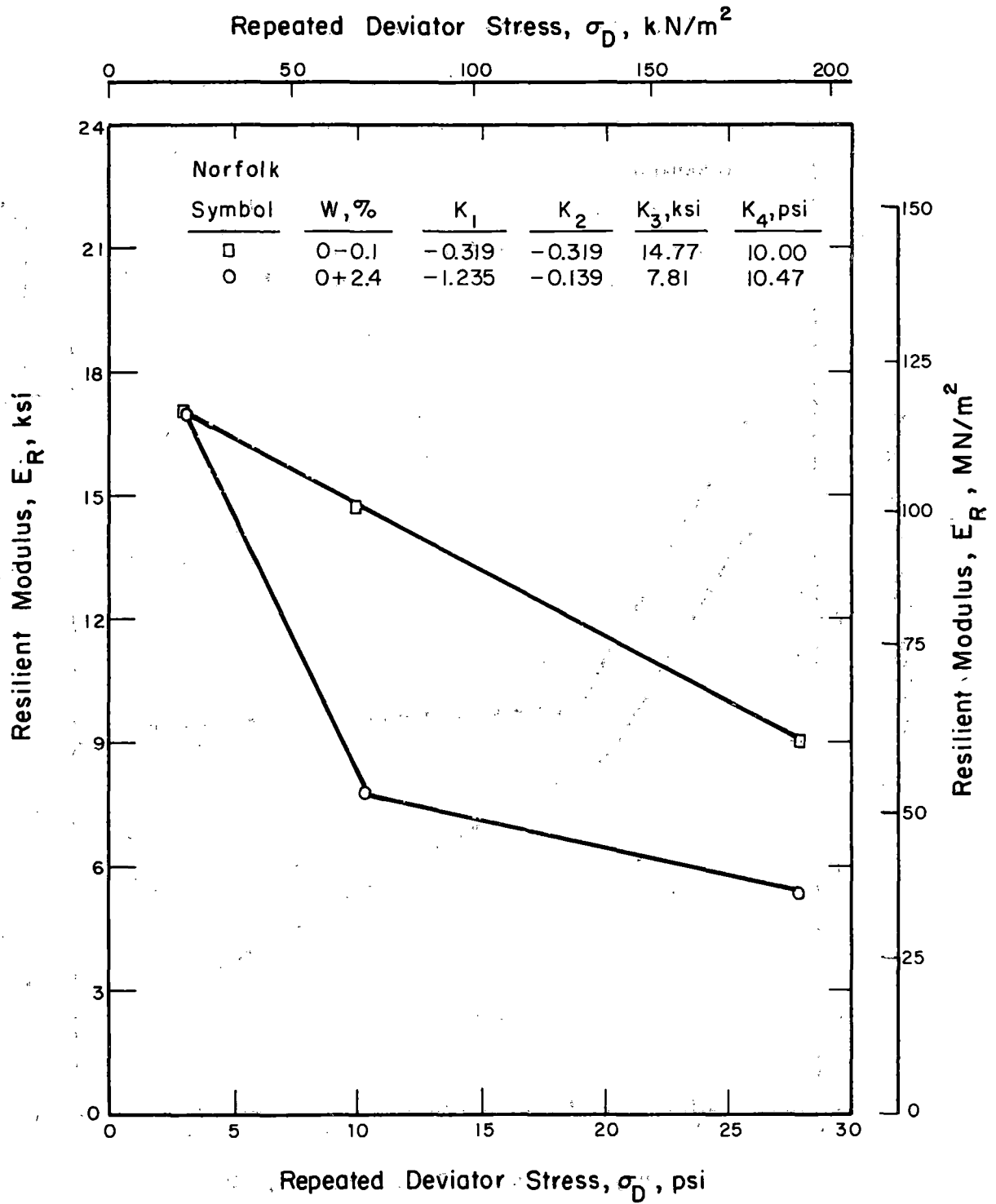


Figure 14.8. Resilient Modulus-Repeated Deviator Stress Relation for Norfolk

## 14.2 Permanent Deformation Test Results

The seven soils that were tested for evaluation of permanent deformation behavior are listed in Table 13.1. Three sets of specimens were prepared for each soil for the following conditions:

1. Optimum moisture content and 95% AASHTO T-99 density
2. Optimum moisture content and 100% AASHTO T-99 density
3. Optimum moisture contents plus 4 percent and 95% percent T-99 density

Figures 14.9 to 14.15 show the plots of permanent strain versus number of load applications at different stress states for the above seven soils, and Figures 14.16 to 14.22 show the plots of accumulated permanent strain versus deviator stress at the end of 5000 load applications. The  $\epsilon_p - N$  data of Figures 14.9 to 14.15 can be fit to the following equation using statistical methods (56).

$$\epsilon_p = AN^b$$

where  $\epsilon_p$  = permanent axial strain

$N$  = number of load applications

$A, b$  = experimentally determined coefficients

The determination of  $A$  and  $b$  for each soil condition is tabulated in Table 14.1. It can be seen that the relationship  $\epsilon_p = AN^b$  represents the data fairly well from a statistical viewpoint. A correlation analysis was performed correlating  $\log A$  to the stress level,  $\sigma_D$ , and  $b$  to the stress level,  $\sigma_D$ . The analysis indicated no significant correlation for the  $b$  coefficient to the stress level,  $\sigma_D$ , for any condition, suggesting that coefficient  $b$  is dependent on soil type only.  $\log A$  did correlate significantly (at the 95 percent level) with the stress level,  $\sigma_D$ , in all cases where there were at least four observations, suggesting that the coefficient  $A$  is a function of the stress level and placement conditions.

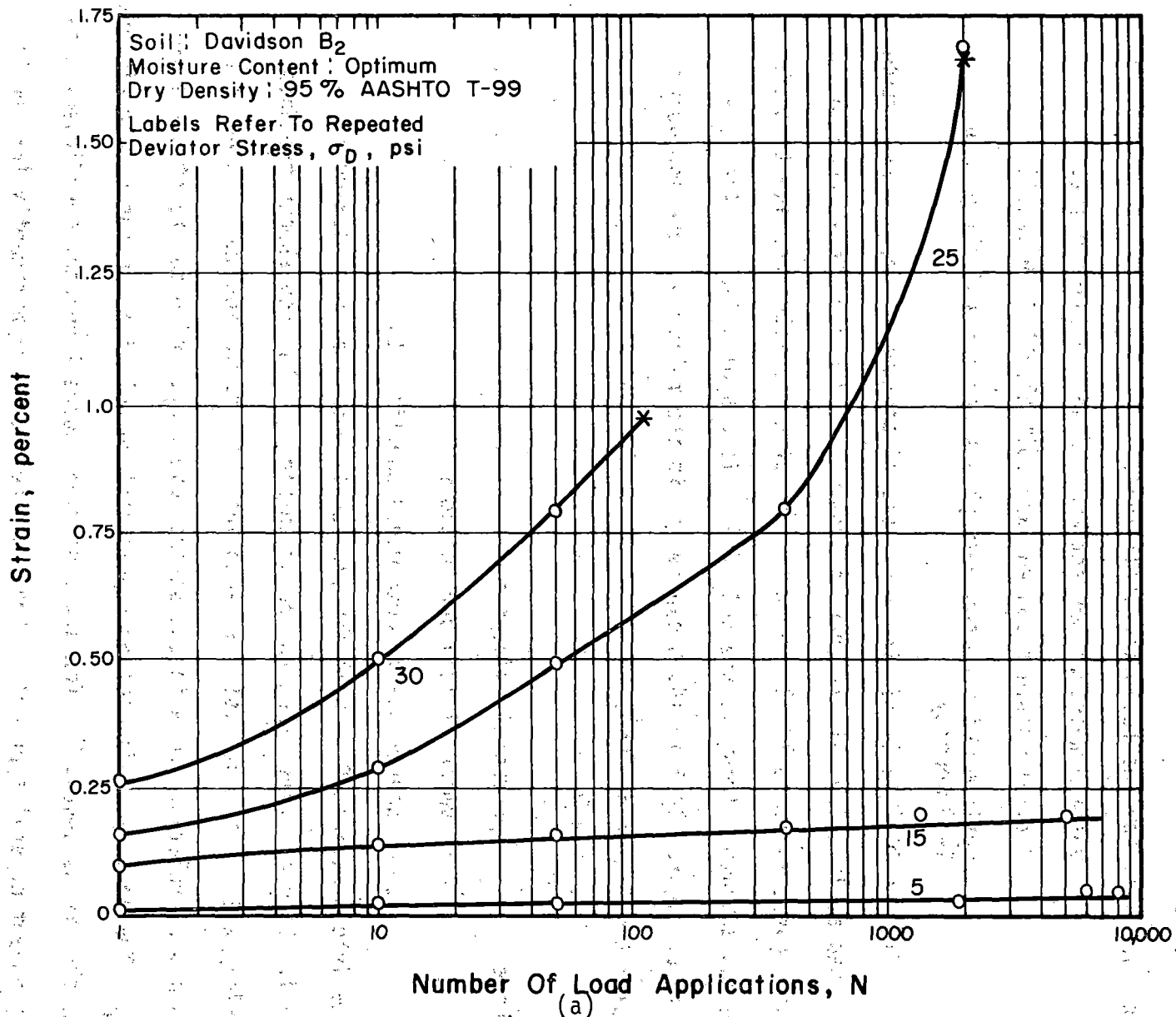


Figure 14.9. Permanent Strain-Number of Load Repetition Relation for Davidson B<sub>2</sub>

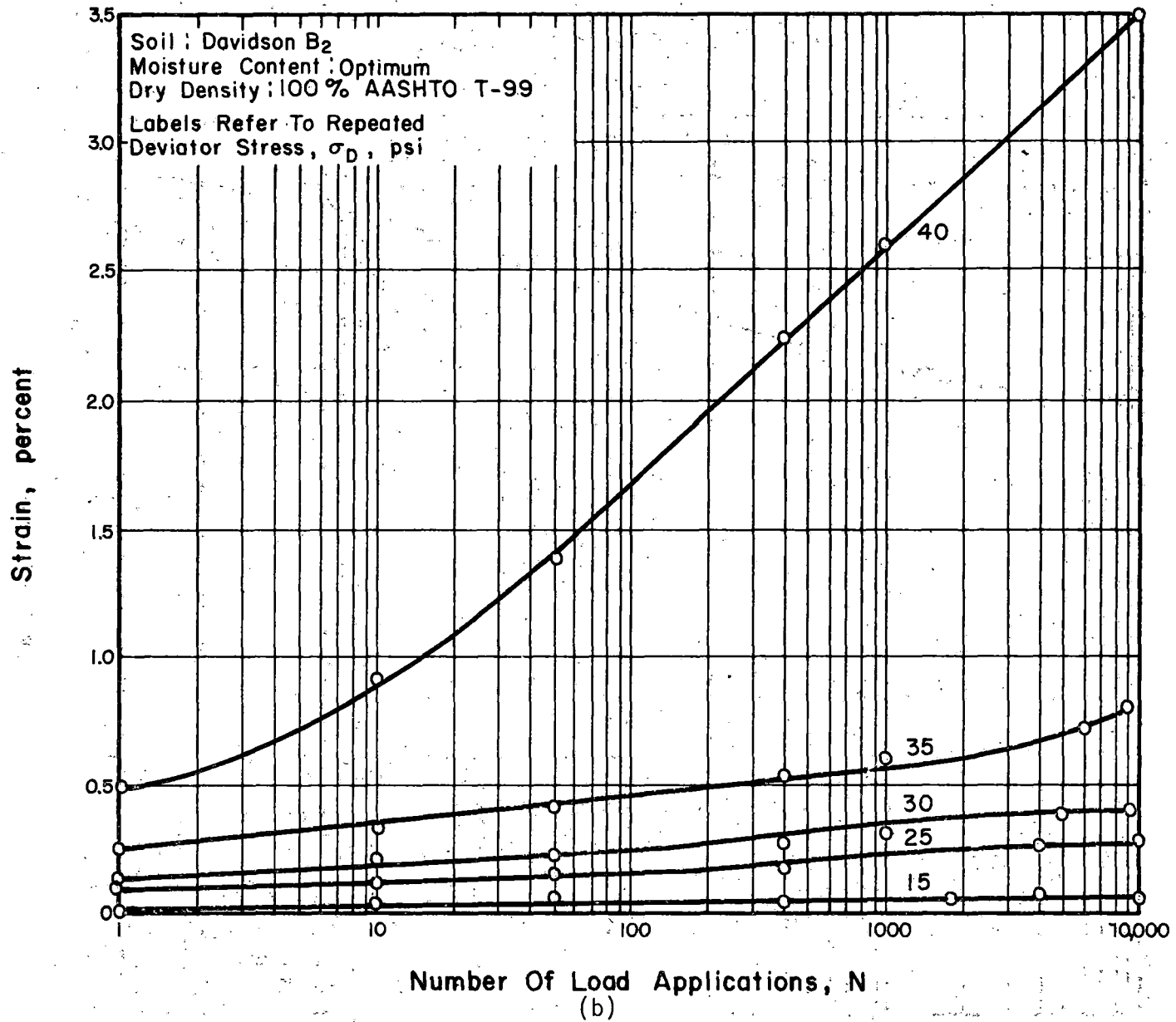


Figure 14.9. Permanent Strain-Number of Load Repetition Relation for Davidson B<sub>2</sub>

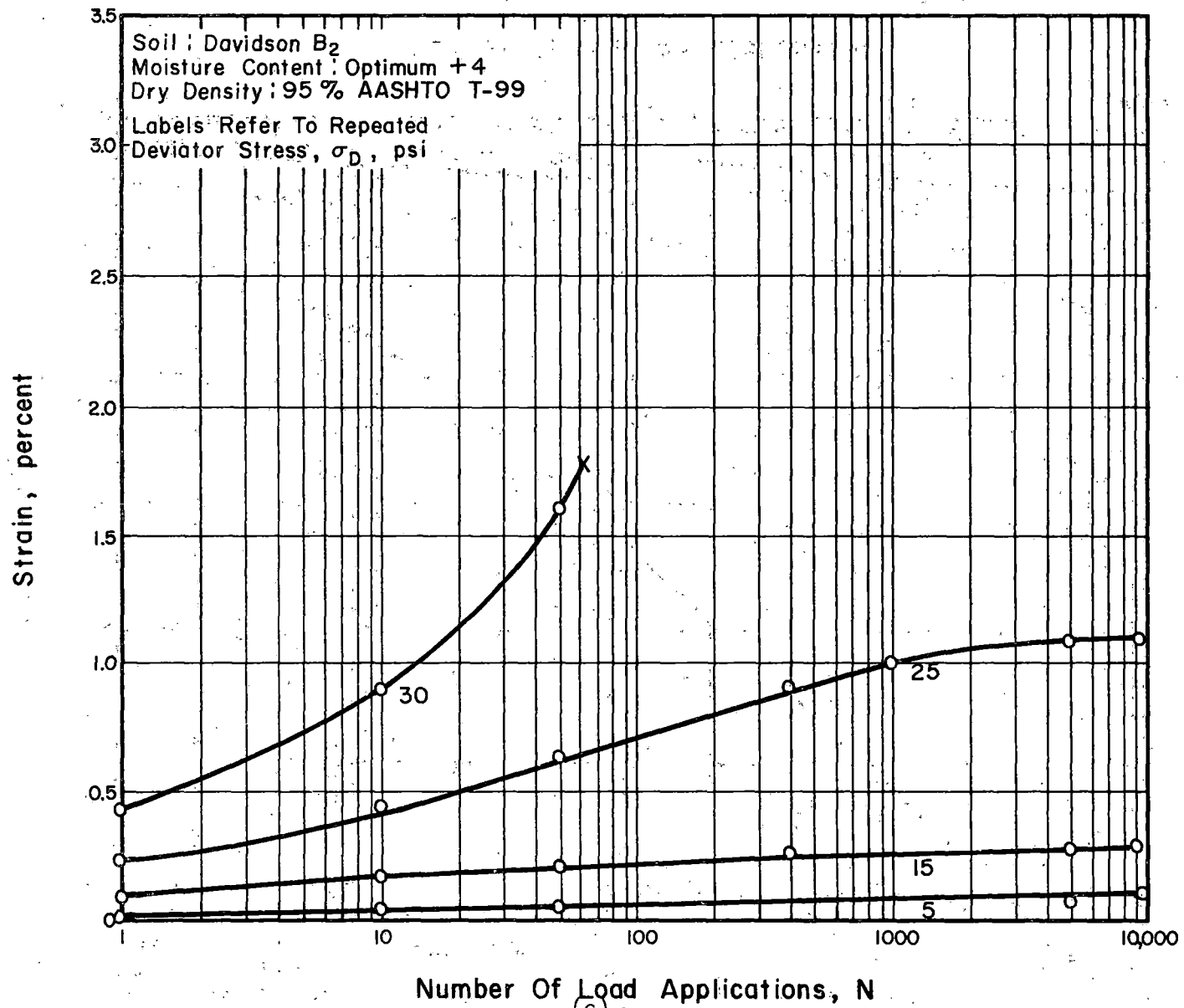


Figure 14.9. Permanent Strain-Number of Load Repetition Relation for Davidson B<sub>2</sub>

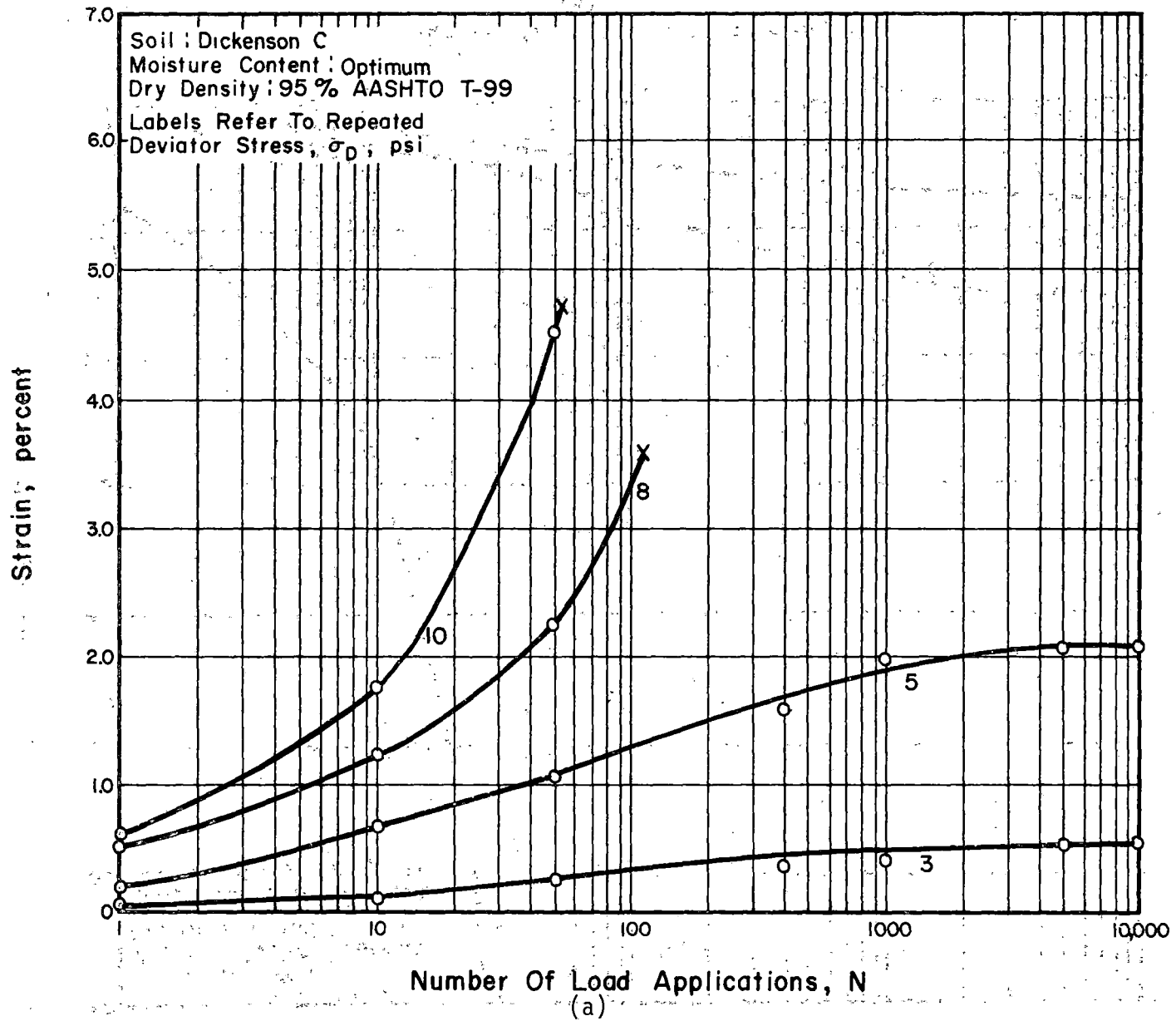


Figure 14.10. Permanent Strain-Number of Load Repetition Relation for Dickenson C

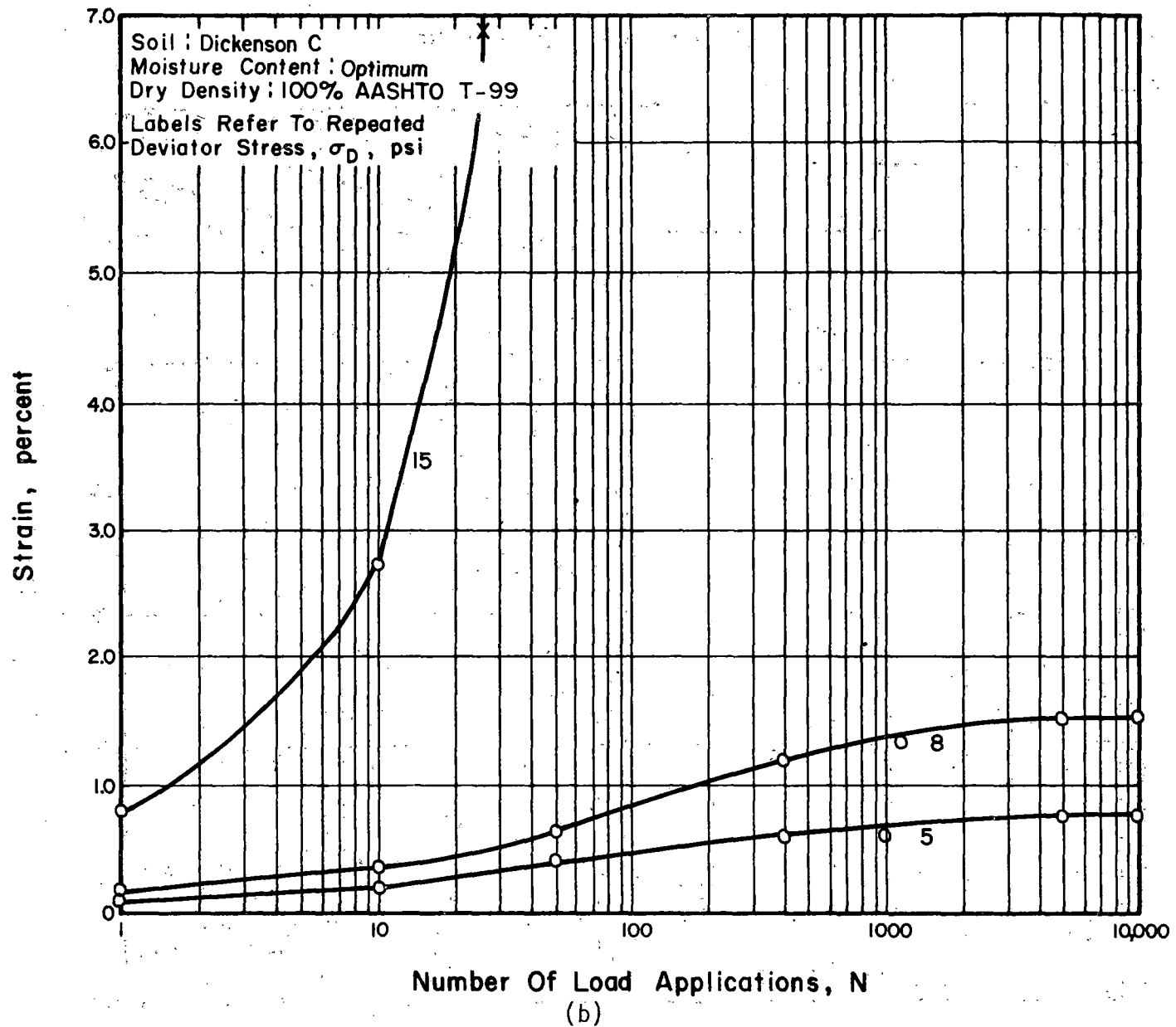


Figure 14.10. Permanent Strain-Number of Load Repetition Relation for Dickenson C

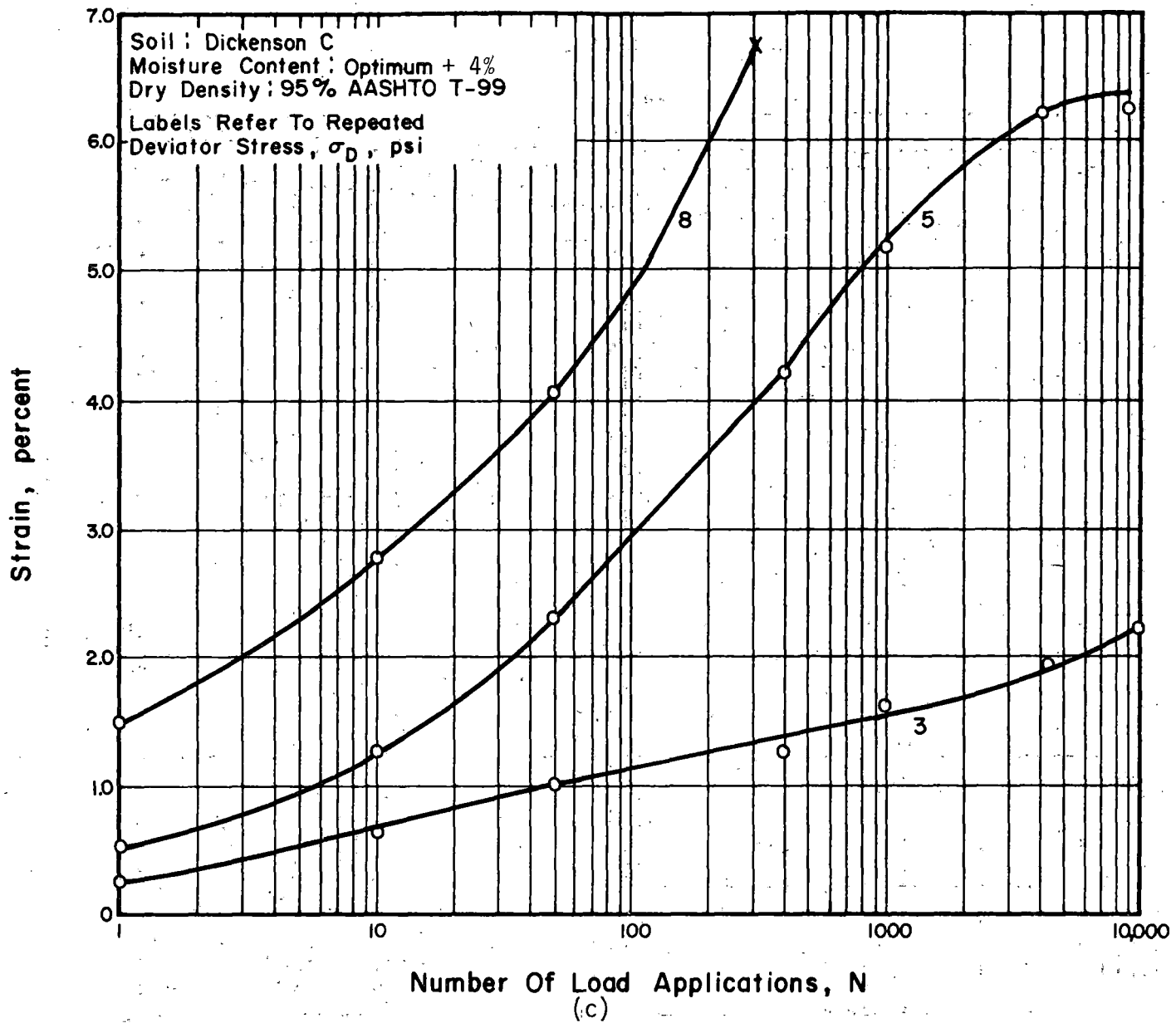


Figure 14.10. Permanent Strain-Number of Load Repetition Relation for Dickenson C

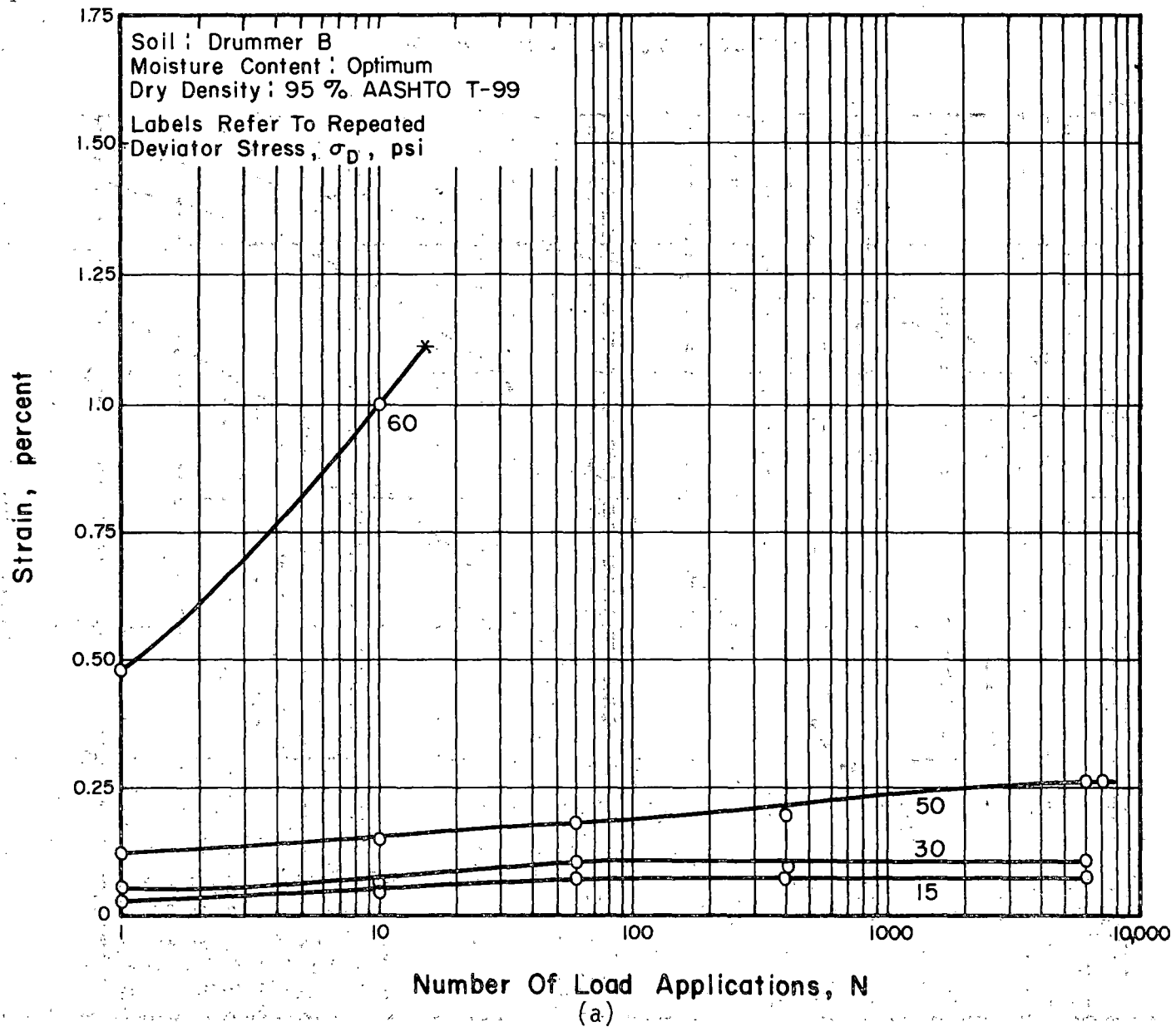


Figure 14.11. Permanent Strain-Number of Load Repetition Relation for Drummer B

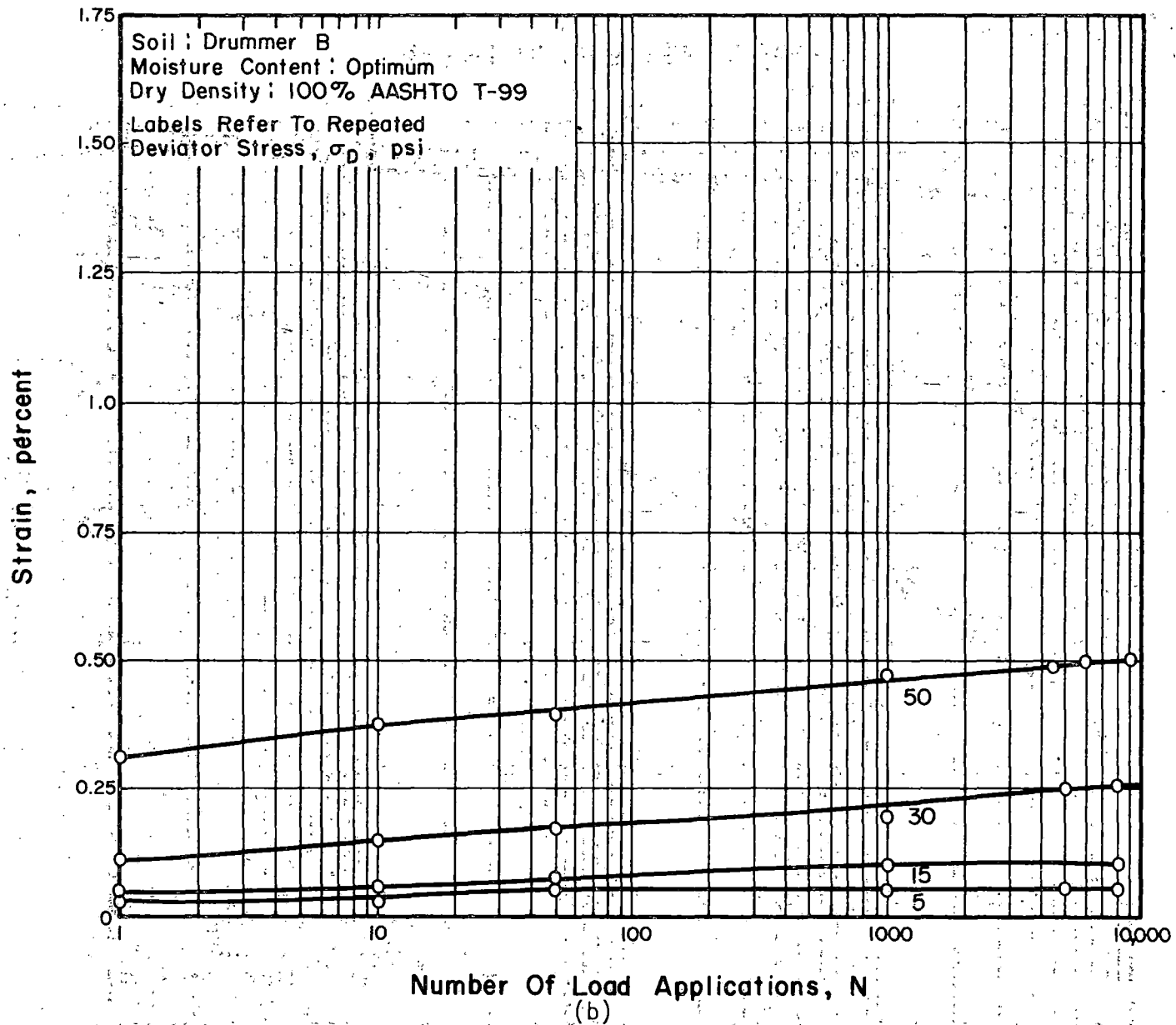


Figure 14.11. Permanent Strain-Number of Load Repetition Relation for Drummer B

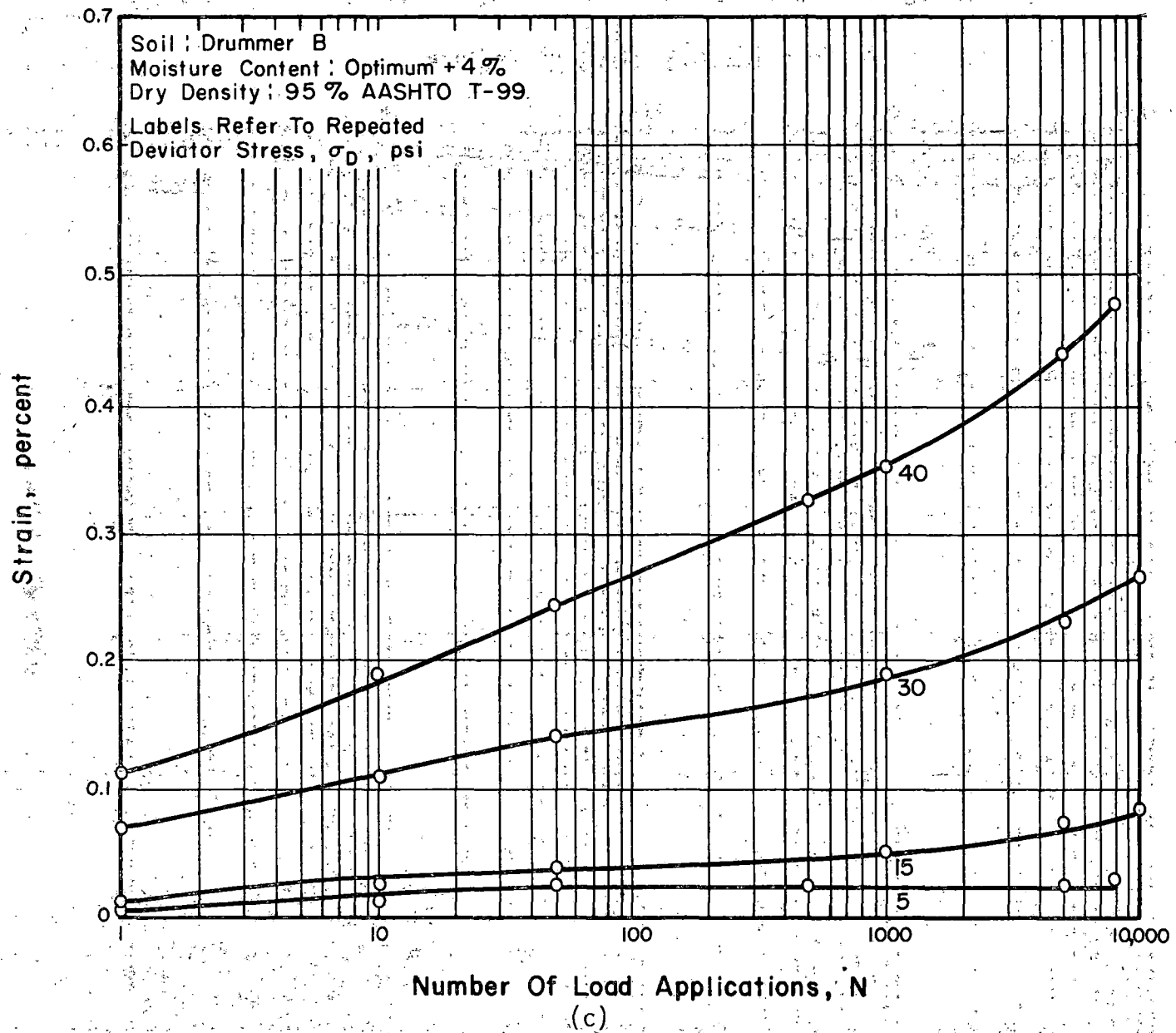


Figure 14.11. Permanent Strain Number of Load Repetition for Drummer B

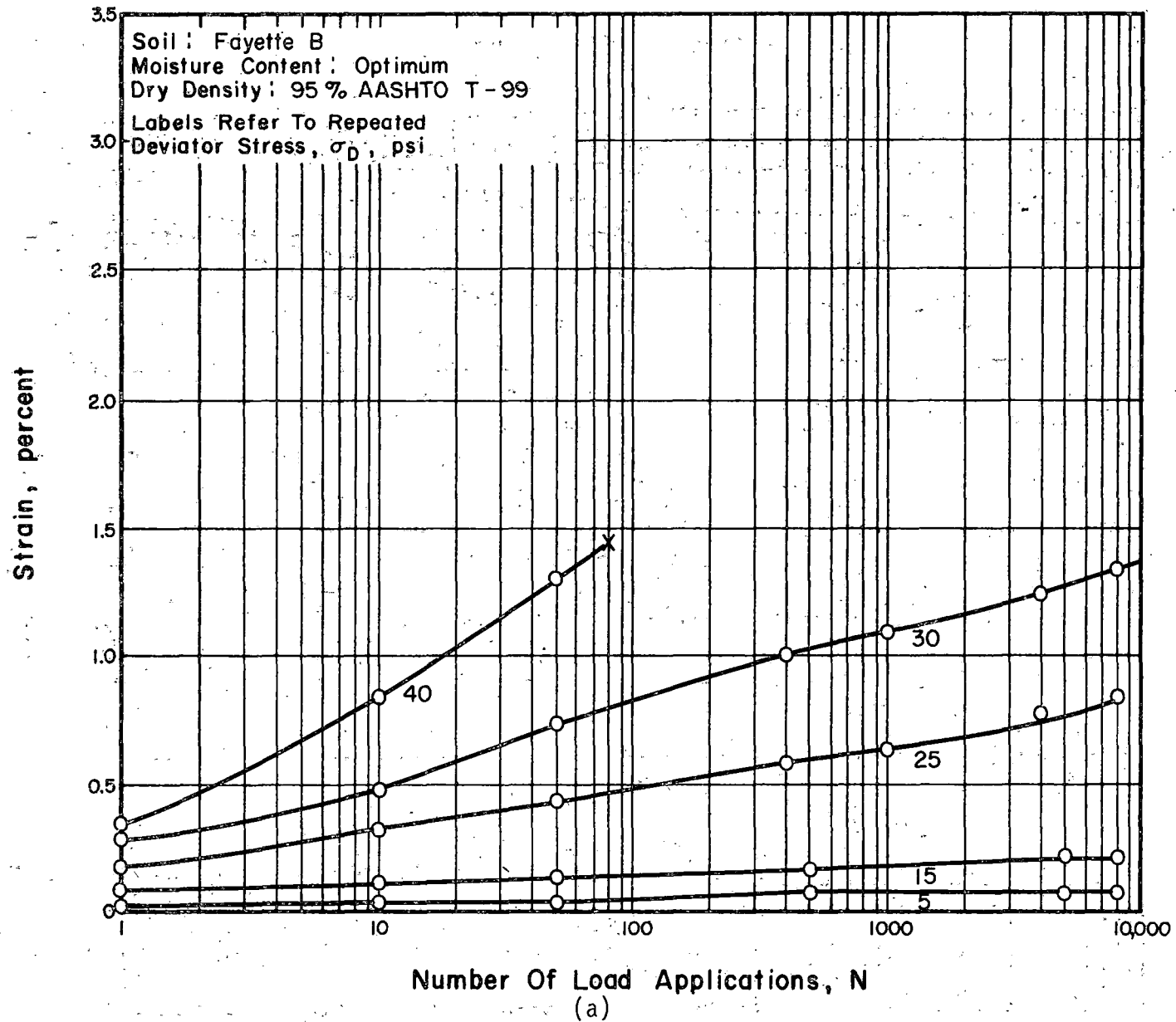


Figure 14.12. Permanent Strain-Number of Load Repetition Relation for Fayette B

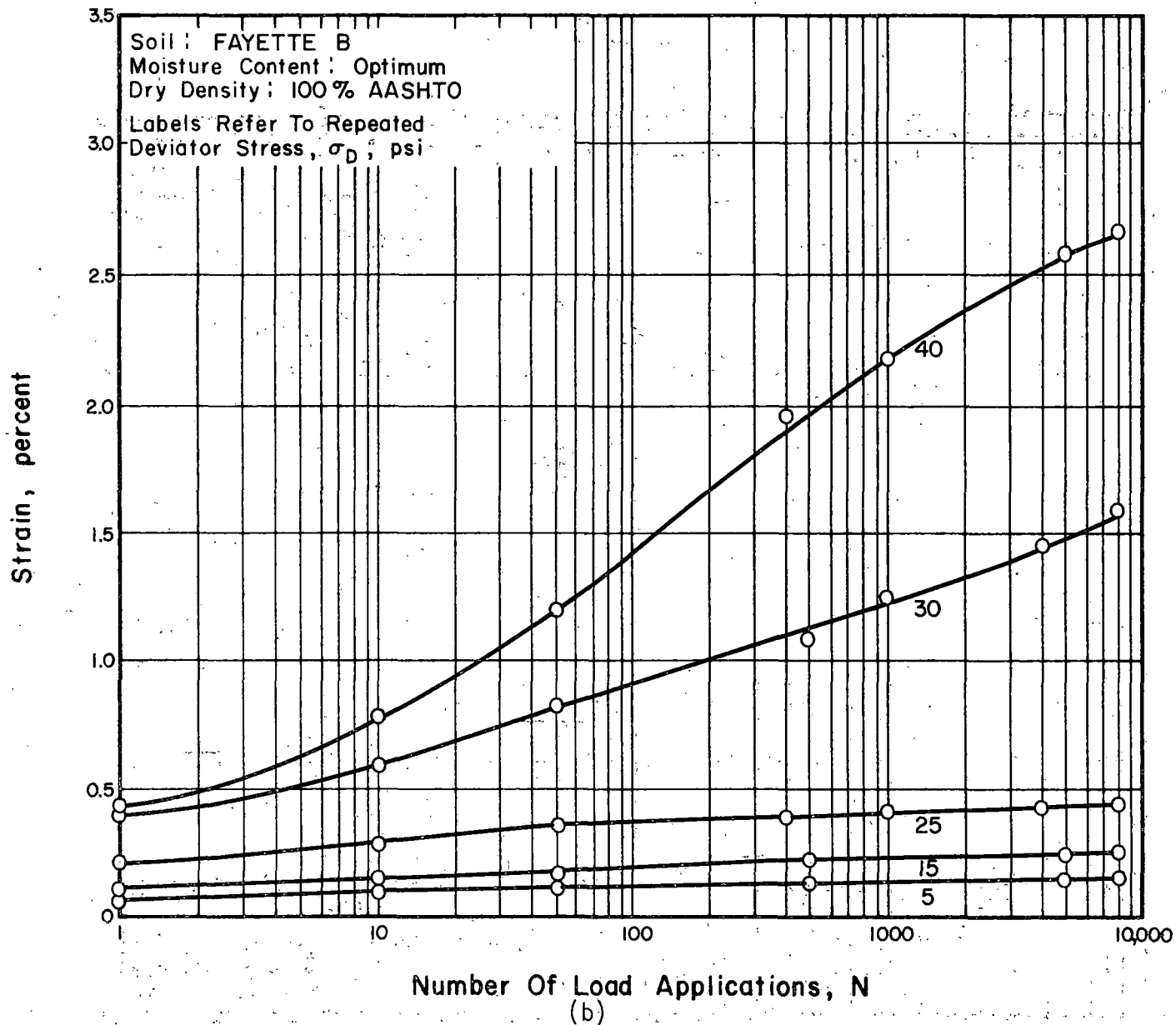


Figure 14.12. Permanent Strain-Number of Load Repetition Relation for Fayette B

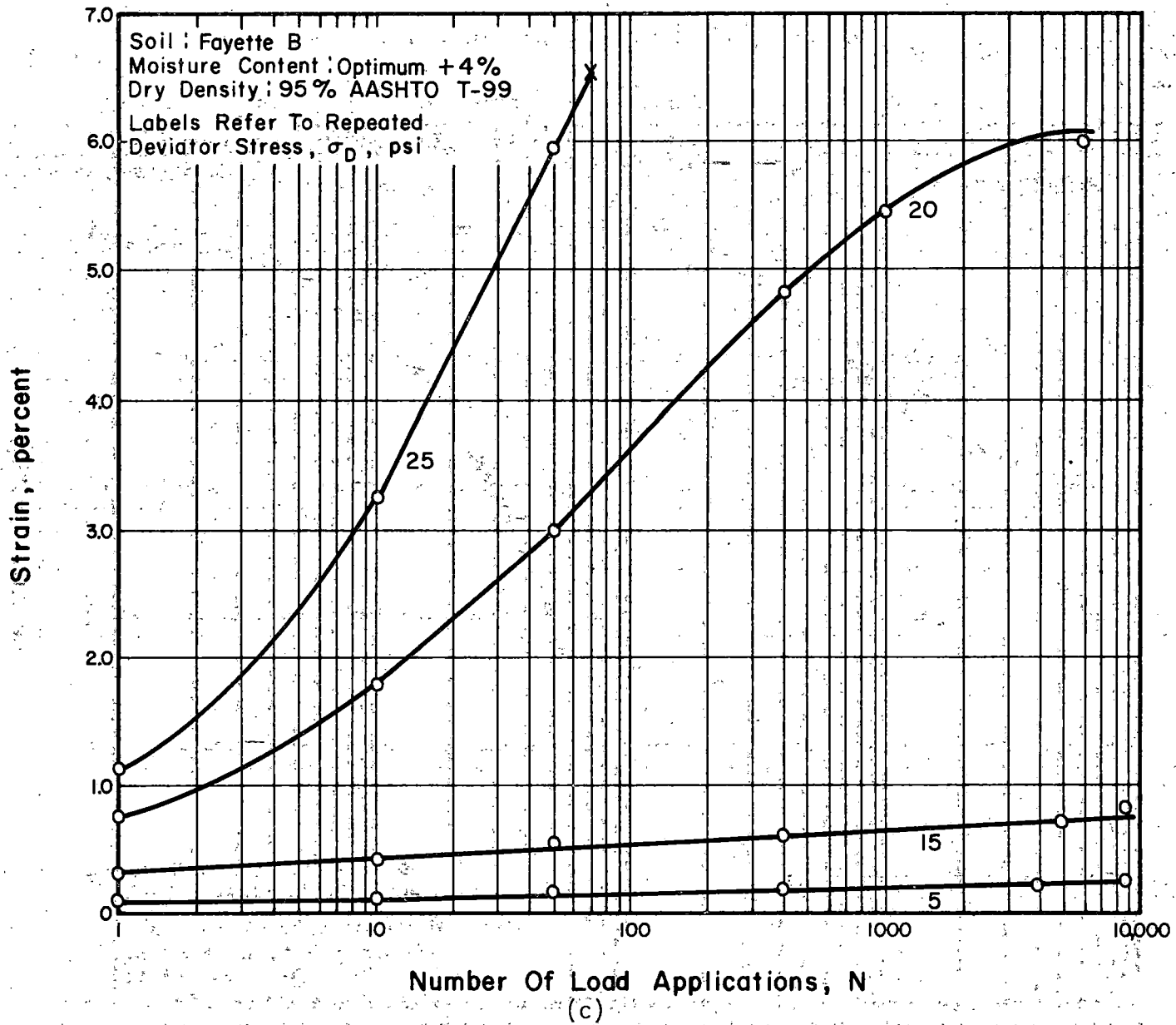


Figure 14.12. Permanent Strain-Number of Load Repetition Relation for Fayette B

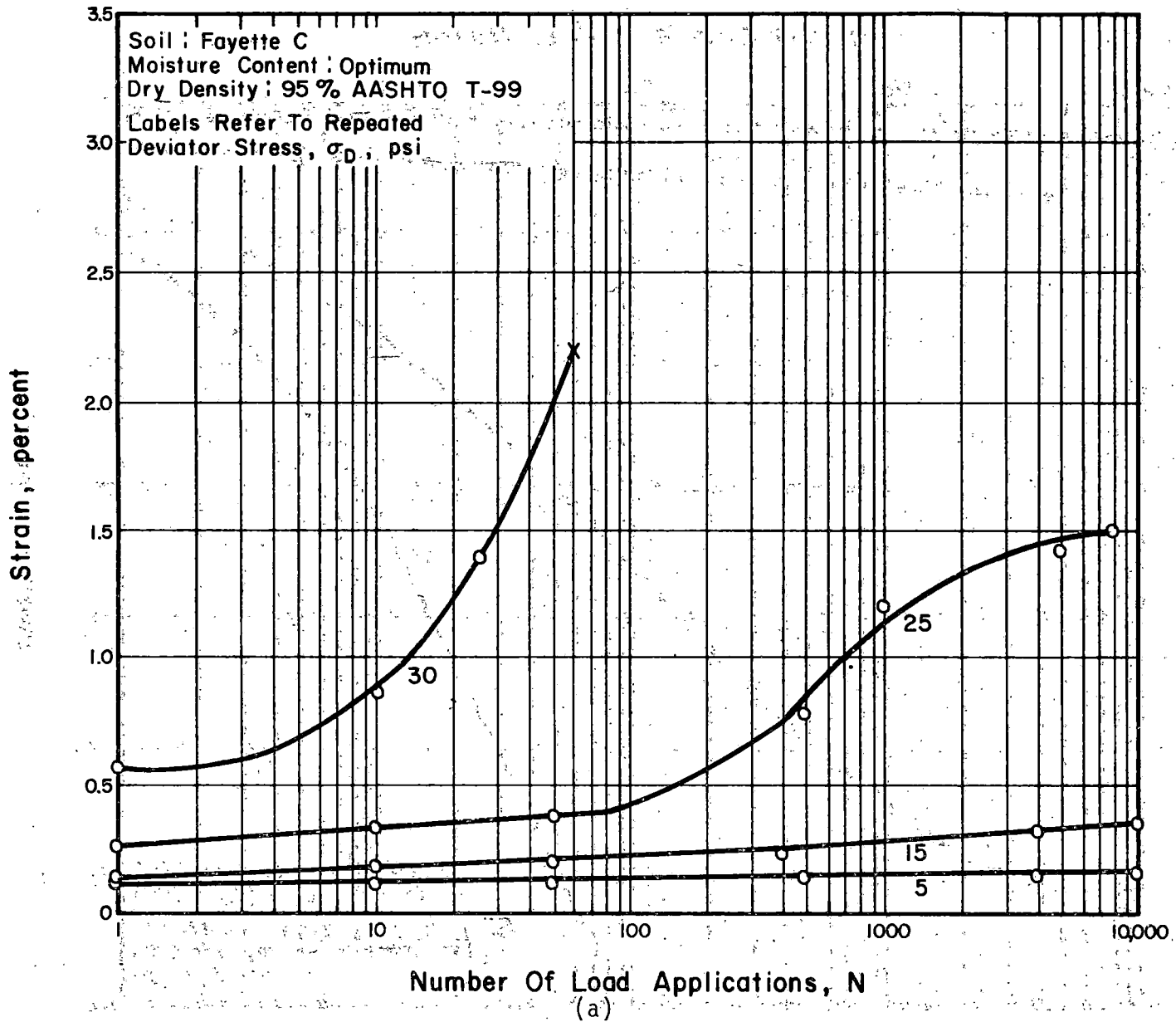


Figure 14.13. Permanent Strain-Number of Load Repetition Relation for Fayette C

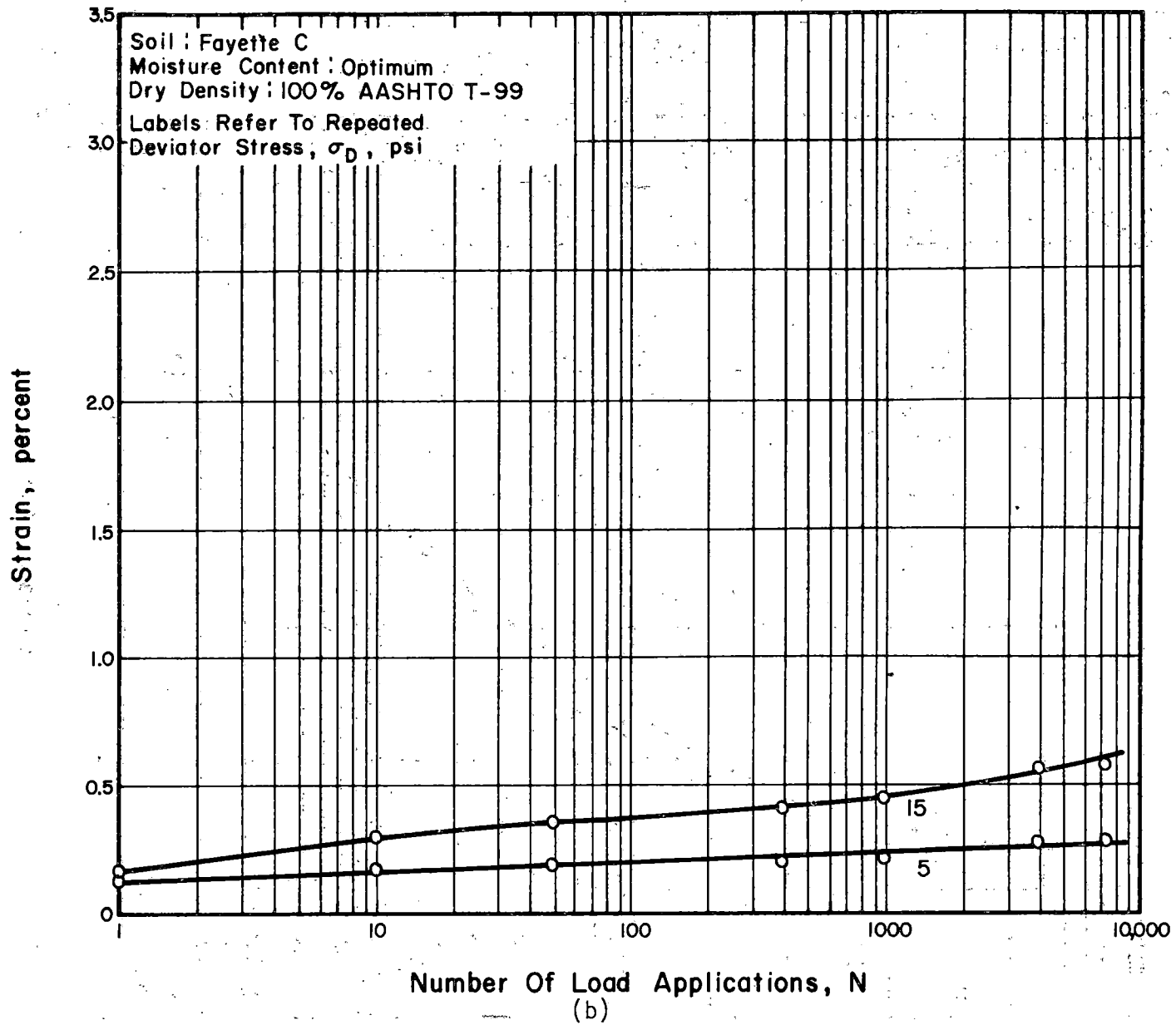


Figure 14.13. Permanent Strain-Number of Load Repetition Relation for Fayette C

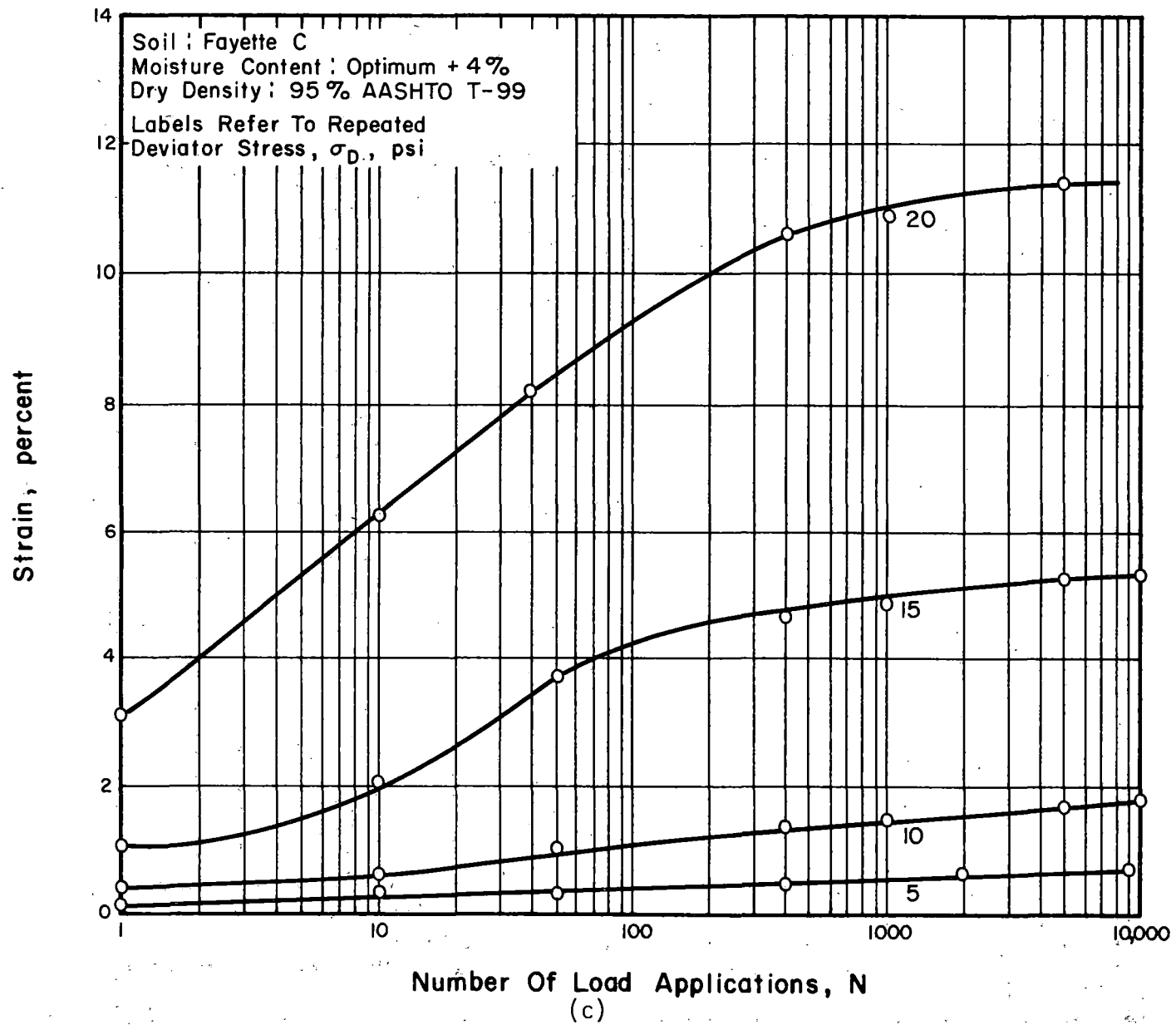


Figure 14.13. Permanent Strain-Number of Load Repetition Relation for Fayette C

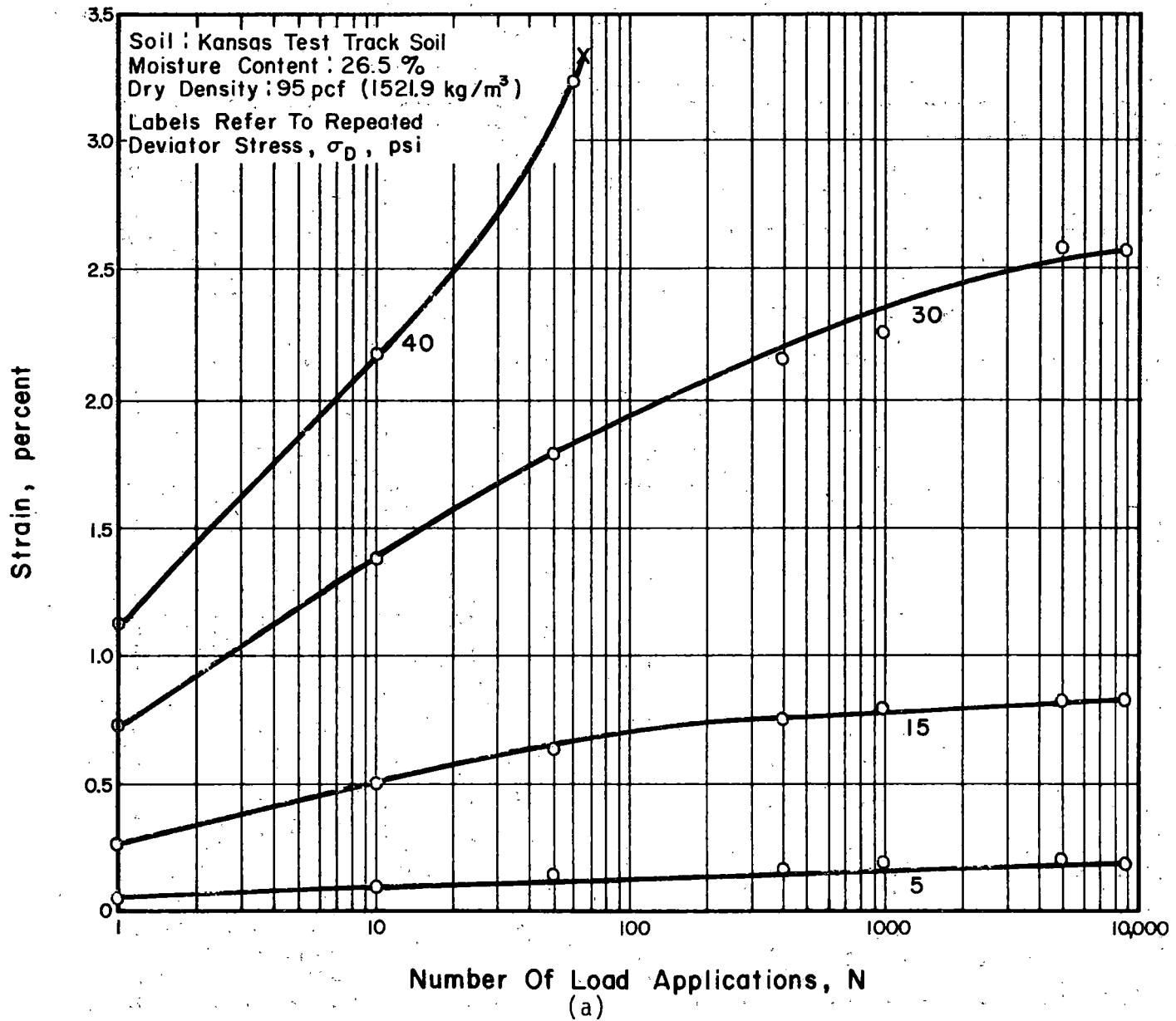


Figure 14.14. Permanent Strain-Number of Load Repetition Relation for the Kansas Test Track Soil

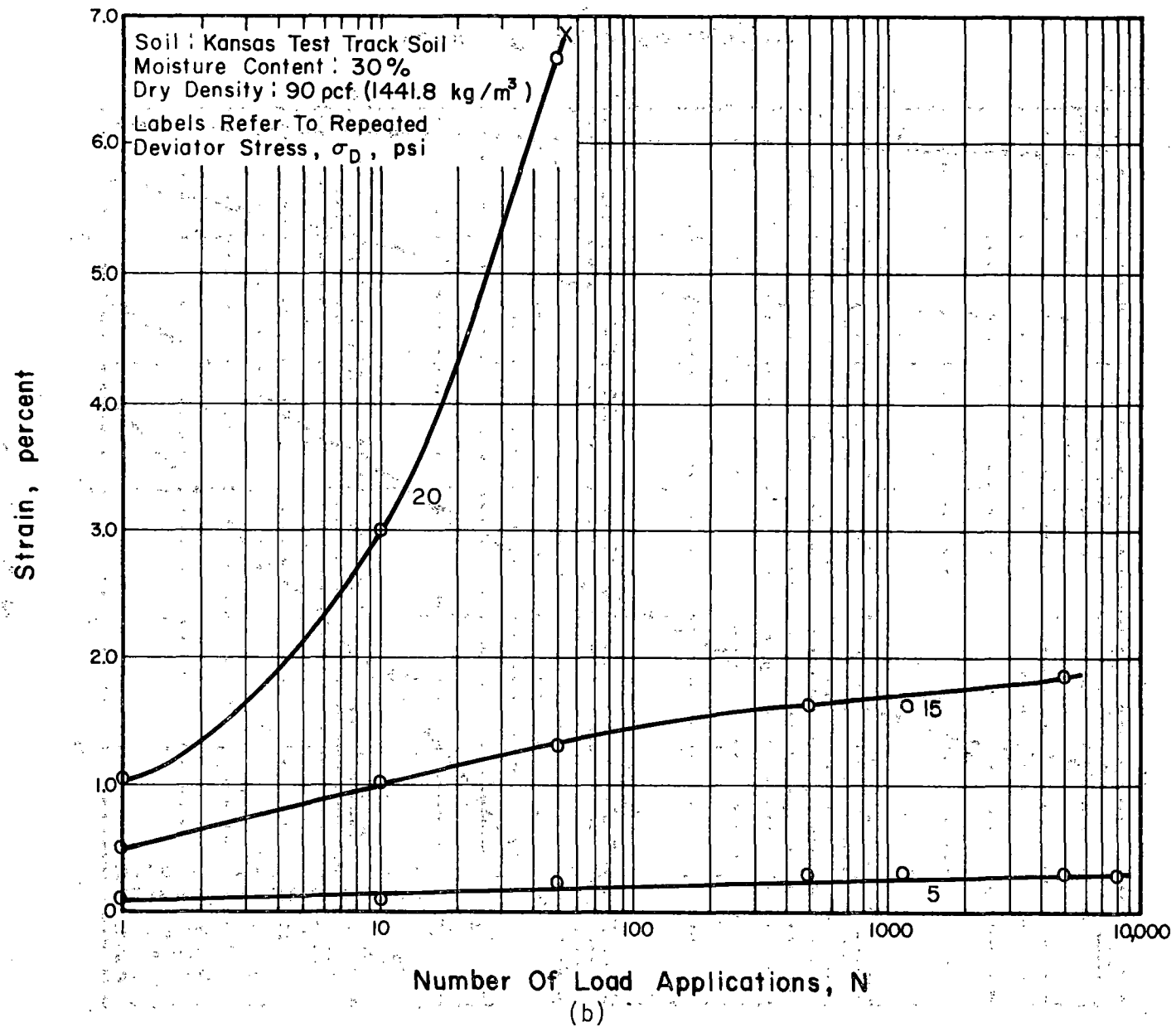


Figure 14.14. Permanent Strain-Number of Load Repetition Relation for the Kansas Test Track Soil

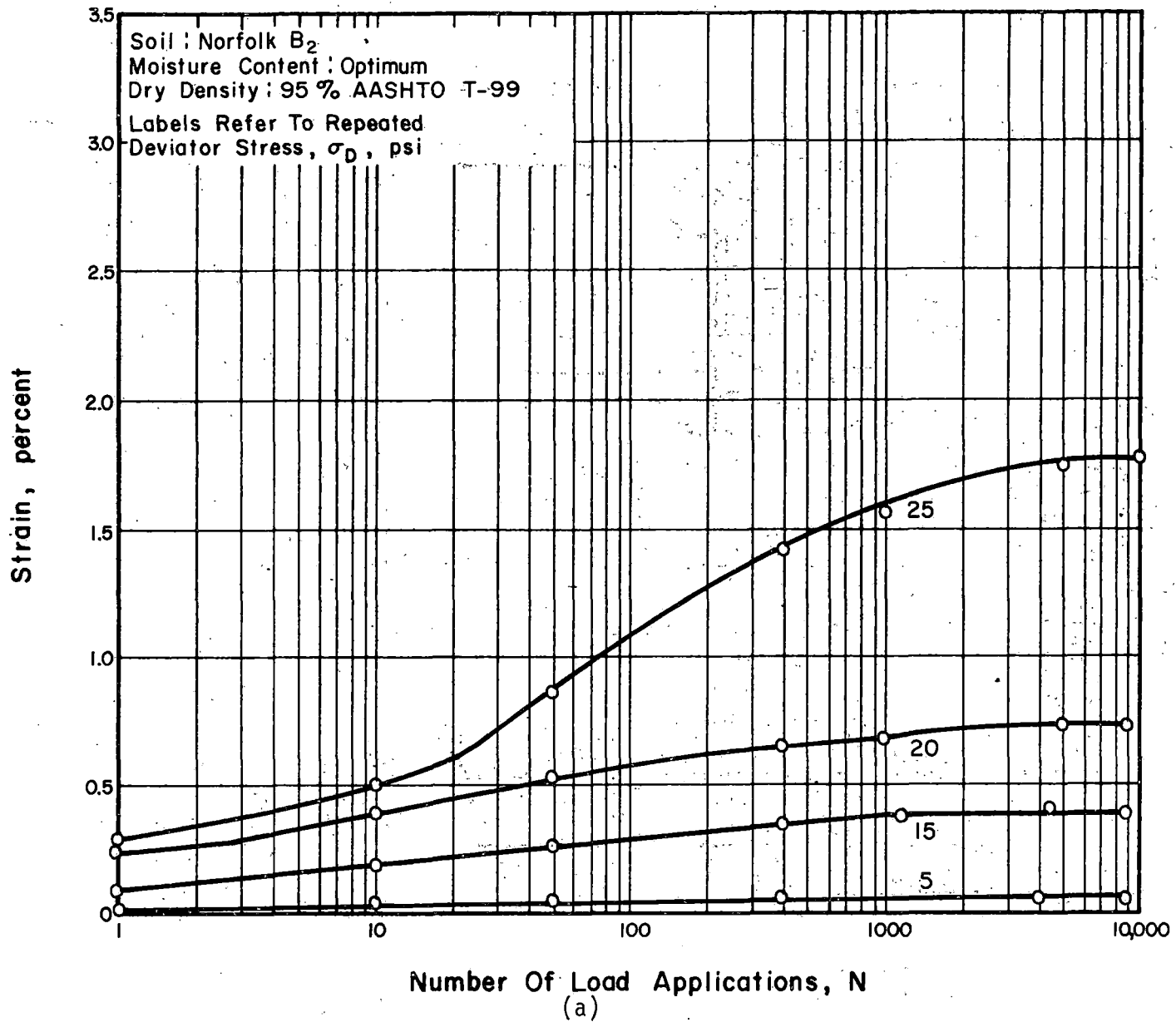


Figure 14.15. Permanent Strain-Number of Load Repetition Relation for Norfolk B<sub>2</sub>

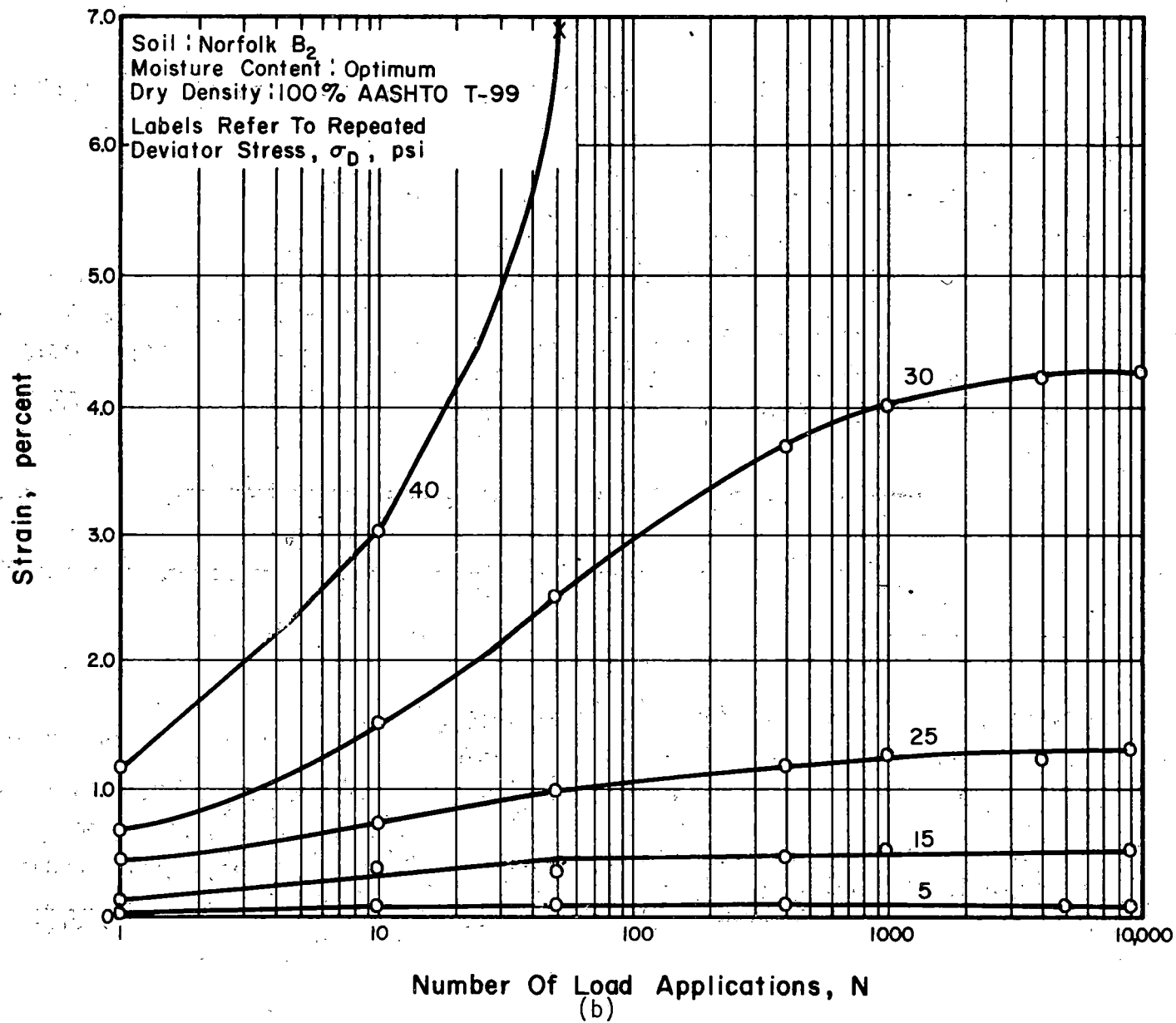


Figure 14.15. Permanent Strain-Number of Load Repetition Relation for Norfolk B<sub>2</sub>

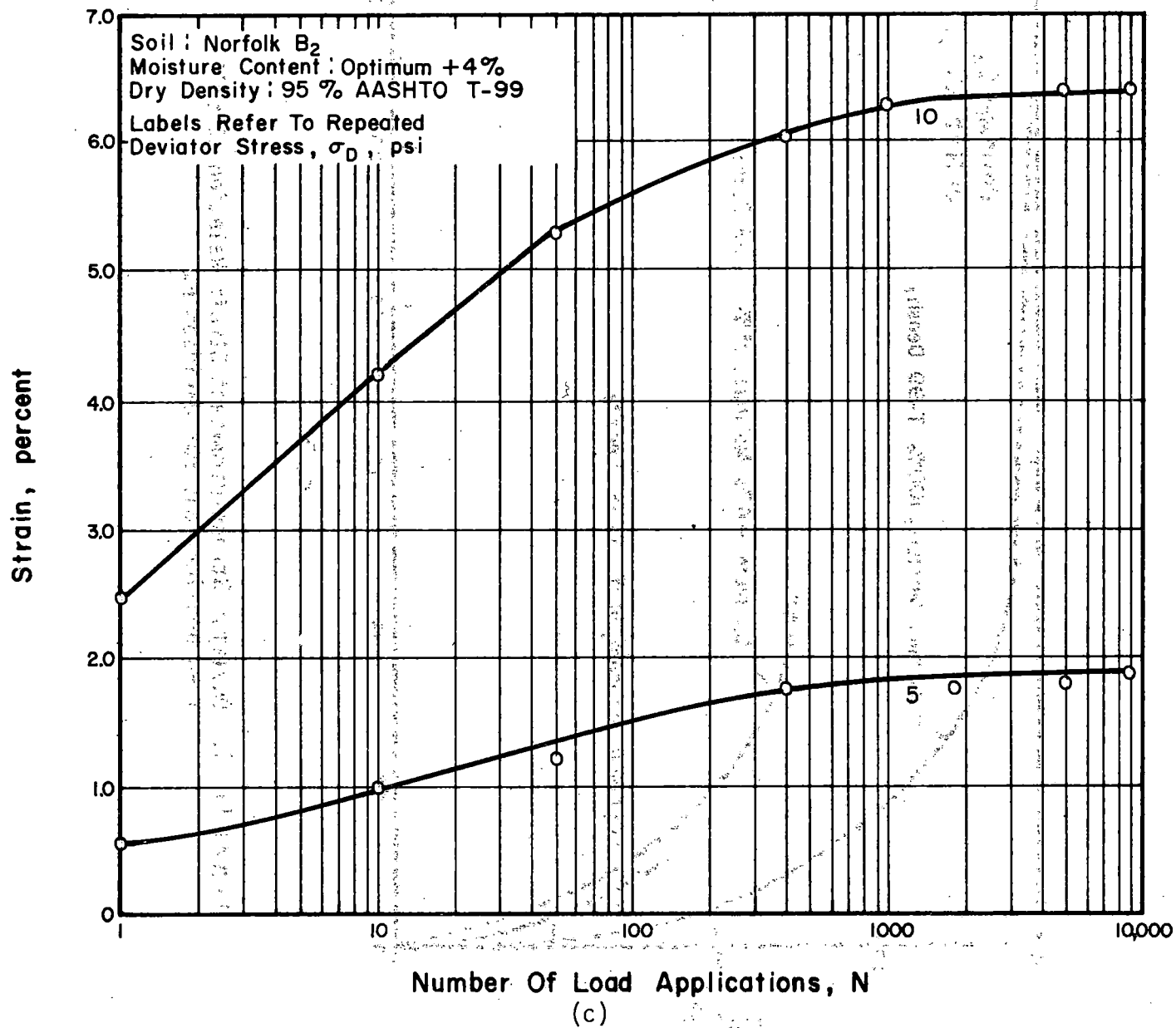


Figure 14.15. Permanent Strain-Number of Load Repetition Relation for Norfolk B<sub>2</sub>

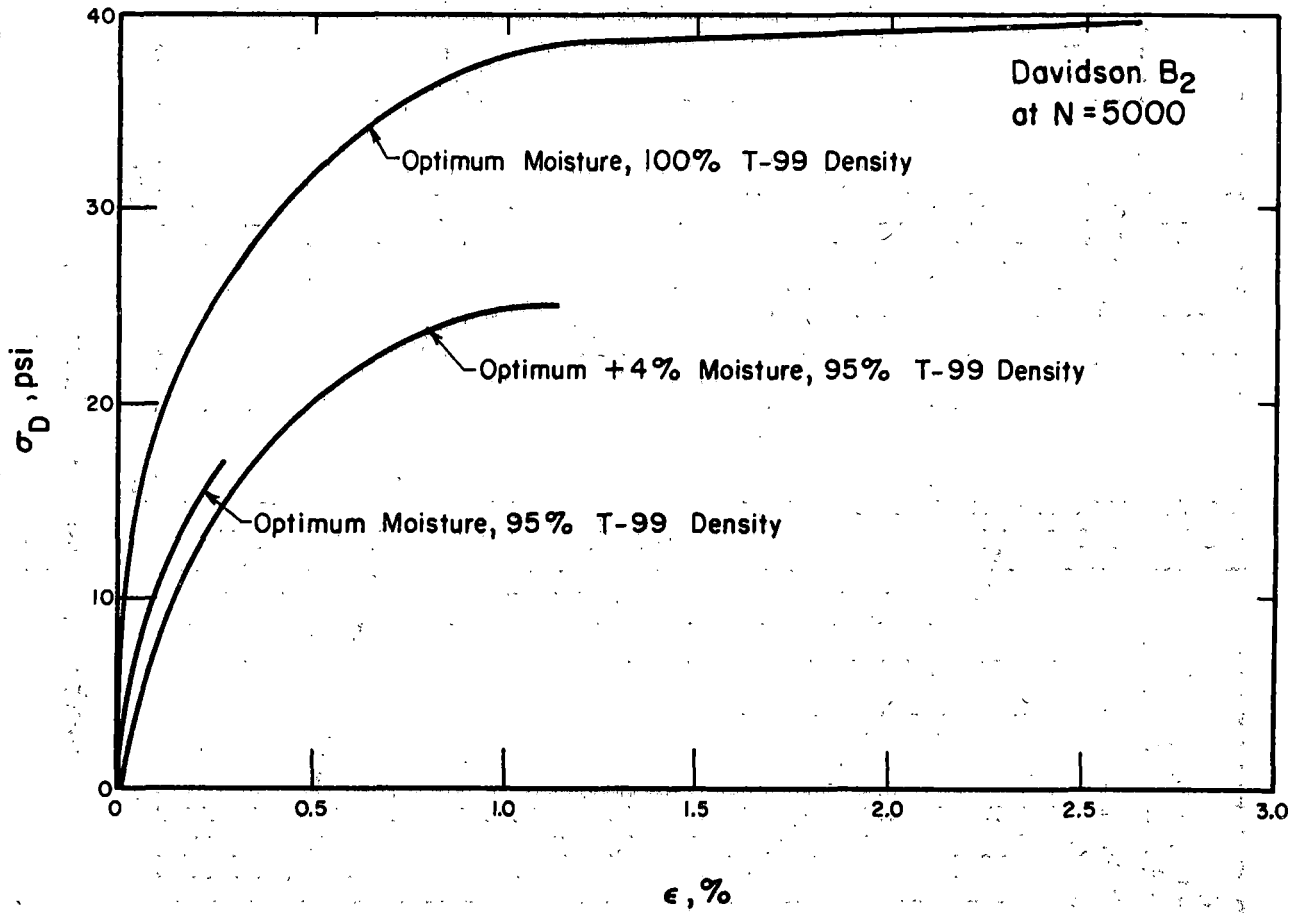


Figure 14.16. Deviator Stress-Permanent Strain Relation at 5000 load applications for Davidson B<sub>2</sub>

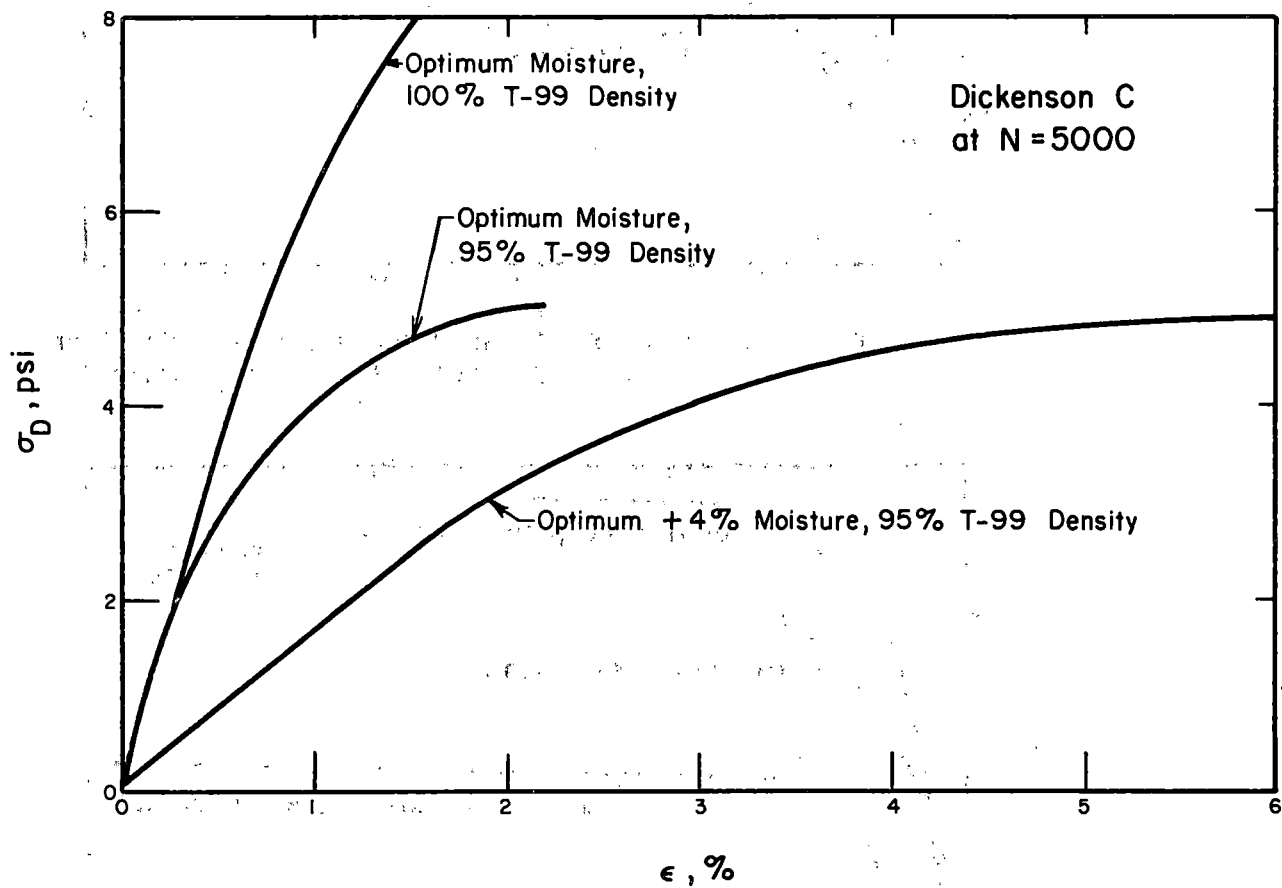


Figure 14.17. Deviator Stress-Permanent Strain Relation at 5000 load applications for Dickenson

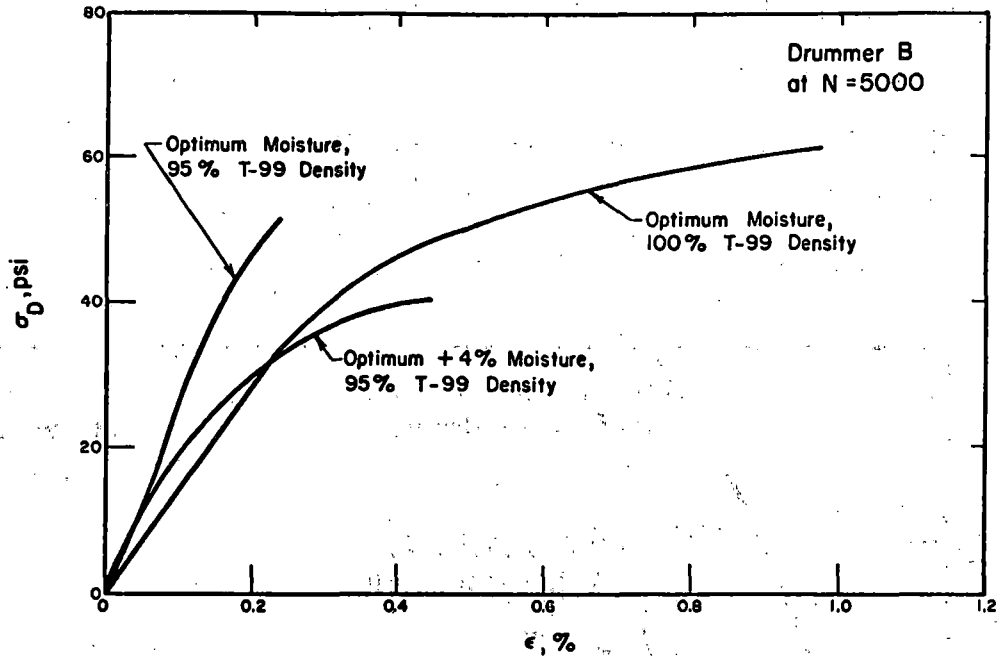


Figure 14.18. Deviator Stress-Permanent Strain Relation at 5000 load applications for Drummer B.

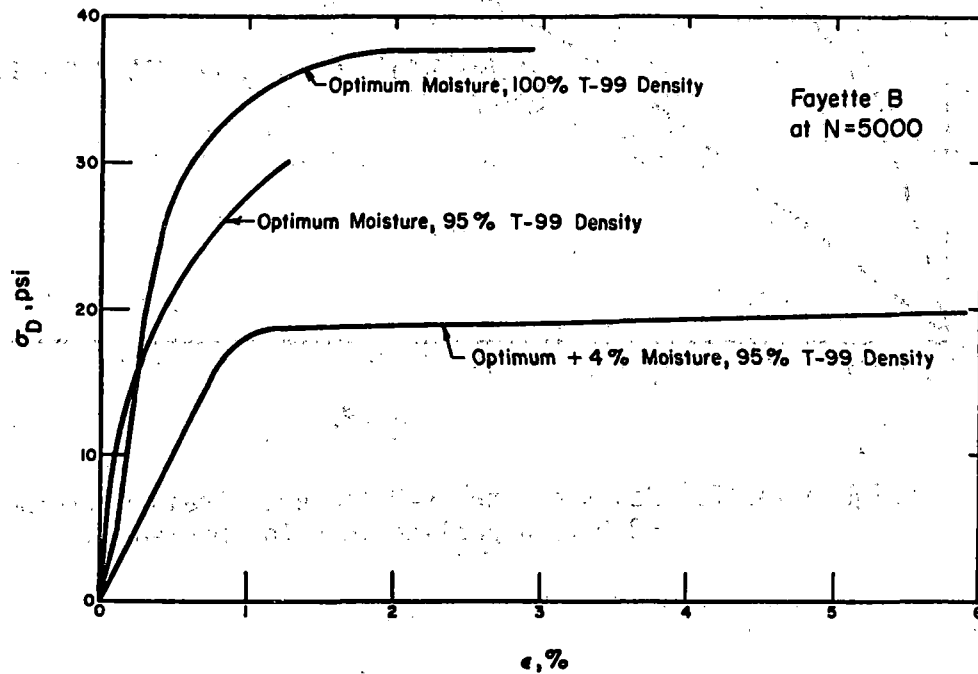


Figure 14.19. Deviator Stress-Permanent Strain Relation at 5000 load applications for Fayette B.

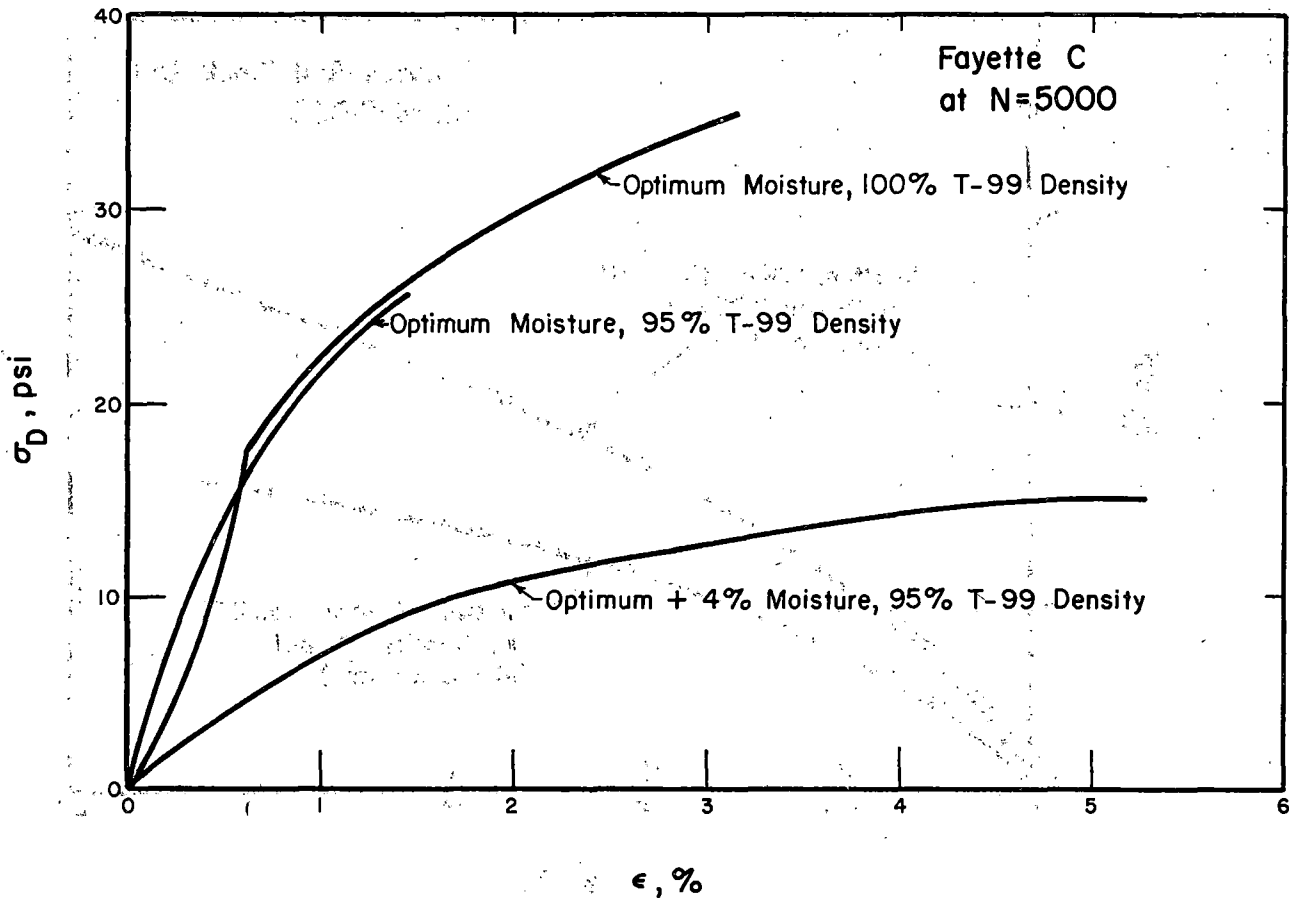


Figure 14.20. Deviator Stress-Permanent Strain Relation at 5000 load applications for Fayette C

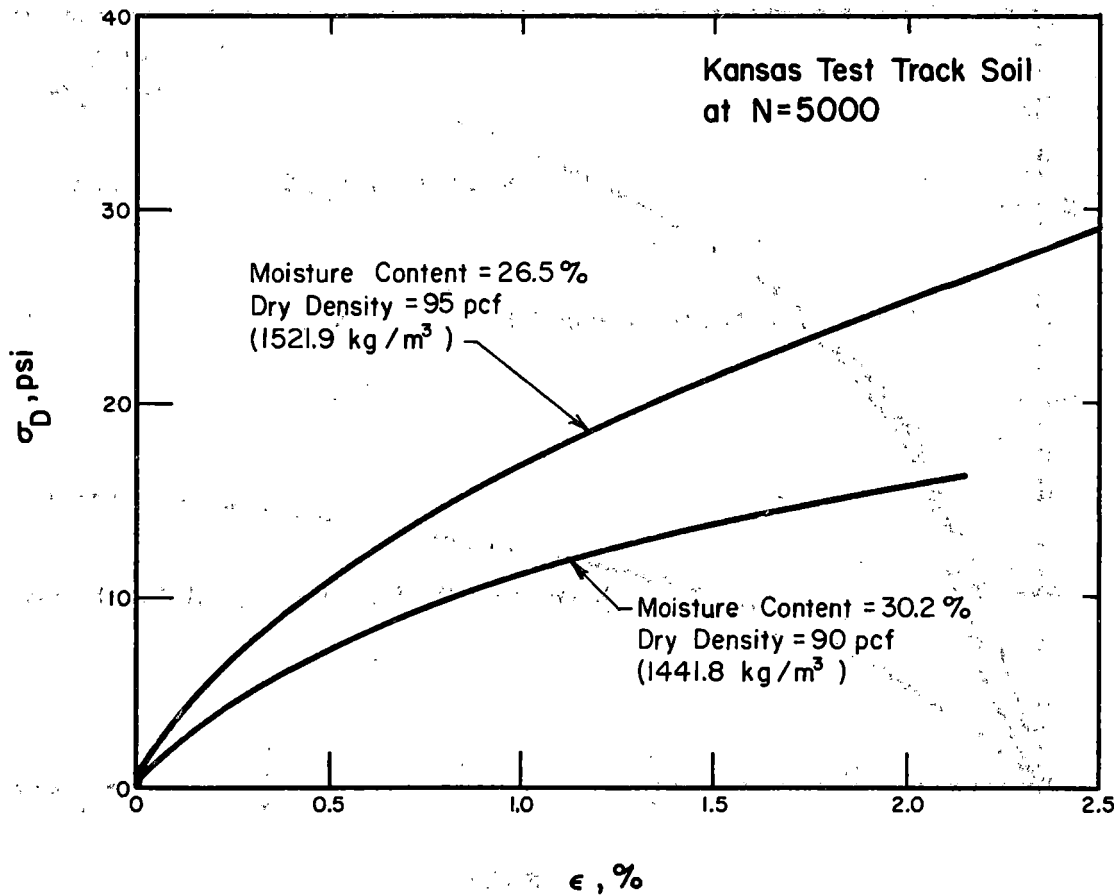


Figure 14.21. Deviator Stress-Permanent Strain Relation at 5000 load applications for the Kansas Test Track Soil

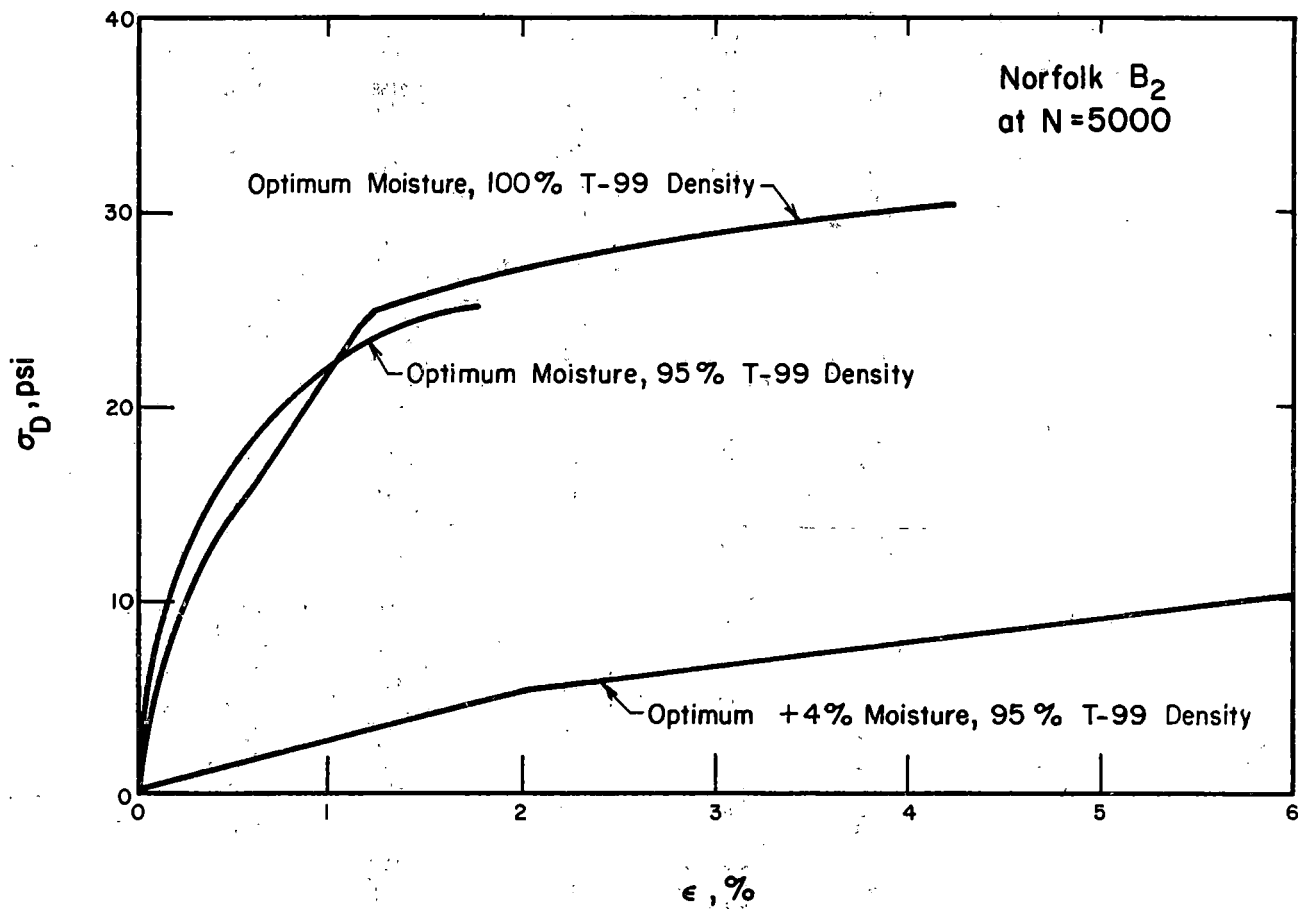


Figure 14.22. Deviator Stress-Permanent Strain Relation at 5000 load applications for Norfolk B<sub>2</sub>

Table 14.1. Permanent Strain Relations for the Soils Used.

Soil	Density % AASHTO T-99	Moisture Content	Applied Deviator Stress $\sigma_d$ , psi	Coefficient b	Coefficient A ( $\times 10^{-4}$ )	
Davidson B <sub>2</sub>	95	opt	5	0.0942	1.61	
	95	opt	15	0.1172	10.89	
	100	opt	15	0.1013	2.84	
	100	opt	25	0.1114	10.14	
	100	opt	35	0.1205	26.42	
	100	opt	40	0.2117	56.18	
	95	opt + 4%	5	0.1071	3.32	
	95	opt + 4%	15	0.0956	13.52	
	95	opt + 4%	25	0.1641	27.10	
	Dickenson C	95	opt	3	0.2796	5.81
95		opt	5	0.2363	33.57	
100		opt	5	0.2521	10.59	
100		opt	8	0.2639	18.75	
95		opt + 4%	3	0.2158	34.12	
95		opt + 4%	5	0.2734	68.08	
Drummer B		95	opt	15	0.0592	4.52
		95	opt	30	0.1038	5.28
	95	opt	50	0.0759	13.06	
	100	opt	5	0.0788	3.12	
	100	opt	15	0.0985	4.90	
	100	opt	30	0.0567	12.76	
	100	opt	50	0.0452	34.04	
	95	opt + 4%	5	0.1052	1.39	
	95	opt + 4%	15	0.2000	1.38	
	95	opt + 4%	30	0.1246	8.20	
Fayette C	95	opt	5	0.0380	10.09	
	95	opt	15	0.1222	11.19	
	95	opt	25	0.2200	21.09	
	100	opt	5	0.0873	12.42	
	100	opt	15	0.1392	18.16	
	100	opt	25	0.1348	43.65	
	100	opt	30	0.1380	70.15	
	95	opt + 4%	5	0.1617	17.02	
	95	opt + 4%	10	0.1756	42.46	
	95	opt + 4%	15	0.1726	138.04	
Fayette B	95	opt	5	0.1839	2.02	
	95	opt	15	0.1010	9.86	
	95	opt	25	0.1667	20.80	
	95	opt	30	0.1726	32.14	
	100	opt	5	0.1015	6.71	
	100	opt	15	0.1053	9.84	
	100	opt	30	0.1466	44.57	
	100	opt	40	0.2029	49.77	
	95	opt + 4%	5	0.1068	8.89	
	95	opt + 4%	15	0.1086	32.28	
Kansas Test Track Soil	90 pcf	30%	5	0.2228	5.28	
	90 pcf	30%	15	0.1346	66.28	
	95 pcf	26.5%	5	0.1503	5.34	
	95 pcf	26.5%	15	0.0963	39.73	
	95 pcf	26.5%	30	0.1273	93.43	
Norfolk B <sub>2</sub>	95	opt	5	0.0967	2.32	
	95	opt	15	0.1306	14.39	
	95	opt	20	0.1102	30.97	
	95	opt	25	0.2068	38.19	
	100	opt	5	0.1066	4.34	
	100	opt	15	0.1127	23.07	
	100	opt	25	0.1056	55.98	
	100	opt	30	0.1976	91.20	
	95	opt + 4%	5	0.1185	72.61	
	95	opt + 4%	10	0.0958	308.32	
	95	opt + 4%	15	0.0873	625.17	

This is also evident from Figures 14.9 to 14.15. The permanent deformation response of the soils is very much stress-dependent with most of the soils exhibiting pronounced increase in the rate of permanent strain with increase in deviator stress. Most of the soils (at given moisture content and density) also exhibit a "threshold stress level" which is defined as the stress level above which the permanent deformation of the soil under repeated loading is rapid and below which the rate of cumulative deformation from additional stress applications is very small.

The effect of one cycle of freeze-thaw on the accumulation of permanent deformation was also evaluated for Drummer B and is shown in Figure 14.23. It can be seen that even one cycle of freeze-thaw is sufficient to produce more detrimental response in the soil specimen as compared to the soil specimen not subjected to any freeze-thaw cycle.

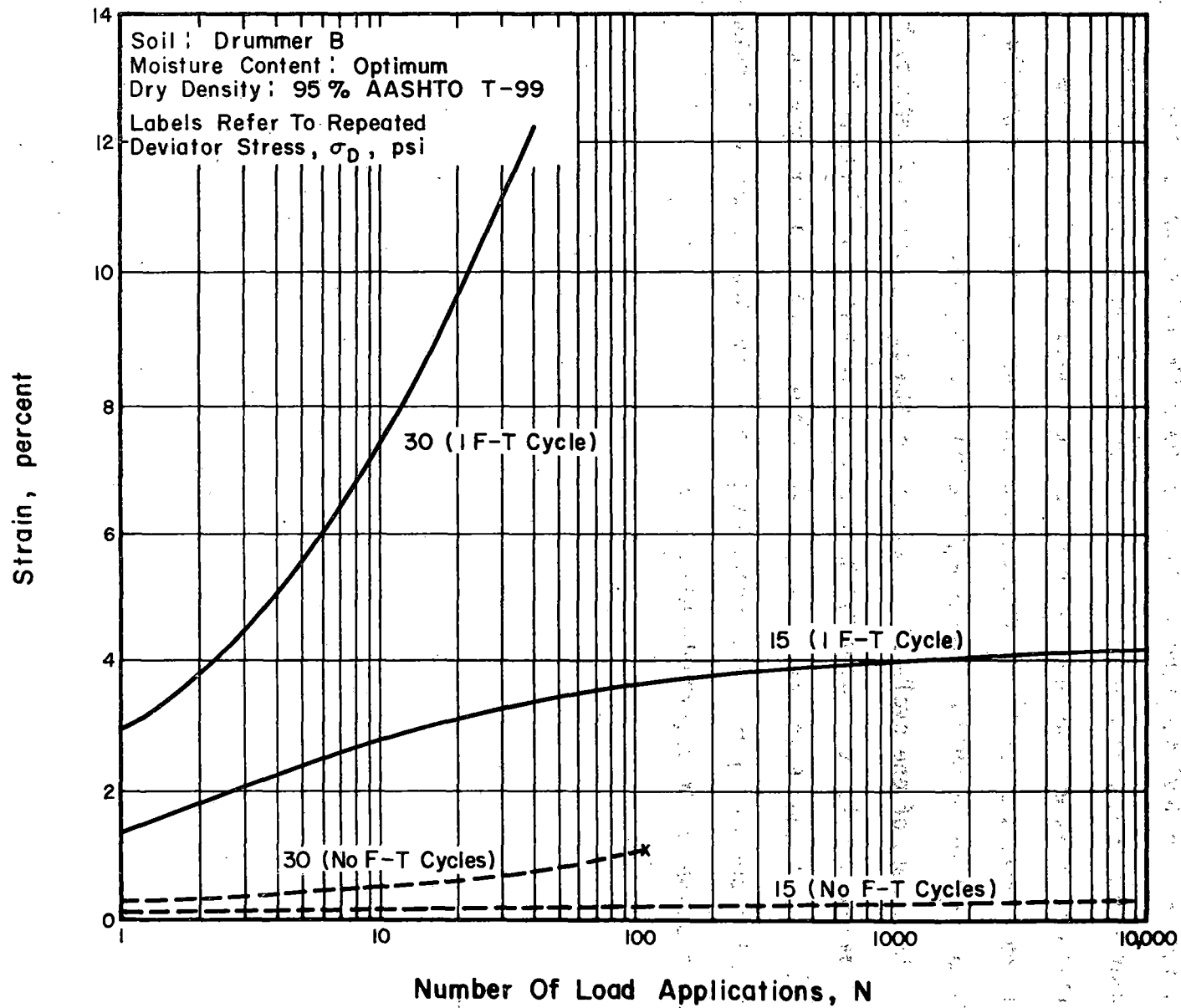


Figure 14.23. Effect of One Freeze-Thaw Cycle on Permanent Deformation for Drummer B

### 14.3 Summary and Conclusions

A number of factors were found to significantly influence the resilient behavior of the five soils included in the resilient response test program. These factors are discussed below.

#### 1. Compaction Condition

Since a single level of density (95% AASHTO T-99) was used in the test program, conclusions can not be drawn directly about the influence of density on resilient response of fine-grained soils. However, a general conclusion that can be drawn from the technical literature is that reduced density leads to greater resilience (lower resilient modulus) (78).

The effect of moisture was found to be very significant. Increasing the moisture content by only about 2 percent led to greatly reduced resilient moduli for the soils tested as shown in Figures 14.1 to 14.8. Expressing the moisture-density relations in terms of degree of saturation, it can be concluded that increasing degree of saturation of fine grained soils leads to increasing resiliency and consequently decreasing resilient moduli.

#### 2. Stress Level

The resilient response of the soils tested was determined at various stress levels and it can be seen from Figures 14.1 to 14.8 that for the soils tested, the resilient modulus is not constant but rather is influenced by the magnitude of the repeated axial stress (deviator stress).

#### 3. Soil Type

Fine-grained soils may exhibit substantially different resilient response characteristics due to inherent variations in soil properties such as plasticity, clay and silt contents, organic matter content, clay mineralogy, etc.

The factors that significantly influenced the permanent deformation test results of the seven soils tested are summarized below.

### 1. Compaction Condition

For most of the seven soils tested, increased moisture content and reduced density led to increased accumulation of permanent strain with increasing number of load applications. Thus specimens compacted at 100 percent AASHTO T-99 density gave better response under repeated loading than those compacted at 95 percent AASHTO T-99 density and specimens compacted at optimum moisture content (95% T-99 density) gave better response than those specimens compacted at optimum plus 4 percent moisture content (95% T-99 density). This is clearly evident from Figures 14.16 to 14.22 which show the permanent strain at the end of 5000 load applications.

Thus, under actual field conditions a soil with a high degree of saturation can be expected to settle very much, accelerating the development of poor track conditions.

### 2. Stress Level

As mentioned previously, the permanent deformation response of the soils tested is stress-dependent with most of the soils exhibiting pronounced increase in the rate of permanent strain with increase in deviator stress. Most of the soils also exhibit a "threshold stress level" which is defined as the stress level above which the permanent deformation of the soils under repeated loading is rapid and below which the rate of cumulative deformation from additional stress applications is very small.

### 3. Freeze-Thaw Effects

Although the effect of freeze-thaw on the accumulation of permanent deformation is presented for only one soil, previous works (80, 81) have also established the detrimental effects of freeze-thaw on soils. Thus, it can be concluded that even one cycle of freeze-thaw is sufficient to greatly reduce the resistance to permanent deformation.

PART D  
CHAPTER 15

TEMPERATURE REGIME CHARACTERIZATION

15.1 Introduction

Environmental exposure conditions have a substantial effect on the instantaneous behavior of the conventional railway track support system (CRTSS), as well as on the long term behavior and performance. The nature of the ballast and subgrade materials and the track support system geometry make the materials sensitive to certain environmental exposure conditions. The environmental factors of significance are temperature and moisture. Certain aspects of the temperature conditions such as freeze-thaw and frost heave are important not only in terms of design of the track support system but also in terms of material quality and property evaluation. The moisture regime that exists in the track support system is also an important consideration. Factors such as precipitation, water table position, permeability of ballast and subgrade materials, and local drainage conditions have an influence on the moisture regime of the system.

Improved CRTSS analysis and design procedures require the quantification of moisture regimes in the track support system both as a function of time and of space.

This part of the report describes investigations made to characterize the temperature regime in a typical track section at two geographical locations: Chicago, Illinois, and Springfield, Illinois. The characterization was made by using a one-dimensional, forward-finite-difference heat-transfer computer model developed by Dempsey (57). The computer model output can be presented as temperature-depth profiles in multi-layer systems.

15.2 Description of the Heat Transfer Model

In general, the program performs the following functions:

1. Reads in climatic data which does not change from year to year for a station,
2. Reads in the daily climatic record,
3. Computes radiation quantity, air temperature and convection coefficient,
4. Calculates the temperature profile in the multi-layer section being analyzed, and
5. Calculates the depth of frost penetration.

The validity of the heat-transfer model has been established in previous studies (57) by comparing predicted temperatures with temperature data from laboratory studies and from the AASHO Road Test at Ottawa, Illinois. Excellent comparisons between theoretical temperatures and measured temperatures indicated that the assumptions, idealizations, and approximations made during the development of the heat-transfer model were valid for predicting temperature profiles for use in studies of multi-layer pavement systems.

A detailed presentation of the development, validation, and utilization of the heat-transfer model can be found in References 57, 58, and 59.

### 15.3. Input Parameters Required for the Heat Transfer Model

The input parameters required for the computer modelling can be divided into two major categories: extrinsic and intrinsic factors.

Among the extrinsic factors, load and climate are the most important.

For this investigation only climatic factors were considered. Climatic factors can be subdivided as follows:

#### 1. Temperature factors

##### a. Air temperature

##### b. Short wave radiation received at the earth's surface

- c. Long wave radiation emitted at the earth's surface
- d. Wind

## 2. Hydraulic factors

- a. Precipitation
- b. Evaporation
- c. Condensation

## 3. Geographical factors

- a. Altitude
- b. Latitude
- c. Degree of Exposure
- d. Nearness of bodies of water

The importance of the above factors has been discussed in detail by Dempsey (57).

Much of this climatic information can be easily acquired. The National Climatic Center, currently located in Asheville, North Carolina, compiles daily climatic data for each of its nationwide weather stations. A typical First Order ESSA (Environmental Sciences Services Association) Weather Bureau daily climatic data card is described in Table 15.1. Information used as input to the heat transfer model includes the station number, date, maximum and minimum daily temperatures, average daily wind velocity, and percent sunshine.

The amount of short wave radiation received at the earth's surface and the amount of long wave radiation emitted at the earth's surface are also necessary input data to the heat transfer model. Methods for obtaining these data are discussed extensively by Dempsey (57).

The intrinsic factors which influence frost action are shown in Figure 15.1. The most important factors are thermal conductivity, heat capacity,

Table 15.1. Description of Climatic Data Card for a First Order ESSA Weather Bureau Station (Reference 57).

<u>Columns</u>	<u>Category</u>										
1 - 5*	Station No.										
6 - 7*	Year										
8 - 9*	Month										
10 - 11*	Day										
12 - 14*	Maximum temperature, F										
15 - 17*	Minimum temperature, F										
18 - 21	Precipitation - midnight to midnight										
22 - 24	Snowfall - midnight to midnight										
25 - 27	Snow depth at 1900 (to be decided on according to records)										
28 - 31	Sea level pressure in a.m. (4 columns - 0630 approx.)										
32 - 35	Sea level pressure in p.m. (4 columns - 1830 approx.)										
36 - 38	Relative humidity at 0630 or 0700										
39 - 40	Relative humidity at 1200 or 1230 (at 1900 from 1901-1915 at SPI)										
41 - 50	Days with the following: <table border="0" style="margin-left: 40px;"> <tr> <td>41 Fog</td> <td>46 Snow</td> </tr> <tr> <td>42 Thunder</td> <td>47 Glaze</td> </tr> <tr> <td>43 Sleet</td> <td>48 Dust Storm</td> </tr> <tr> <td>44 Hail</td> <td>49 Smoke or Haze</td> </tr> <tr> <td>45 Rain</td> <td>50 Blowing Snow</td> </tr> </table>	41 Fog	46 Snow	42 Thunder	47 Glaze	43 Sleet	48 Dust Storm	44 Hail	49 Smoke or Haze	45 Rain	50 Blowing Snow
41 Fog	46 Snow										
42 Thunder	47 Glaze										
43 Sleet	48 Dust Storm										
44 Hail	49 Smoke or Haze										
45 Rain	50 Blowing Snow										
51 - 62	Blank (ice, frozen and river gage headings)										
63	Blank										
64 - 65	Daily prevailing wind direction (to 8 directions) use second number if more than one listed										
66 - 68*	Average daily wind velocity in tenths										
69 - 71*	Percent of possible sunshine										
72 - 74	Mean daily temperature (machine calculated)										
75 - 77	Number of hours of sunshine in tenths										
78 - 79	Degree days - computed from daily mean (65 F - daily mean) (machine calculated)										

\* Data required in heat-transfer model

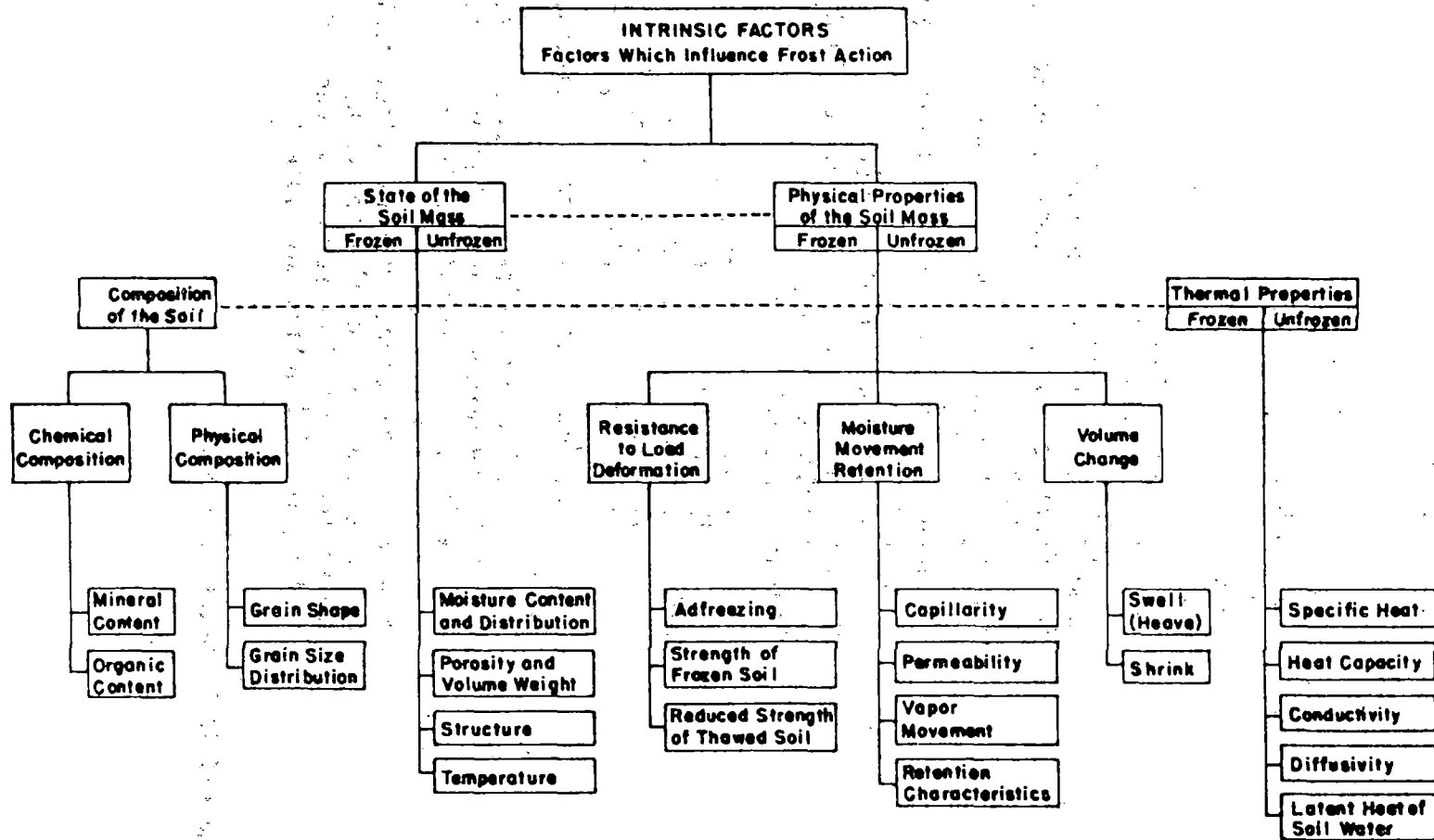


Figure 15.1. Intrinsic Factors Which Influence Frost Action (Reference 57).

and latent heat of fusion. The thermal conductivity,  $K$ , is the quantity of heat which flows normally across a surface of unit area per unit time under a unit thermal gradient and has the units of  $\text{Btu/ft-hr-}^{\circ}\text{F}$  ( $\text{Cal/m-hr-}^{\circ}\text{C}$ ). The heat capacity,  $C$ , is the amount of thermal energy necessary to cause a one degree temperature change in a unit mass of substance and has the units  $\text{Btu/lb-}^{\circ}\text{F}$  ( $\text{Cal/kg-}^{\circ}\text{C}$ ). The latent heat of fusion,  $L$ , is the change in thermal energy in a unit volume of material when the moisture in that material freezes or thaws at a constant temperature. It has the units of  $\text{Btu/ft}^3$  ( $\text{Cal/m}^3$ ).

#### 15.4 Limitations of the Heat Transfer Model

Because the heat transfer model was developed to evaluate the frost action and temperature related effects in multi-layered pavement systems, some of the idealizations, assumptions and approximations made during its development may not pertain to a ballast-subgrade system. The most noticeable deficiency in the heat transfer model as it relates to a ballast-subgrade system is that it does not adequately account for the hydraulic factors, the most important of which is precipitation. The hydraulic factors were ignored in the initial development of the heat transfer model because in general it is assumed that properly constructed pavements prevent the infiltration of surface water (57). Turner and Jumikis (60), Kubler (61), and Moulton and Dabbe (62) have all established that there is a general tendency for the soil moisture content to vary with the seasons; the highest value occurs during the months of spring thaw. Alkinson and Bay (63) found that rainfall during the spring increased the thawing rate in a soil and Franklin (64) found that percolating water can cause rapid changes in soil temperature.

A second shortcoming of the model is that it does not account for the presence of snow cover. The effect of snow cover is difficult to analyze and predict. Snow cover acts as an insulating layer which retards frost penetration during cold periods and retains it during the thawing period. Kubler (61) has found that the depth of frost penetration increases with increasing depths of snow cover.

These shortcomings may all have a significant effect on the characterization of temperature regimes in a ballast-subgrade system. If the effects of variable water contents, percolating water, and snow cover become better understood it will be possible to incorporate them into the heat transfer model to provide a more accurate and representative characterization of temperature regimes in the ballast-subgrade sections.

#### 15.5 Evaluation of the Thermal Properties of Subgrade and Ballast

For the purposes of this investigation an idealized track support system was selected. The idealized section consists of 12 inches (30 cm) of limestone ballast (AREA Gradation No. 4) overlying an A-6 (AASHTO Classification) subgrade soil. Rails and ties were not considered in this study.

In recent years, numerous investigators have performed extensive laboratory and field studies concerning the thermal properties of soils. The most comprehensive treatment of the thermal conductivity of soils was presented by Kersten (65). In his investigation Kersten analyzed the effects of moisture content, mineralogical composition, soil texture, density, and temperature on soil thermal conductivity. Kersten found that the thermal conductivity of a soil generally increased with increasing water content, increasing quartz quality content, increasing particle angularity, and increasing dry density. Kersten also observed that

thermal conductivities increased with increasing soil temperatures in the 40-70°F (4.4 - 21.1°C) range, and that little change in thermal conductivity with temperature was noted in soils at temperatures well below the freezing point.

As a result of this investigation, Kersten developed empirical equations to predict the thermal conductivity of a soil based on soil type, moisture content and dry density. The equations for unfrozen and frozen soil conditions were considered to be accurate within 25 percent. The equations for the unfrozen and frozen conditions, respectively are as follows:

1. For fine grained soil ( $D_{50} \leq 0.074$  mm)

$$\text{Unfrozen: } K_u = \frac{(0.9 \log w - 0.2)10^{0.01\gamma}}{12} \quad (15.1)$$

$$\text{Frozen: } K_i = \frac{0.01(10)^{0.002\gamma} + 0.085w(10)^{0.008\gamma}}{12} \quad (15.2)$$

2. For coarse grained soils ( $D_{50} \geq 0.074$  mm)

$$\text{Unfrozen: } K_u = \frac{(0.7 \log w + 0.4)10^{0.01\gamma}}{12} \quad (15.3)$$

$$\text{Frozen: } K_i = \frac{0.076(10)^{0.013\gamma} + 0.032w(10)^{0.0146\gamma}}{12} \quad (15.4)$$

where  $K_u$  = unfrozen thermal conductivity (Btu/ft-hr-°F)

$K_i$  = frozen thermal conductivity (Btu/ft-hr-°F)

w = water content (percent)

$\gamma$  = dry density (lbs/ft<sup>3</sup>)

$D_{50}$  = particle diameter at 50% passing

For the freezing soil, the thermal conductivity,  $K_f$ , is taken as the average of the unfrozen and frozen thermal conductivities,

$$K_f = \frac{K_u + K_i}{2} \quad (15.5)$$

Additional methods for calculating the thermal conductivity of heterogeneous materials based on a variety of assumptions and simplifications have been presented in References 66, 67, 68, 69, 70, 71, and 72. It has been reported by Johansen (72) that when the thermal conductivities of the components do not differ by more than an order of magnitude, the simple geometric mean equation is satisfactory for computing the thermal conductivity of a saturated soil. The geometric mean equation is:

$$\lambda_c = \lambda_2^n \cdot \lambda_1 (1-n) \quad (15.6)$$

where  $\lambda_c$  = thermal conductivity of a 2 phase component system  
 $\lambda_2$  = thermal conductivity of the solid phase  
 $\lambda_1$  = thermal conductivity of the pore fluid phase  
 $n$  = volumetric fraction of the solid phase

Horai (73) has investigated the thermal conductivity of rock forming minerals. Some of his results are presented in Table 15.2.

Many of the previously mentioned methods or equations may be satisfactorily used to calculate the thermal conductivity of saturated subgrade soil. However, extrapolation of these equations to the computation of thermal conductivities for ballast materials must be carefully analyzed. Johansen (72) states that in rock masses the change in pore fluid from water to air leads to a thermal conductivity ratio,  $\lambda_2/\lambda_1$ , between 100 and 300. Johansen (72) also states that at large ratios of  $\lambda_2/\lambda_1$  (greater than 10), the influence of the microgeometry makes it impossible to predict thermal conductivity of cored rock samples with acceptable accuracy. In such cases only experimental studies can give an adequate degree of accuracy.

This problem is compounded when considering ballast or large sized crushed rock. For porosities on the order of 40-80 percent, air convection and heat radiation begin to play important roles as heat transfer mechanisms.

Table 15.2. Thermal Conductivity of Some Rock Forming Minerals (Reference 73).

MINERAL	AVERAGE K			VARIATION IN K		
	w/m-°C	Cal/m-hr-°C	Btu/ft-hr-°F	w/m-°C	Cal/m-hr-°C	Btu/ft-hr-°F
Quartz	7.7	110.3	4.45	—	—	—
Feldspars						
Orthoclase	2.0	28.7	1.16	1.7-2.3	24.3-33.0	0.98-1.33
Plagioclase						
Albite	2.2	31.5	1.27	1.9-2.3	27.3-33.0	1.10-1.33
Anorthite	1.7	24.3	0.98	—	—	—
Micas						
Muscovite	2.3	32.9	1.33	2.2-2.5	31.5-35.9	1.27-1.45
Phlogopite	2.1	30.0	1.21	1.9-2.3	27.3-33.0	1.10-1.33
Biotite	2.0	28.7	1.16	1.7-2.3	24.3-33.0	0.98-1.33
Pyroxenes	4.3	61.7	2.49	3.8-5.0	54.5-71.6	2.20-2.89
Amphibol	3.5	50.0	2.02	2.5-5.0	35.9-71.6	1.45-2.89
Olivine	4.5	64.4	2.6	3.0-5.0	42.9-71.6	1.73-2.89
Calcite	3.6	51.5	2.08	—	—	—

Only limited information is available regarding the thermal conductivity of large size crushed materials. Vanpelt (74) has presented thermal conductivity data for six crushed stone aggregates in a study which examined the feasibility of using crushed stone in pipe insulation systems. Vanpelt's investigation (74) considered two different types of aggregate, a crushed granitic gneiss and a gravel material consisting mostly of river deposited quartz stone. The gradations of the aggregate tested are shown in Table 15.3. The results of the investigation are summarized in Table 15.4. For the 1 1/2 inch (38 mm) gravel and crushed stone the thermal conductivity varied between 0.2 Btu/ft-hr-<sup>0</sup>F (4.96 Cal/hr-m-<sup>0</sup>C) to 0.3 Btu/ft-hr-<sup>0</sup>F (7.44 Cal/hr-m-<sup>0</sup>C) while the general range for all the materials tested was only 0.166 Btu/ft-hr-<sup>0</sup>F (4.14 Cal/hr-m-<sup>0</sup>C) to 0.3 Btu/ft-hr-<sup>0</sup>F (7.44 Cal/hr-m-<sup>0</sup>C) over the 50 to 80 <sup>0</sup>F (10 to 26.7 <sup>0</sup>C) average mean temperature range.

Calculations of ballast thermal conductivities were attempted using Kersten's equations (15.3 and 15.4), the geometric mean equation (15.6) and Kersten's equations with the w term neglected. With Kersten's equations the values used for  $\gamma$  and w were consistent with the ballast type selected and for the geometric mean equation, values used for  $\lambda_2$  (calcite) and  $\lambda_1$  (air) were based on Horai's recommendations (73). The volumetric fraction of these constituents were determined by a weight-volume analysis of the ballast consistent with the ballast type selected. The results of these calculations are shown in Table 15.5.

As can be seen from Table 15.5, the geometric mean equation and Kersten's equations with the w term neglected predict conductivity values very close to those presented by Vanpelt (74). Kersten's equations with w of 2.2 percent give conductivity values slightly higher than those presented by Vanpelt. Based on these calculations and the work done by Vanpelt,

Table 15.3. GRAIN SIZES OF THE SORTED AGGREGATES (REFERENCE 74)  
(Percent Retained by Weight)

Material	1 1/2"	1"	3/4"	Sieve Sizes		No. 4	Finer Than No. 4
				1/2"	3/8"		
1 1/2" Gravel	12	65	17	3	2	<1	<1
3/4" Gravel		0	7	60	19	11	3
3/8" Gravel				0	<1	68	31
1 1/2" Crushed Stone	3	64	25	7	<1	<1	<1
3/4" Crushed Stone		0	6	71	18	4	1
3/8" Crushed Stone				0	1	69	30

TABLE 15.4 THERMAL CONDUCTIVITY RESULTS OF SIX STONE AGGREGATE SAMPLES (Reference 74).

Material	Dry Density pcf	Void Ratio	Specific Gravity	Heat Flow Direction	$\Delta T$ °F	Average Mean Test Temp °F	Sample Heat Flow (Btu/hrft <sup>2</sup> )	K (Btu/ft-hr-°F)
3/8" Gravel	104.8	.63	2.73	Down	9.5	55.9	3.75	0.218
				Down	24.6	61.5	9.96	0.223
				Down	49.0	75.6	20.49	0.23
	105.3	.62	2.73	Up	10.9	54.6	4.63	0.241
				Up	27.0	63.8	11.91	0.24
				Up	49.1	74.9	21.29	0.237
3/8" Crushed Stone	106.0	.73	2.94	Down	10.5	54.8	3.27	0.173
				Down	49.1	75.4	16.83	0.189
	106.0	.73	2.94	Up	9.4	54.2	3.36	0.197
				Up	24.3	61.6	8.94	0.203
				Up	50.4	75.0	18.05	0.198
				Up	50.4	75.0	18.05	0.198
3/4" Gravel	103.4	.70	2.77	Down	9.7	54.1	4.60	0.232
				Down	50.8	74.6	22.87	0.236
				Up	9.7	54.5	4.96	0.26
	103.2	.68	2.77	Up	25.6	62.3	12.09	0.248
				Up	51.4	73.9	23.52	0.241
				Up	51.4	73.9	23.52	0.241
3/4" Crushed Stone	105.6	.71	2.89	Down	10.0	54.5	3.51	0.184
				Down	47.8	73.4	20.16	0.220
	105.6	.71	2.89	Up	11.6	55.4	5.31	0.237
				Up	25.6	62.2	10.91	0.223
				Up	49.9	74.0	20.60	0.216
				Up	49.9	74.0	20.60	0.216
1 1/2" Gravel	105.9	.60	2.71	Down	10.4	53.5	5.22	0.268
				Down	47.6	73.9	24.48	0.274
	106.6	.59	2.71	Up	11.3	53.9	6.44	0.30
				Up	25.0	61.5	14.03	0.297
				Up	48.9	74.6	26.52	0.287
				Up	48.9	74.6	26.52	0.287
1 1/2" Crushed Stone	102.6	.77	2.91	Down	10.3	54.3	4.21	0.216
				Down	49.9	75.0	21.65	0.229
	103.3	.76	2.91	Up	10.7	54.8	4.37	0.213
				Up	25.4	63.5	10.14	0.209
				Up	49.1	74.1	19.58	0.209
				Up	49.1	74.1	19.58	0.209

Table 15.5. Results of Ballast Thermal Conductivity Calculations.

	Kersten's Equations (Reference 57)		Geometric Mean Equation (Reference 71)		Kersten's Equation neglecting the w%	
	Btu/ft-hr-°F	Cal/m-hr-°C	Btu/ft-hr-°F	Cal/m-hr-°C	Btu/ft-hr-°F	Cal/m-hr-°C
$K_u$	.486	12.0	.265	6.57	.304	7.53
$K_f$	.373	9.24	.262	6.49	.208	5.15
$K_i$	.26	6.44	.259	6.42	.112	2.77

thermal conductivity values for the unfrozen freezing and frozen ballast conditions in the range of 0.26 Btu/ft-hr-<sup>0</sup>F (6.42 Cal/hr-m-<sup>0</sup>C) were selected as input values to the heat transfer model.

Thermal conductivity values for the subgrade were calculated from Kersten's equations (15.1 and 15.2) based on a unit weight of 128.7 lb/ft<sup>3</sup> (2062 Kg/m<sup>3</sup>) and a water content of 17.0 percent. These values were 0.92 (22.8 Cal/hr-m-<sup>0</sup>C) and 1.13 (28.0 Cal/hr-m-<sup>0</sup>C) for the unfrozen and frozen conditions respectively.

In addition to the thermal conductivity equations, Kersten (65) developed equations to compute the thermal heat capacity of a soil water mixture. These equations are as follows for the unfrozen and frozen soil respectively:

$$C_u = \frac{100 C_m + 1.0 w}{100 + w} \quad (15.7)$$

$$C_i = \frac{100 C_m + 0.5 w}{100 + w} \quad (15.8)$$

where  $C_u$  = unfrozen heat capacity (Btu/lb-<sup>0</sup>F)  
 $C_i$  = frozen heat capacity (Btu/lb-<sup>0</sup>F)  
 $C_m$  = a constant (Btu/lb-<sup>0</sup>F)  
 $w$  = water content (percent)

Similar equations were developed by Jumikis (75) and Aldrich (76). Kersten (65) has indicated that a value of  $C_m$  of 0.17 Btu/lb-<sup>0</sup>F represents an average for most soils at temperatures near the freezing point. Kersten has been supported in this view by Aldrich (76). Jumikis (75) and Johnson (76) have concluded however that the thermal heat capacity of dry soil, minerals, and rocks vary within narrow limits and that a value of  $C_m$  of 0.20 Btu/lb-<sup>0</sup>F (0.20 Cal/kg-<sup>0</sup>C) is a good average value. In view of the extensiveness of Kersten's investigations a value of  $C_m$  of 0.17 Btu/lb-<sup>0</sup>F

(0.17 Cal/Kg-<sup>0</sup>C) was selected for this study. This leads to thermal heat capacities for the unfrozen and frozen conditions of 0.188 Btu/lb-<sup>0</sup>F (0.188 Cal/kg-<sup>0</sup>C) and 0.177 Btu/lb-<sup>0</sup>F (0.177 Cal/kg-<sup>0</sup>C) respectively, for the ballast, and 0.29 Btu/lb-<sup>0</sup>F (0.29 Cal/kg-<sup>0</sup>C) and 0.22 Btu/lb-<sup>0</sup>F (0.22 Cal/kg-<sup>0</sup>C) respectively, for the subgrade. Kersten also concluded that factors such as density, particle size and shape, and mineralogical composition have little if any effect on the heat capacity of soils and that the heat capacities for most base, subbase, and subgrade materials are approximately equal.

The latent heat of fusion becomes important when determining the heat capacity of a material during freezing. During freezing, water gives off heat energy known as the latent heat of fusion. This process creates a lag in temperature changes with time which retards the rate of frost penetration. The latent heat effect was incorporated into the heat transfer model by making use of a freezing zone from 32<sup>0</sup>F to 30<sup>0</sup>F (0<sup>0</sup>C to -1.1<sup>0</sup>C). The thermal heat capacity,  $C_f$ , of a material in this zone can be calculated, according to Dempsey (57), by the equation:

$$C_f = \frac{100(w)\gamma^d}{200 \gamma} \quad (15.9)$$

where  $C_f$  = freezing heat capacity (Btu/lb-<sup>0</sup>F)

$\gamma$  = unit weight (lbs/ft<sup>3</sup>)

$\gamma^d$  = dry density (lbs/ft<sup>3</sup>)

w = water content (percent)

This equation yields values of freezing heat capacities of 1.55 Btu/lb-<sup>0</sup>F (1.55 Cal/kg-<sup>0</sup>C) and 10.49 Btu/lb-<sup>0</sup>F (10.49 Cal/kg-<sup>0</sup>C) for the limestone ballast and A-6 subgrade respectively. It should be noted that even at water contents as small as 2.2 percent, the values of these freezing heat capacities are much larger than those for the unfrozen and the frozen conditions.

## CHAPTER 16

## TEMPERATURE REGIME EVALUATION

## 16.1 Initial Analysis

To obtain a sufficiently extensive and accurate characterization of the temperature regime at a particular geographical location a 20 year period of record was analyzed. Two Illinois locations were selected: Chicago and Springfield. Climatic data for the two locations were obtained from the Illinois State Water Survey. A period of record from 1928-1947 was selected. For Chicago, Illinois, a period of seven months per year (October through April) was analyzed. For Springfield, Illinois, the period was reduced to six months (October through March). The values of the intrinsic factors for ballast and subgrade used in the analyses were discussed in Section 15.5 and are summarized in Figure 16.1.

Output parameters considered were:

1. Monthly average mean temperature
2. Monthly average mean temperature above freezing
3. Monthly average mean temperature below freezing and
4. Average number of freeze-thaw cycles per month.

Temperature outputs were generated for the ballast surface and the ballast-subgrade interface. Freeze-thaw cycle data were generated for the ballast surface, the mid-depth of the ballast, the ballast-subgrade interface, and 2 in. (51 mm) below the subgrade surface.

Results of the preliminary analysis are presented in Table 16.1 for the 20-year period of record considered.

The most noticeable observation which can be made from examining and analyzing the data in Table 16.1 is that the characterization does not

Ballast

Depth = 12.0" (30.5)

$\gamma = 98.1 \text{ lbs/ft}^3 \text{ (1571 kg/m}^3\text{)}$

$\gamma_d = 96.0 \text{ lbs/ft}^3 \text{ (1538 kg/m}^3\text{)}$

w% = 2.2%

$K_u = .265 \text{ Btu/ft-hr-}^\circ\text{F (6.57 Cal/m-hr-}^\circ\text{C)}$

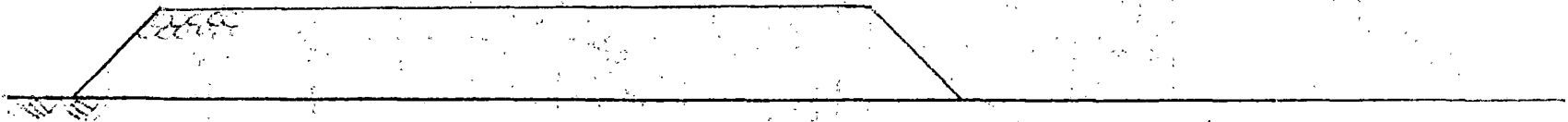
$K_f = .262 \text{ Btu/ft-hr-}^\circ\text{C (6.49 Cal/m-hr-}^\circ\text{C)}$

$K_i = .259 \text{ Btu/ft-hr-}^\circ\text{F (6.42 Cal/m-hr-}^\circ\text{C)}$

$C_u = 0.188 \text{ Btu/lb-}^\circ\text{F (0.188 Cal/kg-}^\circ\text{C)}$

$C_f = 1.55 \text{ Btu/lb-}^\circ\text{F (1.55 Cal/kg-}^\circ\text{C)}$

$C_i = 0.177 \text{ Btu/lb-}^\circ\text{F (0.177 Cal/kg-}^\circ\text{C)}$



Subgrade

Depth = 132.0" (3.35 m)

$\gamma = 128.7 \text{ lbs/ft}^3 \text{ (2062 kg/m}^3\text{)}$

w% = 17.0%

$K_u = 0.92 \text{ Btu/ft-hr-}^\circ\text{F (22.8 Cal/m-hr-}^\circ\text{C)}$

$K_f = 1.02 \text{ Btu/ft-hr-}^\circ\text{F (25.3 Cal/m-hr-}^\circ\text{C)}$

$K_i = 1.13 \text{ Btu/ft-hr-}^\circ\text{F (28.0 Cal/m-hr-}^\circ\text{C)}$

$C_u = 0.29 \text{ Btu/lb-}^\circ\text{F (0.29 Cal/kg-}^\circ\text{C)}$

$C_f = 10.49 \text{ Btu/lb-}^\circ\text{F (10.49 Cal/kg-}^\circ\text{C)}$

$C_i = 0.22 \text{ Btu/lb-}^\circ\text{F (0.22 Cal/kg-}^\circ\text{C)}$

Figure 16.1. Material Properties for Idealized Ballast-Subgrade System.

Table 16.1. Initial Results of Temperature Regime Evaluation.

Station Location	October			November			December			January			February			March			April			Year		
	Ave. $\sigma^{(a)}$	$V_{, \%}^{(b)}$		Ave. $\sigma^{(a)}$	$V_{, \%}^{(b)}$		Ave. $\sigma^{(a)}$	$V_{, \%}^{(b)}$		Ave. $\sigma^{(a)}$	$V_{, \%}^{(b)}$		Ave. $\sigma^{(a)}$	$V_{, \%}^{(b)}$		Ave. $\sigma^{(a)}$	$V_{, \%}^{(b)}$		Ave. $\sigma^{(a)}$	$V_{, \%}^{(b)}$		Ave. $\sigma^{(a)}$	$V_{, \%}^{(b)}$	
<b>AVERAGE MEAN TEMPERATURE</b>																								
<b>Springfield</b>																								
Node 1	70.2	22.0	31.4	51.5	17.3	33.7	39.7	14.6	37.1	36.6	15.6	44.1	41.5	18.0	44.2	53.7	21.3	39.9	—	—	—	49.0	22.0	45.0
Node 7	62.3	2.45	3.93	54.2	3.69	6.84	45.1	2.91	6.51	40.71	2.49	6.21	40.8	2.33	5.71	46.9	3.47	7.36	—	—	—	48.4	8.53	17.7
<b>Chicago</b>																								
Node 1	66.3	20.3	30.6	48.9	16.1	33.0	36.4	13.6	39.0	33.6	14.4	44.2	37.0	16.4	45.5	48.8	19.6	40.3	61.7	22.6	36.7	47.6	21.8	45.9
Node 7	60.5	2.53	4.19	52.2	3.55	6.82	42.8	2.95	6.96	38.5	2.22	5.82	38.0	1.96	5.12	43.4	3.23	7.39	52.0	3.38	6.50	46.9	8.52	18.2
<b>AVERAGE MEAN TEMPERATURE ABOVE FREEZING</b>																								
<b>Springfield</b>																								
Node 1	70.2	22.0	31.4	53.5	16.2	30.2	45.4	11.3	24.8	44.5	10.8	24.2	48.7	14.6	29.8	56.7	20.0	35.2	—	—	—	54.4	19.4	35.6
Node 7	62.3	2.45	3.93	54.2	3.69	6.84	45.1	2.91	6.51	40.7	2.49	6.21	40.8	2.33	5.71	46.9	3.47	7.36	—	—	—	48.4	8.53	17.7
<b>Chicago</b>																								
Node 1	66.4	20.2	30.5	51.5	14.6	28.4	42.6	9.51	22.1	41.9	8.94	21.1	46.1	11.7	25.3	53.1	17.8	33.5	62.0	22.5	36.3	53.5	19.0	35.5
Node 7	60.5	2.53	4.19	52.2	3.55	6.82	42.8	2.95	6.96	38.5	2.22	5.82	38.0	1.95	5.10	43.4	3.23	7.39	52.0	3.38	6.50	46.9	8.52	18.2
<b>AVERAGE MEAN TEMPERATURE BELOW FREEZING</b>																								
<b>Springfield</b>																								
Node 1	None	None	None	23.4	3.06	14.2	20.8	6.24	31.4	18.6	7.58	45.1	19.9	6.02	33.8	23.5	3.80	18.3	—	—	—	19.8	7.35	38.5
Node 7	None	None	None	None	None	None	None	None	None	None	None	None	None	None	None	None	None	None	—	—	—	None	None	None
<b>Chicago</b>																								
Node 1	28.41	0.71	2.64	13.51	3.67	17.2	19.6	7.08	38.2	18.4	8.32	48.9	19.5	7.06	40.9	32.8	3.98	18.6	26.5	1.66	6.2	19.4	8.11	42.8
Node 7	None	None	None	None	None	None	None	None	None	None	None	None	29.7	0.17	0.57	None	None	None	None	None	None	29.7	0.17	0.57
<b>NUMBER OF FREEZE-THAW CYCLES</b>																								
<b>Springfield</b>																								
Node 1	0.0	0.0	0.0	4.1	3.45	8.41	12.8	5.64	44.1	15.9	6.71	42.4	12.9	6.01	46.6	5.85	4.72	72.2	—	—	—	51.5	10.5	20.4
Node 4	0.0	0.0	0.0	0.0	0.0	0.0	0.4	0.68	170	1.0	1.03	102	0.5	0.83	165	0.05	0.22	447	—	—	—	1.95	1.61	82.3
Node 7	0.0	0.0	0.0	0.0	0.0	0.0	0.0	0.0	0.0	0.0	0.0	0.0	0.0	0.0	0.0	0.0	0.0	0.0	0.0	0.0	0.0	0.0	0.0	0.0
Node 8	0.0	0.0	0.0	0.0	0.0	0.0	0.0	0.0	0.0	0.0	0.0	0.0	0.0	0.0	0.0	0.0	0.0	0.0	0.0	0.0	0.0	0.0	0.0	0.0
<b>Chicago</b>																								
Node 1	0.16	0.5	31.76	5.21	3.5	67.0	14.4	5.6	39.1	18.4	6.4	35.0	16.9	4.7	27.9	8.9	5.1	56.8	0.6	1.7	225.3	64.6	13.6	21.0
Node 4	0.0	0.0	0.0	0.0	0.0	0.0	.9	1.1	117.2	1.4	1.4	94.8	.7	.8	139.5	0.16	0.5	317.6	0.0	0.0	0.0	3.20	2.17	68.6
Node 7	0.0	0.0	0.0	0.0	0.0	0.0	0.0	0.0	0.0	0.0	0.0	0.0	0.05	0.23	436	0.0	0.0	0.0	0.0	0.0	0.0	0.05	0.23	436
Node 8	0.0	0.0	0.0	0.0	0.0	0.0	0.0	0.0	0.0	0.0	0.0	0.0	0.0	0.0	0.0	0.0	0.0	0.0	0.0	0.0	0.0	0.0	0.0	0.0

Node 1 - at surface

Node 7 - at ballast - subgrade interface

Node 4 - Mid-depth of ballast

Node 8 - 2 in (5.08 cm) below subgrade surface

(a) Standard deviation,  $^{\circ}\text{F}$

(b) Variance, percent

Note: The average temperatures are given in degrees Fahrenheit.

appear to be representative of anticipated field conditions. For instance at Springfield, no freezing activity was experienced at the ballast-subgrade interface for the entire 20 year period of record, and in Chicago, only one month showed any interface freezing.

A study of the input parameters to the heat transfer model indicated that only two variables, the ballast thermal conductivity and the heat capacity, could vary substantially from their assigned values. Since only limited information was found in the literature about these two variables, it was decided to conduct a series of laboratory tests together with computer simulation of these tests to further evaluate ballast thermal properties.

#### 16.2 Laboratory Evaluation of Ballast Thermal Properties

The laboratory tests and the corresponding computer simulation evaluate ballast thermal conductivity values and also the relative importance of thermal conductivity, heat capacity, density, and water content with respect to heat transfer in ballast.

In the laboratory investigation samples of five types of ballast were prepared to the gradation shown in Figure 16.2. The samples were placed in a dry condition in a styrofoam mold. The mold dimensions were selected so that the ballast samples would be 12 in. (30 cm) high and 8 in. (20 cm) in diameter and protected by not less than 2 in. (51 mm) of styrofoam on the sides and bottom.

During preparation of the samples, thermocouples were placed at the bottom and at the third points so temperature changes within the sample could be accurately monitored with time. Initial temperature readings were 60°F (15.6 °C). The samples were then placed in a constant temperature (22°F, - 5.6°C) cabinet. Temperature readings were taken every hour until all

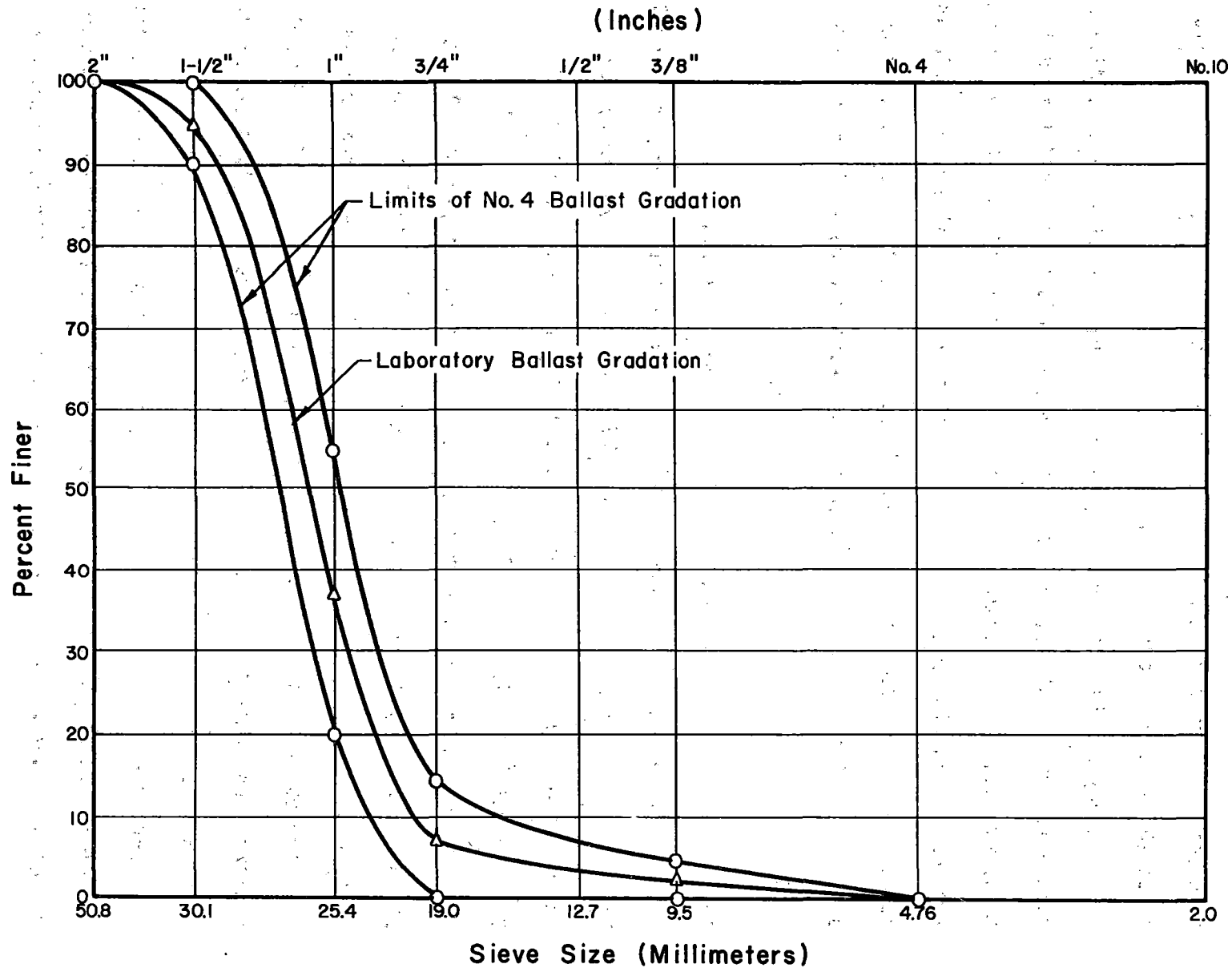


Figure 16.2. Laboratory Gradation Used to Evaluate Ballast Thermal Properties.

the thermocouples had stabilized at approximately 22°F (-5.6 °C). Typical results are included in Figure 16.3 which shows plots of change in temperature,  $\Delta T$ , versus time for three depths.

The results indicate that some air convection is probably taking place in the open graded materials tested. Also, only 28 hours or less was required for all the thermocouples to stabilize to a constant temperature of 22°F (-5.6 °C). It was also found that there appeared to be no lag in temperature changes with time at the freezing point which suggests that the latent heat of fusion effect is either insignificant and may be neglected or more probably that since the samples were prepared in a dry condition, the freezing heat capacity calculated by Equation 15.9 is lower than originally determined.

The computer simulation of the laboratory conditions was carried out using the heat transfer model. The laboratory setup was as shown in Figure 16.4. The variables of thermal conductivity, heat capacity, density, and water content, were examined for the range of values given below:

Ballast Thermal Conductivity	0.20 to 1.0 Btu/ft-hr-°F (4.98 to 24.8 Cal/hr-m-°C)
Ballast Heat Capacity	0.15 to 0.21 Btu/lb-°F (0.15 to 0.21 Cal/kg-°C)
Ballast Density	95.0 to 100 lb/ft <sup>3</sup> (1362 to 1602 kg/m <sup>3</sup> )
Ballast Water Content	0.75 to 2.0 percent

The density and water content values were obtained from the study reported in Part A of this report.

The most prominent intrinsic factor examined affecting temperature changes in the ballast with time is the thermal conductivity. As can be seen from Figure 16.5 there is a significant difference between thermal conductivities of 0.2 Btu/ft-hr-°F (4.98 Cal/m-hr-°C) and 1.0 Btu/ft-hr-°F

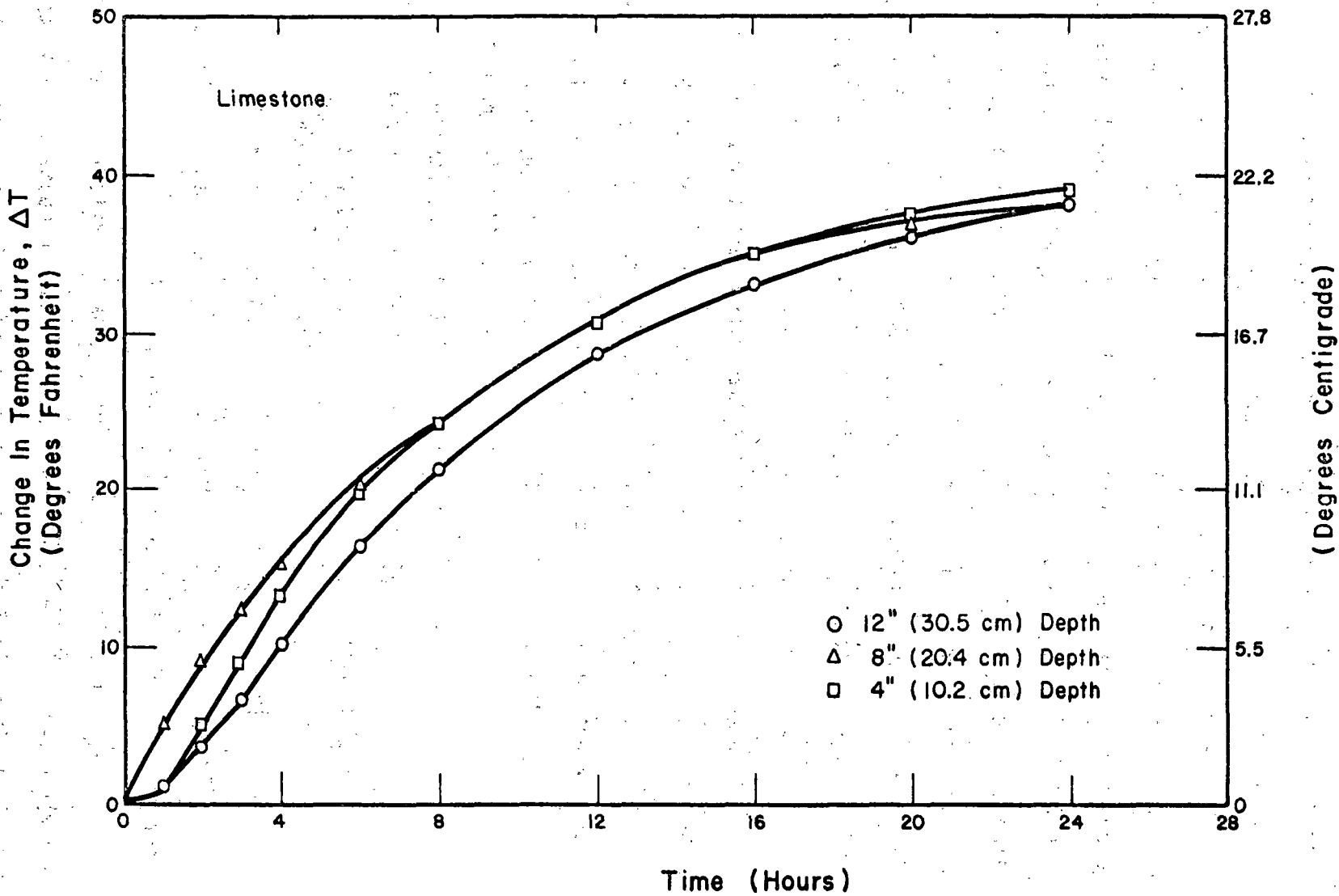


Figure 16.3. Effects of Depth on Heat Transfer in Limestone Ballast.

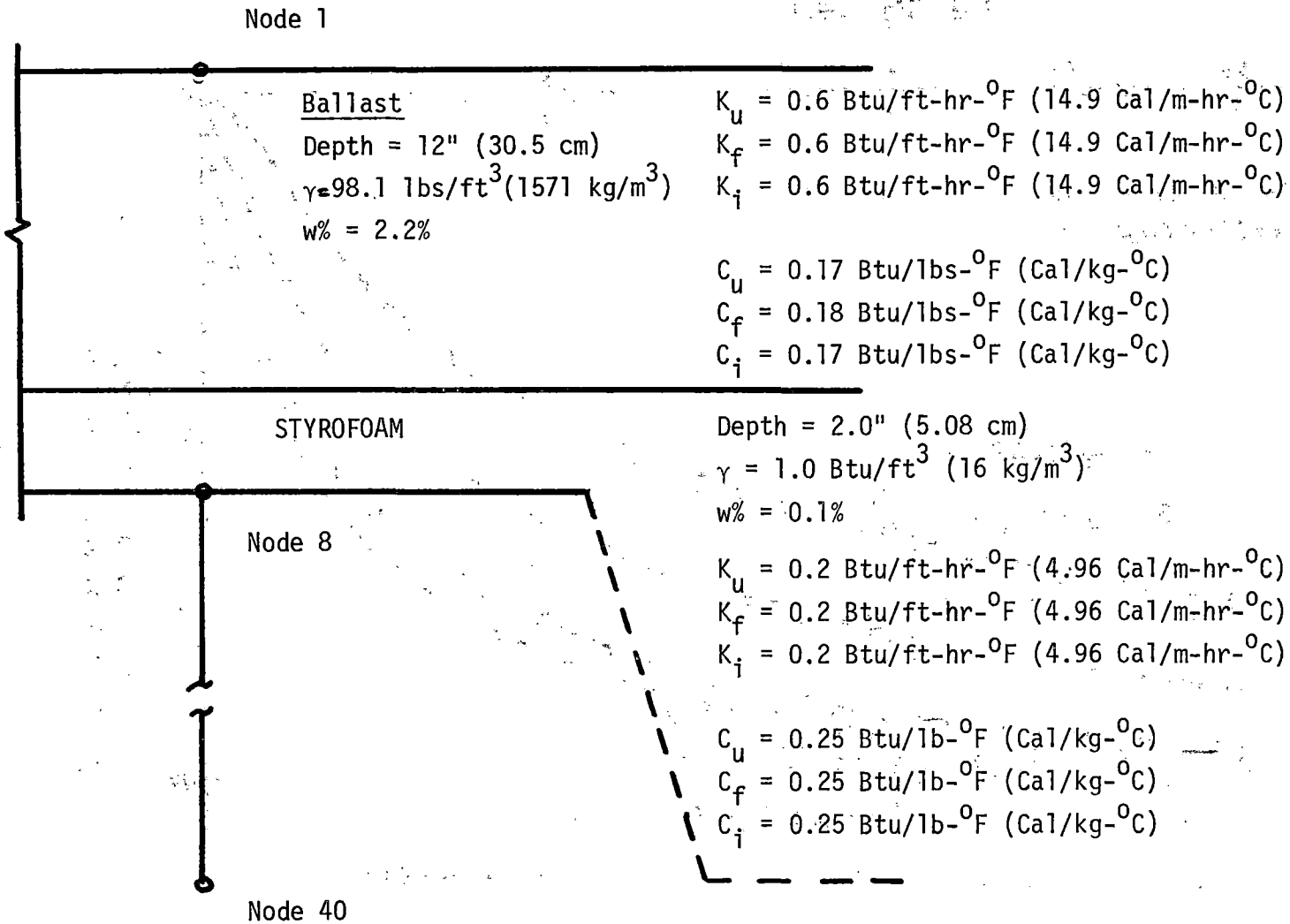


Figure 16.4. Material Properties Used in the Computer Simulation of Laboratory Conditions.

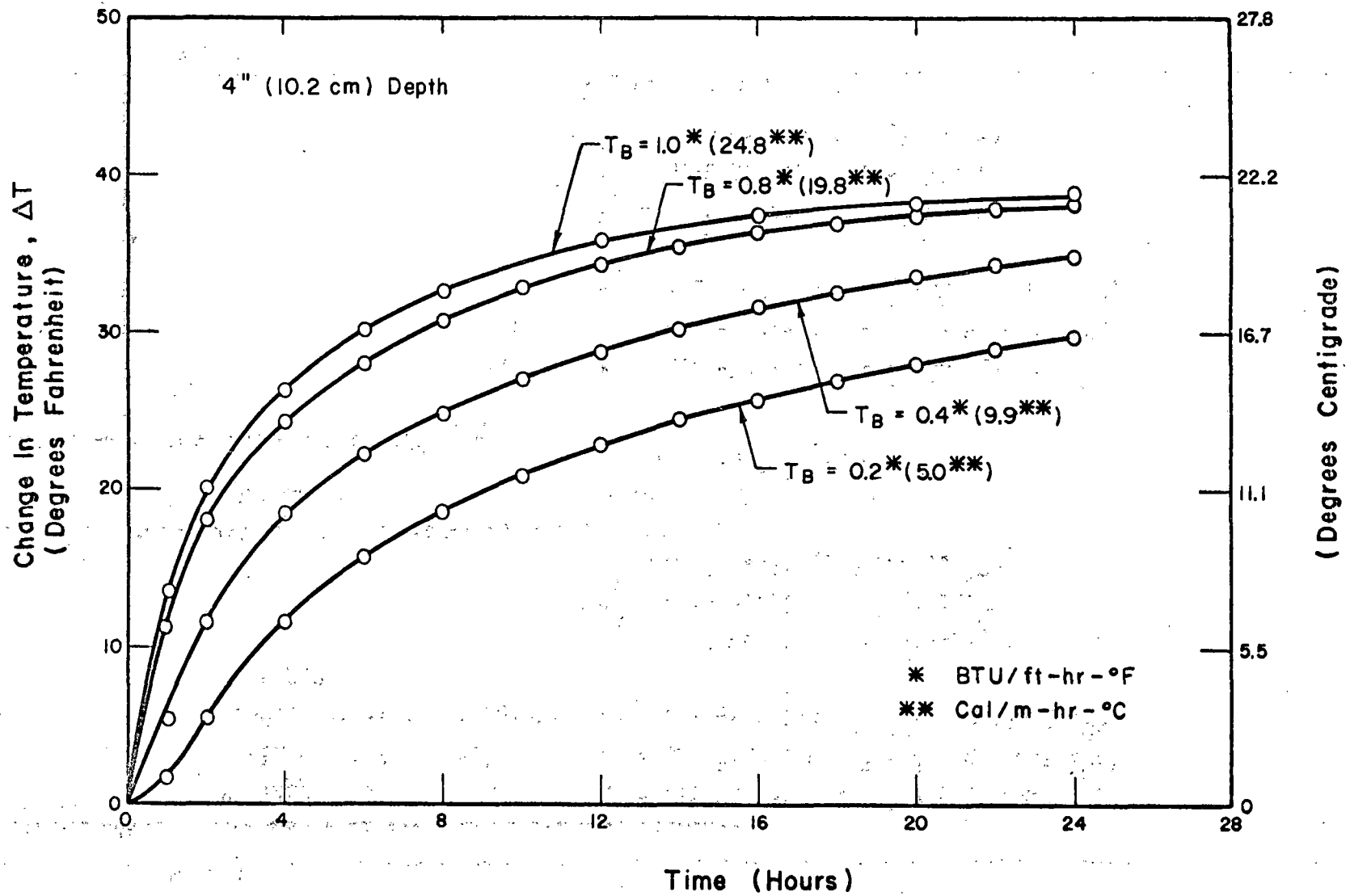


Figure 16.5. Effects of Thermal Conductivity on Heat Transfer in Ballast Materials.

(24.8 Cal/m-hr- $^{\circ}$ C). The difference becomes even more pronounced with depth. The results indicate there is a possible upper bound value for ballast thermal conductivity.

Figure 16.6 shows the effect of varying the heat capacities. It can be seen that the effect is not nearly so great as is the effect of changing the thermal conductivity.

A third ballast property which was varied was the unit weight. A typical result of this simulation is shown in Figure 16.7. Over the range of densities investigated, a comparatively small effect was noted.

The final factor which was varied was the water content of the ballast. No noticeable effect was noted over the range of values (0.75-2.0%) examined.

The primary purpose of the computer simulation and laboratory investigation was to obtain more reliable thermal conductivity values for the unfrozen, freezing and frozen ballast conditions. From a comparison of the results of the laboratory tests and the computer simulations, it was concluded that use of ballast thermal conductivity values from 0.7 to 1.0 Btu/ft-hr- $^{\circ}$ F (17.3 to 24.8 Cal/m-hr- $^{\circ}$ C) were acceptable. Note the values are 3 to 4 times those presented in Table 15.5.

It was concluded that the values of ballast thermal conductivity as computed by Kersten's equations and as presented by Vanpelt were too low to be used in the characterization of temperature regimes in a ballast-subgrade system. Because of convective processes, higher ballast conductivity values would give more realistic characterization of actual field conditions.

### 16.3 Selection of Ballast Thermal Properties

Based on the previous results three changes were made in the input variables originally selected. Additional values of thermal conductivity,  $K_b$ , were selected for analysis. For Chicago, values for  $K_b$  of 0.5 Btu/ft-hr- $^{\circ}$ F

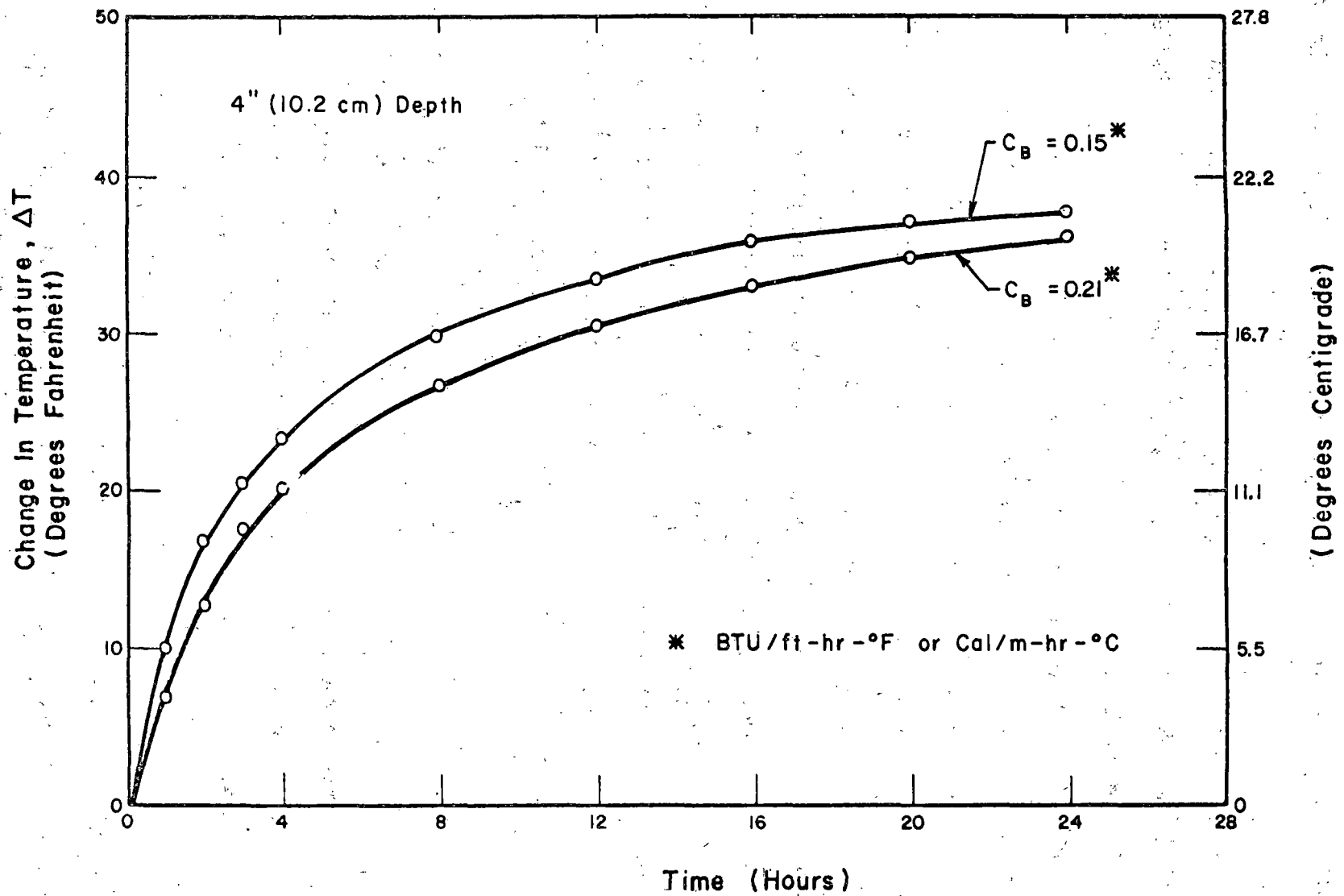


Figure 16.6. Effects of Heat Capacity on Heat Transfer in Ballast Materials.

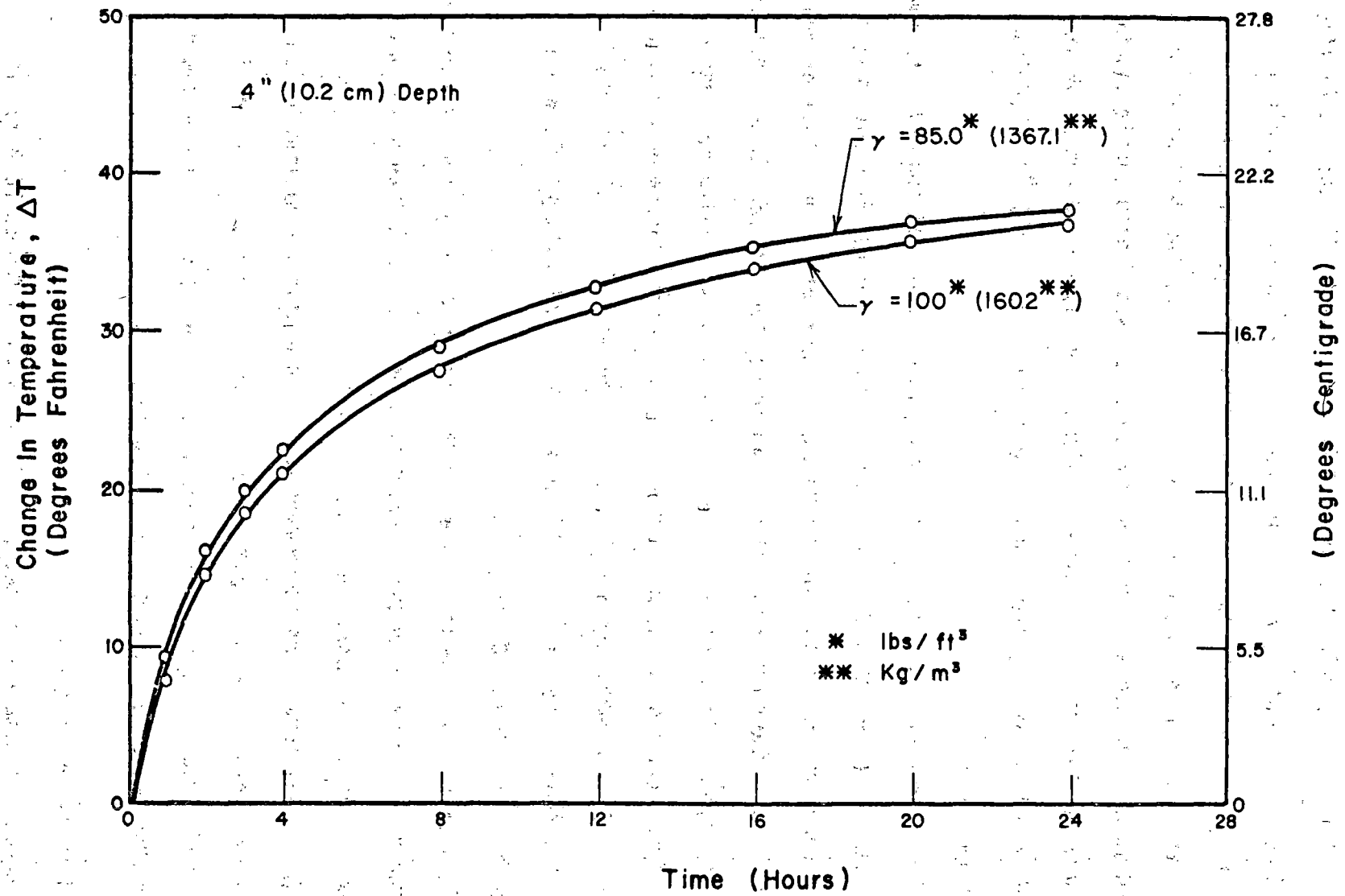


Figure 16.7. Effects of Density on Heat Transfer in Ballast Materials.

(17.39 Cal/m-hr-<sup>0</sup>C), 0.75 Btu/ft-hr-<sup>0</sup>F (18.57 Cal/m-hr-<sup>0</sup>C) and 1.0 Btu/ft-hr-<sup>0</sup>F (24.78 Cal/m-hr-<sup>0</sup>C) were examined. For Springfield, an additional value of  $K_b$  of 1.0 Btu/ft-hr-<sup>0</sup>F (24.78 Cal/m-hr-<sup>0</sup>C) was selected.

As a second change the freezing heat capacity of the ballast was decreased to a value close to that of the unfrozen and frozen conditions to eliminate the latent heat of fusion effect. The effect did not occur in the laboratory tests. A heat capacity value of 0.18 Btu/lb-<sup>0</sup>F (0.18 Cal/kg-<sup>0</sup>C) was selected.

The third change was to decrease the water content of the ballast from 2.2 percent to 0.25 percent. Although the computer simulations indicated that changes in the ballast water content at these small values would have little if any effect on frost action, the reduction was made to be consistent with the decrease in the freezing heat capacity as calculated by Equation 15.9. This reduction in water content also dictated a decrease in the unfrozen and frozen heat capacity as computed by Equations 15.3 and 15.4. These values were adjusted to 0.172 Btu/lb-<sup>0</sup>F (0.172 Cal/kg-<sup>0</sup>C) and 0.17 Btu/lb-<sup>0</sup>F (0.17 Cal/kg-<sup>0</sup>C) respectively.

Because the effects of changes in density on ballast frost penetration were shown by the computer simulations to be slight no further consideration was given to variations in density.

The values noted were incorporated into the heat transfer model and temperature profiles were generated for the 20 year period of record for each station and for each value of ballast thermal conductivity examined. The results are shown in Tables 16.2 and 16.3.

#### 16.4 Discussion of Results

The output data for Chicago, Illinois shown in Tables 16.2 and 16.3 indicate that the surface of the ballast is subjected to an average of

Table 16.2. Results of Temperature Regime Evaluation for Chicago ( $K_B = 0.5$  and  $0.75 \text{ Btu/ft-hr-}^\circ\text{F}$ ).

Station Location	October			November			December			January			February			March			April			Year		
	Ave. $\sigma$ <sup>(a)</sup>	V, <sup>(b)</sup>	V, <sup>(b)</sup>	Ave. $\sigma$ <sup>(a)</sup>	V, <sup>(b)</sup>	V, <sup>(b)</sup>	Ave. $\sigma$ <sup>(a)</sup>	V, <sup>(b)</sup>	V, <sup>(b)</sup>	Ave. $\sigma$ <sup>(a)</sup>	V, <sup>(b)</sup>	V, <sup>(b)</sup>	Ave. $\sigma$ <sup>(a)</sup>	V, <sup>(b)</sup>	V, <sup>(b)</sup>	Ave. $\sigma$ <sup>(a)</sup>	V, <sup>(b)</sup>	V, <sup>(b)</sup>	Ave. $\sigma$ <sup>(a)</sup>	V, <sup>(b)</sup>	V, <sup>(b)</sup>	Ave. $\sigma$ <sup>(a)</sup>	V, <sup>(b)</sup>	V, <sup>(b)</sup>
AVERAGE MEAN TEMPERATURE																								
Chicago ( $K_B = 0.5$ ) *																								
Node 1	66.0	19.0	28.8	48.8	15.2	31.4	36.3	13.0	36.5	33.5	13.7	42.3	36.7	15.7	43.9	48.2	18.6	38.7	61.1	21.3	34.8	47.3	21.0	44.4
Node 7	61.1	3.67	6.01	50.6	4.78	9.48	39.7	3.87	9.84	35.9	2.77	7.71	35.9	2.86	7.92	43.2	4.40	10.1	43.7	45.0	8.38	45.8	0.13	22.2
Chicago ( $K_B = 0.75$ ) *																								
Node 1	65.7	18.0	27.4	48.7	14.6	30.0	36.2	12.4	34.8	33.4	13.0	40.2	36.5	14.9	41.9	47.9	17.7	37.1	60.8	20.3	33.4	47.1	20.3	43.1
Node 7	61.5	4.44	7.24	49.5	5.50	11.2	38.3	4.23	11.1	34.7	3.04	8.73	35.0	3.24	9.20	43.3	5.11	11.7	54.7	4.23	9.55	45.4	11.0	24.2
AVERAGE MEAN TEMPERATURE ABOVE FREEZING																								
Chicago ( $K_B = 0.5$ ) *																								
Node 1	66.1	18.9	28.7	51.4	13.7	26.6	42.7	8.86	20.6	42.0	8.29	19.5	46.0	10.9	23.5	52.8	16.6	31.4	61.5	21.2	34.4	53.4	18.0	33.7
Node 7	61.1	3.67	6.01	50.6	4.78	9.48	39.7	3.87	9.84	36.1	2.66	7.33	36.1	2.78	7.62	43.2	4.40	10.1	53.7	4.50	8.38	46.0	10.0	21.8
Chicago ( $K_B = 0.75$ ) *																								
Node 1	65.8	18.0	27.3	51.1	13.1	25.7	42.1	8.48	20.0	41.5	7.86	18.8	45.3	10.3	22.7	52.0	15.9	30.5	61.2	20.2	32.9	52.9	17.5	33.0
Node 7	61.5	4.40	7.24	49.5	5.50	11.2	38.5	4.19	10.9	35.2	2.77	7.74	35.4	3.04	8.42	43.3	5.11	11.7	54.7	5.23	9.55	45.9	10.73	23.4
AVERAGE MEAN TEMPERATURE BELOW FREEZING																								
Chicago ( $K_B = 0.5$ ) *																								
Node 1	28.9	0.65	2.31	24.7	3.75	16.5	20.8	6.91	35.0	19.6	8.03	43.7	20.3	6.90	37.6	24.6	4.05	17.9	27.8	1.13	4.12	20.6	7.86	39.0
Node 7	None	None	None	None	None	None	30.0	0.0	0.0	29.4	0.32	1.09	28.5	0.88	3.18	None	None	None	None	None	None	29.4	0.37	1.30
Chicago ( $K_B = 0.75$ ) *																								
Node 1	28.9	1.21	4.21	25.0	3.37	14.6	21.1	6.54	32.5	20.1	7.65	40.2	20.9	6.60	34.8	24.9	3.85	16.9	28.2	1.35	4.80	20.9	7.52	36.6
Node 7	None	None	None	None	None	None	29.3	0.37	1.25	20.5	0.75	2.68	28.5	0.70	2.62	None	None	None	None	None	None	28.6	0.77	2.76
NUMBER OF FREEZE-THAW CYCLES																								
Chicago ( $K_B = 0.5$ ) *																								
Node 1	0.15	0.49	326	6.00	3.71	61.9	15.5	5.44	35.2	19.4	5.95	30.7	18.1	4.65	25.8	10.1	5.68	56.3	0.65	1.35	207	69.8	15.1	21.7
Node 4	0.0	0.0	0.0	0.35	0.81	232	3.2	2.59	80.9	5.95	4.22	71.0	5.6	4.19	74.7	1.6	2.21	138	0.0	0.0	0.0	16.7	7.87	47.2
Node 7	0.0	0.0	0.0	0.0	0.0	0.0	0.05	0.22	447	0.75	1.33	177	0.1	0.31	308	0.0	0.0	0.0	0.0	0.0	0.0	0.9	1.48	165
Node 8	0.0	0.0	0.0	0.0	0.0	0.0	0.0	0.0	0.0	0.15	0.67	447	0.05	0.05	447	0.0	0.0	0.0	0.0	0.0	0.0	0.2	0.9	447
Chicago ( $K_B = 0.75$ ) *																								
Node 1	0.10	0.45	447	5.55	3.69	66.5	14.9	5.58	37.6	19.0	6.10	32.2	18.0	47.7	26.6	9.3	5.41	58.2	0.6	1.35	225	67.3	14.6	21.7
Node 4	0.0	0.0	0.0	0.55	1.10	200	4.8	3.43	73.6	8.85	5.50	62.1	8.4	4.75	56.6	2.3	2.96	129	0.0	0.0	0.0	24.9	10.2	40.8
Node 7	0.0	0.0	0.0	0.0	0.0	0.0	0.20	0.41	205	0.75	0.97	129	0.50	1.05	210	0.0	0.0	0.0	0.0	0.0	0.0	1.45	1.67	115
Node 8	0.0	0.0	0.0	0.0	0.0	0.0	0.05	0.22	447	0.80	1.36	170	0.10	0.31	308	0.0	0.0	0.0	0.0	0.0	0.0	0.95	1.57	165

Node 1 - at surface  
 Node 7 - at ballast-subgrade interface  
 Node 4 - Mid-depth of ballast  
 Node 8 - 2 in. (5.08 cm) below subgrade surface

\* - Units are Btu/ft-hr- $^\circ\text{F}$

(a) - Standard deviation,  $^\circ\text{F}$

(b) - Variance, percent

Note: The average temperatures are given in degrees Fahrenheit.

Table 16.3. Results of Temperature Regime Evaluation ( $K_B = 1.0 \text{ Btu/ft-hr-}^\circ\text{F}$ ).

Station Location	October			November			December			January			February			March			April			Year		
	Ave. $\sigma$ <sup>(a)</sup>	V, <sub>%</sub> <sup>(b)</sup>		Ave. $\sigma$ <sup>(a)</sup>	V, <sub>%</sub> <sup>(b)</sup>		Ave. $\sigma$ <sup>(a)</sup>	V, <sub>%</sub> <sup>(b)</sup>		Ave. $\sigma$ <sup>(a)</sup>	V, <sub>%</sub> <sup>(b)</sup>		Ave. $\sigma$ <sup>(a)</sup>	V, <sub>%</sub> <sup>(b)</sup>		Ave. $\sigma$ <sup>(a)</sup>	V, <sub>%</sub> <sup>(b)</sup>		Ave. $\sigma$ <sup>(a)</sup>	V, <sub>%</sub> <sup>(b)</sup>		Ave. $\sigma$ <sup>(a)</sup>	V, <sub>%</sub> <sup>(b)</sup>	
AVERAGE MEAN TEMPERATURE																								
Chicago ( $K_B = 1.0$ )*																								
Node 1	65.6	17.3	26.4	48.7	14.1	29.0	36.2	11.9	33.4	33.4	12.5	38.4	36.4	14.3	40.2	47.8	17.0	35.7	60.8	19.5	32.1	47.1	19.7	42.0
Node 7	61.7	5.01	8.14	49.0	5.97	12.2	37.6	4.46	11.9	34.1	3.33	9.72	34.6	3.58	10.3	43.5	5.61	12.8	55.4	5.78	10.4	45.2	11.5	25.4
Springfield ( $K_B = 1.0$ )*																								
Node 1	—	—	—	51.2	15.1	29.6	39.5	12.8	32.8	36.4	13.6	38.6	40.8	15.7	39.1	52.8	18.5	35.3	—	—	—	44.1	17.2	39.0
Node 7	—	—	—	50.9	6.01	11.9	40.0	4.77	12.0	36.6	4.05	11.1	38.3	4.51	11.8	48.1	6.08	12.7	—	—	—	42.8	8.33	19.5
AVERAGE MEAN TEMPERATURE ABOVE FREEZING																								
Chicago ( $K_B = 1.0$ )*																								
Node 1	65.6	17.3	26.3	50.8	12.7	24.9	41.8	8.16	19.3	40.9	7.58	18.3	44.6	10.0	22.3	51.5	15.3	29.6	61.0	19.4	31.7	52.5	17.0	32.4
Node 7	61.7	5.01	8.14	49.0	5.97	12.2	38.0	4.34	11.4	34.9	2.87	8.07	35.3	3.30	9.18	43.6	5.61	12.8	55.4	5.78	10.4	46.0	11.1	24.2
Springfield ( $K_B = 1.0$ )*																								
Node 1	—	—	—	52.9	14.1	26.5	44.5	9.8	21.9	43.5	9.3	21.2	47.3	12.5	26.3	55.3	17.3	31.3	—	—	—	49.4	14.4	29.1
Node 7	—	—	—	50.9	6.01	11.9	40.2	4.72	11.8	37.2	3.75	9.97	38.7	4.40	11.3	48.1	6.08	12.7	—	—	—	43.3	8.08	18.7
AVERAGE MEAN TEMPERATURE BELOW FREEZING																								
Chicago ( $K_B = 1.0$ )*																								
Node 1	28.7	0.0	0.0	25.4	3.15	13.4	21.5	6.26	30.4	20.4	7.27	37.6	21.2	6.31	32.5	25.1	3.91	16.9	28.3	0.63	2.24	21.2	7.23	34.8
Node 7	None	None	None	None	None	None	29.1	0.53	1.82	28.0	1.05	3.86	28.0	0.99	3.77	29.5	0.0	0.0	None	None	None	28.2	1.05	3.87
Springfield ( $K_B = 1.0$ )*																								
Node 1	—	—	—	25.3	2.86	12.2	22.6	5.56	25.5	20.8	6.77	34.6	21.9	5.46	26.8	25.1	3.45	15.3	—	—	—	21.7	6.63	31.4
Node 7	—	—	—	None	None	None	28.9	0.52	1.79	28.3	1.04	3.79	28.3	0.72	2.69	None	None	None	—	—	—	28.5	0.84	3.03
NUMBER OF FREEZE-THAW CYCLES																								
Chicago ( $K_B = 1.0$ )*																								
Node 1	0.05	0.22	447	4.95	3.32	6.70	14.6	5.60	38.5	18.4	6.44	35.0	17.5	4.76	27.3	8.80	5.09	57.9	0.45	1.19	265	64.7	14.5	22.4
Node 4	0.0	0.0	0.0	0.8	1.28	160	6.4	4.42	69.0	10.5	6.06	58.0	9.45	5.23	55.3	2.85	3.13	110	0.0	0.0	0.0	30.0	11.1	36.9
Node 7	0.0	0.0	0.0	0.0	0.0	0.0	0.75	0.97	129	1.45	2.28	157	0.85	1.69	199	0.05	0.22	447	0.0	0.0	0.0	3.10	3.55	115
Node 8	0.0	0.0	0.0	0.0	0.0	0.0	0.15	0.37	244	0.70	1.17	167	0.45	1.00	222	0.0	0.0	0.0	0.0	0.0	0.0	1.30	2.05	158
Springfield ( $K_B = 1.0$ )*																								
Node 1	—	—	—	3.85	3.25	84.4	12.6	5.73	45.6	15.7	6.38	40.6	13.0	6.11	47.2	5.35	3.9	72.8	—	—	—	50.4	11.0	21.7
Node 4	—	—	—	0.40	0.88	220	5.40	4.52	83.7	7.75	5.43	70.0	6.00	4.90	81.7	1.25	2.27	181	—	—	—	20.8	9.41	45.3
Node 7	—	—	—	0.0	0.0	0.0	0.25	0.64	225	0.75	1.07	143	0.55	1.19	217	0.0	0.0	0.0	—	—	—	1.55	1.82	117
Node 8	—	—	—	0.0	0.0	0.0	0.05	0.22	447	0.40	1.10	274	0.10	0.45	447	0.0	0.0	0.0	—	—	—	0.55	1.23	224

Node 1 - at surface

Node 4 - Mid-depth of ballast

Node 7 - at ballast-subgrade interface

Node 8 - 2 in. (5.08 cm) below subgrade surface

\* - Units are  $\text{Btu/ft-hr-}^\circ\text{F}$

(a) - Standard deviation,  $^\circ\text{F}$

(b) Variance, percent

Note: The average temperatures are given in degrees Fahrenheit.

65-70 freeze-thaw cycles per year. From statistical analysis, there is a 95 percent probability ( $\pm 2$  standard deviations) that during any one year there will be from 35 to 100 freezing and thawing cycles at the surface for the case where  $K_b$  is 1.0 Btu/ft-hr- $^{\circ}$ F (24.8 Cal/m-hr- $^{\circ}$ C). This indicates that the aggregate particles near the surface of the ballast are exposed to an extensive number of freeze-thaw cycles which increase the weathering of the ballast.

Cyclic freeze-thaw is not limited to the surface. As can be seen from Table 16.3, for Chicago (for  $K_b$  of 1.0 Btu/ft-hr- $^{\circ}$ F) at the mid-depth of the ballast, there are on the average 30 freeze-thaw cycles per year. The number decreases to 3.1 cycles per year at the ballast-subgrade interface and 1.3 cycles per year at a depth of 2 in. (51 mm) into the subgrade. Thus in Chicago, the weathering associated with freezing and thawing occurs throughout the full depth of ballast. For smaller values of thermal conductivity ( $K_b = 0.5$  or  $0.75$  Btu/ft-hr- $^{\circ}$ F), the intensity of frost action and resulting weathering decreases with depth.

The freezing and thawing activity in Springfield, is not as intense as in Chicago. As shown in Table 16.3, for  $K_b$  of 1.0 Btu/ft-hr- $^{\circ}$ F, an average of 50.4, 20.8, 1.55, and 0.55 freeze-thaw cycles occur at the surface, the ballast mid-depth, the ballast-subgrade interface, and 2 in. (51 mm) into the subgrade, respectively. Thus, the freezing and thawing in the ballast remains significant. The above characterization was conducted for an idealized CRTSS section of 12 in. (30 cm) of ballast overlying the subgrade soil. Although the idealized section may exist immediately after construction of the section, the thickness of the "unfouled" ballast tends to decrease with time due to ballast intrusion. The intrusion is dependent on several factors including the magnitude of the wheel loads, the amount of traffic, and the

subgrade condition and is accelerated by cyclic freezing and thawing at the ballast/subgrade interface. Since strength loss in soil with increasing freezing and thawing cycles is a well known phenomenon, it is expected that heavy traffic during periods of subgrade thawing will result in accelerated ballast intrusion. As intrusion increases the depth to the interface decreases, the thermal conductivity increases, the number of freeze thaw cycles increases, and the overall strength decreases. Thus the general track condition deteriorates at a faster rate in areas where there is freezing and thawing activity.

## 16.5 Conclusions

From this investigation, the following conclusions can be drawn:

1. The heat transfer model as developed by Dempsey (57) is an excellent tool for the characterization of temperature regimes in an idealized ballast subgrade track support system.

2. Further investigations identifying and measuring the effects of rainfall, internal moisture movement, and snow cover on frost action are needed so that the heat transfer model can be modified and updated to more accurately simulate CRTSS field conditions.

3. More accurate estimates of the thermal conductivities of ballast materials under field conditions are needed as input for the heat transfer model.

4. Further investigation relating the degradation of ballast materials to cyclic freezing and thawing is needed. Information generated by the heat transfer model can be used to determine warming and cooling rates, durations of freezing and thawing cycles, freezing and thawing temperatures, and the number of freezing and thawing cycles. The results could be used in controlled, long term cyclic freezing and thawing tests to examine and determine weathering characteristics of ballast materials.

PART E  
CHAPTER 17

## MATERIALS EVALUATION STUDY SUMMARY AND CONCLUSIONS

## 17.1 Summary

Ballast type materials from several sources were tested in the triaxial apparatus. In service conditions were simulated by utilization of a repeated deviator stress and constant confining pressure. Permanent strain and resilient modulus characteristics were determined; the variables considered included material type and gradation, density, and stress level. Equations relating resilient modulus to the first stress invariant were developed, and the results were analyzed with respect to the variables. The permanent strain results were analyzed with respect to stress level, and comparisons were made between the results according to material characteristics, gradation, and density.

In addition, six types of ballast were tested in the repeated load triaxial apparatus for one million loading cycles each. The compactive effort and gradation for each specimen were the same. The permanent strain behavior and gradation characteristics of the materials were determined. In addition, two specimens were tested at low confining pressure to determine the behavior of rounded versus angular particles.

Ten soils also were tested to determine the resilient and permanent strain characteristics of subgrade materials. The variables included moisture content and freezing and thawing of the samples.

In another portion of the study, laboratory tests and computer simulations were used to determine the thermal properties of ballast. Subsequent thermal regime characterizations were conducted for a typical track structure at two different locations.

## 17.2 Conclusions

The significant conclusions reached during Part A of this study are:

1. The resilient response of a specimen of open graded granular material is independent of stress history so long as the specimen has not been subjected to a stress level which would cause failure.

2. The resilient modulus of open graded materials is appreciably higher than that of dense graded aggregate for a given stress level.

3. The resilient modulus of open graded materials is virtually insensitive to changes in gradation and compaction level. The dependence of resilient response on material type is weak and inconsistent, and therefore no conclusion is drawn with respect to material type.

4. Stress level is the variable most directly influencing the resilient modulus of granular materials. The stress dependent nature of ballast type materials can be characterized by the predictive equation:

$$E_r = K \sigma^n \quad (2.1)$$

5. In sharp contrast to the resilient behavior, plastic strain is affected by stress history. The effect can be explained in terms of primary loading, unloading, and reloading. Large plastic strain results during primary loading. During unloading and reloading elastic strain develops which is accompanied by a small amount of plastic strain.

6. For low stress levels plastic strain is proportional to the logarithm of the number of cycles. As the stress level is increased a "critical value" is reached and the rate of plastic strain accumulation then increases.

7. Plastic strain accumulation is not solely a function of the repeated deviator stress but depends on both the deviator stress and the confining pressure.

8. In general, the No. 5 ballast and the "well graded" specimens tended to resist permanent deformation better than did the No. 4 gradation material.

9. There is a definite dependence of permanent strain behavior on compaction level. In every case the accumulated permanent strain was least for specimens compacted to the highest densities.

10. No definite conclusion can be made with respect to the effects on plastic strain behavior of material properties such as particle index, soundness, Los Angeles abrasion loss, and flakiness index.

Following are the conclusions from Part B:

1. Permanent strain observed at  $10^5$  and at  $10^6$  loading cycles correlated significantly with crushing value. Crushing value appears to be a promising test for predicting resistance to long term, permanent deformation in ballast.

2. Angular materials offer better resistance to permanent deformation at low confining pressures than do rounded materials.

3. The significant correlations for degradation were observed with crushing value, specific gravity (inverse), and density (inverse). No material property correlated significantly with the No. 200 degradation.

4. Long term permanent strain ( $10^5$  and  $10^6$  loading cycles) correlated significantly with the degradation results.

The conclusions from Part C are as follows:

1. The effect of soil moisture was found to be significant. Increasing the moisture content by only about 2 percent led to greatly reduced resilient moduli for the soils tested. Increased degree of saturation of fine grained soils leads to increasing resiliency and consequently decreasing resilient moduli.

2. The resilient response of the soils tested was determined at various stress levels. For the soils tested, the resilient modulus is not constant but is influenced by the magnitude of the repeated axial stress (deviator stress).

3. Fine-grained soils may exhibit substantially different resilient response characteristics due to inherent variations in soil properties such as plasticity, clay and silt contents, organic matter content, clay mineralogy, etc.

4. For most of the soils tested, increased moisture content and reduced density led to increased accumulation of permanent strain with increasing number of load applications. Thus specimens compacted at 100 percent AASHTO T-99 density gave better response under repeated loading than those compacted at 95 percent AASHTO T-99 density and specimens compacted at optimum moisture content (95% T-99 density) gave better response than those specimens compacted at optimum plus 4 percent moisture content (95% T-99 density).

Thus, under actual field conditions a soil with a high degree of saturation can be expected to settle very much, accelerating the development of poor track conditions.

5. The permanent deformation responses of the soils tested are stress-dependent with most of the soils exhibiting pronounced increase in the rate of permanent strain with increase in deviator stress. Most of the soils exhibit a "threshold stress level" which is defined as the stress level above which the permanent deformation of the soils under repeated loading is rapid and below which the rate of cumulative deformation from additional stress applications is very small.

6. Although the effect of freeze-thaw on the accumulation of permanent deformation is presented for only one soil, previous works (80, 81) have also established the detrimental effects of freeze-thaw on soils. Thus, it can be concluded that even one cycle of freeze-thaw is sufficient to greatly reduce the resistance to permanent deformation.

Part D conclusions are as follows:

1. The heat transfer model as developed by Dempsey (57) is an excellent tool for the characterization of temperature regimes in an idealized ballast subgrade track support system.

2. Further investigations identifying and measuring the effects of rainfall, internal moisture movement, and snow cover on frost action are needed so that the heat transfer model can be modified and updated to more accurately simulate CRTSS field conditions.

3. More accurate estimates of the thermal conductivities of ballast materials under field conditions are needed as input for the heat transfer model.

4. Further investigation relating the degradation of ballast materials to cyclic freezing and thawing is needed. Information generated by the heat transfer model can be used to determine warming and cooling rates, durations of freezing and thawing temperatures, and the number of freezing and thawing cycles. The results could be used in controlled, long term cyclic freezing and thawing tests to examine and determine weathering characteristics of ballast materials.

## LIST OF REFERENCES

1. Peck, R. B., First Progress Report of the Joint Investigation of Methods of Roadbed Stabilization, University of Illinois Bulletin, Vol. 43, No. 66, 1946, Reprint Series No. 34.
2. Haynes, J. H., and E. J. Yoder, "Effects of Repeated Loading on Gravel and Crushed Stone Base Course Materials Used in the AASHO Road Test," Highway Research Record No. 39, 1963.
3. Hicks, R. G., and C. L. Monismith, "Factors Influencing the Resilient Response of Granular Materials," Highway Research Record No. 345, 1971.
4. Barksdale, R. D., "Repeated Load Test Evaluation of Base Course Materials," Georgia Institute of Technology, Atlanta, 1972.
5. Allen, J. J., "The Effects of Non-Constant Lateral Pressures on the Resilient Properties of Granular Materials," Ph.D. Thesis, University of Illinois, Urbana, 1973.
6. Tayabji, S. D., "Considerations in the Analysis of Conventional Railway Track Support Systems," Ph.D. Thesis, University of Illinois, Urbana, 1976.
7. Seed, H. B., et al., "Prediction of Flexible Pavement Deflections from Laboratory Repeated-Load Tests," National Cooperative Highway Research Program Report 35, 1967.
8. Morgan, J. R., "The Response of Granular Materials to Repeated Loading," Proceedings, Australian Road Research Board, 1966.
9. Kalcheff, I. V., and R. G. Hicks, "A Test Procedure for Determining the Resilient Properties of Granular Materials," Journal of Testing and Evaluation, Vol. 1, No. 6, ASTM, 1973.
10. Huang, E. Y., "An Improved Particle Index Test for the Evaluation of Geometric Characteristics of Aggregates," Michigan Highway Research Project No. 86546, Houghton, Michigan, July 1965.
11. Ishai, I., and E. Tons, "New Concept and Test Method for a Unified Characterization of the Geometric Irregularity of Aggregate Particles," private communication.
12. Huang, E. Y., et al., "Effect of Geometric Characteristics of Coarse Aggregates on Strength of Soil-Aggregate Mixtures," Proceedings, ASTM, Vol. 64, 1964.

13. Thompson, M. R., "Factors Influencing the Field Stability of Soil-Aggregate Mixtures," Materials Research and Standards, Vol. 7, No. 1, 1967.
14. Hudson, S. B., and H. F. Waller, "Evaluation of Construction Control Procedures - Aggregate Gradation Variations and Effects," National Cooperative Highway Research Program Report 69, 1969.
15. Trollope, D. H., et al., "Stresses and Deformation in Two-Layer Pavement Structures under Slow Repeated Loading," Proceedings, Australian Road Research Board, 1962.
16. Brown, S. F., "Repeated Load Testing of a Granular Material," Proceedings, ASCE, Vol. 100, GT 7, 1974.
17. Allen, J. J., and M. R. Thompson, "Significance of Variably Confined Triaxial Testing," Proceedings, ASCE, Vol. 100, TE 4, 1974.
18. Bishop, A. W., and G. E. Green, "The Influence of End Restraint on the Compression Strength of a Cohesionless Soil," Geotechnique, Vol. XV, No. 3, 1965.
19. Holtz, W. G., and H. J. Gibbs, "Triaxial Shear Tests on Pervious Gravelly Soils," Proceedings, ASCE, Vol. 82, SM 1, 1956.
20. Leslie, D. D., "Large Scale Triaxial Tests on Gravelly Soils," Proceedings, Second Pan American Conference on Soil Mechanics and Foundation Engineering, Vol. 1, 1963.
21. Kondner, R. L., "Hyperbolic Stress-Strain Response: Cohesive Soils," Proceedings, ASCE, Vol. 89, SM 1, 1963.
22. Duncan, J. M., and C.-Y. Chang, "Nonlinear Analysis of Stress and Strain in Soils," Proceedings, ASCE, Vol. 96, SM 5, 1970.
23. Lau, J. S. O., "Repeated Loading Triaxial Tests on Sand," M.S. Thesis, Queen's University, Kingston, Ontario, 1975.
24. Olowekere, D. O., "Strength and Deformation of Railway Ballast Subject to Triaxial Loading," M.S. Thesis, Queen's University, Kingston, Ontario, 1975.
25. "Stresses in the Rails, the Ballast and in the Formation Resulting from Traffic Loads, Summary of the Results Given in Reports Nos. 1-12," Office for Research and Experiments of the International Union of Railways Report D 71/RP 13 (Final Report), Utrecht, Netherlands, 1970.
26. Snyder, J. R., "Repeated Triaxial Testing Machine for Stone with Experimental Evaluations," M.S. Thesis, West Virginia University, Morgantown, West Virginia, 1964.

27. Holubec, I., "Cyclic Creep of Granular Materials," Ontario Joint Highway Research Programme Report No. RR147, University of Waterloo, Waterloo, Ontario, 1969.
28. Wong, R. C. T., "One Dimensional Repeated Loading Test of Railway Ballast," M. S. Thesis, Queen's University, Kingston, Ontario, 1974.
29. Bishop, C., "Some Vibration and Repeated Loading Tests on Railway Ballast," Undergraduate Report, Queen's University, Kingston, Ontario, 1975.
30. Brown, S. F., and A. F. L. Hyde, "Significance of Cyclic Confining Stress in Repeated-Load Triaxial Testing of Granular Material," Transportation Research Record No. 537, 1975.
31. Lade, P. V., and J. M. Duncan, "Stress-Path Dependent Behavior of Cohesionless Soil," Proceedings, ASCE, Vol. 102, GT 1, 1976.
32. "Deformation of Railway Ballast under Repeated Loading (Triaxial Tests)," Office for Research and Experiments of the International Union of Railways Report D 117/RP 5, Utrecht, Netherlands, 1974.
33. Manual for Railway Engineering, American Railway Engineering Association, 1973.
34. Report of Committee 1, Proceedings, American Railway Engineering Association, Vol. 58, 1957.
35. Annual Book of ASTM Standards, American Society for Testing and Materials, Philadelphia, 1975.
36. AASHTO Materials, 11th ed., American Association of State Highway and Transportation Officials, Washington, D. C., 1974.
37. British Standard 812, Methods for Sampling and Testing of Mineral Aggregates, Sands, and Filters, British Standards Institution, 1967.
38. Huang, E. Y., Unpublished Report, 1974.
39. Robnett, Q. L., et al., "Technical Data Bases Report - Ballast and Foundation Materials Research Program," U. S. Department of Transportation Report No. FRA/OR & D-76-138, 1975. PB No. 251,771.
40. Duncan, J. M., and P. Dunlop, "The Significance of Cap and Base Resistant," Proceedings, ASCE, Vol. 94, SM 1, 1968.
41. Rostron, J. P., et al., "Density Standards for Field Compaction of Granular Bases and Subbases," Research Results Digest 57, National Cooperative Highway Research Program, 1974.
42. Thompson, O. O., "Evaluation of Flexible Pavement Behavior with Emphasis on the Behavior of Granular Layers," Ph.D. Thesis, University of Illinois, Urbana, 1969.

43. Cedergren, H. R., Drainage of Highway and Airfield Pavements, John Wiley and Sons, New York, 1974.
44. Knutson, R. M., "Factors Influencing the Repeated Load Behavior of Railway Ballast," Ph.D. Thesis, University of Illinois, Urbana, 1976.
45. Heath, D. L., and M. J. Shenton, "The Behavior of Track Ballast Under Repeated Loading Conditions," British Railways Report No. E.610D, 1968.
46. Chung, K. M. P., "Some Triaxial Tests on Railway Ballast," Undergraduate Report, Queen's University, Kingston, Ontario, 1974.
47. Report of Committee 1, Proceedings, American Railway Engineering Association, Vol. 54, 1953.
48. Report of Committee 1, Proceedings, American Railway Engineering Association, Vol. 56, 1955.
49. "Evaluation of Construction Control Procedures," National Cooperative Highway Research Program Report 34, 1967.
50. "Effects of Different Methods of Stockpiling and Handling Aggregates," National Cooperative Highway Research Program Report 46, 1967.
51. Eske, M., and H. C. Morris, "A Test for Production of Plastic Fines in the Process of Degradation of Mineral Aggregates," ASTM, STP No. 277, 1960.
52. Report of Committee 1, Proceedings, American Railway Engineering Association, Vol. 59, 1958.
53. Dalton, C. J., "Field Durability Tests on Ballast Samples as a Guide to the Significance of the Specification Requirements," Canadian National Railways Technical Research Centre, St. Laurent, Quebec, 1973.
54. Robnett, Q. L., et al., "Development of a Structural Model and Materials Evaluation Procedures," Ballast and Foundation Materials Research Program, Department of Civil Engineering, University of Illinois at Urbana-Champaign, (to be published by U. S. Department of Transportation).
55. Robnett, Q. L., and M. R. Thompson, "Interim Report - Resilient Properties of Subgrade Soils, Phase I - Development of Testing Procedure," Civil Engineering Studies, Transportation Engineering Series No. 5, Illinois Cooperative Highway Research Program Series No. 139, Department of Civil Engineering, University of Illinois at Urbana-Champaign, 1973.
56. Monismith, C. L., et al., "Permanent Deformation Characteristics of Subgrade Soils in Repeated Loading," paper prepared for presentation at the 54th Annual Meeting of the Transportation Research Board, 1975.
57. Dempsey, B. J., "A Heat-Transfer Model for Evaluating Frost Action and Temperature Related Effects in Multilayered Pavement Systems," Ph.D. Thesis, University of Illinois, Urbana, Illinois, 1969.

58. Dempsey, B. J., and M. R. Thompson, "A Heat Transfer Model for Evaluating Frost Action and Temperature Related Effects in Multilayered Pavement Systems," Highway Research Record No. 342, 1970.
59. Marek, C. R., and B. J. Dempsey, "A Model Utilizing Climatic Factors for Determining Stresses and Deflections in Flexible Pavement Systems," Proceedings of the Third International Conference on the Structural Design of Asphalt Pavements, London, 1972.
60. Turner, K. A., Jr., and Jumikis, A. R., "Subsurface Temperatures and Moisture Contents in Six New Jersey Soils, 1954-1955," Highway Research Bulletin 135, 1956.
61. Kubler, G., "Influence of Meteorologic Factors on Frost Damage in Roads," Highway Research Record No. 33, 1963.
62. Moulton, L. K., and Dubbe, E. C., "A Study of the Relationship Between Air Temperatures and Depth of Frost Penetration as Related to Pavement Performance of West Virginia's Highways," State Road Commission Report No. 7, Engineering Experiment Station, West Virginia University, Morgantown, West Virginia, 1968.
63. Atkinson, A. B., and Bay, C. E., "Some Factors Affecting Frost-Penetration," Transactions of American Geophysical Union, Vol. 21, Part 3B, The National Research Council of the National Academy of Sciences, 1940.
64. Franklin, T. B., "The Effect of Weather Changes on Soil Temperatures," Proceedings, Royal Society of Edinburgh, Vol. 40-41, 1920.
65. Kersten, M. S., "Thermal Properties of Soils," Bulletin No. 28, University of Minnesota, Engineering Experiment Station, Minneapolis, 1949.
66. DeVries, D. A., "Thermal Conductivity of Soil," Department of Science and Industrial Research, Building Research Station L. C. 759, 1956.
67. Smith, W. O., "Thermal Conductivity of Dry Soils," Soil Science, Vol. 53, 1942.
68. McGaw, R., "Heat Conduction in Saturated Granular Materials," Highway Research Board Special Report No. 103, 1969.
69. Kunii, D., and J. M. Smith, "Heat Transfer Characteristics of Porous Rocks," A. I. Ch.E. Journal, Vol. 6, No. 1, 1960.
70. Haskin, Z., and S. Shtrikuan, "A Variational Approach to the Theory of Effective Magnetic Permeability of Multiphase Materials," Journal Applied Physics, Vol. 33, 1962.
71. Johansen, Ø., "A Method for Calculation of Thermal Conductivities of Soils," Part 1, General Theory, Frost i Jord, No. 7, 1973.
72. Johansen, Ø., "Thermal Conductivity of Rock and Soil," Frost i Jord, No. 16, 1975.

73. Horai, K., "Thermal Conductivity of Rock Forming Minerals," Journal of Geophysical Research, Vol. 76, 1971.
74. Vanpelt, D. J., "Thermal Conductivity Measurements of Crushed Stone and Gravel Aggregate," Technical Note, U. S. Army Cold Regions Research and Engineering Laboratory, Hanover, New Hampshire, 1976.
75. Jumikis, A. R., Thermal Soil Mechanics, Rutgers University Press, New Brunswick, New Jersey, 1966.
76. Aldrich, H. P., Jr., "Frost Penetration Below Highway and Airfield Pavements," Highway Research Bulletin 135, 1956.
77. Johnson, A. W., "Frost Action in Roads and Airfields," Highway Research Board, 1952, Special Report No. 1, 1952.
78. Thompson, M. R., and Robnett, Q. L., "Resilient Properties of Subgrade Soils," Final Report, Civil Engineering Studies, Transportation Engineering Series No. 14, Department of Civil Engineering, University of Illinois at Urbana-Champaign, 1976.
79. Minerals Yearbook, 1972, Bureau of Mines, U. S. Department of the Interior, Vol. I, Published, 1974.
80. Thompson, M. R., and Dempsey, B. J., "Durability Testing of Stabilized Materials," Final Report, Civil Engineering Studies, Transportation Engineering Series No. 11, Department of Civil Engineering, University of Illinois at Urbana-Champaign, 1974.
81. Robnett, Q. L., and Thompson, M. R., "Effect of Lime Treatment on the Resilient Behavior of Fine-Grained Soils," Transportation Research Record No. 560, Transportation Research Board, 1976.

**PROPERTY OF FRA  
RESEARCH & DEVELOPMENT  
LIBRARY**

Material Evaluation Study: Ballast and Foundation  
Materials Research Program, 1977, R. Knutson,  
M. Thompson, T. Mullin, S. Tayabji, US DOT,  
FRA, 01-Track & Structures